THE UNIVERSITY
of EDINBURGH

The Association of Structural Brain Networks with Cognition in Suspected Epilepsy and Epilepsy Surgery

Julie Woodfield

Doctor of Philosophy
College of Medicine and Veterinary Medicine
Deanery of Clinical Sciences
University of Edinburgh

2020

Abstract

The human brain can be modelled as a network of interconnected anatomical regions using structural magnetic resonance imaging data. Understanding variations in network structure could help understand variations in higher brain functions such as cognition. This thesis investigates whether brain network structure is associated with cognition in patients investigated for suspected epilepsy and in those undergoing epilepsy surgery. Epilepsy is frequently associated with cognitive impairments and seizures are known to disrupt both structural and functional brain networks.

First, a systematic literature review was undertaken to compare structural brain networks in epilepsy with healthy controls. Patients with epilepsy were found to have less efficient networks with increased average path lengths compared to healthy controls. Networks constructed from cortical thickness covariance also showed increased clustering coefficients compared to controls.

Second, the association between network structure and cognitive dysfunction in a cohort of children undergoing investigation for suspected epilepsy was analysed. Patients with cognitive dysfunction had networks with longer average path lengths, longer normalised average path lengths, and lower global efficiency, even after controlling for the number and weight of network edges. These findings were consistent across network construction methods.

Third, in a cohort of children undergoing resective epilepsy surgery, a post-operative increase in intelligence quotient was associated with increased global efficiency in the structural network within the healthy, contralateral non-operated hemisphere.

Although cognition was associated with clinical features such as seizure frequency and age at onset of seizures, differences in network characteristics could not be completely explained by differences in clinical features. Different modelling techniques created different representative models but findings were broadly consistent across model types.

This thesis suggests that the widespread alterations in brain structure described in epilepsy may lead to less efficient brain networks which could contribute to cognitive dysfunction. Adequately treating seizures in those with an efficient underlying brain network structure may facilitate cognitive development and allow patients to achieve their cognitive potential.

Lay Summary

The organisation of the brain can be thought of as a network of regions connected by paths down which signals travel. Modelling the brain as a network allows the structure of the network to be investigated. This thesis investigates whether the structural organisation of the brain network is associated with how well the brain functions. This is investigated in people who experience seizures. Seizures occur fairly commonly in the population and are frequently associated with changes in brain function and structure that can have an impact on quality of life. Investigating brain network structure and its association with brain function in people who experience seizures may help influence the way in which seizure disorders are treated to maximise brain function.

First, a systematic review of existing studies was undertaken to collate studies that have compared brain network structure between healthy participants and those who have epilepsy, which is a condition characterised by seizures. Participants with epilepsy were found to have less efficient networks compared to healthy controls. Less efficient brain networks may be associated with the frequent memory, language, and cognitive problems that people with epilepsy can experience.

Second, the association between brain network structure and the presence of learning difficulties in a group of children undergoing brain scans to investigate potential seizures was analysed. Networks were constructed from brain scans using several different methods, and although these produced slightly different models with slightly different values, children with learning difficulties consistently had less efficient networks than those without. This suggests that brain network structure is associated with global brain function.

Third, a group of children with medication resistant epilepsy who were undergoing surgery for epilepsy were investigated. A more efficient network structure within the non-operated side of the brain was associated with an improvement in intelligence quotient following surgery. This suggests that treating seizures adequately in those with an underlying well organised brain structure may facilitate better cognitive development and outcomes.

This thesis provides evidence that brain network structure is altered in patients with seizures, and this alteration can be associated with brain function. When seizures are treated by surgery, having a good underlying brain network structure is associated with an improvement in brain function.

Acknowledgements

I would like to thank Mark Bastin and Richard Chin, my PhD supervisors at the University of Edinburgh and Kees Braun, my supervisor at the University Medical Centre, Utrecht for their suggestions, feedback, and guidance during the PhD, and for providing access to extra data sets during the course of my PhD. This project would never have happened without the support of the Edinburgh Clinical Academic Track programme at the University of Edinburgh who employed me and allowed me to pursue an area that interests me. I would particularly like to thank Jo Ness for making everything happen, along with all of the directors and co-directors involved over the last few years.

All of the data in this final thesis comes from the University Medical Centre in Utrecht, and I would like to acknowledge Kees Braun, Monique van Schooneveld, Martijn van den Heuvel and Suzanne Koudijs for sharing the data and their ideas with me. I would also like to thank everyone who made the project happen in Utrecht including Eltje Bloemen, Helene Willems-van Paridon, Tim Veersema, Herm Lamberink, Bert van den Munckhof, and Anne Mooij. Without these people I would not have found anywhere, acquired any data, had forms filled in correctly, met the correct people, managed to use a computer, or navigated the canteen to find lunch. Thank you to everyone in Utrecht for making me feel welcome and included, and helping with everything.

I would also like to thank everyone in Edinburgh who supported data acquisition, data processing, project management, and my writing at the Royal Hospital for Sick Children and Child Life and Health, particularly Janice Fyall, Ailsa McLellan, Becky Black, Matthew Hunter, Tomi Ajetunmobi, and Michael Yoong. In addition, thank you to the Edinburgh neurosurgical team for the persistent encouragement to finish the PhD thesis.

Declaration

I declare that this thesis was composed by myself, that the work contained herein is my own except where explicitly stated otherwise in the text, and that this work has not been submitted for any other degree or professional qualification except as specified.

(*Julie Woodfield*)

Table of Contents

List of Figures

List of Tables

Chapter 1

Introduction

1.1 Chapter Abstract

Epilepsy is a common disorder of brain network function that manifests clinically with seizures. Seizures may be controlled with anti-epileptic drugs (AEDs). However, in some cases AEDs are ineffective at preventing or controlling seizures. Both seizures and the use of AEDs are commonly associated with cognitive dysfunction. Surgical resection of the epileptogenic focus or surgical disruption of seizure circuits may be considered in those with medication resistant epilepsy. Post-operative freedom from seizures and AEDs can lead to improvements in cognitive function. Understanding how brain network structure is associated with cognitive ability and changes in cognitive ability in those experiencing seizures could lead to a better understanding of how brain network structure influences and facilitates cognition, and how management strategies can be designed to ensure the best possible cognitive outcomes for patients experiencing seizures.

The complex network of interconnected neurones that make up the human brain can be modelled and analysed using structural magnetic resonance imaging (MRI) data. This thesis aims to investigate how brain networks are structured to facilitate complex cognitive functioning and how networks are altered in response to seizures and therapeutic interventions to manage seizures. First, the brain network structure of those with and without epilepsy will be compared. Then the association of network structure and cognitive functioning in children with suspected epilepsy will be investigated. Finally, the effects of surgery to resect epileptogenic foci on cognitive function will be assessed to investigate how brain network structure can facilitate any cognitive improvement post operatively. This will establish how seizures affect brain network structure, how changes in network structure might affect cognitive function, and how brain network structure mediates the effects of therapeutic interventions in those with seizures. This could lead to improved prediction of cognitive outcomes in patients undergoing medical and surgical therapy for epilepsy, and therefore the development of individual strategies that aim to maximise efficient network structure and cognitive outcomes.

1.2 Background

The human brain functions to process incoming signals and co-ordinate responses. On a basic level this facilitates necessary reactions to changes in the internal and external environment, and on a more complex level, allows learning, memory, intelligence, and personality. The structure and organisation of the central nervous system enables these functions.

1.2.1 Brain development

Human brain development begins in the embryo with the infolding of ectoderm to form the neural tube as shown in Figure 1.1. Complex folding of the rostral part of the neural tube gives rise to the embryonic brain. By day 25, the prosencephalon, mesencephalon, and rhombencephalon can be identified.[1] The cerebral hemispheres and thalamus arise from further development and folding of the prosencephalon. The basal ganglia develop from the medial and lateral ventricular eminences bulging into the lateral and third ventricles.[1] Neurones and glia are initially formed in the germinal matrix or ventricular zone, and afterwards the subventricular zone, and migrate towards what will become the pial surface of the cerebral hemispheres, forming the cortical plate, and later the layers of the cerebral cortex.[2]

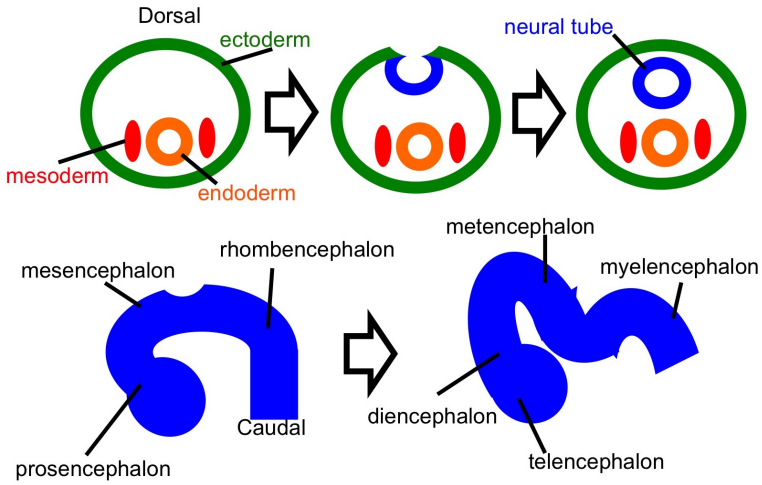

Figure 1.1: ***Embryonic brain development***. ***Top row:*** *primary neurulation. The neural plate of the ectoderm folds, leading to the neural groove and finally the neural tube. This occurs by day 30.* ***Bottom row:*** *dorsal and ventral induction. The brain is subdivided into the prosencephalon, mesencephalon, and rhombencephalon. The mesencephalic flexure appears by day 25. By day 30, the prosencephalon has further subdivided into the telencephalon and diencephalon. The cerebral hemispheres develop from the telencephalon and rapidly enlarge to cover the diencephalon, which gives rise to the thalamus. The pontine flexure divides the rhombencephalon into the metencephalon and myelencephalon.*

During the foetal period of development (from approximately eight weeks) the cerebral hemispheres increase in size, growing posteriorly to create the occipital pole, frontally to create the frontal pole, and laterally to create the temporal pole, gradually burying the insula. The complex pattern of sulci and gyri continues to develop, along with increasing complexity of the subcortical structures. Continued radial migration of neurones creates within hemisphere ascending and descending neuronal tracts.[3]

Tangential migration contributes to within hemisphere connections, and the cerebral commissures and the corpus callosum arise from the embryonic lamina terminalis in a rostrocaudal direction.[1,4] At the time of birth, oligodendrocytes have begun myelination of the major fibre tracts of the brain, and final differentiation of cortical neurones has occurred, creating the structure of the brain that allows performance of both simple and complex functions.

1.2.2 Brain structure

The basic unit of signal processing in the brain is the neurone, shown in Figure 1.2. Neurone dendrites can sense inputs, and summation of these input signals can lead to either hyperpolarisation and prevention of signal propagation or depolarisation of the axon membrane and propagation of an action potential to the nerve terminal, resulting in the release of neurotransmitters across synapses and input into other neurones. Within neurones signals are propagated as electrical currents and between neurones synapses use neurotransmitters as chemical signals that act on cell membrane receptors. The adult human brain contains an estimated 86 billion neurones[5] and these are anatomically arranged into white matter containing many myelinated axons, and grey matter, consisting mostly of cell bodies. The grey matter of the cerebral cortex and basal ganglia is shown in Figure 1.3. Major white matter tracts surrounding these areas of grey matter are shown in Figure 1.4. This macroscopically visible division organises regions into grey matter nuclei with multiple cell bodies receiving inputs and processing signals and white matter tracts that convey information to and from these regions, creating an effective network for signal processing.

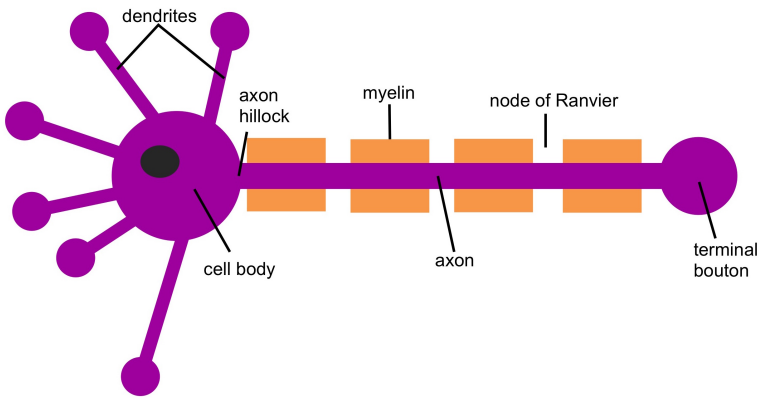

Figure 1.2: ***Diagram of a neurone***. *Neurones may have many thousands of branching sensory dendrites which synapse with other neurones or sensory receptors. Axons carry information away from the cell body and are encased in the central nervous system by oligodendroglia which form a myelin sheath. At rest the inside of the cell has a negative membrane electrical potential with respect to the exterior. Dendritic responses to changes at their synapses can cause depolarisation or hyperpolarisation at the axon hillock. If sufficient depolarisation occurs the axon rapidly depolarises and an action potential of depolarisation travels down the axon, causing release of neurotransmitters at the axon terminal synapses. The myelin sheath allows fast saltatory conduction of the action potential to the next node of Ranvier, where membrane depolarisation occurs to continue the depolarisation along the length of the axon.*

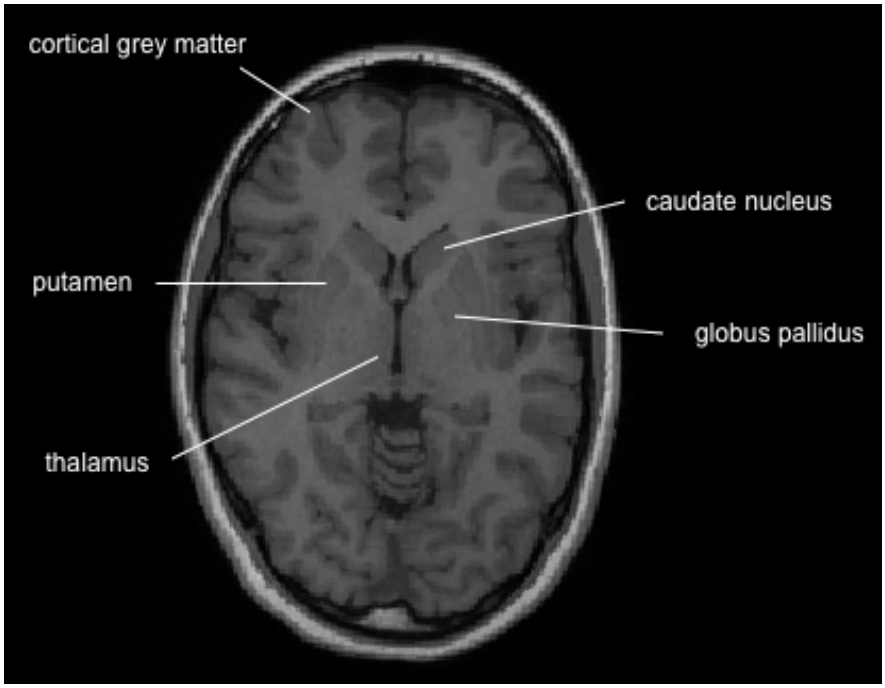

Figure 1.3: ***Grey matter anatomy***. *Axial T1-weighted MRI slice showing the grey matter of the basal ganglia (caudate, putamen, globus pallidus), thalamus, and the cerebral cortex. Grey matter appears hypointense to white matter on this T1-weighted image.*

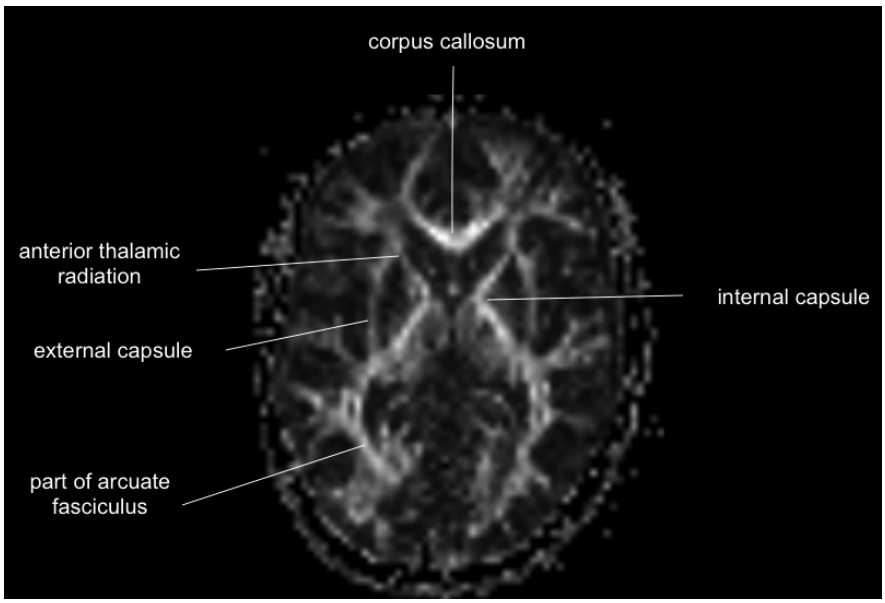

Figure 1.4: ***White matter anatomy***. *Axial fractional anisotropy (FA) MRI slice highlighting white matter tracts. This FA map shows white matter tracts with high FA as hyperintense.*

The cortical grey matter is further subdivided into anatomical regions that support different functions. Brodmann first divided the cortical grey matter into regions based on the cellular structure of the Nissl stained cortical layers in the early 1900s.[6,7] His last published maps[7] are reproduced in Figure 1.5. Although Brodmann's areas were defined post mortem by cytoarchitectonic appearances, many regions are linked to specific functions such as the precentral gyrus with its giant pyramidal cells serving the primary motor area and the area striata of the calcarine fissure representing the primary visual cortex.[6,8]

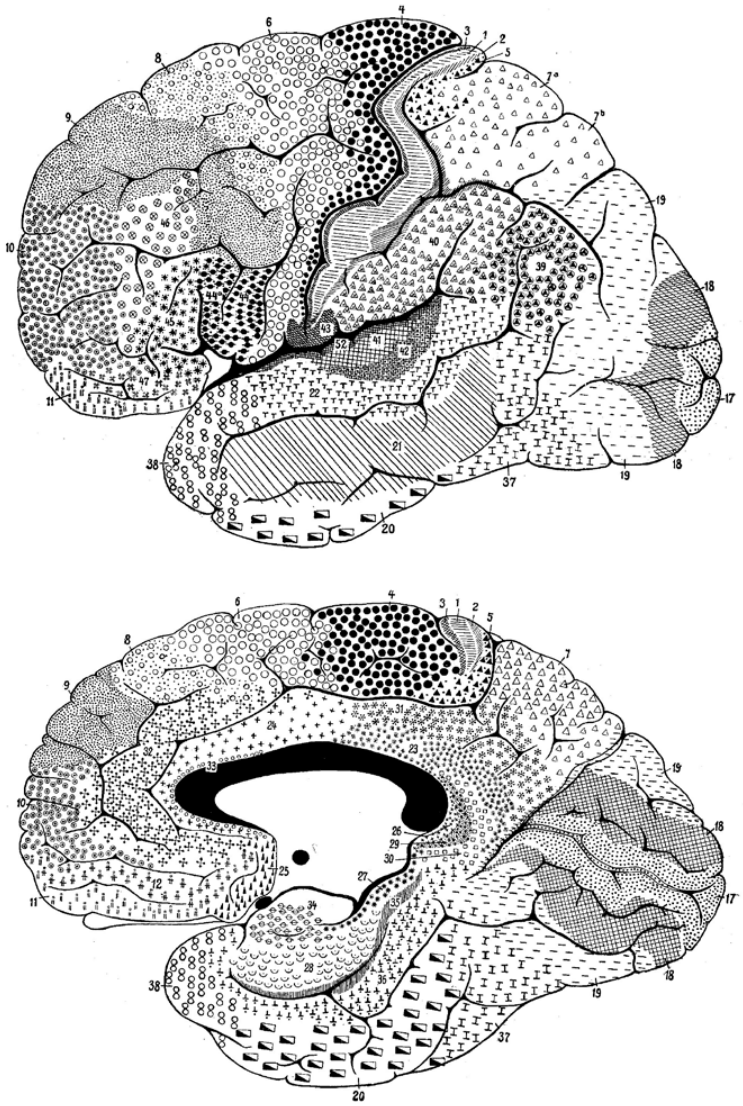

Figure 1.5: ***Brodmann maps***. *The later modified version of Brodmann's maps. Lateral view of the left hemisphere (above) and medial view of the right hemisphere (below). Numbers represent named Brodmann regions. Region descriptions can be found in references Brodmann, 1909*[6] *and Judas, 2012.*[7]

Anatomic localisation within the human brain has been investigated using direct electrical stimulation during awake craniotomy.[8] This led to Penfield's maps of motor and sensory function in the pre and post central gryi (see Figure 1.6 and the well known homunculus).[8] However, cortical mapping confirmed that functions could be interrupted or stimulated at a wide range of locations, with motor function found

in primary sensory cortex and vice versa[8] and interruption of speech and language function found following stimulation of a wide range of locations across the lateral surface of the cerebral hemisphere.[9] Therefore, function is not determined only by one cortical region but relies on the interplay of multiple cortical circuits. This hodotopical view of brain function takes into account cortical regions subspecialised in structure and function along with the multiple neuronal network connections,[10] and can be applied not only to motor, sensory, or speech function, but also to higher mental processes such as learning and memory.[11]

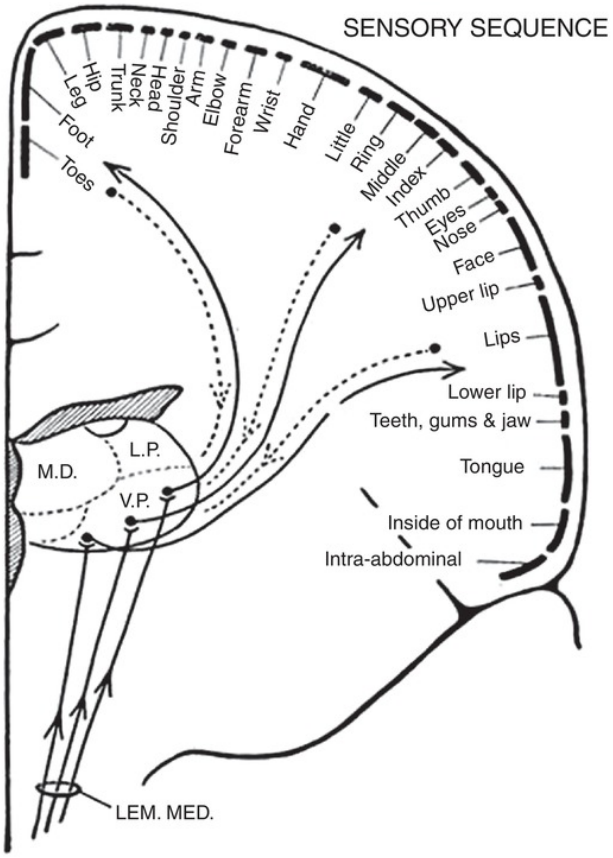

Figure 1.6: ***Penfield's sensory sequence***. *The sensory sequence in the Rolandic cortex as determined by Penfield and reproduced from Penfield and Jasper, 1954.*[8]

1.2.3 Investigating brain structure

Until the advent of cross sectional imaging, only post mortem[6] or intra-operative analyses[8] of human brain structure were possible, and much knowledge was extrapolated from animal models. However, MRI can now be used to image brain structure in vivo. Standard T1-weighted and T2-weighted MRI (shown in Figure 1.7) is created by stimulating hydrogen nuclei by applying a radiofrequency (RF) pulse at 90 degrees to the magnetic field in the scanner (B_0). T1-weighted relaxation or spin-lattice relaxation is the time it takes for the hydrogen nucleus to recover 63% of its original magnetisation.[12] In spin-echo imaging, a 180 degree RF pulse is applied to rephase the spins of the hydrogen ions, creating a spin-echo, which occurs at the echo time (TE). The TE is twice the time from the initial 90 degree RF

pulse to the rephasing 180 degree RF pulse. The T2-weighted or spin-spin relaxation is the time it takes for 63% of the transverse magnetisation to be lost.[12] The receiver coil detects precessing magnetisation as voltage. The repetition time (TR) is the time until the 90 degree RF pulse is reapplied. Spatial localisation in MRI is achieved through the use of gradient coils which alter the magnetic field slightly within the bore of the scanner. If each location in the scanner has a slightly different magnetic field, the hydrogen ions will precess at a slightly different frequency. MRI sequences can be acquired either in two dimensional (2D) or three dimensional (3D) space. MRI shows clear differences between the appearance of grey and white matter - this can be seen on standard clinical T1-weighted and T2-weighted imaging in Figure 1.7.

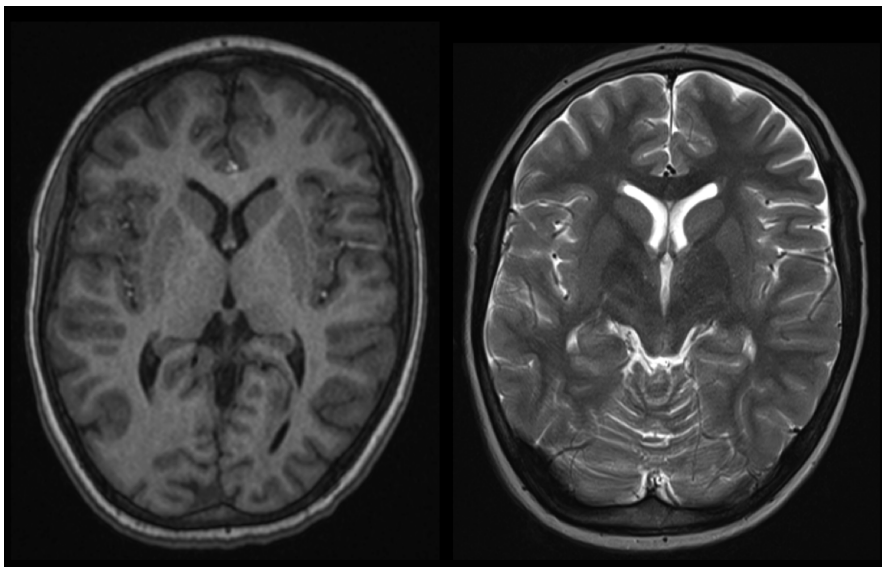

Figure 1.7: ***Standard T1-weighted and T2-weighted MRI****. Axial slices of T1-weighted (left) and T2-weighted (right) MRI sequences showing grey and white matter. White matter appears hyperintense on T1-weighted and hypointense on T2-weighted images. Cerebrospinal fluid is hypointense on T1-weighted and hyperintense on T2-weighted images. (MRI: magnetic resonance imaging)*

MRI can also be used to probe the structure of white matter tracts using diffusion tensor imaging (DTI), which measures the diffusion of water within the brain. Water molecules in the brain show free diffusion in areas without cellular barriers, such as within the cerebrospinal fluid of the ventricles, but show highly ordered diffusion along the direction of white matter tracts with restricted diffusion at angles perpendicular to the white matter tracts. Diffusion is measured on MRI by adding a diffusion gradient to a T2-weighted sequence, usually a single-shot spin-echo echo planar imaging (EPI) sequence, which allows random patient motion to be frozen out. This gradient is cancelled by a second gradient following the 180 degree refocusing pulse. However, molecules that have moved are out of phase with the others, which leads to signal loss in voxels with high water diffusion.[13] The b-value in seconds (s)/millimetre $(mm)^2$ is dependent on the magnitude, duration, and time interval of the diffusion gradient and higher b-values lead to higher signal drop out.[14] Diffusion along different directions in tissue can be assessed by varying the direction of the diffusion sensitising gradients.[15] At least six diffusion gradient directions must be obtained for a three dimensional representation of diffusion and for DTI the more directions measured, the more accurate representation.The diffusion weighted imaging (DWI) signal is compared

to the signal in the pure T2-weighted image to calculate the apparent diffusion coefficient (ADC) map with the geometric mean of each direction at the measured b value then being divided by the b=0 or non diffusion weighted T2-weighted EPI to cancel out the T2-weighted effects.[13,15] The ADC is measured in mm^2/s. Examples of how these images appear are shown in Figure 1.8

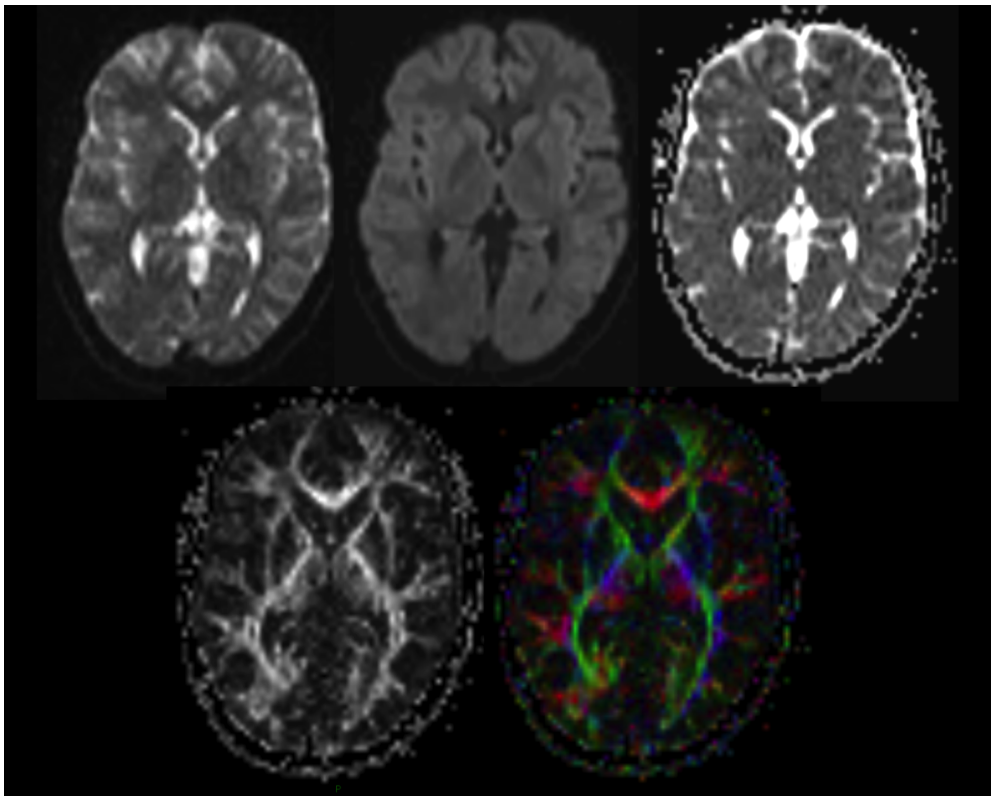

Figure 1.8: ***Diffusion MRI***. *Axial slices showing the b=0 EPI with hyperintense cerebrospinal fluid and hypointense white matter. The b=1000 image has signal drop out in areas of high diffusion so cerebrospinal fluid appears hypointense. The ADC map identifies regions with high diffusion as hyperintense. The FA maps depict the FA at each voxel. White matter can be seen prominently on these images due to the increased FA along the direction of white matter bundles. Standard colour coding for the colour FA map is shown with left-right fibres in red, craniocaudal fibres in blue and anteroposterior fibres in green. Colour intensity is proportional to the FA. (MRI: magnetic resonance imaging; ADC: apparent diffusion coefficient; FA: fractional anisotropy)*

The diffusion tensor is calculated in three dimensions. In the x, y, and z dimensions, the diffusion tensor (D) is:

$$\mathsf{D} = \begin{bmatrix} D_{xx} & D_{xy} & D_{xz} \\ D_{xy} & D_{yy} & D_{yz} \\ D_{xz} & D_{yz} & D_{zz} \end{bmatrix}$$

This can be decomposed into a set of three eigenvectors or principle directions and eigenvalues (λ_1, λ_2 and λ_3). This decomposition can occur at each voxel to give voxel-wise eigenvalues and eigenvectors.[15] The principle axis within each voxel is the eigenvector with the largest eigenvalue. Diffusion can be isotropic, of equal magnitude in all directions, or anisotropic, where diffusion occurs

more prominently in one direction. FA ranges from zero to one and is a measure of how much of the diffusion occurs along the principle axis (λ_1). This is calculated as:[14,16]

$$\text{FA} = \sqrt{\frac{1}{2}} \frac{\sqrt{(\lambda_1 - \lambda_2)^2 + (\lambda_2 - \lambda_3)^2 + (\lambda_3 - \lambda_1)^2}}{\sqrt{\lambda_1^2 + \lambda_2^2 + \lambda_3^2}}$$

Graphical examples of low and high FA and eigenvectors are shown in Figure 1.9. FA maps on axial MRI slices are shown in Figure 1.8. FA is often colour coded so that the direction of fibres can be appreciated visually as in Figure 1.8.

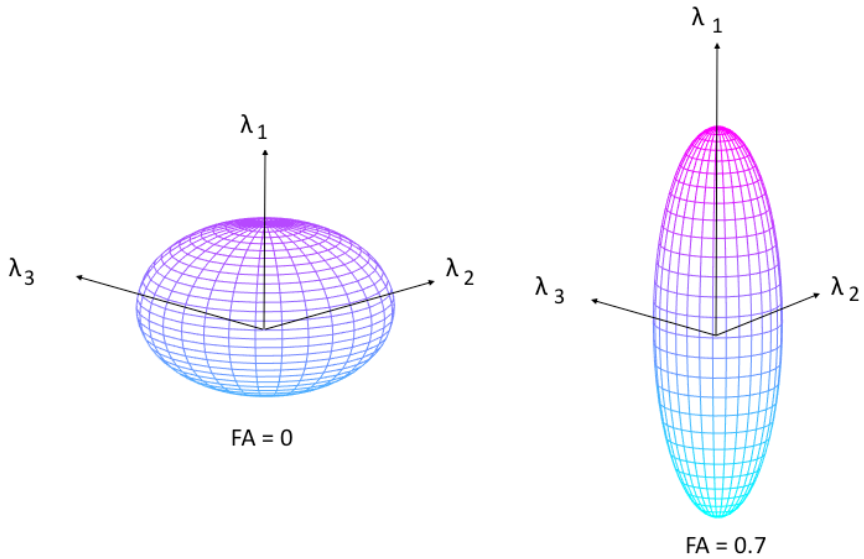

Figure 1.9: ***Diffusion tensor models***. *Isotropic diffusion on the left represented by a sphere with an equal magnitude of diffusion in all three directions* ($\lambda_1 = \lambda_2 = \lambda_3$). *Anisotropic diffusion on the right represented by an ellipse where the magnitude of* λ_1 *is greater than that of* λ_2 *or* λ_3. λ_1, λ_2, *and* λ_3 *are the eigenvalues for the three principle directions of the diffusion tensor model.*

Anisotropy has consistently been shown to be higher in white matter compared to grey matter,[15–18] and this is true of both myelinated and unmyelinated white matter fibres,[16,18] with anisotropy increasing prior to myelination during development.[19,20] Increased FA in white matter likely reflects a combination of myelination, total axonal membrane thickness, the degree of order of fibres, the density and spacing of fibres, and membrane permeability.[15] The increased FA in white matter and tendency of the principle direction to be along the white matter bundle can be used to reconstruct white matter tracts through the process of tractography. Reconstructing white matter tracts from MRI data can be performed using many different algorithms which can be broadly divided into deterministic or probabilistic methods. Deterministic streamline methods start from a seed point and trace the fibre along the principle eigenvector at each voxel until stopping criteria are achieved.[21,22] A visual representation of the principle eigenvector in each voxel is displayed in Figure 1.10. Voxels containing multiple fibres, crossing fibres, or kissing fibres or noisy MRI acquisitions may cause premature stopping of fibres, ambiguous fibre directions, or anatomically unlikely results from these techniques.[23] Probabilistic tractrography algorithms aim to overcome these disadvantages by fitting a probability distribution of

likely orientations at each voxel rather than using the principle direction of the fibre within each voxel obtained from the DTI model.[24–26] This enables white matter tract mapping based on the probability that any two locations are connected. Other technical approaches to improving the anatomical representation of tractography include data acquisition using high angular resolution diffusion imaging[27] or diffusion spectrum imaging,[28] or algorithms that use energy minimisation techniques[29,30] or shape matching techniques.[31] However, long range fibres, difficult fibre arrangements, and corticocortical fibres remain challenging to accurately depict using all diffusion techniques.[24,32] Despite this, animal models have consistently shown good accuracy of diffusion techniques in reproducing similar anatomy to post mortem tract tracing studies.[30,32–34]

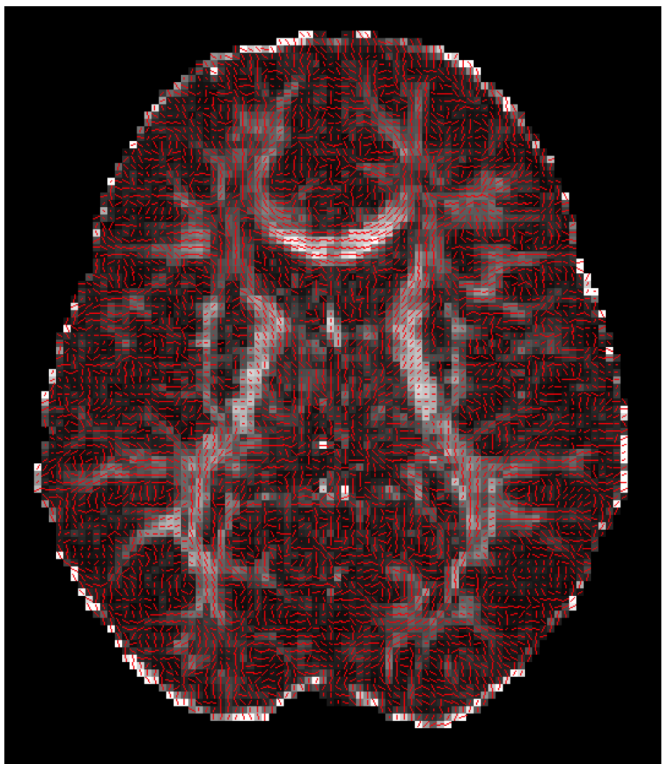

Figure 1.10: ***Voxel principle directions***. *The principle direction of the eigenvector at each voxel is displayed by a red line overlying the MRI voxel. These principle directions are used to create streamlines by following the principle directions from a particular seed point until too acute an angle or too low an FA value is reached.*

1.2.4 Investigating brain function

Knowledge regarding brain functioning and anatomical subspecialisation of human cortical regions was initially derived from lesioning studies or intra-operative functional mapping (see Figure 1.6).[8,9] Electrical patterns of brain activity can also be recorded from the surface using electrophysiological techniques such as electroencephalography (EEG), which measures changes in current passing through the substance of the brain. The EEG has a high temporal but low spatial resolution, although this can be improved by recording invasively using implantable electrodes.[35] In addition, electrical activity in specific pathways such as motor, sensory, visual, or auditory pathways can be assessed

using evoked potentials or electromyography. Functional imaging techniques such as functional Magnetic Resonance Imaging (fMRI) have also been developed to assess neurological brain function. Functional MRI detects regional changes in deoxyhaemoglobin concentration caused by upregulation of oxygen usage in metabolically active brain regions. Because deoxyhaemoglobin is paramagnetic, changes in its concentration result in changes in T2-weighted relaxation times on single shot EPI.[36] In contrast to EEG, fMRI has a low temporal but high spatial resolution.

Clinical investigation of both basic and higher brain functions has long been carried out, and assessments range from practical assessments of ability to carry out activities of daily living such as the modified Rankin Scale (mRS)[37] to measures of consciousness, such as the Glasgow Coma Scale (GCS),[38] or to detailed neuropsychological assessment of cognitive function such as with an Intelligence Quotient (IQ) test. Modern IQ tests are scored with reference to a normal population, where the median population score is mathematically adjusted to 100 points and one standard deviation is mapped to 15 points, so that anyone who takes the test and scores the same as the median score of the normal population achieves a score of 100 points.[39] IQ tests attempt to measure the general factor of cognitive ability or *g* that is believed to underly general cognitive abilities.[40]

1.2.5 Modelling brain networks

1.2.5.1 Network creation

Brain networks can be modelled on both a microscopic and macroscopic scale. The building blocks of signal processing are the neurones and synapses that create electrical circuits, and mapping each of these connections would create a vastly complex brain network model. The complete neurological system of the worm *Caenorhabditis elegans* has been completely mapped.[41] However, *C. elegans* has only 302 neurones and approximately 5000 synapses, unlike the 86 billion neurones[5] and many more synapses of the human brain. Even attempts at complete mapping of *Drosophila* neural circuits have been restricted to one particular circuit,[42] and mapping of all individual neurones of a human brain has never been achieved. Thus, brain network modelling is undertaken on a macroscopic scale using the techniques to investigate brain structure and function described above.

Networks are described as consisting of links or edges between regions, described as nodes as shown in Figure 1.11. Nodes in brain networks are usually representative of anatomical regions and are determined from anatomical MRI. Nodes may represent cortical grey matter or deep grey matter structures. The edges of brain networks may represent either structural or functional connectivity. Structural connections can be determined from white matter streamlines or tracts between nodes or through the covariance of nodes in shape, volume or thickness.[25,43] In animal studies, structural connections can also be investigated by post mortem tract tracing.[44,45] Functional connections can be determined from temporal correlations between nodes in electrophysiological measurements such as EEG data, or from either task dependent or resting state temporal correlations in fMRI data.[46] Brain networks can be constructed either from the whole brain or from a particular region or functional network of interest, for example the visual system. The description of brain elements and their connections is referred to as the connectome.[47]

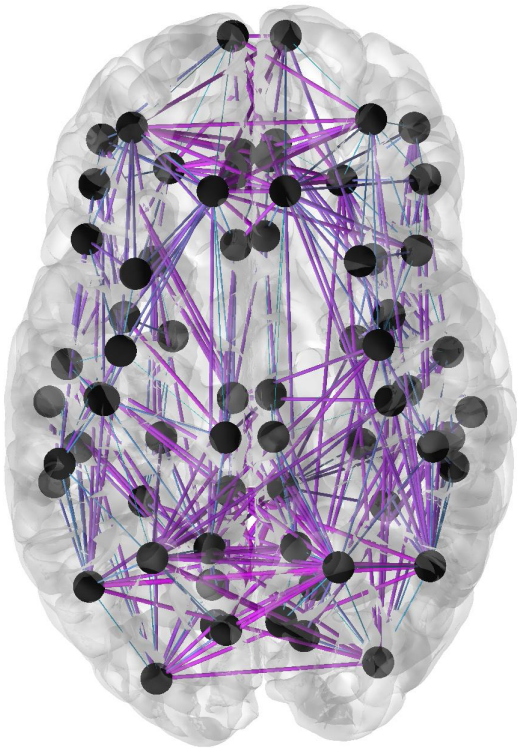

Figure 1.11: ***Brain network model***. *Modelled brain network, superior view. Black dots are network nodes and purple lines are network edges. Thickness and colour of network edges represent the strength of connection. The nodes are placed within anatomical regions.*

Macroscopic brain networks are constructed using mathematical modelling techniques that aim to represent the underlying brain structure or function. However, all techniques have limitations and at each stage of network construction, there are limitations in methods and choices of technique that can affect how closely the resulting model is able to reflect underlying brain structure.

The choice of network node can range from individual MRI voxels to large anatomical regions, and nodes may be chosen in advance based on existing anatomical theories or determined by the data used to construct edges. Different anatomical parcellation schemes will lead to different numbers of nodes. Commonly used parcellation schemes include the Desikan-Killiany atlas,[48] distributed with Freesurfer software,[49] and used in this thesis. This subdivides the cortex into 68 regions, in contrast to the automated anatomical labelling (AAL) atlas,[50] distributed with statistical parametric mapping (SPM) software,[51] which facilitates parcellation into either 90 or 124 cortical region of interests (ROIs). These two parcellation schemes are compared visually in Figure 1.12. The number of nodes and the anatomical location of nodes can affect network measures.[52–54] Larger nodes may lead to a larger numbers of edges at each node, leading to a higher network density, which will affect network measures.[52,55] Using smaller nodes, for example individual voxels, can lead to spurious results from MRI artefacts due to motion, poor signal to noise ratio or data smoothing affecting volumes larger than individual nodes.[55,56]

Network edges can be determined through either functional measures such as fMRI or EEG, or structural measures such as diffusion MRI or covariance of region volume or thickness measures.

Figure 1.12: ***Parcellation schemes***. *Parcellation schemes commonly used for brain network studies. Left: Desikan-Killiany atlas distributed with Freesurfer, with 68 cortical regions. AAL atlas distributed with SPM, with 90 cortical regions.*

Where diffusion MRI is used to establish edges, the resulting network structure is constrained by the limitations of establishing streamlines. Diffusion MRI is limited in its ability to trace long fibres, short association fibres, crossing fibres, and kissing fibres.[23,57] Network edges can be constructed from DTI data using various different techniques, including the number of streamlines, the density of streamlines, or the average FA along the streamlines, and all of these techniques will create networks with slightly different parameters.[55,58] The choice of network construction technique from DTI can affect the calculated network characteristics.[55,58] Network edges can also be constructed using the covariance of cortical volume or thickness measures.[43] Cortical networks derived from correlations in thickness measurements do not have the short and long range fibre tracking issues of DTI derived networks, and cortical thickness measurements on MRI have been shown to reflect histological post mortem cortical thickness,[59] proving that cortical thickness can be accurately measured using MRI during life. Networks obtained via cortical thickness correlations show similar patterns of connectivity to those built from DTI or tract tracing data, as well as functional brain networks.[43,60–62].

The biological basis for correlations in cortical thickness or volume measurements across individuals is proposed to be attributed to regional mutual developmental or environmental influences.[43,63–65] The thickness and arrangement of cell layers within the cortex on Nissl staining has long been associated with functional subspecialisation of cortical regions,[6] suggesting that thickness can be used a representation of differential function. Correlations in cortical thickness and volume occur across individuals within functional systems such as visual or language systems, suggesting that cortical regions involved in co-ordinating a function show variance of structural measurements within a population.[60,64–66] In addition, developmental changes in cortical thickness correlation networks have been reported.[67] Cortical development and parcellation is based on radial and tangential migration of neurones to create cytoarchitectonic areas.[2,68] Cortical thickness is dependent on the number and arrangement of neuronal and glial cells and both genetic and environmental influences on these

processes occur.[68] Development or change in the structure and thickness of cortical regions can result from reciprocal connectivity via axonal connections.[43,67] Anatomical connectivity may develop or change in response to developmental or environmental influences, and in the same way that connected regions show synchronous electrical activity, they have also been reported to show similar structure, including of thickness measurements.[60,66] This may be due to similar functional demands on regions, on similar developmental origins, which may be associated with similar neurotransmitter or chemical exposure, leading to similar structure.[64–66,66,68]

There are, therefore, a multitude of different methods of establishing network nodes and edges to model brain networks. Constructing networks using different methods of determining edges will always lead to slightly different network characteristics and slightly different models of the underlying brain network structure. In addition, all structural networks require thresholding to remove spurious connections, establish binary networks, or to fix network density across networks to facilitate network comparison.[43,54,56,69,70] Differences in techniques of network construction lead to slightly different representations of the underlying brain network. Each technique will have its own limitations and advantages in modelling brain structure. Until technology allows modelling at the individual neurone level, the limitations of techniques to model brain network structure will need to be taken into account when considering conclusions drawn from macroscopic brain structural network models. The relative advantages and disadvantages of each technique in representing brain network structure reflect that all techniques are only models of the complex connectivity within the human brain.

1.2.5.2 Brain network analysis

Brain networks can be analysed using graph theory, the branch of mathematics dedicated to describing and analysing networks. To facilitate this analysis, brain networks are depicted as adjacency matrices as in Figure 1.13. Each node (n) in the network has a column and row in the matrix and each matrix entry a_{ij} represents the edge between each node n_i and node n_j.[47,71] Graphs can be binary where edges either exist or do not exist and each entry in the matrix a_{ij} is restricted to the values zero or one, or weighted where a_{ij} may take any value from zero to the maximum weight. Analysing brain networks as adjacency matrices allows all the mathematical tools of graph theory to be applied to describe and compare the network, including straightforward measures such as node degree (the number of edges a node has), clustering coefficient (the average proportion of neighbouring nodes connected to a node), and path length (the number of edges required to be traversed to join any two nodes).[46,47,71,72] In addition, more complex network analysis developed in other fields of network science can be applied to brain networks,[71] which opens up the field of connectomics to take advantage of measures developed in other areas of informatics research. The main network measures discussed in this thesis are described briefly in Table 1.1. A detailed description of the calculation of network measures analysed in the data chapters of this thesis is in the Methods chapter in Section 3.8.2.

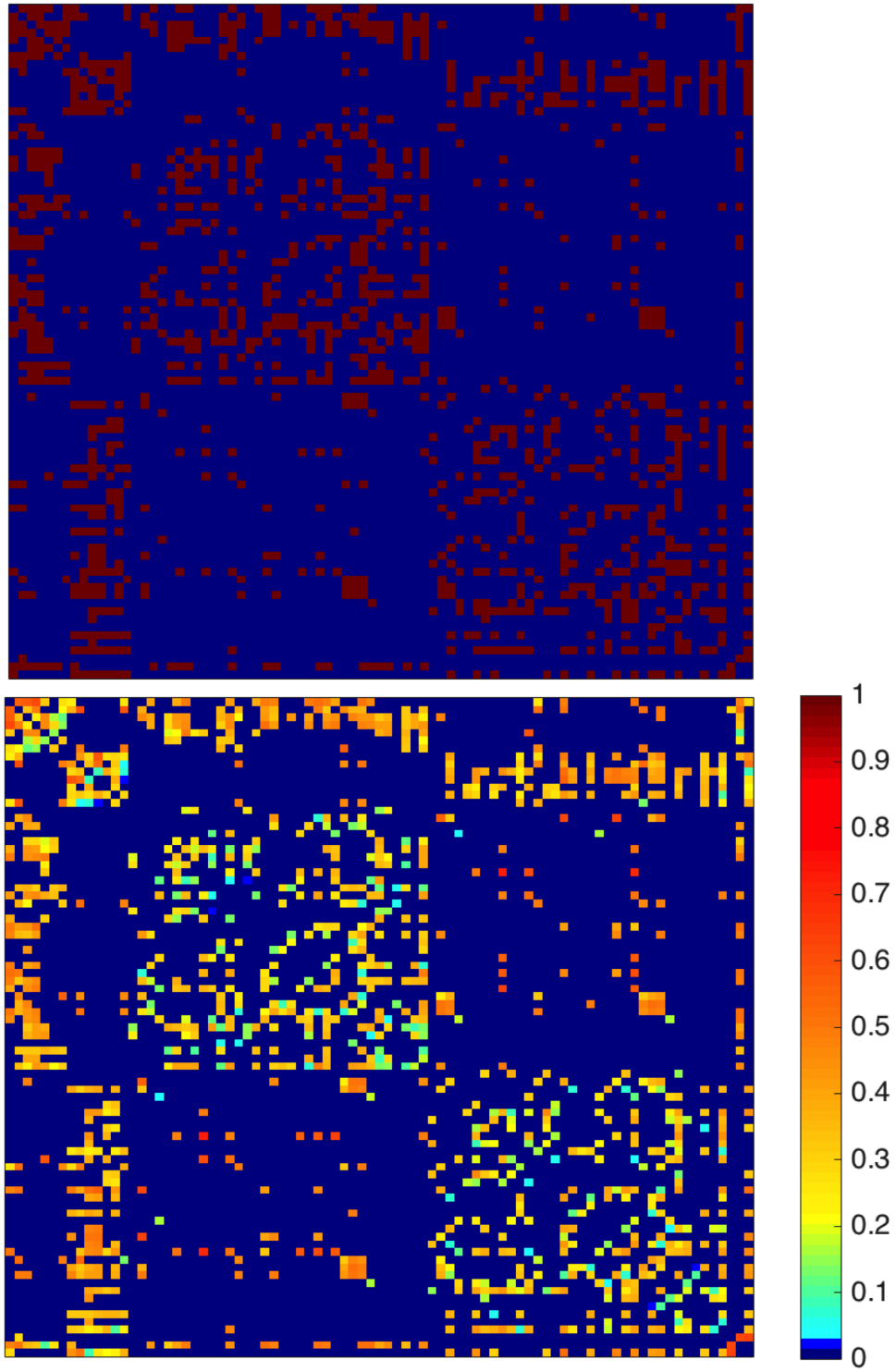

Figure 1.13: ***Brain network adjacency matrices***. *Each row and column represents a single node or anatomical region and the colour-coded entry represents the edge or connection between those two nodes. The colour bar shows the value associated with each colour. Above is a binary network where edges either exist and have a value of one (dark red) or do not exist and have a value of zero (dark blue). Below is a weighted network where existing edges can take any value depending on the network construction method. Edges that do not exist have a zero (dark blue) entry.*

Measure	Symbol	Description
Binary Measures		
network density / sparsity	D	number of edges present in network as a proportion of all possible edges
node degree	k_i	number of edges connected to the node
degree distribution	$P(k)$	degrees of all nodes in the network
shortest path	d_{ij}	minimum number of edges between two nodes
characteristic path length	L	mean shortest path length between all nodes in the network
normalised characteristic path length	λ	characteristic path length divided by characteristic path lengths calculated for random networks of the same size and density
network global efficiency	E_{glob}	mean inverse shortest path length between all nodes in the network
node clustering coefficient	t_i	the fraction of neighbours of a node also connected to each other
network clustering coefficient	C	mean clustering coefficient of all nodes in the network
normalised clustering coefficient	γ	network clustering coefficient divided by the clustering coefficients calculated for random networks of the same size and density
betweenness centrality	b_i	fraction of all shortest paths in the network that pass through the node
modularity	Q	extent to which a network may be subdivided into non-overlapping groups
rich club coefficient	ϕ_k	the proportion of edges present between nodes once all nodes of a lower degree are removed from the network
small worldness statistic	σ	normalised clustering coefficient divided by normalised characteristic path length
Weighted Measures		
node strength	S_i	sum of weights of all edges connected to the node
network strength	S	mean of all node strengths
mean edge weight	k_i^w	mean of all edges in network
shortest path length	d_{ij}^w	total sum of the inverse of edge weights between two nodes
weighted clustering coefficient	t_i^w	average geometric mean of the product of the edge weights of triangles surrounding the node
rich club coefficient	ϕ_k^w	the proportion of edges present between nodes once all nodes of a lower rank of weight are removed from the network

Table 1.1: ***Common network measures.*** *Commonly used network measures. Binary networks have edge weights of either zero or one. Weighted networks have edge weights ranging from zero to the maximum edge weight. Where weighted networks have different descriptions of network measures these are listed in the second part of the table under weighted measures. Where the description of the weighted measure is the same of the description for the binary measure, these are listed only once in the first part of the table under binary measures.*

1.2.5.3 Brain network characteristics

There are several consistent network organisational findings amongst studies of brain networks. Watts and Strogatz first described the small world organisation of the the neural network of the worm *Caenorhabditis elegans*.[72] The nomenclature of small world networks arose from the prior description of social networks in which there are only a few number of steps required to connect all people in the world with each other.[73] A small world network has high local clustering along with a few long range connections, and this leads to low average path lengths within the network.[72] Mathematically, the small worldness of the network can be calculated as the clustering coefficient divided by the path length after both have been corrected to random networks with the same degree distributions (see Table 1.1 for the description of the small worldness statistic, σ).[74,75] Human brain networks with edges derived from both functional and structural data have consistently shown a small world organisation with a small worldness statistic greater than one.[25,43,46,57,76–78] In addition, human brain networks have been described as having a few highly connected nodes or hubs which have a high degree.[70,79,80] These hubs also show a tendency to be connected to other hub nodes, forming a so called rich club.[80,81] Thus, various different methodologies have provided evidence that mapping the brain as a macroscopic network can provide insight into the underlying properties of the human brain connectome.

1.2.5.4 Association of brain network characteristics with function

The theory that a healthy structural global brain network is necessary for normal brain functioning has been developed through finding alterations in global network structure in neurological diseases such as Alzheimer's Disease,[54,78] schizophrenia,[62,82] and epilepsy.[83–85] In addition individual differences in cognitive function have been reflected in global brain network properties. An association of whole brain network properties with intelligence was initially demonstrated in functional brain networks. A shorter normalised average path length in resting-state fMRI networks was associated with a higher full scale IQ measured using the Wechsler Adult Intelligence Scales (WAIS) in a healthy group of 19 volunteers with above average IQ.[86] This negative correlation of normalised average path length with full scale IQ on the WAIS was reproduced in 30 healthy controls using whole brain resting-state fMRI networks, although the correlation was not found to be statistically significant.[87] However, an attempt to replicate this functional network association in approximately 1000 adults from the human connectome project failed to show any association between fMRI derived network measures and a measurement of intelligence taken from the weighted sum of crystallised and fluid intelligence from a cognition toolbox.[88] It is not clear whether the measures of intelligence, the different ranges of intelligence measures in the populations studied, or different pre-processing schemes for network creation and analyses have contributed to these conflicting results, or whether the smaller studies have suffered from publication bias of positive results.

The association between structural brain networks and intelligence has also been investigated in a few published studies. In 79 healthy adults, those with a WAIS full scale IQ greater than 120 points were shown to have increased global efficiency and shorter average path lengths in both binary and weighted structural networks created using DTI streamlines across multiple parcellation schemes.[89] Structural networks built from DTI streamlines have also shown an association between longer path lengths and

general cognitive ability in schizophrenics.[82] DTI network density, average path length, and global efficiency were also associated with a *g* score derived from subtests of the Wechsler Intelligence Scales for Children (WISC) in 43 eight to twelve year old high functioning children.[90] However, these findings are not consistently reported. A study investigating older community dwelling adults without known cognitive dysfunction found an association between average path length and global efficiency measured from whole brain DTI derived structural networks and IQ measured using the WAIS only in those over 75 years, but not in those aged between 60 and 75 years.[91] Another study found 32 healthy controls had an association between increased global efficiency and decreased average path length with WAIS determined full scale IQ, but that this relationship was not present in 74 schizophrenic patients with slightly lower IQ scores but DTI networks generated using exactly the same methodology.[92] The association between cortical thickness covariance networks and IQ has been investigated in one previous study which found higher global efficiency, higher modularity, and lower local efficiency with increased Performance Intelligence Quotient (PIQ) but not with increased Verbal Intelligence Quotient (VIQ) measured using the Weschler Abbreviated Scale of Intelligence in healthy children with high IQ scores.[93] These studies provide some evidence of an association between structural network average path length and global efficiency with IQ, but as with functional networks, the associations are inconsistently reported.

Potential explanations for discrepancies between studies include differences in network construction or analysis, differences in populations studied, and differences in measures of intelligence used. Graph theory measures are dependent upon data processing choices such as thresholds, parcellation schemes, network density, and whether or not the network is weighted, as well as being dependent on the quality of the underlying MRI data.[52,58,74] Different measures of intelligence may in fact be measuring slightly different constructs, and this may account for some of the different findings between studies.[94,95] In addition, different findings may reflect the different populations being studied. Many of the studies have been carried out only in highly performing individuals, and the range of network measures and the range of performance on measures of intelligence may be too small to detect any clinical or statistical difference between individuals within the study sample.[89,90,93] The finding of an association between path length and IQ only in those over 75 years but not in younger people suggests the possibility of a range within which there may not be a detectable association, but that after a certain threshold of network dysfunction, this association becomes relevant.[91] Mathematically, reduced covariance in the sample reduces measured correlation. There have not been any studies investigating IQ and average path length in poorly performing populations.

Although few studies have investigated the association between intelligence and global whole brain network measures, individual differences in intelligence have been previously associated with structural brain measures such as brain volume, regional grey matter volumes, cortical thickness, white matter FA, and axonal density.[90,94–98] Findings across specific association cortex regions and the white matter tracts linking them have led to the development of structural models of intelligence such as the parieto-frontal integration theory.[95] At the heart of models of how the brain functions to allow general cognitive ability or intelligence is the suggestion that multiple processing regions are involved and efficient integration of information between regions is essential. This theoretically fits with the findings from the small number of structural connectome studies that decreased average path lengths and

increased global efficiency in whole brain networks is associated with increased IQ. Investigating structural brain networks, which necessarily reflect individual differences in cortical region size or thickness, and the strength of connections between them due to their construction methods, may help elucidate how the organisation of brain structure facilitates effective cognitive functioning.

1.2.6 Brain networks in epilepsy

1.2.6.1 Description of epilepsy

Epilepsy is a disease of the brain defined by:

- at least two unprovoked seizures occurring more than 24 hours apart,
- or one unprovoked seizure and a probability of further seizures similar to the general recurrence risk after two unprovoked seizures,
- or the diagnosis of an epilepsy syndrome.[99]

Epilepsy is common, affecting approximately 1% of the world's population, and although the condition is usually managed with AEDs, one third of cases are medication resistant.[100] Epilepsy is increasingly viewed as a disorder of brain networks with the physiological effects of ictal seizure discharges affecting normal signal processing within the brain but also interictal widespread disruption of brain structure and function.[100–102] Therefore, epilepsy is an interesting and appropriate model in which to study disorders of brain networks.

1.2.6.2 Cognition in epilepsy

Population based studies consistently report an increased frequency of psychiatric, cognitive, and social comorbidities in people with epilepsy compared to those without.[103,104] Cognitive deficits are found in 25-40% of people with epilepsy.[104–106] Cognitive impairment in epilepsy can negatively impact quality of life, and is associated with increased healthcare needs and increased mortality.[103,104,106–109] The relationship between epilepsy and cognition is complex. Cognitive impairment in epilepsy is associated with structural brain changes,[110] an early age of onset of epilepsy,[111,112] a longer duration of epilepsy,[113] an encephalopathic aetiology,[113,114] increased seizure frequency,[108,109] lower socioeconomic status,[104] and the use of AEDs.[115] These associations suggest that structural brain changes, brain function, seizure factors, epilepsy factors, epilepsy treatments, and the genetic and environmental influences on the person can all influence cognition in those with epilepsy.

Structural brain lesions are associated with cognitive dysfunction in epilepsy.[103,110] Structural brain changes may directly result in epilepsy, for example following a traumatic brain injury.[110] Alternatively, structural brain changes may arise as a result of epilepsy. For example, the hippocampal changes that occur as a result of temporal lobe epilepsy.[110] Lesions associated with epilepsy may result in specific anatomically predictable neurological or psychological deficits, such as language and memory problems in temporal lobe epilepsy. However, those with lesional epilepsies may also show generalised cognitive dysfunction not necessarily expected from the location of the lesion,[111,113] and cognitive difficulties are

also found in those with non-lesional epilepsies.[103] Further, even those who have focal seizures clinically may have widespread structural alterations in cortical, subcortical, and white matter structures.[116–119] Therefore, structural lesions may both cause seizures and arise as a result of seizures, and may be associated with dysfunction of both specific domains of cognitive function and more generalised measures of cognition.

Seizure burden may also contribute to cognitive impairment in epilepsy. More frequent seizures, a higher number of seizures, a longer duration of epilepsy, and status epilepticus are associated with cognitive impairment.[108–110] In addition, generalised tonic clonic seizures are associated with worse cognitive function than partial seizures,[110] suggesting seizure type or extent of brain involvement may be important in contributing to cognitive dysfunction. As cognitive impairment occurs both immediately following seizures, but also in seizure free periods, and more frequently following status epilepticus, it is possible that frequent or prolonged seizures may contribute to altered brain structure or function, leading to cognitive impairment. Alternatively, cognitively impaired brains may have a tendency to more frequent or prolonged seizures. Epilepsy is more frequent amongst those with an intellectual disability than in the general population.[106] Therefore, causality in the relationship between cognitive impairment and generalised or more frequent seizures is not clear.

Some epilepsy syndromes are genetic, such as tuberous sclerosis,[110] and it is likely that cognitive impairment, structural brain abnormalities, and epilepsy all occur as a result of the genetic abnormality. However, even syndromes with genetic mutations such as tuberous sclerosis have variable clinical presentations, and some people with tuberous sclerosis will not have epilepsy or intellectual disability. This suggests that epigenetic and environmental factors must also play a role in the development of epilepsy and cognitive impairment even when there is a clear genetic influence and clear structural brain changes.

One important external influence on cognitive function in epilepsy is AED therapy. Polypharmacy with AEDs and particular AEDs such as topiramate, have been linked to cognitive impairment and deterioration in IQ scores with a dose-response effect.[110,115] However, interpreting this relationship is also not straightforward, as it is likely that higher doses of AEDs and a greater number of AEDs are used by those with uncontrolled seizures. Therefore it is not necessarily clear what effect the medication has on cognition over and above the seizures that it is treating. However, the difference in cognitive side effects reported with different AEDs, and the presence of cognitive side effects even when seizures are controlled does suggest that medication can play a role in cognitive impairment.

The association between epilepsy, seizures, cognition, and brain structure is therefore complex and multifactorial. Uncontrolled or prolonged seizures in a susceptible brain may contribute to cognitive impairment, as may the treatment for this situation with high doses or numbers of AEDs. Alternatively, underlying genetic, structural, or aetiological influences may produce brains that are more susceptible to both poor cognitive function and seizures. A better understanding of how factors such as higher socioeconomic status, higher educational attainment, fewer AEDs, and better controlled seizures protect against structural brain changes and cognitive dysfunction in epilepsy could aid with planning treatments that maximise cognitive potential in affected individuals. Cognitive impairment in epilepsy greatly impacts quality of life, healthcare service use, morbidity, and mortality, and the relationship between cognitive function and epilepsy is complex. Recognition of the importance of cognitive function

in epilepsy led to the International League Against Epilepsy (ILAE) including the following statements in their research priorities for Europe: identification of factors that lead to cognitive impairment; investigation of the relationship between disease development and cognitive and behavioural comorbidity, elucidating the role of the latter as a precursor as well as a consequence of seizure occurrence; search for metabolic, functional, or molecular biomarkers that could allow early identification of patients at risk for the development of severe cognitive impairment; and elucidation of the mechanisms responsible for AED related cognitive impairment.[120]

1.2.6.3 Epilepsy surgery

In appropriate cases surgical procedures to resect the epileptic focus or prevent the spread of seizures can greatly reduce the burden of epilepsy. Studying children undergoing epilepsy surgery provides an opportunity to study epileptic patients before and after seizure freedom or reduction is achieved through resection of the epileptogenic focus without changing the underlying aetiology and genetic background of the child. If patients become both seizure free and AED free post operatively, they provide a model for studying the association of cognition, epilepsy, and structural brain changes with the seizures and pharmacological treatments eliminated. Determining which factors lead to improved cognitive outcomes following epilepsy surgery could lead to a better understanding of why cognitive deficits occur in epilepsy as well as improving surgical selection, counselling, and outcomes.

Case series reporting seizure freedom following epilepsy surgery in childhood suggest overall rates of complete seizure freedom in 66% of temporal lobe resections, 46% of occipital and parietal resections, and 27% of frontal lobe resections.[121] However, seizure freedom alone may not predict ongoing health and social care needs. Cognitive and developmental outcomes are important determinants of the success of epilepsy surgery,[122] but current understanding of which children may show improvement post-operatively remains poor.[100] Those undergoing epilepsy surgery start with a cognitive disadvantage, with approximately 60% having a pre-operative IQ lower than 80.[111,113] A literature review of seven studies of memory and IQ outcomes in children undergoing epilepsy surgery concluded that overall no deterioration was seen in IQ in contrast to adult epilepsy surgery patients.[123] A further systematic review including only studies with more than 20 patients that used reliable change indices or standardised regression based changes to assess change in neuropsychological scores found three studies assessing IQ and reported an overall risk of IQ loss of 11% and overall probability of IQ gain of 16% in children.[124] Using slightly different inclusion criteria, sixteen studies reporting a 10 point change in either IQ or Developmental Quotient (DQ) in children after epilepsy surgery were identified in a more recent review and pooled estimates from this meta-analysis suggested that 19% of children showed improvement in IQ or DQ after surgery.[125] Aetiology, timing of surgery, contralateral MRI abnormalities, and cessation of AEDs have all been shown to predict IQ change following surgery.[125–127] Five years following temporal lobectomy in childhood, a cohort of operated children showed an increase in their IQ compared to those who had not undergone surgery, and this was associated with both a decrease in AED use and increased grey matter volumes.[122] As the follow up period, AED therapy, epileptic focus, surgical procedure, and methods of determining change in IQ have been inconsistent in existing studies, it is difficult to draw conclusions regarding cognitive outcomes of paediatric epilepsy surgery. However, there is a suggestion that IQ scores can change following epilepsy surgery in childhood, and

investigating factors that predict improvements in IQ post-operatively might aid the understanding of the underlying mechanism for how cognition is affected in epilepsy.

1.2.6.4 Network findings in epilepsy

Cognitive function in epilepsy may be influenced by the underlying cause of the epilepsy, the effect of seizures, the effect of genetic or environmental influences, the treatment of epilepsy, the effect of structural brain changes caused by any of these, or any combination of the above. Structural brain networks have been associated with cognitive function, and measures of network integration such as average path length and global efficiency are associated with scores on IQ tests or general cognitive ability as described in Section 1.2.5.4. Understanding how structural brain networks are different in epilepsy, and whether any differences are associated with cognition could help the understanding of how and why cognitive dysfunction occurs in epilepsy. An improved understanding of the structural correlates of cognition in epilepsy could aid treatment planning, and patient and carer counselling.

Networks in epilepsy have been studied both during seizures and between seizures. Ictal neurophysiological recordings have suggested that during seizures network recordings move away from a small world topology toward a more regular lattice network topology, where all nodes are connected to their neighbours,[72] and that this may be related to synchronous neuronal discharges.[102,128,129] Between seizures, functional networks derived from temporal correlations in EEG signals or fMRI task dependent or resting state data have also suggested a loss of small world characteristics with increased local clustering and increased path lengths.[101,130,131] Increased local clustering and increased path lengths in epilepsy have also been reported in structural networks derived from DTI streamlines and cortical thickness covariance networks.[83,101,132,133] Therefore, it is likely that epilepsy can cause widespread changes in global brain function and structural organisation. However, many studies have small sample sizes, use different network construction techniques, and study different sub populations of epilepsy, making it difficult to draw robust conclusions from individual studies.[100,101] Hence, a systematic review is undertaken on this topic in Chapter 2.

Within epilepsy populations, the association of network characteristics with cognition has been studied in a small number of patients. In 39 children with new onset epilepsy, the ratio of clustering coefficient to characteristic path length derived from cortical thickness networks was found to be reduced in those with lower IQ scores.[134] In a separate group of 39 adults wth focal epilepsy, cognitive impairment was associated with lower clustering coefficients and higher path lengths.[133] A small group of nine patients with cognitive impairment and frontal lobe epilepsy had a higher path length and clustering than those with epilepsy and no cognitive impairment or healthy controls, but the difference was not statistically significant.[131] In contrast, Widjaja *et al.* found no significant correlation between global network properties and IQ in 45 children with focal epilepsy.[135] All of these studies investigated children or adults with IQ scores around the population mean of 100 points rather than the poorly performing groups in whom extra-temporal epilepsy surgery in childhood is usually undertaken. In addition, sample sizes are small and findings have not been reproduced. Thus there is a need to assess whether these studies are reproducible and whether cognitive changes in children with epilepsy do have a structural correlate in graph theory measures. Further the association with cognitive outcome following epilepsy

surgery has not been studied, and this would provide the opportunity to assess whether network characteristics are correlated with cognitive performance and whether the status of pre-operative networks can predict post-operative cognitive changes. Establishing whether DTI structural and network characteristics are associated with cognition in this group of children with structural focal abnormalities could allow a better understanding of the mechanisms causing global cognitive difficulties in epilepsy. Establishing whether post operative cognitive outcome can be predicted from the DTI characteristics pre-operatively could improve surgical selection, timing, and counselling, and lead to future opportunities to modulate white matter networks to improve cognitive outcomes.

1.3 Objectives

The aim of this thesis is to investigate the association between the organisation of structural brain networks and cognitive function. This will be investigated in patients with epilepsy or suspected epilepsy who provide a population with a disorder of functional brain networks and a range of cognitive impairment. Understanding this association may provide insight into the optimum brain network structure for the performance of complex cognitive tasks. This could lead to the development and adjustment of interventions that prevent further deterioration of network structure and loss of cognitive function.

To achieve these aims, structural brain networks derived from MRI of the brain will be investigated. Networks will be modelled using anatomical regions as nodes and both DTI and cortical thickness covariance as edges. First, it will be necessary to understand whether there are differences in network structure that are associated with the presence of epilepsy or seizures. To investigate the existing evidence for this, a systematic review of the literature comparing MRI derived structural brain networks in patients with epilepsy and those without epilepsy will be carried out. This will establish whether there are changes in structural networks that should be considered that may be associated with the diagnosis of epilepsy. An increase in both measures of integration, such as average path length, and measures of segregation, such as clustering coefficients have been reported in people with epilepsy. The systematic review will aim to synthesise all studies comparing structural brain networks in epilepsy with healthy controls to determine the strength and consistency of the existing evidence base for an increase in clustering coefficients and average path lengths in epilepsy. Consistent and robust evidence for altered structural characteristics of brain networks across subjects with epilepsy would provide evidence for altered network structure being associated with the high frequency of cognitive dysfunction in epilepsy.

Secondly, a cohort of children investigated for seizures with structural anatomical MRI and DTI will be investigated. Within this cohort, the association of structural brain network characteristics with cognitive impairment will be investigated. This will test the hypothesis of whether an increased average path length in structural networks is associated with cognitive impairment in children who are investigated for seizures. This will establish whether previous studies finding increased path lengths with lower IQ scores or cognitive function are reproducible, and whether this finding also occurs in a population of children undergoing investigation for seizures. Both cortical thickness covariance networks and DTI networks will be created in this cohort to assess whether results are reproducible across different

network model construction methods. This will investigate whether network construction methods played a part in the previously reported inconsistent results of studies of the association between network average path length and cognitive function.

Finally a cohort of children with medication resistant epilepsy who have undergone resective epilepsy surgery will be investigated. The association of network structure with pre-operative cognition and post-operative change in cognition will be investigated. The hypothesis is that measures of integration, such as path length or global efficiency, which have previously been reported to be associated with cognitive function, might predict post-operative change in IQ. Children undergoing epilepsy surgery provide a well investigated cohort who have epilepsy but may potentially be rendered seizure free or have a significant reduction in seizure burden post operatively. This cohort will test the hypothesis that post-operative change in cognition might be constrained by the organisation of pre-operative structural brain networks. If structural networks require low average path lengths for improved performance on IQ tests, then those with high average path lengths pre-operatively may not show an increase in IQ post-operatively even with seizure and AED freedom. Ultimately a better understanding of whether measures of integration such as network average path length are associated with cognitive ability in epilepsy may aid in the understanding the mechanisms of how epilepsy is associated with global cognitive dysfunction.

1.4 Thesis Outline

This thesis is divided into chapters which answer the following questions.

- Do people with epilepsy have structural brain networks with higher clustering coefficients and average path lengths compared to healthy controls? This will be answered with a systematic review of the literature that includes studies that assessed whether there was a difference in brain structural network organisation between people with epilepsy and a control group. This systematic review is in Chapter 2.
- Is the average path length of structural networks associated with cognitive impairment in children with suspected epilepsy? This question will be addressed using a cohort of children investigated for seizures. Both DTI and cortical thickness covariance brain networks will be modelled. Global and hemispheric network characteristics will be assessed for an association with cognitive impairment and IQ scores. Specifically, increased average path lengths and decreased global efficiency are hypothesised to be associated with cognitive dysfunction as these represent poor network integration and efficiency. In addition, as clustering coefficients may be increased in those with epilepsy, and cognitive impairment is associated with epilepsy, an association between higher network clustering and cognitive dysfunction is hypothesised. The two types of network model construction methods will be compared with regards to structure and findings to assess whether findings are consistent across different network models. Experimental methods will be described in Chapter 3 and the results will be described in Chapter 4.
- Is structural network average path length in the healthy hemisphere associated with pre-operative IQ or post-operative change in IQ in children undergoing epilepsy surgery? This hypothesis will

be assessed in a cohort of children with medication resistant epilepsy undergoing epilepsy surgery. Pre-operative structural cortical thickness covariance networks of the hemisphere contralateral to the surgical site will be constructed for groups with and without cognitive impairment and network characteristics compared between the two groups. Then the cohort will be divided into those with an increase in IQ post-operatively and those without an increase in IQ. Structural cortical thickness covariance networks will be constructed for the two groups and the global characteristics compared. The hypothesis is that those with an efficient underlying brain structure with lower network average path lengths will show an increase in IQ following adequate treatment of epilepsy through surgery, but that those with poor underlying brain structure and longer average path lengths will not show an improvement in IQ. The methods will be described in Chapter 3 and the findings will be described in Chapter 5.

Finally, the data generated from these experiments will be discussed and compared to existing findings, and likely explanations for the findings will be reviewed in Chapter 6.

Chapter 2

Systematic Review of Whole Brain Structural Connectomes in Epilepsy

2.1 Chapter Abstract

Epilepsy is increasingly viewed as a whole brain network disorder. Epileptic discharges spread through abberant epileptic networks to manifest as seizures. Even patients with partial seizures or a structurally abnormal epileptogenic focus have widespread structural and functional abnormalities throughout the whole brain. These generalised network abnormalities may be associated with the comorbidities seen in epilepsy, such as cognitive dysfunction. A systematic literature review was performed to investigate the differences in whole brain structural connectomes derived from MRI between patients with epilepsy and healthy controls. Twenty-seven relevant studies were identified and analysed. Studies used different network construction and analysis methods. Five of nine studies investigating network average path length found an increased average path length in patients with epilepsy. Seven of ten studies investigating global efficiency found a decreased global efficiency in patients with epilepsy. None of the eight studies investigating the normalised average path length found a difference between patients with epilepsy and healthy controls. Studies using different network construction techniques had different findings in clustering coefficients between patients with epilepsy and healthy controls. Meta-analysis was not performed due to the heterogeneity in network construction methods, analysis methods, and numerical estimates of network measures. In conclusion, findings depend on the modelling techniques employed and the methods of calculating or normalising the network measures investigated, and are difficult to generalise or combine between studies.

2.2 Introduction

Epilepsy is characterised by the abnormal spread of synchronous electrical discharges through brain networks. This manifests clinically as seizures. Epilepsy can be associated with widespread abnormal brain white and grey matter structure, even when there is a clearly abnormal epileptogenic focus. For example, changes in structural white matter have been reported in the opposite hemisphere in those

with temporal lobe epilepsy.[136] In addition, localised and generalised cortical thinning and changes in DWI parameters have been reported in several studies of epileptic brains.[117,137] It may be widespread pathological epileptogenic tissue that causes or allows synchronous uncontrolled firing of neurones.[117,138] However, seizures themselves may also produce widespread brain structural changes via methods such as excitotoxicity.[117,139] This has led several groups to investigate whether there are overall structural brain organisational changes in epilepsy that may be associated with or caused by repeated epileptic discharges.

To investigate overall brain structure, the brain can be modelled on a macroscopic scale as a connectome.[47] A brain connectome or network typically consists of a number of anatomical regions as the network nodes.[47] The edges or connections can be determined using functional neurophysiological or imaging methods, or using structural measures from MRI.[46] Networks can then be mathematically analysed using graph theory.[46] Global and widespread changes in brain structure and function in epilepsy, such as cortical thinning and changes in DWI parameters[117,137] may lead to changes in network structure and function.

To determine the overall pattern of structural network changes associated with epilepsy, this review aims to systematically identify, collate, and describe studies investigating differences in structural networks between those with epilepsy and healthy controls. Assessing any changes in structural networks that are associated with a diagnosis of epilepsy will aid the understanding of how seizures can affect brain structural organisation or how brain structural organisation might facilitate seizures. Understanding any changes in brain network structure between the epileptic brain and healthy brains will lay the foundation in this thesis for the further investigation of changes in cognition in epilepsy and their association with how networks are structured and organised. To understand how brain network structure is altered with cognition within epilepsy, it is important to first understand any differences between brain network structure in epilepsy and health.

2.3 Objectives

This systematic literature review will compare structural whole brain networks derived from MRI for patients with epilepsy and healthy controls. Networks will be compared in terms of global graph theory measures, including average path lengths, clustering coefficients, small worldness, and global efficiency.

2.4 Methods

2.4.1 Search strategy

Electronic searches were carried out in MEDLINE, EMBASE, Scopus, and Web of Science Core Collection. Reference lists of included studies were hand searched to identify any potentially relevant studies. Scopus was used to identify studies that had cited the included studies and these lists were also screened for potentially relevant studies. Search strategies are shown in Tables 2.1, 2.2, 2.3, and

2.4. Searches were initially carried out in June 2015, and the review was updated in January 2017. Results presented here are from the January 2017 update.

1	(connectivity or connectome* or network* or (graph adj1 theor*)).mp.
2	exp Connectome/
3	(seizure* or epilep* or convulsion*).mp
4	exp Epilepsy/ or exp Seizure/
5	(MRI or DTI or 'magnetic resonance' or 'diffusion tensor' or (cortical adj2 thickness)).mp
6	diffusion tensor imaging/ or magnetic resonance imaging/ or diffusion magnetic resonance imaging/
7	1 or 2
8	3 or 4
9	5 or 6
10	7 and 8 and 9

Table 2.1: ***MEDLINE search strategy.*** *Search strategy used in Ovid MEDLINE 1946 to June Week 2 2015, Ovid MEDLINE(R) In-Process and Other Non-indexed Citations June 15, 2015, Ovid MEDLINE(R) Daily Update June 15, 2015, and Ovid MEDLINE(R) Epub Ahead of Print June 15, 2015. The search was updated on 16th January 2017 in Epub Ahead of Print, In-Process and Other Non-Indexed Citations, Ovid MEDLINE(R) Daily and Ovid MEDLINE(R) 1946 to Present (December Week 2016).*

1	(connectivity or connectome* or network* or (graph adj1 theor*)).mp
2	exp connectome/
3	(seizure* or epilep* or convulsion*).mp
4	exp "seizure, epilepsy and convulsion"/
5	(MRI or DTI or 'magnetic resonance imaging' or 'diffusion tensor imaging' or (cortical adj2 thickness)).mp
6	nuclear magnetic resonance imaging/ or diffusion tensor imaging/ or diffusion weighted imaging/
7	1 or 2
8	3 or 4
9	5 or 6
10	7 and 8 and 9

Table 2.2: ***EMBASE search strategy.*** *Search strategy used in Ovid EMBASE 1974 to 2015 June 15. Updated on Monday 16th January 2017 in Ovid EMBASE 1980 to 2017 Week 3.*

TITLE-ABS-KEY(connectivity OR connectome OR network OR (graph W/1 theor*))
AND
TITLE-ABS-KEY(seizure OR epilep* OR convulsion)
AND
TITLE-ABS-KEY(mri OR dti OR ”magnetic resonance” OR ”diffusion tensor”
OR (cortical W/2 thickness))

Table 2.3: ***Scopus search strategy.*** *Search strategy used in Ovid Scopus on 16th June 2015. This search was repeated on 16th January 2017.*

TOPIC:(connectivity OR connectome OR network OR (graph NEAR/1 theor*))
AND
TOPIC:(seizure OR epilep* OR convulsion)
AND
TOPIC:(mri OR dti OR ”magnetic resonance” OR ”diffusion tensor”
OR (cortical NEAR/2 thickness))

Table 2.4: ***Web of Science search strategy.*** *Search strategy used in Web of Science Core Collection on 17th June 2015. This search was repeated on 16th January 2017.*

2.4.2 Inclusion criteria

Studies were included if they assessed whole brain structural networks constructed from MRI in patients with epilepsy. Studies had to have a healthy control group without epilepsy for comparison. Studies comparing subgroups of epilepsy patients were not included if they did not have a healthy control group for comparison. Networks had to be assessed using graph theory techniques. Studies assessing functional brain networks constructed from fMRI, EEG, or other functional techniques were excluded. Studies that assessed specific pathways or limited anatomical regions rather than whole brain or hemispheric networks were also excluded. Studies that did not perform any quantitative analysis of networks were also excluded. Studies investigating machine learning techniques to correctly classify epilepsy and healthy controls using network characteristics were included when they described the differences in network characteristics between the group with epilepsy and the healthy controls. There were no restrictions on language or age of participants.

2.4.3 Outcome measures

Graph theoretical metrics were compared between those with epilepsy and those without epilepsy. Specifically, the following metrics were extracted and compared between groups:

- average path length (L)
- normalised average path length (λ)

- clustering coefficient (C)
- normalised clustering coefficient (γ)
- global efficiency (E_{Glob})
- small worldness (σ)

Other generalised network measures such as modularity, degree distribution, and vulnerability to network attack are also described where these were assessed by studies. The efficacy of machine learning techniques to distinguish between structural networks of those with and without epilepsy is described. Localised network features such as differences in specific hub nodes, specific network edges identified by network based statistics techniques, and local node efficiencies are not described as this review concentrates on global whole brain or hemispheric measures. Association of network measures with clinical epilepsy characteristics or cognition is described where this is included in studies.

2.4.4 Data collection

Two people independently screened all titles and abstracts identified by the search to identify those that were potentially relevant. The full text was sourced and reviewed independently by two people for all abstracts identified as potentially relevant. When there was disagreement about the abstracts, the full text was sourced. When there was disagreement about the full text, this was resolved by consensus. Data was extracted from all included studies. Where numbers were not printed in the text or tables, these were read from graphs by adjusting the paper on screen to a suitable scale and calculating the plotted values. Supplementary material was checked for further information. When values were given for left and right epilepsy groups, or frontal and temporal epilepsy groups, these were averaged to give a single epilepsy group for comparison taking into account the number of people per hemisphere or anatomical region. This was performed so that controls were only entered once even if they were used as controls for more than one epilepsy group. When subgroups of epilepsy included patients with epilepsy and patients with epilepsy plus a comorbidity (e.g. cognitive difficulties, anxiety), the group with just epilepsy without the comorbidity was taken as the epilepsy group to ensure all differences seen were attributable to epilepsy rather than the comorbidity. When values for network analyses were stated over a range of thresholds the value as close as possible to a density of 0.2 was used in the tables to ensure consistent comparisons of networks at a fixed density.

2.4.5 Quality assessment

Studies were assessed for quality and risk of bias using the Quality Assessment of Diagnostic Accuracy Studies - 2 (QUADAS-2) tool.[140] This was applied as though the network analysis was the index test, and the diagnosis of epilepsy was the reference standard.

2.4.6 Data analysis

For each network measure, the findings from each study are combined in tables. No meta-analysis was performed due to the heterogeneity in patient groups and network construction and analysis methods. A descriptive narrative of the findings was undertaken.

2.4.7 Data reporting

This systematic review follows the structure recommended in the Preferred Reporting Items for Systematic Reviews and Meta-Analyses (PRISMA) guidelines.[141]

2.5 Results

2.5.1 Results of the search

Literature searching identified a total of 2897 studies after removal of duplicates. Of these 79 abstracts were potentially relevant and these were selected for full text review. Following full text review 27 studies were included in the final analysis. No further studies were identified by checking reference lists of included studies or studies citing included studies. The PRISMA[141] flow diagram in Figure 2.1 shows the study identification and selection process with reasons for abstract exclusion. When more than one reference referred to the same study population, these were combined and analysed as a single study.

2.5.2 Description of studies

2.5.2.1 Populations studied

The populations studied are described in Table 2.5. The majority of studies (17/27) were undertaken in patients with temporal lobe epilepsy (TLE). However, there were also two studies of childhood absence epilepsy (CAE),[142,143] one of juvenile myoclonic epilepsy (JME),[144] two including frontal lobe epilepsy (FLE),[131,133] two including patients with generalised tonic clonic seizures (GTCS)[145,146] and two including patients with idiopathic epilepsies.[145,147] Six studies included children[131,134,135,142,147,148] and the rest were performed in adults.

2.5.2.2 Network construction techniques

Structural networks were constructed from MRI using a range of different techniques. Details of network construction techiques are in Table 2.6. Studies used between 52 and 1024 nodes in network construction. The main anatomical atlases used to determine node anatomical regions were atlases distributed with Freesurfer[48,49] or the AAL atlas.[50,51] Twenty studies used diffusion MRI to determine edges between nodes, and the remainder used covariance of anatomical regions in terms of either thickness or volumes. With edges constructed from region covariance, edge weights were determined

by either raw correlation values or *p* values. Binary covariance networks were constructed using a correlation threshold, a *p* value threshold, or thresholding to an absolute or a relative density. Diffusion imaging edge weights were determined through the number of streamlines, corrected for volume region or surface area, or using the FA along the streamlines. Networks were analysed across a full range of network densities, although networks tended to have densities lower than 0.5. Studies analysing covariance networks all constructed group level networks. Diffusion MRI networks tended to be constructed on an individual level, but many were analysed as group level averaged networks.

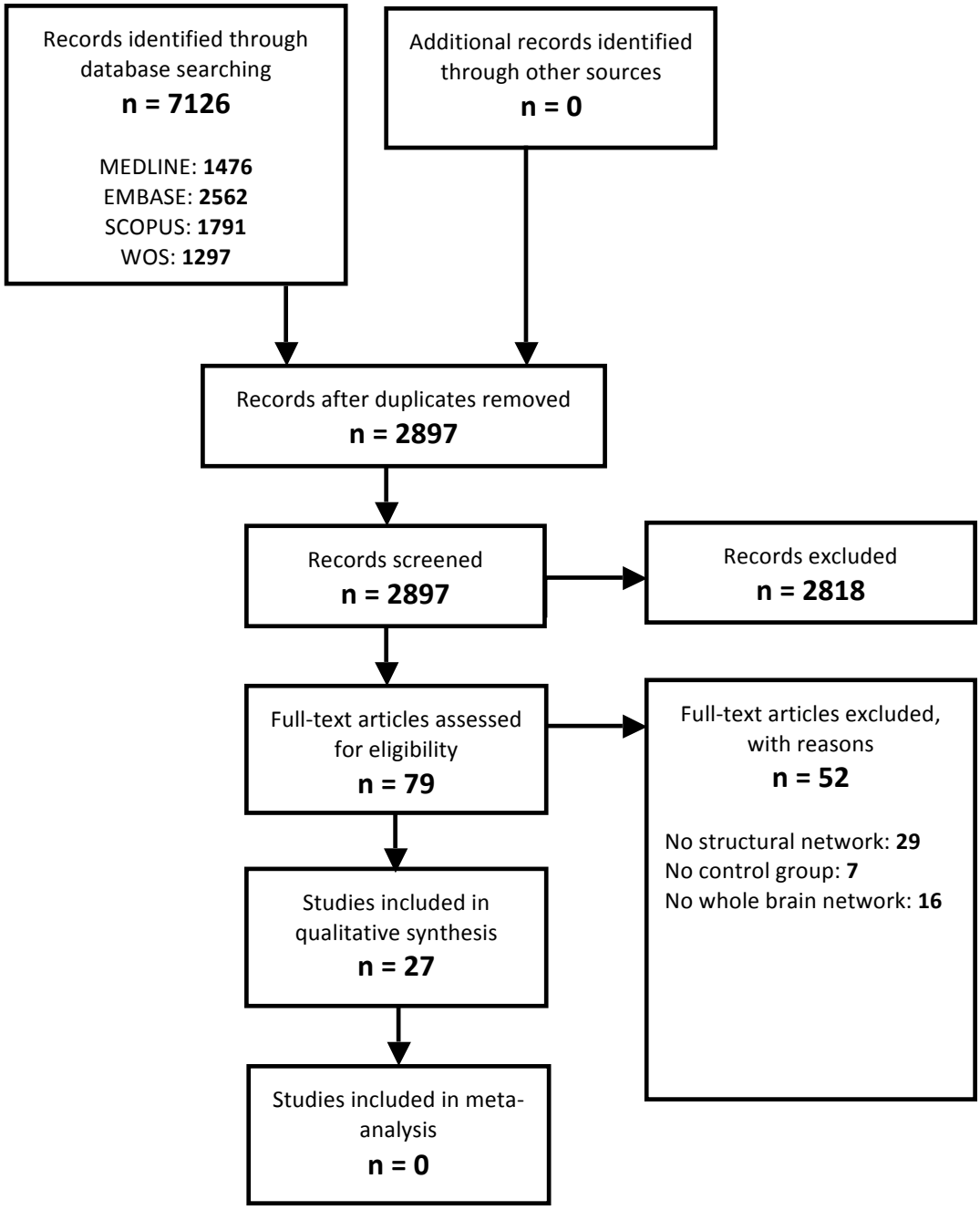

Figure 2.1: ***PRISMA flow diagram.*** *Number of studies identified and reasons for exclusions at each stage of the review process.*

Study	Type of Epilepsy	No. Patients	Age (yrs) mean±SD median (range)	Male No (%)	No. Controls	Age (yrs) mean±SD median (range)	Male No (%)
Raj 2010	TLE	27	39 ± 8	10 (37)	30	39 ± 10	10 (33)
Bernhardt 2011	TLE	122	36 ± 10	52 (43)	47	36 ± 10	23 (49)
Zhang 2011	IGE with GTCS	26	24 ± 7		26	24 ± 7	
Vaessen 2012	TLE or FLE	32	41 ± 13	15 (47)	23	41 ± 13	9 (39)
Liao 2013	GTCS	59	25 ± 7	38 (64)	59	25 ± 7	37 (63)
Besseling 2014	Rolandic	22	11 ± 2	14 (64)	22	11 ± 2	11 (50)
Besson 2014	TLE	39	40 ± 10	18 (46)	28	40 ± 10	13 (46)
Bonilha 2014	All	39	13 ± 3	14 (36)	28	13 ± 3	11 (39)
DeSalvo 2014	Left TLE	24	33 ± 17	10 (42)	24	33 ± 17	9 (38)
Lemkaddem 2014	TLE	22	34 ± 10	9 (41)	21	34 ± 10	13 (62)
Liu 2014	Left TLE	16	38 ± 13	8 (50)	21	38 ± 13	
Vaessen 2014	FLE	26	11 (8-13)		36	11 (8-13)	
Xu 2014	Left TLE	14	24	10 (71)	22	24	13 (59)
Xue 2014	CAE	17	9 ± 2	10 (59)	18	9 ± 2	10 (56)
Caeyenberghs 2015	JME	35	27 ± 8	10 (29)	35	27 ± 8	10 (29)
Chiang 2015	TLE	24	38 ± 13	8 (33)	11	38 ± 13	6 (55)
Curwood 2015	CAE	30	21 ± 2	15 (50)	56	21 ± 2	23 (41)
Douw 2015	TLE	49	37 ± 13	23 (47)	23	37 ± 13	7 (30)
Fang 2015	TLE	43	27 ± 8	25 (76)	39	27 ± 8	22 (56)
Munsell 2015	TLE	70	40 (16-68)	27 (38)	48	40 (16-68)	26 (54)
Widjaja 2015	Focal	45	14 ± 3		28	14 ± 3	
Yasuda 2015	TLE	156	48 ± 11	60 (39)	116	48 ± 11	39 (34)
Garcia-Ramos 2016	IGE+ILRE	62	13 ± 3	33 (53)	48	13 ± 3	21 (46)
Kamiya 2016	TLE	44	33 ± 12	21 (48)	14	31 ± 8	6 (43)
Li 2016	GTCS	50	26 ± 8	31 (62)	60	26 ± 8	32 (53)
Sone 2016	TLE	15	49 ± 10	8 (53)	14	50 ± 9	7 (50)
Wirsich 2016	Right TLE	7	33 ± 10	4 (57)	13	32 (20-59)	7 (54)

Table 2.5: ***Populations studied*** *Clinical and demographic features of populations studied. Age is mean with SD or median with range, in years. Blank cells represent data not available from the papers. Data are rounded to zero decimal places, and are calculated from values given in the paper or supplementary material when required. (SD: standard deviation; TLE: temporal lobe epilepsy (both right and left onset included unless stated); GTCS: generalised tonic clonic seizures; FLE: frontal lobe epilepsy; JME: juvenile myoclonic epilepsy; CAE: childhood absence epilepsy; IGE: idiopathic generalised epilepsy; ILRE: idiopathic localisation related epilepsy)*

Study	Field Strength	Parcellation Scheme	No. Nodes	Edge Type	Edge Construction	Density	Threshold	Weighted or Binary	Individual or Group	Corrections
Raj 2010	4T	Freesurfer DK	72	Thick Vol Curv	Gibbs Model	0.15		Both	Group	sex
Bernhardt 2011	1.5T	AAL	52	Cort.Thick.	Corr.	0.05-0.4		Binary	Group	age sex mean Cort.Thick.
Zhang 2011	3T	AAL	90 1024	DTI	NOS, StrD FA, FAxNOS	0.18	> 1 SL	Weighted	Individual	
Vaessen 2012	3T	AAL	90	DTI	SL Vol/TIV		SL in all subjects	Both	Individual	
Liao 2013	3T	AAL	90 1024	GM Vol	partial Corr.	0.14-0.3	cost function	Weighted	Group	age, sex TIV
Besseling 2014		Probabilistic anatomical landmark	137	DTI	NOS/ROI Vol.	0.01-0.75		Weighted	Individual	
Besson 2014	3T	Freesurfer Destrieux	164	DTI	Ave FA		$> 75\%$ subjects	Weighted	Individual	age age at onset
Bonilha 2014	1.5T	Freesurfer Destrieux	171	Vol.	Corr.	0.15-0.5		Binary	Group	TIV
DeSalvo 2014	3T	Freesurfer DK	1015	DTI	StrD		2-50cm	Weighted	Individual	

Study	Field Strength	Parcellation Scheme	No. Nodes	Edge Type	Edge Construction	Density	Threshold	Weighted or Binary	Individual or Group	Corrections
Lemkaddem 2014	3T	Freesurfer	84	DTI	GFA ICVF ODI			Weighted	Individual	
Liu 2014	1.5T	AAL	78	DTI	NOSxFA ROI Vol.		>3 SL	Weighted	Individual	
Vaessen 2014	3T	Freesurfer	205	DTI	SL Vol. TIV		>2 SL	Weighted	Individual	
Xu 2014	1.5T	AAL	90 1024	DTI	FAxNOS NOS, FA		>3 SL	Weighted	Individual	
Xue 2014	3T	AAL	90	DTI	NOS max NOS		max spanning tree	Weighted	Individual	
Caeyenberghs 2015	3T	AAL	116	DTI	NOS			Binary	Individual	
Chiang 2015	3T	AAL	90	DTI	StrD		>3 SL	Weighted	Individual	
Curwood 2015	1.5T	Freesurfer	915	Cort.Thick.	Corr.	0-1	$p<0.05$	Weighted	Group	age sex TIV
Douw 2015	3T	Freesurfer Lausanne	1000	DTI	NOSxROI SA			Weighted	Individual	
Fang 2015	1.5T	AAL	116	DTI	NOS/ROI Vol.			Weighted	Individual	
Munsell 2015	3T	Freesurfer Lausanne	82	DTI	NOS			Weighted	Individual	
Widjaja 2015	3T	AAL	82	DTI	NOS/ROI Vol.			Weighted	Individual	

Study	Field Strength	Parcellation Scheme	No. Nodes	Edge Type	Edge Construction	Density	Threshold	Weighted or Binary	Individual or Group	Corrections
Yasuda 2015	3T	Freesurfer DK	80	GM Vol.	Corr.	0.05-0.4	$p < 0.05$	Binary	Group	age gender GM Vol
Garcia-Ramos 2016	1.5T	Freesurfer DK	85	Cort Vol.	Corr.	0.05-0.4		Weighted	Group	ICV
Kamiya 2016	3T	Freesurfer DK	83	DTI	NOS			Weighted	Individual	
Li 2016	3T	AAL	90	DTI	StrD, NOS	0.23		Weighted	Individual	
Sone 2016	3T	AAL	90	Vol.	Corr.	0.1-0.5	$p < 0.05$	Binary	Group	age gender
Wirsich 2016	3T	AAL	512	DTI	NOS	0.44-0.46	$> 1SL$	Weighted	Individual	

Table 2.6: ***Network construction methods*** *Methods used to construct networks from structural MRI data. (T: Tesla; DK: Freesurfer Desikan-Killiany atlas; Thick.: thickness; Vol.: volume; Curv.: curvature; AAL: automated anatomical labelling atlas; DTI: diffusion tensor imaging; Cort.Thick.: cortical thickness; Corr.: correlations; NOS: number of streamlines; StrD: streamline density; FA: fractional anisotropy; TIV: total intracranial volume; SL: streamlines; ROI: region of interest; GM: grey matter; GFA: generalised fractional anisotropy; ICVF: intracellular volume fraction; ODI: orientation dispersion index; SA: surface area)*

2.5.2.3 Network analysis techniques

The global network parameters examined in each study are shown in Table 2.7. A range of analysis techniques were investigated by different studies, although most used some form of measurement of integration, for example path length, and segregation, for example clustering coefficient.

Study	L	λ	C	γ	σ	E_{Glob}	S	hubs	k	BC	Q	SF coupling	machine learning	other
Raj 2010	✘	✘	✔	✘	✘	✘	✔	✔	✔	✔	✔	✔	✔	
Bernhardt 2011	✔	✔	✔	✔	✔	✘	✘	✔	✔	✘	✘	✘	✘	resilience
Zhang 2011	✘	✔	✘	✔	✔	✘	✔	✔	✘	✘	✘	✔	✘	
Vaessen 2012	✔	✘	✔	✘	✘	✘	✘	✘	✘	✘	✘	✘	✘	density EW
Liao 2013	✘	✔	✔	✔	✔	✘	✔	✘	✔	✘	✘	✘	✘	
Besseling 2014	✘	✔	✘	✔	✘	✘	✘	✘	✘	✘	✔	✘	✘	
Besson 2014	✘	✘	✘	✘	✘	✘	✘	✘	✔	✔	✘	✘	✘	
Bonilha 2014	✘	✘	✔	✘	✘	✔	✘	✘	✔	✔	✘	✘	✘	resilience
DeSalvo 2014	✘	✘	✘	✘	✘	✔	✘	✘	✘	✘	✔	✘	✘	
Lemkaddem 2014	✘	✘	✔	✘	✘	✔	✔	✔	✘	✘	✘	✘		
Liu 2014	✔	✔	✔	✔	✔	✔	✔	✔	✔	✔	✘	✘	✘	
Vaessen 2014	✔	✘	✔	✘	✘	✘	✘	✘	✘	✘	✔	✔	✘	
Xu 2014	✔	✔	✔	✔	✔	✔	✘	✔	✔	✔	✘	✘	✘	resilience
Xue 2014	✔	✔	✔	✔	✔	✔	✔	✘	✘	✘	✘	✘	✘	
Caeyenberghs 2015	✘	✔	✘	✔	✔	✘	✘	✔	✘	✔	✘	✘	✘	
Chiang 2015	✘	✘	✘	✘	✘	✘	✘	✘	✘	✘	✘	✔	✘	
Curwood 2015	✘	✘	✔	✘	✔	✘	✔	✘	✔	✘	✘	✘	✘	
Douw 2015	✘	✘	✘	✘	✘	✘	✘	✔	✘	✘	✔	✔	✘	
Fang 2015	✘	✘	✘	✘	✘	✘	✘	✘	✘	✘	✘	✘	✔	
Munsell 2015	✘	✘	✘	✘	✘	✘	✘	✘	✘	✘	✘	✘	✔	
Widjaja 2015	✔	✘	✔	✘	✔	✔	✔	✘	✘	✘	✘	✘	✘	
Yasuda 2015	✘	✘	✔	✘	✘	✔	✘	✔	✘	✔	✘	✘	✘	
Garcia-Ramos 2016	✘	✘	✘	✘	✘	✘	✘	✘	✘	✘	✔	✘	✘	transitivity
Kamiya 2016	✘	✘	✘	✘	✘	✘	✘	✘	✘	✔	✘	✘	✔	
Li 2016	✘	✘	✔	✘	✘	✔	✔	✔	✘	✘	✘	✔	✘	rich club
Sone 2016	✔	✘	✔	✘	✔	✔	✘	✔	✘	✔	✔	✘	✘	transitivity
Wirsich 2016	✔	✘	✘	✘	✘	✘	✘	✔	✘	✘	✘	✔	✘	transitivity rich club

Table 2.7: ***Network analyses*** *Calculated network characteristics examined by studies. (L: average path length; λ: normalised average path length; C: clustering coefficient; γ: normalised clustering coefficient; σ: small worldness; E_{Glob}: global efficiency; S: mean network strength; k: degree distribution or mean average degree; BC: betweenness centrality; Q: modularity; SF coupling: structural functional coupling; EW: edge weight)*

2.5.3 Comparison between epilepsy and healthy controls

2.5.3.1 Average path length and global efficiency

Thirteen studies investigated the network average path length or the normalised average path length.[83,131,133,135,142,144,145,148–153] Results available from these studies are summarised in Tables 2.8 and 2.9. Five of nine studies found an increased average path length in patients with epilepsy compared to healthy controls and four of nine studies found no difference in average path length. None of the eight studies investigating normalised average path length (λ) found any difference between patients with epilepsy and healthy controls. No studies found a decreased path length or average path length in epilepsy. Two studies did not test for a statistically significant difference, but presented numerical results. Due to the wide range of network construction techniques and the wide range in values, meta-analysis was not undertaken.

Path Length (L)			
	mean(SD)		
Study	Epilepsy	Controls	Findings
Bernhardt 2011	1.98	1.95	$\leftrightarrow$
Vaessen 2012	63.3 (9.6)	60.9 (10)	$\uparrow$
Liu 2014	1.06 (0.4)	0.97 (0.2)	$\uparrow$
Vaessen 2014	0.33 (0.006)	0.33 (0.005)	$\leftrightarrow$
Xu 2014	2.15 (0.22)	1.93 (0.16)	$\uparrow$
Xue 2014	30 (7.8)	22 (4.0)	$\uparrow$
Widjaja 2015	33.4 (1.4)	32.1 (1.1)	$\uparrow$
Sone 2016	2	2.05	$\leftrightarrow$
Wirsich 2016	40.0	43.0	$\leftrightarrow$

Table 2.8: ***Average path length in epilepsy and healthy controls.*** *Group mean and standard deviation read from paper or from graph, or calculated from values given in tables or graphs. Measurement for density closest to 0.2 taken where measurements for a range of densities were stated in the paper. Where group values are given without standard deviations, standard deviations are missing. (SD: standard deviation, ?: no statistical testing performed by authors, $\uparrow$: metric is higher in epilepsy, $\downarrow$: metric is lower in epilepsy, $\leftrightarrow$: no difference between epilepsy and healthy controls)*

The global efficiency (E_{Glob}) is the inverse of the average path length. This was investigated by 10 studies,[134,135,142,150–152,154–157] of which seven found a decreased global network efficiency in patients with epilepsy compared to healthy controls. Two studies found no difference in global efficiency between epilepsy and healthy controls, and one study found an increase in global efficiency in epilepsy compared to healthy controls. Study findings are shown in Table 2.10

There was no difference in findings of global efficiency and path lengths between studies using volume or covariance networks versus DTI networks, or across studies with large or smaller numbers of study participants. There were no differences in the normalised average path length, despite studies showing differences in the average path length between epilepsy and healthy controls. This suggests that the difference in path length may be accounted for by differences in the number or strength of edges

between the epilepsy and healthy control groups.

Normalised Path Length (λ)			
	mean(SD)		
Study	Epilepsy	Controls	Findings
Bernhardt 2011	1.04	1.03	$\leftrightarrow$
Zhang 2011	1.15 (0.005)	1.15 (0.005)	$\leftrightarrow$
Liao 2013			$\leftrightarrow$
Besseling 2014	1.97 (0.05)	1.96 (0.05)	$\leftrightarrow$
Liu 2014	1.19 (0.2)	1.18 (0.2)	?
Xu 2014	4.39 (0.35)	4.01 (0.42)	?
Xue 2014			$\leftrightarrow$
Caeyenberghs 2015	1.03 (0.04)	1.03 (0.05)	$\leftrightarrow$

Table 2.9: ***Normalised average path length in epilepsy and healthy controls.*** *Group mean and standard deviation read from paper or from graph, or calculated from values given in tables or graphs. Measurement for density closest to 0.2 were taken for inclusion where measurements for a range of densities were stated in the paper. Where group values are given without standard deviations, standard deviations are missing. Where findings are given without numerical values, these were not given in the paper. (SD: standard deviation, ?: no statistical testing performed by authors, $\uparrow$: metric is higher in epilepsy, $\downarrow$: metric is lower in epilepsy, $\leftrightarrow$: no difference between epilepsy and healthy controls)*

Global Efficiency (E_{Glob})			
	mean(SD)		
Study	Epilepsy	Controls	Findings
Bonilha 2014	0.52	053	$\downarrow$
DeSalvo 2014			$\uparrow$
Lemkaddem 2014	0.15 (0.007)	0.16 (0.004)	$\downarrow$
Liu 2014	0.95 (0.36)	1.03 (0.28)	$\downarrow$
Xu 2014	0.47 (0.05)	0.52 (0.04)	$\downarrow$
Xue 2014	0.033 (0.006)	0.044 (0.010)	$\downarrow$
Widjaja 2015	0.041 (0.001)	0.042 (0.001)	$\downarrow$
Yasuda 2015			$\downarrow$
Li 2016		$\leftrightarrow$	
Sone 2016	0.55	0.55	$\leftrightarrow$

Table 2.10: ***Global efficiency in epilepsy and healthy controls.*** *Group mean and standard deviation read from paper or from graph, or calculated from values given in tables or graphs. Measurement for density closest to 0.2 taken for inclusion where measurements for a range of densities were stated in the paper. Where group values are given without standard deviations, standard deviations are missing. Where findings are given without numerical values, these were not given in the paper. (SD: standard deviation, ?: no statistical testing performed by authors, $\uparrow$: metric is higher in epilepsy, $\downarrow$: metric is lower in epilepsy, $\leftrightarrow$: no difference between epilepsy and healthy controls)*

2.5.3.2 Clustering coefficient

Nineteen studies investigated differences in network average clustering coefficient between patients with epilepsy and healthy controls.[83,85,131,133–135,142–146,148–152,155,156,158] Studies that only investigated nodal clustering coefficients and did not investigate the network average clustering coefficient are not included. Study findings are displayed in Tables 2.11 and 2.12. Five of the 15 studies investigating average clustering coefficients found an increased clustering coefficient in epilepsy compared to healthy controls, seven studies found no difference, and three studies found a decreased average clustering coefficient in epilepsy compared to healthy controls. Of the nine studies reporting the normalised average clustering coefficient, six studies found no difference between patients with epilepsy and healthy controls, one study found a decreased normalised average clustering coefficient in patients with epilepsy and two studies did not test for an association. Meta-analysis was not undertaken due to the wide ranging methodologies and resulting values.

Clustering Coefficient (C)			
	mean(SD)		
Study	Epilepsy	Controls	Findings
Raj 2010			↔
Bernhardt 2011	0.38	0.33	↑
Vaessen 2012	0.018 (0.003)	0.018 (0.003)	↓
Liao 2013	0.158	0.126	↑
Bonilha 2014	0.53	0.50	↑
Lemkaddem 2014	0.138 (0.005)	0.147 (0.004)	↓
Liu 2014	0.38 (0.08)	0.38 (0.05)	↔
Vaessen 2014	1.9 (0.09)	1.92 (0.07)	↔
Xu 2014	0.33 (0.02)	0.34 (0.02)	↔
Xue 2014	0.013 (0.003)	0.016 (0.004)	↓
Curwood 2015	0.13	0.125	↑
Widjaja 2015	0.004 (0.0005)	0.004 (0.0004)	↔
Yasuda 2015			↑
Li 2016			↔
Sone 2016	0.50	0.54	↔

Table 2.11: ***Clustering coefficient in epilepsy and healthy controls.*** *Group mean and standard deviation read from paper or from graph, or calculated from values given in tables or graphs. Measurement for density closest to 0.2 were taken for inclusion where measurements for a range of densities were stated in the paper. Where group values or standard deviations are missing these could not be found in the papers. (SD: standard deviation, ?: no statistical testing performed by authors, ↑: metric is higher in epilepsy, ↓: metric is lower in epilepsy, ↔: no difference between epilepsy and healthy controls)*

Only one study found a difference in the normalised clustering coefficient between epilepsy and healthy controls, which may suggest that any group differences are due to different numbers or strengths of network edges. Studies which found an increased clustering coefficient in epilepsy all used covariance methods to construct networks, whilst studies which found a decreased clustering coefficient in epilepsy

all used diffusion MRI methods to construct networks, so the different construction methods may account for the different findings. All covariance network studies found an increase in clustering coefficient except one study. However, several DTI network studies found no difference in clustering coefficient.

Normalised Clustering Coefficient (γ)			
	mean(SD)		
Study	Epilepsy	Controls	Findings
Bernhardt 2011	1.85	1.86	$\leftrightarrow$
Zhang 2011	2.52 (0.11)	2.60 (0.05)	$\downarrow$
Liao 2013			$\leftrightarrow$
Besseling 2014	3.35 (0.11)	3.35 (0.11)	$\leftrightarrow$
Liu 2014	2.81 (1.16)	2.52 (0.69)	?
Vaessen 2014	1.9 (0.09)	1.92 (0.07)	$\leftrightarrow$
Xu 2014	4.39 (0.35)	4.01 (0.42)	?
Xue 2014			$\leftrightarrow$
Caeyenburghs 2015	3.72 (0.38)	3.86 (0.60)	$\leftrightarrow$

Table 2.12: ***Normalised clustering coefficient in epilepsy and healthy controls.*** *Group mean and standard deviation read from paper or from graph, or calculated from values given in tables or graphs. Measurement for density closest to 0.2 taken for inclusion where measurements for a range of densities were stated. Where group values or standard deviations are missing these could not be established from the paper. (SD: standard deviation, ?: no statistical testing performed by authors, $\uparrow$: metric is higher in epilepsy, $\downarrow$: metric is lower in epilepsy, $\leftrightarrow$: no difference between epilepsy and healthy controls)*

2.5.3.3 Small worldness

The small worldness statistic σ, (calculated as $\frac{\gamma}{\lambda}$), was investigated by 10 studies. The findings are shown in Table 2.13. One study found an increased small worldness statistic in patients with epilepsy, four studies found no difference between patients with epilepsy and healthy controls, and three studies found a decreased small worldness statistic in patients with epilepsy compared to healthy controls. Two studies did not test for a statistically significant difference between the groups.

2.5.3.4 Network average strength

The average network strength or overall strength of the network for weighted networks was investigated by eight studies.[135,142,143,145,146,149,150,155] Only studies investigating global average network strength are included. Studies investigating the distributions of node strengths are not included in this analysis. Two of the eight studies found increased overall network strength in epilepsy compared to healthy controls, three studies found no difference, and three studies found decreased network strength in epilepsy compared to healthy controls.

Small Worldness Statistic (σ)			
	mean(SD)		
Study	Epilepsy	Controls	Findings
Bernhardt 2011	1.76	1.8	↔
Zhang 2011	2.4 (0.26)	2.6 (0.26)	↓
Liao 2013	1.8	1.9	↔
Liu 2014	2.35 (0.72)	2.14 (0.50)	?
Xu 2014	3.89 (0.26)	3.53 (0.37)	?
Xue 2014			↔
Caeyenburghs 2015	3.61 (0.44)	3.77 (0.85)	↔
Curwood 2015	1.7 (0.08)	1.5 (0.15)	↑
Widjaja 2015	2.08 (0.15)	2.00 (0.14)	↓
Sone 2016	1.1	1.14	↓

Table 2.13: ***Small worldness in epilepsy and healthy controls.*** *Group mean and standard deviation read from paper or from graph, or calculated from values given in tables or graphs. Measurement for density closest to 0.2 taken for inclusion where measurements for a range of densities were stated. Where group values or standard deviations are missing, these could not be established from the papers. (SD: standard deviation, ?: no statistical testing performed by authors, ↑: metric is higher in epilepsy, ↓: metric is lower in epilepsy, ↔: no difference between epilepsy and healthy controls)*

Network Strength (S)			
	mean(SD)		
Study	Epilepsy	Controls	Findings
Zhang 2011	10.1 (0.50)	10.5 (0.99)	↔
Liao 2013	5.5	5	↑
Lemkaddem 2014	6.7 (1.0)	7.3 (0.7)	↓
Liu 2014	0.18 (0.24)	0.19 (0.14)	↔
Xue 2014	0.46 (0.12)	0.6 (0.14)	↓
Curwood 2015			↑
Widjaja 2015	0.70 (0.02)	0.72 (0.03)	↓
Li 2016			↔

Table 2.14: ***Network average node strength in epilepsy and healthy controls.*** *Group mean and standard deviation read from paper or from graph, or calculated from values given in tables or graphs. Measurement for density closest to 0.2 taken for inclusion where measurements for a range of densities were stated. Where group values or standard deviations are missing, these could not be established from the paper. (SD: standard deviation, ?: no statistical testing performed by authors, ↑: metric is higher in epilepsy, ↓: metric is lower in epilepsy, ↔: no difference between epilepsy and healthy controls)*

2.5.3.5 Other network comparisons between epilepsy and healthy controls

Global network resilience to attack was examined by three studies (see Table 2.7).[83,134,151] All of these found that the global networks of patients with epilepsy were more vulnerable to targeted attacks of

nodes with high degree, strength, or betweenness centrality, than those of healthy controls. However, vulnerability to random attacks, where any node is removed from the network, had similar effects on network measures between patients with epilepsy and healthy controls.

Machine learning techniques for identifying patients with epilepsy from brain connectomes were assessed by four studies.[158–161] These all showed the ability of machine learning techniques to correctly classify epilepsy patients and healthy controls on the basis of MRI derived structural networks and their parameters.

Several studies also examined node degree distributions, node betweenness centrality and locations of hubs (see Table 2.7).[83,84,134,143–145,149–152,155–159,162] Studies found various changes in hub locations, and differences between individual anatomical regions and node statistics. However, these results are not summarised here as this review concentrates on global network properties rather than changes in individual nodes or regions.

Decomposition of the network into different modules was examined by seven studies,[131,147,148,152,154,159,162] and results were variable between studies, with some showing differences in module composition and modularity, and others finding no difference in modularity statistics. Other parameters investigated are shown in Table 2.7.

2.5.3.6 Epilepsy characteristics

Within the epilepsy patient groups, various associations of epilepsy characteristics with network measures were investigated. Vaessen *et al.*[133] found drug load was negatively associated with C and had a non significant positive association with L. However, they found no association between network measures and the number of seizures or duration of epilepsy.[133] Lemkaddem *et al.* found an association between the age of onset of epilepsy and L,[155] and Xue *et al.* found an association between the duration of epilepsy and a lower network strength.[142] However, three studies reported no association between any network measures investigated and epilepsy clinical variables including the age at seizure onset, duration of epilepsy, drug load, or seizure frequency.[135,150,151]

2.5.4 Quality and completeness of studies

Quality assessment using the QUADAS-2[140] tool is shown in Table 2.15. Patient selection concerns were identified in studies where the patients were not stated to be selected in a consecutive manner and methods of selection were unclear. Several studies did not state reasons for patient exclusions and these were identified as having potential problems with patient flow and timing. Applicability concerns were only raised when it was not clear from the study methods how patients were diagnosed with epilepsy. None of the studies stated that network analyses were performed blinded to the patient groups, but studies did state that imaging adjustment was performed without knowledge of patient group. Overall, studies had few applicability or bias concerns as assessed by the QUADAS-2 tool.

Study	Risk of Bias				Applicability Concerns		
	Patient Selection	Index Test	Reference Standard	Flow and Timing	Patient Selection	Index Test	Reference Standard
Raj 2010	?	✔	✔	?	✔	✔	✔
Bernhardt 2011	✔	?	✔	?	✔	✔	✔
Zhang 2011	?	?	✔	?	✔	✔	✔
Vaessen 2012	?	?	?	?	✔	✔	✔
Bonilha 2013	✔	?	✔	?	✔	✔	✔
Liao 2013	?	✔	✔	?	✔	✔	✔
Besseling 2014	?	?	✔	?	✔	✔	✔
Besson 2014	✔	?	✔	?	✔	✔	✔
Bonilha 2014	?	?	✔	?	✔	✔	✔
DeSalvo 2014	?	?	✔	?	✔	✔	✔
Lemkaddem 2014	?	?	✔	?	✔	✔	✔
Liu 2014	?	?	✔	?	✔	✔	✔
Vaessen 2014	?	?	✔	✔	✔	✔	✔
Xu 2014	?	?	✔	?	✔	✔	✔
Xue 2014	✔	?	?	✔	✔	✔	✔
Caeyenberghs 2015	?	?	✔	?	✔	✔	✔
Chiang 2015	?	?	✔	?	✔	✔	✔
Curwood 2015	?	?	✔	?	✔	✔	✔
Douw 2015	✔	?	✔	✔	✔	✔	✔
Fang 2015	?	?	✔	?	✔	✔	✔
Munsell 2015	?	?	✔	?	✔	✔	✔
Widjaja 2015	?	?	✔	?	✔	✔	✔
Yasuda 2015	✔	?	✔	✔	✔	✔	✔
Garcia-Ramos 2016	?	?	✔	?	✔	✔	✔
Kamiya 2016	?	?	✔	?	✔	✔	✔
Li 2016	?	?	✔	?	✔	✔	✔
Sone 2016	?	?	✔	?	✔	✔	✔
Wirsich 2016	?	?	✔	✔	✔	✔	✔

Table 2.15: **Study quality** The QUADAS-2 tool was used to assess study quality. Network construction and analysis was applied to the tool as the index test to diagnose epilepsy. (✔: low risk; ✘: high risk; ?: unclear risk due to insufficient information in the study report)

2.6 Discussion

2.6.1 Summary of main results

Twenty seven studies were identified that investigated differences in whole brain structural networks derived from MRI between patients with epilepsy and healthy controls. Nineteen studies used diffusion MRI to create network edges and the remainder used covariance of region volume or thickness. Meta-analysis was not performed due to the heterogenous study designs, analysis methods, and numerical estimates of network measures calculated. Five of nine studies found an increased path length in patients with epilepsy compared to healthy controls, but no studies showed a difference in normalised average path length. Five of six studies of covariance networks found an increased clustering coefficient in epilepsy compared to healthy controls. However, DTI studies all found a decreased clustering coefficient or no difference in clustering coefficient. Eight of nine studies found no difference in the normalised clustering coefficient between epilepsy and healthy controls. There were no trends for differences in the small worldness statistic or average network strength between those with epilepsy and healthy controls in the identified studies.

A higher average path length and a lower global efficiency in patients with epilepsy compared to healthy controls could be accounted for pathologically by a global loss of white matter with fewer streamlines in patients with epilepsy in the DTI derived networks.[136,137] For the covariance networks, although regional and local increases in correlation may occur in epilepsy,[117] if globally these changes are not occurring in a co-ordinated pattern, this may still lead to fewer longer range connections, and therefore longer overall path lengths. There was no consensus amongst studies with regards to changes in clustering coefficients in epilepsy. This may be due to the different network construction techniques used by studies. Regional changes in cortical thickness or volumes seen in epilepsy patients[138,163] may lead to increased covariance between nearby regions and therefore increased clustering coefficients in covariance networks. However, decreases in longer range connections, or global loss of white matter,[117] which may be better represented using DTI derived networks may lead to lower clustering coefficients in DTI derived networks.[117]

Studies investigating the normalised average path length, where the metrics are normalised to networks with the same degree or overall edge weights, found values above 1, suggesting that in epilepsy, the overall brain structure of higher path lengths than regular networks, is maintained. In addition, all studies reported small world networks in the epilepsy groups with $\sigma > 1$. However, few studies showed any group differences between those with epilepsy and healthy controls in the normalised metrics λ, γ, or σ. The elimination of group differences through normalisation of metrics suggests that any differences in metrics between groups is either being driven by overall network structure, or is not a robust enough finding to withstand normalisation due to small reported group differences. Small numerical differences between groups could be driven by small numbers of participants in the groups, or a lack of sensitivity in network measures to group differences, meaning that differences between groups must be large before network measures can reliably identify them. These two possibilities could be addressed by increased the number of participants in groups, or by improving the sensitivity of network construction methods to small anatomical changes.

Of the few studies that investigated the relationship of the severity of epilepsy with network metrics, only half found any associations between network measures and epilepsy characteristics. This may be due to well characterised, similar epilepsy groups. For example a group of patients with left TLE being investigated for a surgical programme in a single centre may have a small range of epilepsy characteristics such as number of daily seizures and duration of epilepsy as they have been subselected as suitable for that programme and that study. It may also be due to small group numbers in many studies. However, a few studies did find a dose-response relationship with epilepsy characteristics, where more severe epilepsy suggested more network disruption compared to healthy controls. With the current evidence base, it is difficult to know whether this provides further evidence in addition to the findings in path length and clustering between groups that there is an overall difference in structural brain networks between epilepsy and healthy controls.

2.6.2 Completeness, quality, and applicability of evidence

The risk of bias in applicability and study conduct as assessed with the QUADAS-2 tool was generally low. This tool is designed for studies of diagnostic accuracy and was applied as though the network analysis was the index test, and the diagnosis of epilepsy was the reference standard. This tool was used as no suitable tool for assessing quality and risk of bias in connectome studies has yet been developed. However, this tool did not assess all sources of bias or quality in these studies. For example, no specific assessment of choice of threshold for network construction, methods of correcting for group differences, or consistent reporting of results was carried out. This led to most studies having an unclear risk of bias surrounding the network analysis, which was reviewed as the index test.

Studies included few numbers of patients, with epilepsy groups ranging from seven to 156 participants per study. This is likely due to the intensity of image processing and network matrix processing and analysis required to create and analyse MRI derived structural networks. Further, all studies used slightly different network construction techniques, with a wide variety of atlases, number of network nodes, edge types, and network densities. This meant that networks were not comparable between studies, and numerical estimates of network measures varied widely. This prevented any meta-analysis being undertaken and restricted the analysis options available. Several studies calculated group network measures and used permutation testing to test statistical associations, which is a reliably documented method for assessing group differences in network analysis. However, these analyses also do not lend themselves easily to meta-analysis unless measures of dispersion are also provided along with the group estimate and *p* value, and this was not the case in most studies. This also contributed to the decision not to undertake meta-analysis for these studies. Larger studies using similar methodologies that create individual rather than group networks would lend themselves to meta-analysis more easily.

Abstract screening and study selection was performed by two people independently, which decreases the chance of potentially relevant papers being missed by this review. Checking forward citations and reference lists meant that it is unlikely that any studies were missed by this review. The lack of clear network parameters documented in papers or supplementary material meant that these were required to be calculated from graphs or figures, which may have introduced mistakes into the review methodology. Ideally, data extraction would be double checked by a second reviewer or authors would

provide accurate figures. However, contacted authors did not respond with figures where these were missing or only available to be read from graphs.

2.6.3 Recommendations for Reporting

The advantages of meta-analysis are that results of smaller studies can be combined to increase the number studied, the statistical power, and improve estimates of the effect size of the association. Performing meta-analysis based on a systematic review aims to avoid the selective weighting and inclusion and the consequent inherent risk of bias that can result from narrative reviews without clear inclusion and exclusion criteria and an aim to include all available literature. Combining estimates is particularly important in areas where small numbers are enrolled in studies, such as this investigation into connectome differences in epilepsy. Small numbers result from a smaller pool of patients with the condition of interest compared to the general population and the resources and time required to process data for connectome studies. However, the studies identified by this review could not be combined in a meta-analysis despite a reasonable number of studies addressing the same research questions. This was due to the heterogeneity of populations, network construction methods, and network analysis methods, and variability in study reporting. Many sources of heterogeneity are inherent in the question addressed. Epilepsy covers a wide range of clinical syndromes and conditions. Structural networks can be constructed and analysed in multiple different ways, with advantages and disadvantages to each technique, and no generally accepted gold standard for each step of the processing and analysis pathway. However, consistent reporting of studies would aid in meta-analysis of those studies with similar analysis methods of similar populations. The minimum dataset required to be reported to allow an evidence synthesis and meta-analysis of connectome differences in epilepsy compared to healthy controls is:

- description of the population studied and the comparison population, including inclusion and exclusion criteria
- description of connectome creation, including parcellation scheme and number of nodes, any data thresholding, network density choices, choice of edge construction method and description of edge construction, and any corrections of the data for population characteristics
- description of methods of calculation of network measures
- value and measure of dispersion of either group level or individual network for each measure assessed in each group
- whether data was processed and analysed blinded to group allocation, and steps taken to minimise bias and improve accuracy during data processing

These points could be used as minimum reporting criteria in future studies of graph theory measures to facilitate assessment of study quality and risk of bias and allow meta-analysis. This would facilitate the combination of published studies to create estimates of correlation or effect sizes for the association of network measures with epilepsy.

2.7 Conclusions

Twenty seven studies have investigated structural network differences between patients with epilepsy and healthy controls. Heterogeneity in study populations, network construction and analysis methods, and data reporting meant study estimates could not be combined for meta-analysis. An increased average path length and decreased global efficiency was found in epilepsy compared to healthy controls, but this finding was not consistent across studies. Higher clustering coefficients were found in patients with epilepsy in studies of structural covariance, but not in studies of DTI derived connectomes. Most studies found no differences between patients with epilepsy and healthy controls in the normalised average path length and clustering coefficient, suggesting any differences may be due to network construction methods rather than global network organisation. Recommendations for reporting and assessment of future studies of structural connectomes in epilepsy have been made.

Chapter 3

Study Methods

3.1 Chapter Abstract

This thesis aims to address whether structural network characteristics are associated with cognitive function in suspected epilepsy and epilepsy surgery. To achieve this, two clinical cohorts were investigated. This chapter provides a detailed description of the methods used in Chapters 4 and 5 to identify and anlayse the clinical cohorts. The methods used to collect the study data and establish subgroups are described. Then, the creation of connectomes from structural MRI data is described. Finally the analyses of the structural networks and the statistical analysis of the network characteristics with the clinical characteristics of the cohorts is described.

3.2 Aims

Chapter 4 investigates a cohort of children undergoing an epilepsy research protocol MRI for investigation of suspected seizures. Both cortical thickness and DTI based brain networks were created from structural MRI data for the children in this cohort. The association of structural network measures with cognitive dysfunction and IQ was investigated. The two types of network were compared with each other to assess the robustness of the findings, and the influence of markers of epilepsy severity on the network characteristics were investigated.

Chapter 4 investigates children undergoing epilepsy surgery who have had appropriate investigation and follow up with MRI and neuropsychology. In this cohort, cortical thickness networks were created and the association with pre-operative and post-operative IQ scores was investigated. This investigated whether the findings from the first cohort were applicable in a second different cohort of children with epilepsy, and whether structural network measures can be used to predict cognitive outcomes following epilepsy surgery.

3.3 Description of the Cohorts

3.3.1 Suspected epilepsy cohort

Between 2004 and 2009 children undergoing an MRI for known or suspected epilepsy at the University Medical Center Utrecht (UMCU) underwent brain imaging using a specific research epilepsy protocol MRI scan. The details of children imaged using this protocol were recorded in a research database at the time of scanning. From this database, children between the ages of one year and 17 years whose MRI scan was available on the UMCU Picture Archiving and Communications System (PACS) were selected for inclusion in the suspected epilepsy cohort. Children under the age of one year were excluded because poor grey white differentiation at this age makes automated MRI segmentation unreliable. The upper age cut off was set at 17 years to create a cohort that only included paediatric patients. Many epilepsy syndromes tend to occur in specific age groups,[164] and the onset of epilepsy during childhood is more frequently associated with cognitive dysfunction.[103] The cohort was restricted to paediatric patients to decrease the heterogeneity of patients and to ensure the results are applicable to the groups of children encountered in paediatric clinical practice. Clinical data was extracted from the electronic patient record system of the UMCU and the research database created at the time of MRI imaging. Clinical data collected included demographics, age at the onset of seizures, duration of seizures, seizure types, epilepsy diagnoses, medication, and the results of EEG, MRI, and other clinical investigations. The results from this cohort are presented in Chapter 4.

3.3.2 Epilepsy surgery cohort

A multicentre epilepsy surgery cohort was planned, and children meeting the following inclusion criteria were sought.

Inclusion criteria:

- Undergone or undergoing resective epilepsy surgery in an epilepsy surgery centre
- Between the ages of 1 year and 17 years at the time of surgery
- Both DTI and 3D T1-weighted non-contrast MRI performed pre-operatively
- Assessment of IQ both pre-operatively and at one year or later post operatively

Patients under one year of age were excluded due to the difficulties in automated segmentation of grey and white matter below this age. Patients above 17 years at the time of operation were excluded to ensure the results were applicable and valid for the paediatric population. A 3D T1-weighted MRI scan was essential for segmentation into anatomical ROIs to act as nodes for network creation. A pre-operative IQ score was necessary to compare baseline network characteristics with baseline pre-operative cognition, and a post-operative IQ score was necessary to assess whether the baseline network characteristics could predict the change in IQ following resective surgery. Patients who had undergone resective procedures, such as lobectomy, functional hemispherectomy, or lesion resection were included and those who had undergone palliative procedures such as callosotomy or had bilateral

seizure onset were excluded so that the population had similar seizure and cognitive outcome expectations.

Initial discussions were held between the Royal Hospital for Sick Children (RHSC), Edinburgh, United Kingdom (UK), Boston Children's Hospital (BCH), United States of America (USA), and the UMCU, The Netherlands to create a multi-centre surgical cohort. The cohorts identified at each centre are described below.

3.3.2.1 Royal Hospital for Sick Children, Edinburgh

All children who had undergone resective epilepsy surgery in Edinburgh were identified from the database of the Scottish national paediatric epilepsy surgery service. Data was available from February 2012 when the service began. Scottish national PACS was searched to identify patients with suitable pre-operative imaging, and Research Ethics Committee (REC) and National Health Service (NHS) Lothian Research and Design (R&D) approval was sought to add DTI for research purposes to the pre-operative imaging of children undergoing epilepsy surgery. This was approved and commenced from March 2015. Paper neuropsychology records for NHS Lothian were searched to identify and record the standard clinical epilepsy surgery pre-operative and post-operative neuropsychological assessments for patients assessed within NHS Lothian. The national paediatric epilepsy surgery service database and NHS Lothian electronic patient records were searched to identify the clinical details of the eligible participants.

During the process of data collection and analysis there was a formal review of the location of the Scottish paediatric epilepsy surgery service and it was not possible to continue with data collection or analysis for the Scottish service at this time. It also became apparant that very few children had neuropsychology assessments documented in NHS Lothian, and therefore pre-operative and post-operative IQ scores were available for fewer than 10 patients. Due to this, the results from this cohort are not presented in this thesis.

3.3.2.2 Boston Children's Hospital

Patients who had undergone resective epilepsy surgery were identified by collaborators in Boston via their epilepsy surgery service database. Neuropsychology test results were entered into this database. A data sharing agreement was agreed for the anonymous analysis of these patients. MRI scans for this same group of patients were transferred electronically. On receipt of the MRI scans, it was apparent that the group of patients were imaged on multiple different MRI platforms with only up to three patients sharing each of several markedly different DTI sequences. The neuropsychology scores for this cohort were not initially entered into the database, and sourcing these led to a long delay in acquiring patient data. Because of the concern over eliciting whether differences in network measures were due to the different scanner platforms and sequences rather than differences in patient cognition and clinical characteristics, and the delay in acquiring neuropsychological data, results from this cohort are also not presented in this thesis.

3.3.2.3 University Medical Centre Utrecht

All children who had undergone epilepsy surgery and had attended both a pre-operative and a post-operative neuropsychological assessment at the UMCU were identified from the records of the paediatric neuropsychology department. The UMCU PACS was searched for each of the children to identify whether a pre-operative 3D T1-weighted non-contrast MRI sequence and a DTI sequence had been performed. As only a few patients had undergone DTI imaging pre-operatively, and neuropsychology data was not available from the other two centres, the inclusion criteria were changed so that patients with only 3D T1-weighted imaging and no DTI sequence could also be included. Only MRI scans within the two years prior to the operation were considered to ensure comparison with contemporaneous neuropsychological assessment results. Children without a 3D T1-weighted MRI scan within two years prior to the operation date were excluded. Demographic and clinical data was acquired for all patients from the electronic record system of the UMCU, the Dutch paediatric epilepsy surgery database, and other surgical epilepsy databases at the paediatric neurology department. Data collected included demographics, epilepsy characteristics, medication, and surgical outcome. All clinical data were entered into custom databases and spreadsheets. The results from this cohort are reported in Chapter 5.

3.4 Research Approvals and Data Sharing Agreements

Research approval and data sharing agreements were agreed for the epilepsy surgery cohorts from the RHSC, BCH, and UMCU. The South East Scotland REC committee confirmed a favourable ethical opinion for the study in March 2015. NHS Lothian R&D approval was granted for this project in April 2015. This study initially only included patients with DTI MRI sequences acquired for clinical use or added to the pre-operative MRI planning scan for research purposes. In patients in whom the DTI sequence was added for research purposes, ethical approval was only granted for patient or parent consent in patients up to the age of 16 years as in Scotland the provisions of the Adults with Incapacity (Scotland) Act 2000 apply to those over the age of 16 years and parents cannot consent on behalf of their children unless they hold power of attorney. Due to the lack of patients with pre-operative DTI imaging available, a substantial amendment to facilitate the use of all retrospective data in patients up to 18 years of age who had undergone resective epilepsy surgery and only had 3D T1-weighted imaging available was added and approved by the South East Scotland REC and NHS Lothian R&D department in June 2015. This was to facilitate analysis with cortical thickness connectomes in the surgical cohort once it became clear that there would be insufficient patients with pre-operative DTI available to analyse DTI derived networks.

In July 2015, the Dutch Medical Ethics Committee (METC) of the UMCU considered the study and confirmed that the Medical Research Involving Human Subjects Act (WMO) did not apply and that official approval of the study was not required. This allowed the retrospective use of patient clinical, neuropsychological, and imaging data for the purposes of assessing the relationship between network characteristics and cognition in patients undergoing epilepsy surgery. To allow data transfer between the UMCU and the University of Edinburgh, a clinical trial agreement was required by the University of

Edinburgh. This was approved by both parties in July 2015.

At BCH, ongoing Institutional Review Board (IRB) approval for research assessment of the paediatric epilepsy surgery programme was already in place and had undergone a continuing review in May 2015. A data transfer agreement for the transfer of anonymous data between the University of Edinburgh and BCH was agreed in May 2016. This required appropriate clinical trials insurance to be arranged by the University of Edinburgh prior to any data transfers being accepted. Confirmation of appropriate insurance was provided by the University of Edinburgh in February 2016.

3.5 Data Management

At each epilepsy surgery centre, each individual patient was assigned a unique anonymous study number. The link between patient details and the unique study number was stored on a password protected computer on the clinical hospital network at the clinical site. Access to the file linking patient identity and study number was restricted to acquiring and linking the clinical data, neuropsychology data, and MRI data. Study data was then stored only linked to the unique study number on University of Edinburgh computers. Data transferred to the University of Edinburgh only included the unique study number and did not include any patient identifiable data. Anonymous data from UMCU was transferred using an encrypted password protected hard disc carried on the person of the researcher. Anonymous data from BCH was transferred over a secure encrypted data transfer service. Anonymous data from the RHSC was acquired and entered directly into co-located University of Edinburgh computers from the NHS Lothian network. On the University of Edinburgh network, data was stored in password protected files on a password protected network, and backed up regularly. Data was processed using local computers and servers within the University of Edinburgh network.

3.6 Neuropsychology Methods

All neuropsychology assessments were carried out at the patient's local epilepsy surgery centre or local hospital by trained paediatric neuropsychologists. All assessments were carried out for clinical purposes and no additional research assessments were performed. In the epilepsy surgery cohort, neuropsychological assessment was carried out pre-operatively and at two years post operatively, and all patients were assessed. In the paediatric seizure cohort, neuropsychological assessments were carried out when clinically indicated at the request of the clinicians caring for the patient, and not all patients underwent formal neuropsychological assessment. All children underwent neuropsychological testing in their native language.

3.6.1 IQ assessment

Age and developmentally appropriate instruments were used to assess IQ. Due to the 1 year to 17 years age range in these cohorts, it would not have been appropriate to test all patients using the same instrument. The IQ tests used in the cohorts in this thesis are shown in Table 3.1 along with each test's

appropriate age range. Numbers of patients undertaking each test type are reported with the test results in Chapters 4 and 5. Post-operative assessments were carried out using the same instrument as pre-operatively. When patients scored lower than the lowest score possible on the test, this was recorded as not achieving an IQ score. When IQ scores could not be calculated, but the assessing neuropsychologist believed it was appropriate to calculate a DQ, this was calculated as:

$$\text{DQ} = 100 * \frac{\text{mental age}}{\text{calendar age}}$$

Both IQ and DQ scores were combined and used in analyses. All tests used had a population normal mean of 100 points and a standard deviation of 15 points, so were combined on this population normed scale and were not converted to *z* scores. The difference between pre-operative and post-operative scores was calculated as the post-operative score minus the pre-operative score. Total Intelligence Quotient (TIQ), VIQ, and PIQ scores were all recorded when these were available from the instruments used, but only TIQ was used in the final analyses. This was to ensure that all test results used were attempting to measure the same underlying construct of general cognitive ability.

Neuropsychological Test	Age Range
Wechsler Preschool and Primary Scales of Intelligence (WPPSI)	3-7 years
Wechsler Intelligence Scales for Children (WISC)	5-17 years
Wechsler Adult Intelligence Scales (WAIS)	16-17 years
Snijders-Oomen Niet-verbale Intelligentietest (SON)	3-7 years
Kaufman Adolescent and Adult Intelligence Test (KAIT)	15-17 years
Bayley Scales of Infant Development (BSID)	16-165 months

Table 3.1: ***IQ test and age range*** *IQ tests, their abbreviations, and the age ranges tested during neuropsychological assessment.*

3.6.2 Diagnosis of cognitive impairment

For the suspected epilepsy cohort described in Chapter 4, the UMCU electronic patient records and paediatric neurology databases were searched to establish if the child had a diagnosis of Intellectual Disability (ID) documented by a neuropsychologist or paediatrician caring for that child. If the child had a documented diagnosis of an ID or if they attended special education due to significant educational needs, they were assigned to the group with cognitive impairment. If the child had documented evidence that there were no concerns about their cognitive development or educational attainment, they were assigned to the cognitively normal group. Children with special educational needs only due to physical disability who did not also have cognitive dysfunction or an ID and who were documented to have normal cognitive and educational development, were assigned to the group without cognitive difficulties. If there was no documentation regarding an ID, no neuropsychology assessment, or no documentation of educational attainment, then these children were not assigned to either group, and were excluded from analyses of cognitive impairment. The diagnosis of ID or special educational needs was independently clarified from each child's medical records by two doctors on two separate occasions.

In the epilepsy surgery cohort, a diagnosis of cognitive impairment was determined using the IQ score. Those who scored between 70-130 points, within two standard deviations of the population mean of 100 were considered to have scored within the normal range of the test. Those who scored below 70 points, or who were unable to be assigned a IQ or DQ score due to severe impairment were considered to have cognitive impairment.

3.6.3 Assessment of change in IQ

A clinically meaningful change in IQ was taken as a change in full scale or total IQ of at least 10 points, as agreed and described in previous studies investigating IQ change.[125,126,165] In the epilepsy surgery cohort patients were divided into two groups. One group had a post-operative increase in IQ of at least 10 points, and the other group did not. A change in IQ of fewer than 10 points was taken as no change in IQ. Any decrease in IQ of at least 10 points was also recorded.

3.7 Imaging Methods

3.7.1 MRI acquisition

All MRI scans were acquired as part of routine clinical care. No additional research scans were acquired in the cohorts of patients whose results are reported in this thesis. In the suspected epilepsy cohort all scans were acquired on a 1.5 T Philips Achieva with a SENSE 8 channel head coil. The 3D volume T1-weighted scan was a fast field echo sequence with a TR of 25ms, an TE of 4.6ms, a flip angle of 30°, a field of view (FOV) of 256x256mm^2, and a slice thickness of 1mm to give a near isotropic voxel size of 0.94x0.94x1mm. The acquisition time for this sequence was 2mins11s. The DTI sequence consisted of a single EPI b=0s/mm^2 image followed by 15 diffusion directions at a b value of 800s/mm^2. Acquisition parameters were TR=1382ms, TE=60ms, flip angle=90°, FOV=128x128mm^2, slice thickness=2mm, voxel size = 1.75x1.75x2mm, and an acquisition time of 2mins12s.

In the epilepsy surgery cohort 3D T1-weighted MRI was performed as a pre-operative assessment or for surgical planning purposes as part of routine clinical care according to one of the following protocols:

1. 1.5T Phillips Achieva with SENSE head coil. TR:25ms, TE:4.6ms, flip angle:30°, FOV:256x256, voxel size: 0.94x0.94x1
2. 1.5T Phillips Achieva with SENSE head coil. TR:8.2ms, TE:3.7ms, flip angle:8°, FOV:256x256, voxel size: 1x1x1
3. 1.5T Phillips Intera with SENSE head coil. TR:25ms, TE:7ms, flip angle:30°, FOV:256x256, voxel size: 1x1x1
4. 1.5T Phillips Intera with SENSE head coil. TR:8.2ms, TE:3.7ms, flip angle:8°, FOV:256x256, voxel size: 1x1x1

3.7.2 MRI processing

Anonymised MRI data labelled with unique study numbers were exported from PACS in Digital Imaging and Communications in Medicine (DICOM) format and transferred to the University of Edinburgh servers as described in section 3.5. DICOM files were converted to Neuroimaging Informatics Technology Initiative (NifTI) format using dcm2nii.[146]

3.7.2.1 Processing of 3D T1-weighted sequences

Each patient's 3D T1-weighted sequence was visually inspected for quality and pathology. It was not possible to extract meaningful data from scans with excessive artefact, so these were excluded from the study. Examples of significant movement, ring, streak, or implant artefacts leading to exclusion from the study are shown in Figure 3.1. The numbers of patients with artefacts leading to exclusion in each cohort are reported in Sections 4.5.1.1 and 5.4.1. All scans had been previously reported by a consultant radiologist aware of the patient's clinical history. Any reported abnormalities were identified and recorded.

The 3D T1-weighted sequence was processed using Freesurfer software, which is documented and available online (http://surfer.nmr.mgh.harvard.edu/). Briefly, the brain was extracted using a watershed and surface deformation procedure,[166] the Talairach transformation was computed, and volumetric segmentation of deep grey matter structures and subcortical white matter structures was performed.[49] Then the grey:white matter boundaries and grey matter:cerebrospinal fluid (CSF) boundaries were defined using intensity normalisation and automated topology correction to place the boundaries at the location with the greatest shift in signal intensity.[167] Surface based registration was performed by inflation of the cortical surface and parcellation into cortical units matching sulcal and gyral folding patterns.[168] Parcellation was completed using the Desikan-Killiany atlas.[48] At each surface vertex, cortical thickness was calculated as the distance from the grey:white boundary to the grey:CSF boundary.[169]

All segmentations and parcellations were manually checked for quality and accuracy. Manual checks were undertaken in all subjects following: (1) brain extraction, (2) tissue segmentation, and (3) cortical and subcortical parcellation. In addition, if an error message occurred or data processing stalled, additional manual checks were performed. To check brain extraction, the volume extracted was overlaid on the original T1-weighted data in each subject. Images were visually checked for unintentional inclusion of dura or skull and missing brain within the brain volume. Each slice in all three planes was checked. Following tissue segmentation, white matter and grey matter volume maps were overlaid on the original T1-weighted data and the extracted brain. White and grey matter boundaries were visually checked against the macroscopic appearance of the T1-weighted volume on each slice in all three planes. To check cortical and subcortical segmentations, the segmentations with labels were overlaid on the original T1-weighted volume and each labelled region was checked in its complete volume in all three planes. This was checked through existing knowledge of approximate region boundaries and for symmetry where appropriate. The list of segmented structures was also checked to ensure no regions were missing from the parcellation. All processed images and file names were labelled with the

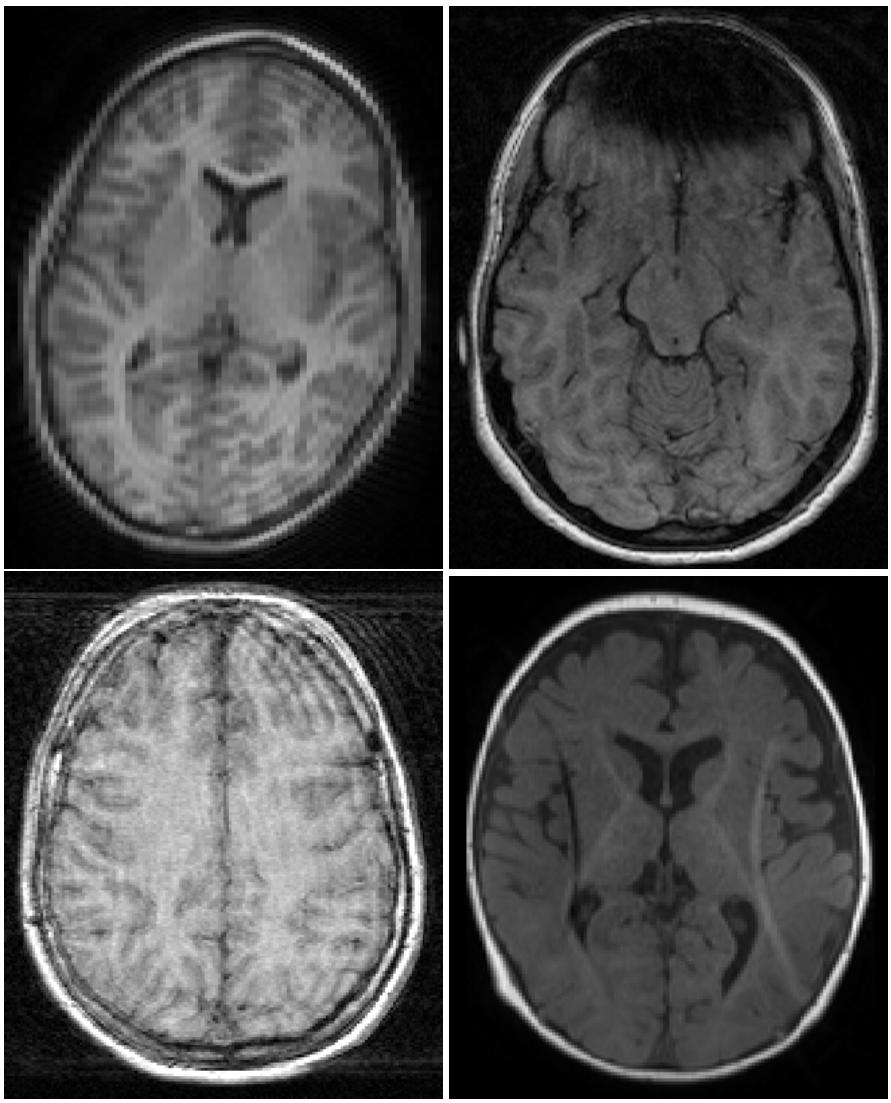

Figure 3.1: ***Participants excluded due to MRI artefact***. *Axial MRI example scans of participants who were excluded due to imaging artefacts degrading the data and preventing accurate automated analysis*

anonymised study number. Although I had full access to all data including group allocations, and IQ scores, the image processing was carried out completely separately in batches on a separate computer without these files, and it would not have been practical to remember group allocations or IQ scores or check these whilst checking multiple processed images or performing manual editing. Although manual editing is a potential source of bias within the processing pipeline, this was performed in preference to including visibly inaccurate data in the analyses or excluding multiple subjects from the analyses due to inaccurate automated processing.

When Freesurfer software was not able to process the MRI data, or segmentations or parcellations were inaccurate, manual adjustments were made to the Freesurfer processing stream. In some cases with abnormal anatomy, initial registration to the Talairach atlas failed. This was performed manually using Freesurfer tools when necessary. When left and right hemispheres were not correctly identified as such in patients with hemispheric abnormalities, manual seed points for the corpus callosum were set. To

adjust brain masks after skull stripping was performed, the watershed parameters and use of the atlas were adjusted to improve the brain extraction. When an accurate brain mask could not be generated after rerunning brain extraction with adjusted parameters, the brain mask was manually edited slice by slice within Freesurfer. The segmentation of grey matter, white matter and CSF was found to be inaccurate in regions with pathology and in regions with lower signal intensity than the rest of the brain. A problem with lower overall signal intensity was frequently identified in the temporal lobes. To correct the tissue boundaries, control points were used in the white matter to manually set the intensity of the voxel to that of white matter, or the white matter template was manually edited. An example of manual correction of the temporal grey white boundary using control points is shown in Figure 3.2.

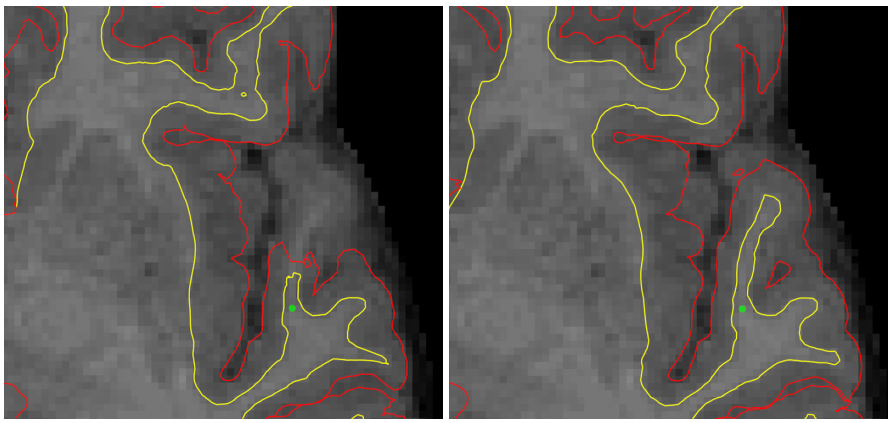

Figure 3.2: ***Correction of white matter segmentation using control points.*** *Left: Example of low intensity in the temporal lobe causing inaccurate identification of the grey white boundary and therefore of the pial surface. A control point (green dot) was added to set the intensity of that voxel to that of white matter. Right: The new white matter and pial surface boundaries following regeneration of the surfaces using the control point to reset the level at which white matter should be identified in this region. (green dot: control point location, yellow line: white matter surface, red line: pial surface)*

When hemispheric abnormalities compromised whole brain accurate segmentations, right or left hemispheres were processed separately, or only the healthy hemisphere was processed. When abnormal anatomy caused shift or absence of subcortical regions, and this affected the accuracy of cortical segmentations, cortical processing was performed ignoring the prior subcortical segmentation. Region labels of segmentations were edited as required by renaming voxels using the Freesurfer interface. After each step, the processing stream was re-run from the appropriate step, and the results were re-examined for quality and accuracy. This led to multi-stage processing for some scans, particularly those showing extensive pathology. An example of a scan that required multiple manual interventions for accurate segmentation and parcellation is shown in Figure 3.3.

Accurate whole brain segmentation and parcellation was attempted in all cases without significant artefact. Some pathological findings, such as small white matter abnormalities, or deep small infarcts, did not interfere with accurate segmentation, parcellation, and cortical thickness measurements. Lesions such as tumours or cortical dysplasia interfered with accurate assessment and measurements only in the gyri, lobe, or hemisphere affected. In these cases, as long as the rest of the brain was accurately processed, the inaccurate region was recorded and excluded from analysis. In some cases, extensive bilateral pathology interfered with processing, and no accurate segmentation or parcellation

could be performed. Examples of these cases are shown in Figure 3.4. When a single hemisphere could not be accurately segmented and parcellated, patients were excluded from further analyses. The numbers of patients removed from the analyses due to extensive bilateral pathology in the cohorts are reported in Sections 4.5.1.1 and 5.4.1.

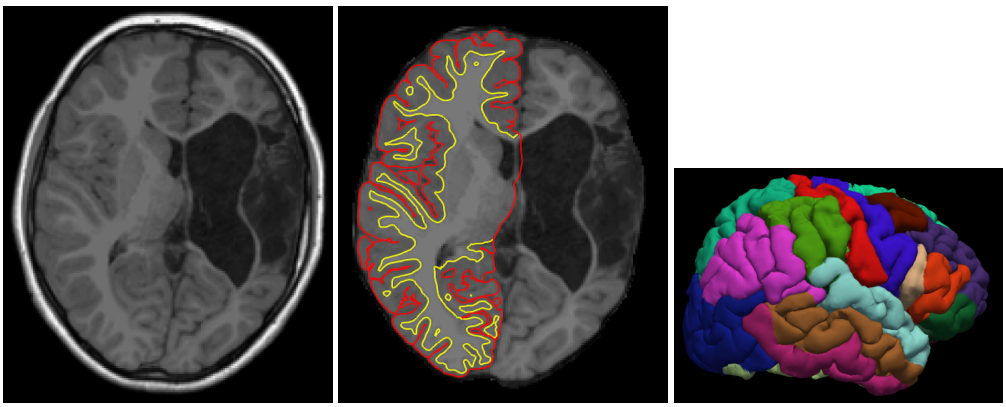

Figure 3.3: ***Manual intervention of Freesurfer pipeline.*** *This scan required manual Talairach registration, manual specification of the corpus callosum seed point to correctly separate the right and left hemispheres, and separate processing of the left hemisphere. Left: original T1 axial volume scan. Middle: Brain extracted data with pial surface outlined in red and the white matter surface outlined in yellow. Right: Accurately segmented right hemisphere. The left hemisphere could not be accurately segmented due to the extensive pathological changes and was not used in the analysis*

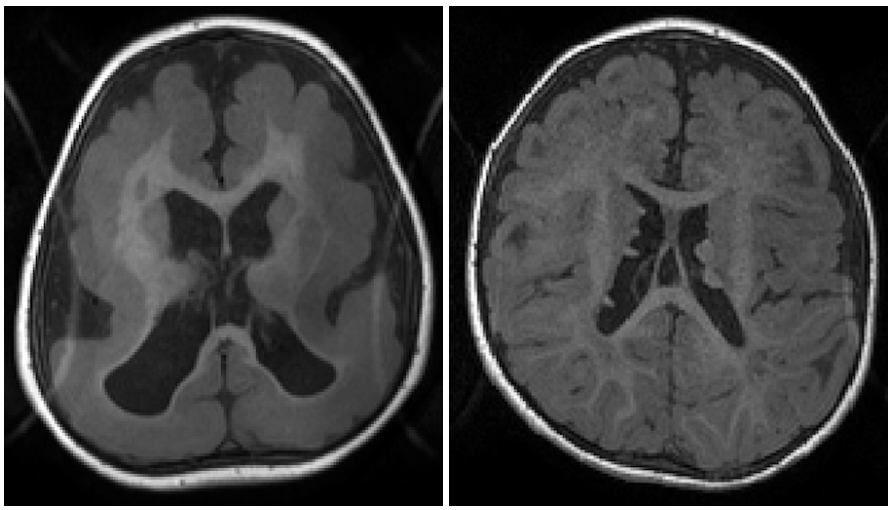

Figure 3.4: ***Participants excluded due to bilateral pathology*** *Examples of participants who were excluded due to the presence of bilateral extensive pathology that prevented accurate segmentation and parcellation. Left: Four year old patient with lissencephaly. Right: 18 month old patient with tuberous sclerosis and multiple bilateral cortical and subcortical tubers.*

3.7.2.2 Processing of DTI sequences

The DTI sequences were processed at the UMCU. Patient motion and eddy current distortions were corrected by aligning all 15 diffusion weighted scans to the b=0s/mm^2 image.[170] Diffusion tensors were estimated deterministically at each voxel and the main diffusion direction was selected as that voxel's principal eigenvector using robust estimation of tensors by outlier rejection.[171] The FA at each voxel was calculated. FA is determined by the eigenvalue of the diffusion tensor's eigenvector that points along the principal axis (λ_1) and the eigenvalues of two remaining radial axes (λ_2) and (λ_3) and was calculated as:[14,16]

$$\mathrm{FA} = \sqrt{\frac{1}{2}} \frac{\sqrt{(\lambda_1-\lambda_2)^2+(\lambda_2-\lambda_3)^2+(\lambda_3-\lambda_1)^2}}{\sqrt{\lambda_1^2+\lambda_2^2+\lambda_3^2}}$$

Whole brain streamlines were generated using the fiber assignment by continuous tracking (FACT) algorithm.[172] Eight seed points were placed in each white matter voxel and the stopping criteria used were an FA of less than 0.1 in the voxel, a turning angle of more than 45 degrees, or exit of the streamline from the brain mask volume. Linear registration of the DTI sequence to the 3D T1-weighted sequence was performed to allow alignment of the Freesurfer segmentation with the generated streamlines. These methods of determining streamlines are in established use for network creation.[81]

3.8 Network Methods

3.8.1 Network construction

3.8.1.1 Cortical thickness networks

A single group cortical thickness network was constructed for each patient group described in Chapters 4 and 5. Whole brain cortical thickness networks were constructed using anatomical regions as nodes and the correlation in cortical thickness between these regions as edges. The 68 regions of the Desikan-Killiany atlas[48] were taken as the network nodes. Atlas regions and the order in which they are displayed in this thesis are shown in Table 3.2. Cortical thickness in each of the 68 regions was measured using Freesurfer as described in Section 3.7.2. Networks were constructed in MATLAB Release 2015b (The Mathworks Inc, Massachusetts, United States). The pearson product moment correlation of the cortical thickness of each region was calculated and used as the weight of the edge between each pair of regions, as per previous studies.[83,134,143]

In addition to using the cortical thickness measurements to create networks, age and sex corrected cortical thickness measurements were also used in an attempt to mitigate the effects of age and sex on the network findings. To correct for age and sex, a linear model predicting the cortical thickness measurement from the age and sex of the patients was fitted for each of the 68 regions, and the standardised residual from these models at each region was used instead of the original cortical thickness measurement. The pearson product moment correlation for each region pair was again

calculated, and these correlations were used as the edge strengths between each region for the age and sex corrected cortical thickness networks. These, and similar methods have previously been used in studies of cortical thickness networks.[83,143,149]

Single hemisphere cortical thickness networks were constructed using the 34 Desikan-Killiany regions from a single hemisphere (right or left). Both raw cortical thickness measurements and age and sex corrected residuals were used to determine edge strengths in single hemisphere networks.

The correlation matrices were used as the connectivity or adjacency matrices for each group. Self-self connections were set to zero and negative correlations were removed as is frequently described in connectome analysis of both structural and functional data due to the lack of clarity over interpretation of negative correlations and inability of current mathematical graph theory analysis to deal with negative edge weights.[74] The matrices were thresholded using absolute thresholding to remove all weights below the threshold value or by proportional thresholding to maintain the proportion of weights above the threshold value. Thresholds were applied at 0.1 intervals from zero to one. The threshold at which both group networks remained fully connected was used for group comparisons. This was to facilitate the calculation of network average path lengths and is a technique described in previous analyses of cortical thickness connectomes.[52,83,173] Cortical thickness networks were also thresholded to create sparse networks as described previously,[52] aiming for densities of around 0.2 for comparison to DTI derived networks. Networks of similar densities were compared because of the reliance of many graph parameters on the density of the network.[70] The reasoning for the choice of thresholds at which network characteristics were calculated in each group is discussed in the methods, results, and discussion sections of Chapters 4 and 5. Both weighted and binary networks were investigated. To create binary cortical thickness networks, all edge weights that remained after thresholding were set to one. Non-existent edge weights were set to zero. The processing pipeline to create cortical thickness networks is shown in Figure 3.5.

3.8.1.2 DTI networks

DTI networks were created in MATLAB using the 68 cortical regions of the Desikan-Killiany atlas, plus the 14 subcortical regions, and three brain stem regions segmented with Freesurfer. These were created by Martijn van den Heuvel. The 85 ROIs are described and numbered in the order displayed in adjacency matrices in this thesis in Table 3.2. The existence and weights of edges between these nodes were determined using two methods. A NOS adjacency matrix was formed by counting the NOS that connected each pair of nodes. NOS network weights were examined with both raw streamline counts and after normalisation of streamline counts so that they followed a gaussian distribution and were in the range from zero to one. This was achieved using the normalisation tools distributed with the Brain Connectivity Toolbox (BCT),[74] and is as described in previous studies.[81,174] An FA weighted network adjacency matrix was formed by averaging the FA values in all voxels traversed by the streamlines connecting each pair of nodes. Average FA fall between zero and one due to FA only taking values between zero and one and were analysed without any normalisation. The processing pipeline to create DTI based networks is shown in Figure 3.5.

Streamline counts generated from white matter seeds may introduce bias into measurements through

over-representation of long white matter matter fibres due to seeding in white matter, under-representation of fibres travelling long distances due to problems with tractography algorithms reconstructing long distance white matter tracts, preference for algorithms to end streamlines at gyri rather than sulci, and an increased number of streamlines beginning or ending at cortical nodes with larger volumes or surface areas.[175] Various attempts have been made to correct for these errors, including correcting the number of streamlines for the volume or surface area of the node, use of average tract FA, introducing a threshold number of streamlines, normalising streamline counts using various methods, using the volume or cross sectional area of the path of the streamline, or dealing only with binary networks.[175] This thesis uses tract average FA, binary networks, and normalisation of streamline counts to assess for any influence of bias introduced through streamline counts. Where raw streamline counts are used in this thesis, these are always compared to other methods of correcting for streamline bias. Raw streamline counts are used as the raw method of network construction. Correction of the number of streamlines to streamline density was not undertaken as correction using FA values already corrects for the previously mentioned biases.

Binary networks were created from both the FA and NOS weighted adjacency matrices by setting all existent connections to have a weight of one. These are referred to as the FA and NOS binary networks. Individual binary and weighted FA and NOS networks were analysed for each participant. Group averaged DTI networks were also created for some analyses. To create the group averaged networks, only connections appearing in at least 60% of all subjects within the group were retained. Each remaining edge was weighted with the average weight of those subjects in whom the edge existed. Group averaged networks were created for both the FA and NOS networks, and were analysed as both weighted networks and binary networks. The binary group averaged connectivity matrices were created by setting all existing edge weights to one and non existent edge weights to zero.

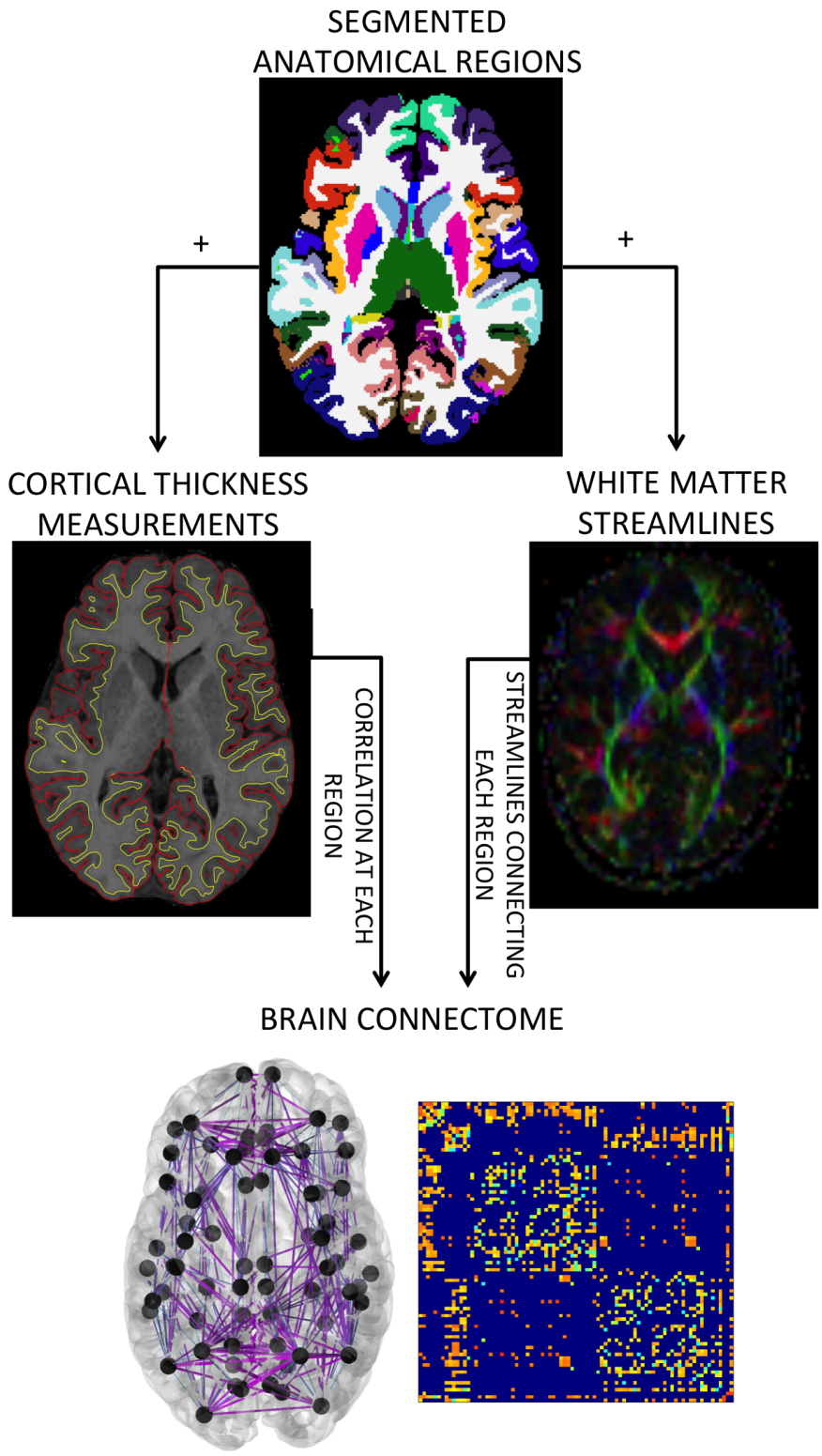

Figure 3.5: ***Network creation pathway.*** *Data processing steps to create connectomes from structural MRI data. Anatomical regions were segmented using the Freesurfer Desikan-Killiany atlas. For cortical thickness networks (left), the cortical thickness at each region was calculated as the distance between the white matter boundary outlined in yellow and the cortical surface outlined in red. The pearson correlation coefficient of the cortical thickness measurements at each region was used as the edge weight. For DTI networks (right), streamlines were generated between each cortical region and the number of streamlines or the average FA along the streamline was used as the edge weight. For both network types, self-self connections were set to zero. Networks or connectomes can be displayed anatomically (bottom left) with nodes placed in anatomical regions and edges placed between connected nodes, or as adjacency matrices (bottom right), where the edges are represented as filled in yellow-red squares and each node is a row or column in the matrix. (DTI: diffusion tensor imaging, FA:fractional anisotropy)*

Region	DTI Region Number	Cort.Thick. Region Number
left thalamus	1	
left caudate	2	
left putamen	3	
left pallidum	4	
left hippocampus	5	
left amygdala	6	
left accumbens area	7	
right thalamus	8	
right caudate	9	
right putamen	10	
right pallidum	11	
right hippocampus	12	
right amygdala	13	
right accumbens area	14	
left bank of the superior temporal sulcus	15	1
left caudal anterior cingulate cortex	16	2
left caudal middle frontal gyrus	17	3
left cuneus cortex	18	4
left entorhinal cortex	19	5
left fusiform gyrus	20	6
left inferior parietal cortex	21	7
left inferior temporal gyrus	22	8
left isthmus of cingulate cortex	23	9
left lateral occipital cortex	24	10
left lateral orbital frontal cortex	25	11
left lingual gyrus	26	12
left medial orbital frontal cortex	27	13
left middle temporal gyrus	28	14
left parahippocampal gyrus	29	15
left paracentral lobule	30	16
left pars opercularis	31	17
left pars orbitalis	32	18
left pars triangularis	33	19
left pericalcarine cortex	34	20
left postcentral gyrus	35	21
left posterior cingulate cortex	36	22
left precentral gyrus	37	23
left precuneus cortex	38	24
left rostral anterior cingulate cortex	39	25
left rostral middle frontal gyrus	40	26
left superiorfrontal gyrus	41	27
left superior parietal cortex	42	28
left superior temporal gyrus	43	29
left supramarginal gyrus	44	30
left frontal pole	45	31

Region	DTI Region Number	Cort.Thick. Region Number
left temporal pole	46	32
left transverse temporal cortex	47	33
left insula	48	34
right bank of the superior temporal sulcus	49	35
right caudal anterior cingulate cortex	50	36
right caudal middle frontal gyrus	51	37
right cuneus cortex	52	38
right entorhinal cortex	53	39
right fusiform gyrus	54	40
right inferior parietal cortex	55	41
right inferior temporal gyrus	56	42
right isthmus of cingulate cortex	57	43
right lateral occipital cortex	58	44
right lateral orbital frontal cortex	59	45
right lingual gyrus	60	46
right medial orbital frontal cortex	61	47
right middle temporal gyrus	62	48
right parahippocampal gyrus	63	49
right paracentral lobule	64	50
right pars opercularis	65	51
right pars orbitalis	66	52
right pars triangularis	67	53
right pericalcarine cortex	68	54
right postcentral gyrus	69	55
right posterior cingulate cortex	70	56
right precentral gyrus	71	57
right precuneus cortex	72	58
right rostral anterior cingulate cortex	73	59
right rostral middle frontal gyrus	74	60
right superiorfrontal gyrus	75	61
right superior parietal cortex	76	62
right superior temporal gyrus	77	63
right supramarginal gyrus	78	64
right frontal pole	79	65
right temporal pole	80	66
right transverse temporal cortex	81	67
right insula	82	68
brain stem	83	
left ventral dorsal columns	84	
right ventral dorsal columns	85	

Table 3.2: ***Network region descriptions.*** *Descriptions of network regions for DTI and Cort.Thick. networks. Numbering of nodes is in the order displayed in all adjacency matrices in this thesis. (DTI: diffusion tensor imaging; Cort.Thick.: cortical thickness)*

3.8.2 Network measures

Connectivity matrices for the networks were analysed using the Brain Connectivity Toolbox[74] in MATLAB. The network measures analysed in this thesis are described in the following sections. To define the network measures, the following notation is used:

- n is the number of nodes in the network
- N is the set of all nodes in the network
- l is the number of edges in the network
- L is the set of all edges in the network
- l^w is the sum of all edge weights in the network
- i and j are nodes in the network
- ij is the link between nodes i and j
- a is the binary adjacency matrix or undirected binary graph
- a_{ij} is the presence of an edge between nodes i and j in a binary network. The value of a_{ij} is one when an edge exists between nodes i and j and zero when there is no edge between nodes i and j.
- w is the weighted adjacency matrix or undirected weighted graph
- w_{ij} is the weight of the edge between nodes i and j in the weighted network

3.8.2.1 Density

Network density is the number of edges present in the network as a proportion of all the possible edges that could be present in the network. Density was calculated as:

$$\text{density} = \frac{l}{\frac{1}{2}n(n-1)}$$

Example binary and weighted versions of the same example network are shown in Figure 3.6. These networks have seven nodes, and therefore 21 potential edges. They only have 8 edges, which is equivalent to a density of 0.38. Density is identical for weighted and binarised networks as it does not depend on edge weights.

3.8.2.2 Degree

The degree of each node, known as k_i, is the number of edges connected to that node. For each node i, the degree is calculated as:

$$k_i = \sum_{j \in N} a_{ij}$$

In Figure 3.6, node A has a degree of 2, and node B has a degree of 3. To describe the degree of the network (k), the mean of each node's degree was taken. Edge weights are not taken into account when calculating the degree so binarised networks have the same degree as their weighted equivalents, as can be seen in Figure 3.6.

3.8.2.3 Node strength

Node strength (k_i^w) is the sum of all the edge weights of edges connected to that node. For each node i, the node strength is:

$$k_i^w = \sum_{j \in N} w_{ij}$$

The mean network strength is the mean of all node strengths across all nodes in the network. Node strength is only applicable to weighted networks. In Figure 3.6, the strength of node E is 1.5, and the strength of node A is 1.1.

3.8.2.4 Edge weight

The edge weight for each edge is set during the construction of the weighted networks. The mean network EW is the mean of all the edge weights in the network.

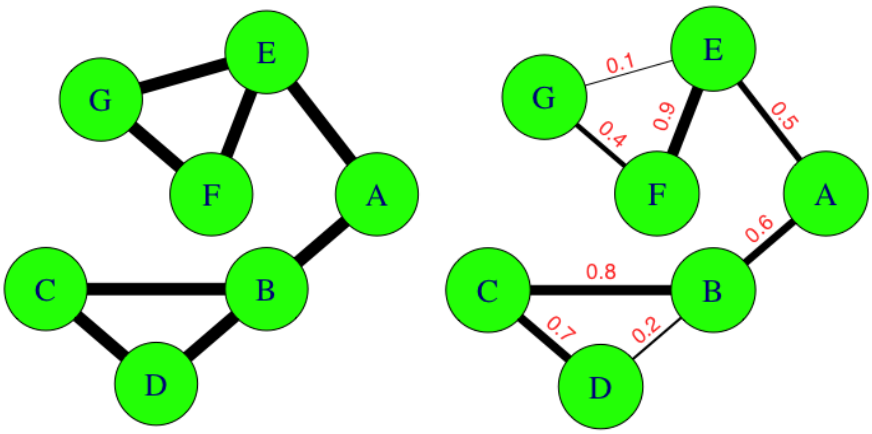

Figure 3.6: ***Example binary and weighted networks.*** *Left: Binary network. Edges that are present in the network have a weight of one. Edges are black lines. Nodes are the green circles. Right: Weighted network. Edge weights vary from zero (not present) to one, and are represented by the thickness of the edge. Edge weights are given in red text.*

3.8.2.5 Path length

Paths within networks are sequences of nodes and edges. The shortest path between any two nodes in a binary network is the minimum number of edges that require to be traversed to reach the target node. The average shortest path length across the network (L) is also known as the characteristic path length. To calculate this, first the shortest path length or shortest distance d was calculated between each pair of nodes i and j using Dijkstra's algorithm,[176] and recorded in the distance matrix. For binary networks, the shortest path length between two nodes is the minimum number of edges between the nodes. For example, in the binary network in Figure 3.6, the shortest path length between nodes G and A is 2. There is also a path between nodes G and A that traverses node F and has a total of 3 edges, but this is a longer path between the two nodes in the binary network. For weighted networks, the edge weights were first converted to lengths by inverting the edge weights. Weight inversion is necessary in networks derived from brain imaging because higher edge weights represent more efficient connections and therefore shorter edge distances. The shortest path length between any two nodes in a weighted network is the sum of the inverted edge weights between the two nodes. For example in the weighted network in Figure 3.6, the weighted shortest path length between nodes G and A is actually the path that passes through node F. The direct path from G to A has a path length of 12 ($\frac{1}{0.1} + \frac{1}{0.5}$), whereas the path from G to F to E to A has a path length of 5.6 ($\frac{1}{0.4} + \frac{1}{0.9} + \frac{1}{0.5}$).

The characteristic path length (L) of the network is the mean of the shortest path lengths between all nodes in the network,[72] and was computed as:

$$L = \frac{1}{n} \sum_{i \in N} \frac{\sum_{j \in N, j \neq i} d_{ij}}{n-1}$$

In the above equation d_{ij} represents either the binary or the weighted shortest distance between nodes.

When networks are not fully connected, and there is no path between two nodes, the path length cannot be calculated as defined, as when the shortest path of zero is inverted, the matrix entry becomes infinity. When shortest path lengths were calculated in disconnected networks, the values of infinity were removed from the distance matrix and set to zero and the mean shortest path length was calculated on only non zero entries in the matrix to avoid this problem.

3.8.2.6 Global efficiency

The global efficiency of the network (E_{Glob}) is the mean of the inverse shortest path length between each node.[177] Network global effeciency was calculated as:

$$E_{Glob} = \frac{1}{n} \sum_{i \in N} \frac{\sum_{j \in N, j \neq i} d_{ij}^{-1}}{n-1}$$

In this equation d_{ij} represents either the binary or the weighted shortest distance between nodes. Unlike path length, global efficiency is defined for disconnected networks. When there is no edge between two nodes, the distance becomes infinity, but the inverse of infinity is taken as zero, and therefore it is possible to calculate global efficiency regardless of whether the network is fully connected.[177]

3.8.2.7 Clustering coefficient

The binary clustering coefficient C_i for each node is the fraction of the neighbours of a node that are also connected to each other.[72] The binary network clustering coefficient (C) is the mean of the clustering coefficients across all nodes in the network and was calculated as:

$$C = \frac{1}{n} \sum_{i \in N} \frac{2t_i}{k_i(k_i - 1)}$$

In this equation, k_i is the degree of node i and t_i is the number of triangles around node i. The number of triangles around node i was calculated in the binary networks as:

$$t_i = \frac{1}{2} \sum_{j,h \in N} a_{ij} a_{ih} a_{jh}$$

In the binary network in Figure 3.6, node E is connected to nodes G, F, and A and has a degree of 3. It is possible for nodes A, F, and G to have 3 edges between them, but only the edge between nodes F and G exists. This gives node E a clustering coefficient of $\frac{1}{3}$. Alternately, it is possible for there to be 3 triangles around node E (1: E,G,F; 2: E,G,A; 3: E,F,A). Only one of these three triangles is fully formed giving a clustering coefficient of $\frac{1}{3}$.

The weighted clustering coefficient of a node is defined as the average intensity of the triangles around that node, where the intensity is calculated as the geometric mean or cubed root of the product of the three edge weights.[178] The network weighted clustering coefficient was calculated as the mean of each node's clustering coefficient. Prior to calculating the weighted clustering coefficient, all edge weights were scaled by the largest weight in the network by dividing each weight by the maximum edge weight. This was as per the original description of the weighted clustering coefficient to ensure that the definition of the weighted clustering coefficient approached the binary clustering coefficient as edge weights became binary.[178] After scaling of the edge weights, the intensity of triangles around each node was calculated as:

$$t_i^w = \frac{1}{2} \sum_{j,h \in N} \left(w_{ij} w_{ih} w_{jh}\right)^{\frac{1}{3}}$$

Then the weighted clustering coefficient (C) was calculated for the network by calculating the mean of each node's clustering coefficient C_i across the network.

3.8.2.8 Betweenness centrality

The betweenness centrality of a node is the fraction of all shortest paths in the network that pass through that node,[179] and was calculated as:

$$\text{betweenness centrality}_i = \frac{1}{(n-1)(n-2)} \sum_{h,j \in N, h \neq j, h \neq i, j \neq i} \frac{\rho_{hj}(i)}{\rho_{hj}}$$

In this equation, ρ_{hj} is the number of shortest paths between h and j that pass through i.[74] The weighted and binary betweenness centrality are calculated in the same manner, but using the weighted or binary shortest path lengths respectively for that node.

3.8.2.9 Normalisation of metrics

Network measures were normalised by comparison to randomised reference networks. Symbols, definitions, and equations for the normalised measures are shown in Table 3.3, and descriptions of the normalised measures are displayed in Chapter 1 in Table 1.1. For each individual or group network, random reference networks were created with the same number of nodes, edges, and node degrees as the original network. This was achieved using the randomisation tool provided by the BCT.[74] One thousand random networks were computed for each of the DTI networks and the patient cortical thickness networks. For the permuted networks, only 100 of the 1000 networks were each randomly rewired 100 times due to the long computing time required to achieve 1000 random reference networks for each of 1000 permutations.

After creation of the randomly rewired networks, each of the network measures in Table 3.3 was calculated for each of the randomly rewired networks. To calculate the normalised metrics, the original metric was divided by the mean of that metric from the randomly rewired networks.

	Symbol		
Metric	Original	Normalised	Calculation
Shortest path length	L	λ	$\frac{L}{mean(Lrand)}$
Clustering coefficient	C	γ	$\frac{C}{mean(Crand}$

Table 3.3: ***Normalised metrics.*** *Definitions and symbols representing original and normalised network metrics.The subscript 'rand' indicates the metric calculated from the randomly rewired metrics.*

3.8.2.10 Small world coefficient

The small world coefficient (σ) is defined as:

$$\sigma = \frac{\gamma}{\lambda}$$

where γ is the normalised mean network clustering coefficient and λ is the normalised mean network shortest path length[72,75] as described in Section 3.8.2.9. Networks are described as having a small world organisation when $\sigma > 1$[75] or when λ is about one and γ exceeds one.[72]

3.9 Statistical Methods

Networks were viewed in MATLAB Release 2015b (The Mathworks Inc, Massachusetts, United States) or in BrainNet viewer.[180] Statistical testing was carried out using R version 3.4.0 "You Stupid Darkness"

(The R Foundation for Statistical Computing, 2017) and MATLAB. For group comparisons t tests were used for numerical data following a normal distribution, Mann Whitney U tests were used for numerical data that did not follow a normal distribution, and X^2 tests were used for categorical data. Histograms and Q-Q plots were used to assess whether data followed a normal distribution. Multiple comparisons were accounted for by controlling the false discovery rate (FDR) to be 5% and FDR corrected *p* values are reported.[181] These are also known as *q* values but are referred to as corrected *p* values in this thesis. To calculate the adjusted *p* values, for each assessment of network measures, the p.adjust command was used in R with the setting "BH."[181] The input was the list of *p* values for each network analysis, so each *p* value was adjusted for 32 comparisons (2 network types and 16 network measures, for example the list in Table 4.10). For multivariable analyses, logistic regressions were performed for categorical outcome data and linear (gaussian) regressions were performed for numerical data. For all models, the model fit, residuals and standard errors were analysed.

For group comparisons using the cortical thickness data, permutation testing was performed. This involved randomly assigning group labels to participants to create 1000 random group permutations. The participants were randomly assigned to two groups in 1000 different ways. For each of these 1000 different allocations, a cortical thickness network was created for each of the two groups. For each of these 2000 networks (2 for each permutation), network metrics were calculated and the difference between the two groups for each metric was calculated. This led to a distribution of 1000 group differences for each metric, which could be plotted and analysed. The *p* values were calculated using the number of times a value greater than that encountered in the experimental data was seen in the random group permutations, divided by 1000 (the number of permutations). This is an established method for determining statistical significance in connectomics research, and is applicable when the underlying probability distribution of the metrics or group differences in unknown.[81,83,174]

3.10 Contributions

The suspected epilepsy cohort database was established by Suzanne Koudijs and Kees Braun at the UMCU. The list of potential eligible patients for the epilepsy surgery cohort was provided by Monique van Schooneveld at the UMCU. For both of the cohorts I analysed the patient records to establish which patients were eligible for the studies and to record clinical features and neuropsychology assessment results. I extracted the MRI from the UMCU PACS system for all patients. I performed all Freesurfer segmentations, including corrections. Processing of DTI and creation of DTI whole brain networks was performed by Martijn van den Heuvel at the UMCU. I created all cortical thickness connectomes. I created all single hemisphere connectomes, binary connectomes, thresholded connectomes, or connectomes produced from adjusted edge weights. I performed all connectome analysis and statistical analysis for this thesis.

Chapter 4

Suspected Epilepsy Cohort

4.1 Chapter Abstract

Cognitive impairment is a common and significant comorbidity in paediatric epilepsy. Difficulties with cognition may be attributed to the underlying pathological process causing seizures, or the disruption of normal processing pathways by ictal discharges. Widespread structural brain changes have been reported in both focal and generalised onset epilepsies. This chapter investigates whether the organisation of structural brain networks derived from cortical thickness measurements or white matter streamlines is associated with cognitive impairment or IQ scores in children investigated for seizures. Cognitive impairment was found to be associated with lower network densities, lower average node degrees, lower average node strengths, and lower average network edge weights. Children with cognitive impairment had higher average path lengths and lower network global efficiency in networks created from DTI NOS and streamline averaged FA. These findings persisted when corrections were made for network density or average edge weight, suggesting differing network topologies contributes to the difference in network average path lengths between the groups. Cortical thickness networks thresholded to similar densities as the DTI networks also showed higher average path lengths. However, these findings were not reproducible at high network densities in the cortical thickness networks. DTI network average path lengths were also associated with IQ scores, providing further evidence for an association between network organisation and cognition. These findings were robust in the subgroup of children who later had a definite diagnosis of epilepsy. The relationship between cognition and network average path length also remained significant when seizure frequency and number of AEDs were included in multivariable analyses. In conclusion, cognitive impairment is associated with less efficient network organisation, and this finding is robust across several network construction and analysis methods. However, network construction does affect some findings, and the conclusions are limited by the small sizes of some of the analysed subgroups.

4.2 Introduction

The organisation of the human brain can be modelled as a structural network consisting of nodes or regions and the edges or links that connect them.[46] On a macroscopic scale, MRI is used to determine anatomical network nodes using segmented cortical and subcortical structures. Edges can be determined using covariance of ROI properties[43] or DTI to map streamlines between regions.[62]. The application of graph theory to macroscopic human structural MRI derived networks or connectomes has shown the human brain to be highly organised with a small world topology.[46,72] Further, shorter network average path length and higher global efficiency of structural brain networks have been associated with higher IQ scores or measures of cognitive function in healthy adults,[89], normally developing children[90], and in the healthily ageing elderly.[182] Structural network organisation has also been associated with cognitive abilities in some disease states such as Alzheimer's Disease,[78] and schizophrenia.[82]

Brain network organisation is of particular interest in those with epilepsy due to the disorder of brain networks associated with seizure onset and propagation. A diagnosis of epilepsy is associated with global functional and structural whole brain network changes, and epilepsy is increasingly viewed as a disorder of brain networks.[100,102] There is also an increased frequency of cognitive deficits in those with a diagnosis of epilepsy,[103] and even focal onset epilepsies may lead to generalised cognitive dysfunction not necessarily expected from the location of the epileptogenic focus.[111,113] Cognitive deficits are associated with an early age of onset of epilepsy[111,112] and a longer duration of epilepsy.[113] Due to this, and the potential impact of epilepsy during development, the effect of epilepsy on cognition is of particular importance during childhood. Childhood epilepsy, particularly when medication resistant, can lead to significant intellectual disability that impacts on development and future adult attainment. Approximately 60% of children undergoing epilepsy surgery have IQ scores lower than 80.[111,113] The frequency and severity of cognitive problems in childhood epilepsy may be associated with the alteration of whole brain functional and structural networks in epilepsy.

Only a few studies have investigated whether structural network topology is associated with cognition in childhood epilepsy. A small group of nine patients with cognitive impairment and frontal lobe epilepsy had a higher path length and clustering than those with epilepsy and no cognitive impairment or healthy controls, but the difference was not statistically significant.[131] In a second study of children with non-lesional localisation related epilepsy undergoing epilepsy surgery there were no significant correlations between global network properties and IQ.[135] In 39 children with new onset epilepsy, the ratio of clustering coefficient to characteristic path length derived from cortical thickness networks was found to be reduced in those with lower IQ scores.[134] Decreased path length and increased clustering coefficients in DTI structural networks were associated with increased IQ in 39 adults with frontal or temporal lobe epilepsy.[133] However, in all of these studies, the mean IQ of the patients with epilepsy was very close to the population mean of 100 points rather than the poorly performing group whose lower cognitive performance can have a significant impact on daily activities. As the ability to complete an IQ test relies upon a certain baseline level of function that may exclude those with a significant intellectual disability, it is not known how children with epilepsy and very poor cognitive performances compare to those with epilepsy and cognitive function within the normal range. Further, sample sizes are small and findings have not been reproduced. Thus there is a need to assess whether these studies

are reproducible and whether cognitive changes in children with epilepsy do have a structural correlate in graph theory measures. This chapter aims to investigate whether children investigated for suspected epilepsy who have significant cognitive impairment differ from those whose cognitive performance is within the normal range in terms of the organisation of their whole brain structural networks as derived from MRI.

4.3 Objectives

This chapter aims to answer the following questions in a cohort of children investigated for suspected epilepsy.

- Is cognitive impairment associated with longer average path lengths and lower global efficiency in structural brain networks?
- Is IQ associated with longer average path lengths and lower global efficiency in structural brain networks?
- Is there an association between seizure characteristics, cognition, and the clustering coefficient or average path length of structural brain networks?

4.4 Methods

A paediatric suspected epilepsy cohort was established as described in detail in Chapter 3 in Section 3.3.1. This cohort consisted of children between the ages of one year and 17 years who had undergone a specific epilepsy protocol MRI brain scan on a single MRI scanner at the UMCU for the investigation of suspected seizures. The MRI scan included the 3D T1-weighted sequence and the DTI sequence described in Section 3.7.1. The 3D T1-weighted volume was segmented and parcellated using Freesurfer as described in Section 3.7.2. Whole brain structural covariance cortical thickness networks were created using both raw cortical thickness measurements and residual cortical thickness measurements after regressing the effects of age and sex using a linear model. Networks were formed using the 68 cortical regions of the Desikan-Killiany atlas[48] as nodes. Region descriptions for these nodes are listed in Table 3.2. Both binary and weighted networks were created and analysed. The DTI data was used to generate streamlines between these same cortical regions as well as the subcortical regions listed in Table 3.2. DTI networks were created using both the NOS and the average FA along the streamlines to determine edge weights as described in Section 3.8.1.2. Both binary and weighted networks were created from the DTI data. The processing pipeline for MRI structural network creation is shown in Figure 3.5. Network measures were computed using tools from the BCT[74] in MATLAB. Methods for calculation of network measures are described in Section 3.8.2.

Demographic and clinical epilepsy characteristics for the patients in the paediatric suspected epilepsy cohort were gathered from databases within the paediatric neurology department at the UMCU and from the UMCU electronic patient records. All patients included in this cohort had experienced an event that was thought to be a seizure, and had subsequently been investigated for this. Details of the clinical

history, examination, EEG, and any other investigations prior to and after the MRI undertaken were recorded and analysed. Final diagnoses and seizure types were established from review of the medical notes to establish the opinion of the paediatric neurologist in charge of the patient. Those described as having a focal onset epilepsy had MRI, EEG and clinical semiology concordance. Those described as having generalised epilepsy had generalised onset of seizures. Some of the children in this cohort did not meet the requirement for a final diagnosis of epilepsy, and sometimes it was unclear whether the event was actually a seizure. In all descriptions of seizures and timings, the event investigated as a possible seizure is referred to, even when this is later investigated and thought not to be a seizure. The term 'seizure' in this chapter refers to all of the suspicious events investigated. Some patients in this cohort had a well established diagnosis of epilepsy. In these patients, the timing of their first seizure is taken as the time of epilepsy onset even if this was not the event that prompted re-investigation with an MRI.

Cognitive assessments had been undertaken in this cohort as clinically indicated. Not all patients underwent formal neuropsychological testing. All neuropsychological testing was carried out by a paediatric neuropsychologist as described in Section 3.6. Where possible, patients were assigned a TIQ or DQ score using one of the age appropriate instruments listed in Table 3.1. TIQ and DQ scores were analysed together as raw scores as described in Section 3.6. Patient records were also searched to find out whether the child had an established diagnosis of an ID. When the patient's paediatrician, paediatric neurologist, or paediatric neuropsychologist had documented a diagnosis of an ID or the child had documented special educational needs due to an ID, they were assigned to the cognitive impairment category. If the patient's medical records documented that there were no concerns regarding their learning, education, or development, they were assigned to the no cognitive impairment category. When this information was not documented in the patient's record, this was treated as missing data, and the child was not assigned to either group.

To assess the relationships between structural network measures and cognition in children investigated for seizures, the calculated network measures were compared between the group with cognitive impairment and the group without. Network measures were also compared directly with IQ scores in the patients in whom these were available. Global network measures were compared between the two groups. Network findings were also compared between the different types of networks. The influence of epilepsy characteristics on the association between structural network measures and cognition was also assessed in the DTI networks. Statistical testing was carried out in MATLAB and R as described in Section 3.9.

4.5 Results

4.5.1 Description of the suspected epilepsy cohort

4.5.1.1 Creation of the cohort

Between 2004 and 2009, 130 children underwent the epilepsy protocol MRI for investigation of suspected seizures and their details were entered into a research database. This database was

interrogated to establish which patients could be included in the present study. Patients under the age of one (n=9) or over the age of 18 (n=1) at the time of the MRI were excluded. MRI scans were reviewed and those whose MRI scans were not found on the PACS system at the UMCU (n=6), those with bilateral pathology on imaging (n=5), and those whose imaging had artefacts preventing analysis (n=4) were also excluded. Examples of artefacts leading to exclusion from this study are shown in Figure 3.1. Patients with bilateral pathology preventing reasonable interpretation of grey and white matter segmentations or cortical parcellations, such as multiple cortical or subcortical tubers, widespread white matter signal changes, and extensive infarcts were excluded due to difficulty establishing the boundary between grey and white matter. The presence of lissencephaly or extensive perinatal infarcts leading to altered patterns of sulcal and gyral folding led to inaccurate cortical parcellation, and these patients were also excluded. Examples of imaging findings leading to exclusion due to pathological findings on MRI are shown in Figure 3.4. Reasons for exclusion from this cohort are displayed in the patient flow diagram in Figure 4.1. In total 105 patients were included in the suspected epilepsy cohort.

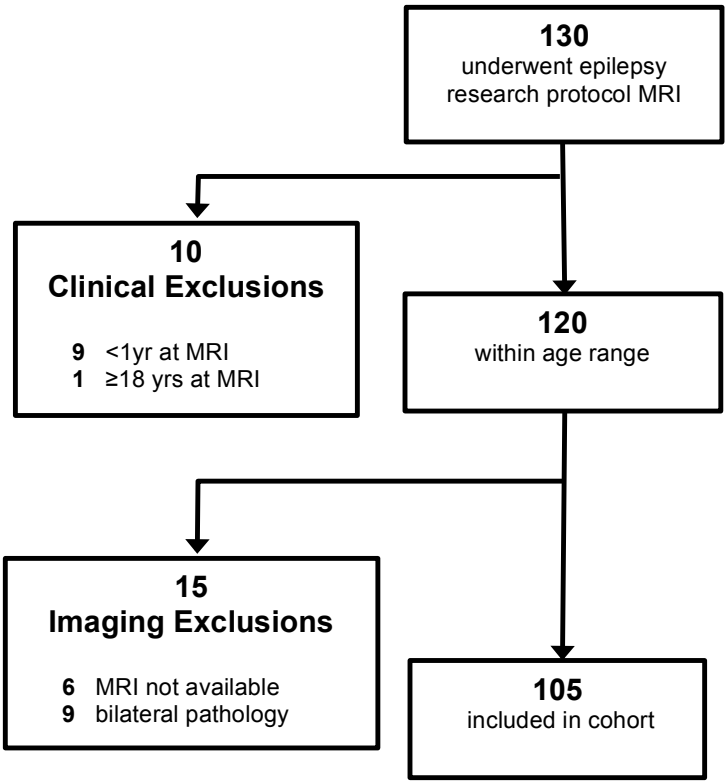

Figure 4.1: ***Paediatric epilepsy cohort.*** *Numbers of patients initially identified and consecutively scanned with the research MRI protocol. The flow diagram shows the reasons for exclusion from the cohort.*

4.5.1.2 Demographics

The cohort consists of 62 (59%) males and 43 females (41%). At the time of undergoing MRI, patients were aged between one year and 17 years. The median age was 6 years and the age range distribution is shown in Figure 4.2.

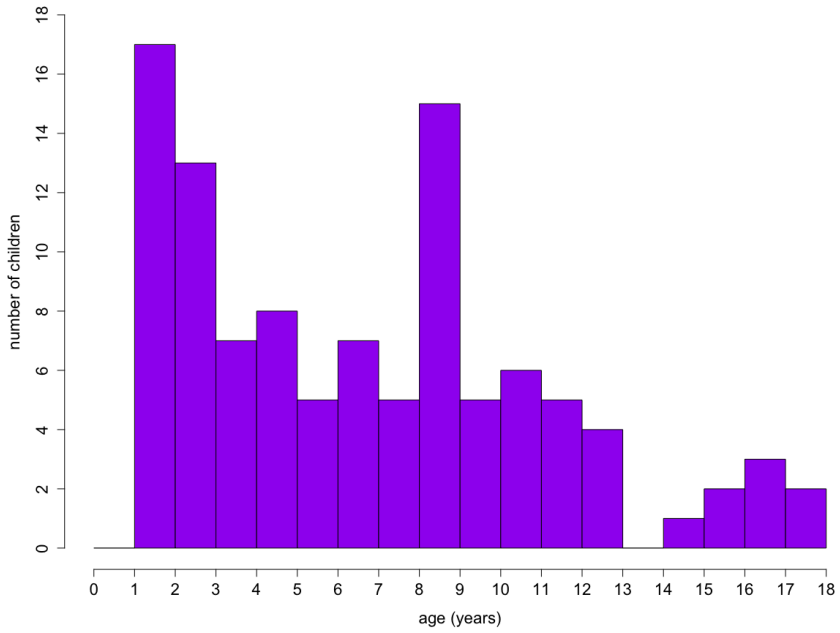

Figure 4.2: ***Age at MRI.*** *Age distribution at the time of undergoing MRI (MRI: magnetic resonance imaging)*

4.5.1.3 Clinical characteristics

The date of first seizure, or the date of the first event thought to be a seizure was available for 90 (86%) patients. In the remaining patients, the date of the event was not documented in the medical notes. All events investigated as seizures are referred to as seizures in the following graphs and tables. Patients were between 1 day old and 16 years old at the time of their first seizure. The median age at first seizure was one year and the distribution of the age at first seizure is shown in Figure 4.3.

The time interval between the first seizure and the MRI scan ranged from 4 days to 11 years. In some children this MRI was the first investigation for seizures, whereas others had undergone multiple previous investigations. The median duration between the first seizure and the MRI scan was 18 months, and 52 (58%) patients had undergone the epilepsy protocol MRI scan within one year of their first seizure. The interval between first seizure and MRI is shown in Figure 4.4.

Data on seizure frequency at the time of MRI scanning was available for all patients. Thirty-two (30%) patients were experiencing daily seizures and 39 (40%) were seizure free. Seizure frequency for the remainder is shown in Figure 4.5. Seizure freedom was defined as having only had one event with no further events, or having been on AEDs and free of seizures for the last six months.

The number of AEDs being taken at the time of the MRI was available for 93 patients. Data for the remainder were not available in the patient records. The number of AEDs ranged from zero to four. The largest number of patients (34, 37%) were not taking any AEDs. The distribution of the number of AEDs being taken by each patient is shown in Figure 4.6. No patients had stopped taking AEDs so all patients who were not taking any AEDs at the time of the MRI had not started AED therapy.

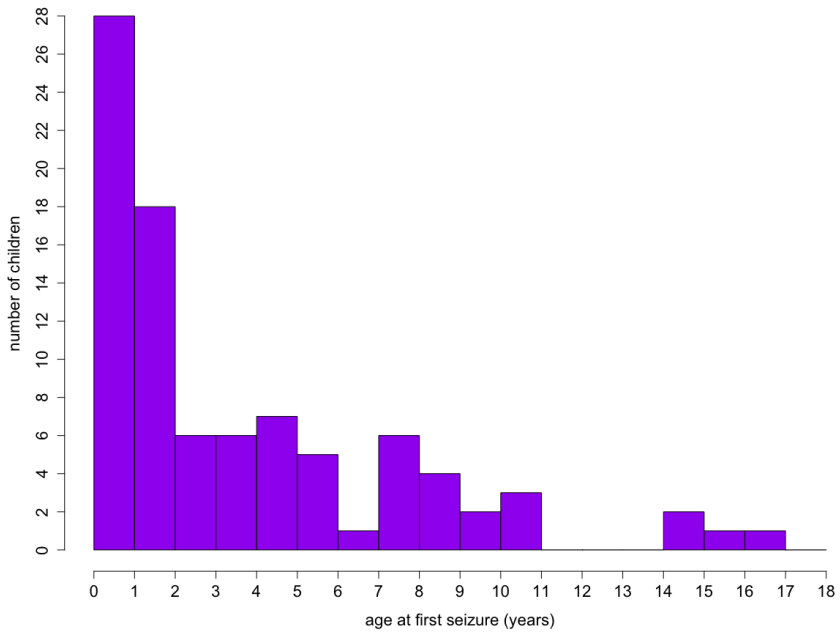

Figure 4.3: ***Age at first seizure.*** *Age in years at the time of the first seizure.*

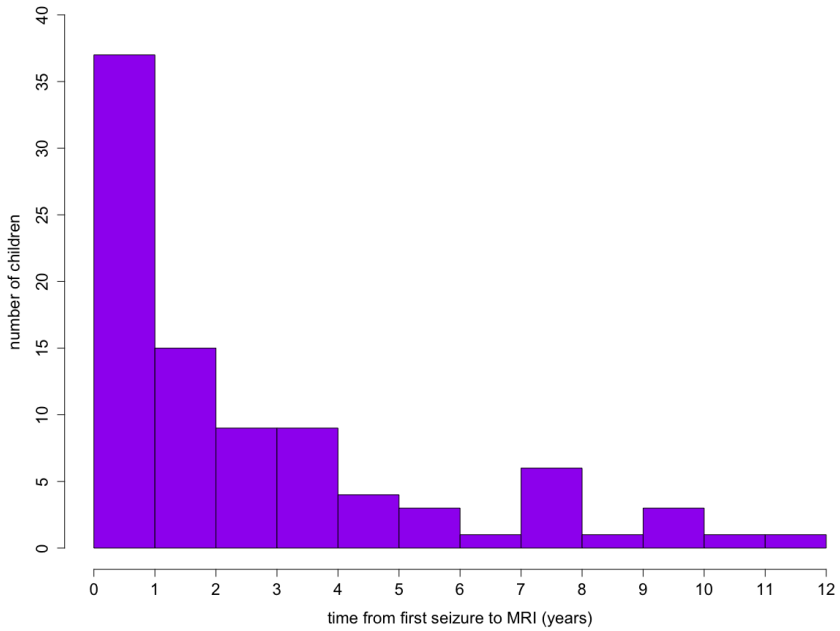

Figure 4.4: ***Time interval from first seizure to MRI.*** *Number of years from the first seizure to the time of MRI scanning (MRI: magnetic resonance imaging)*

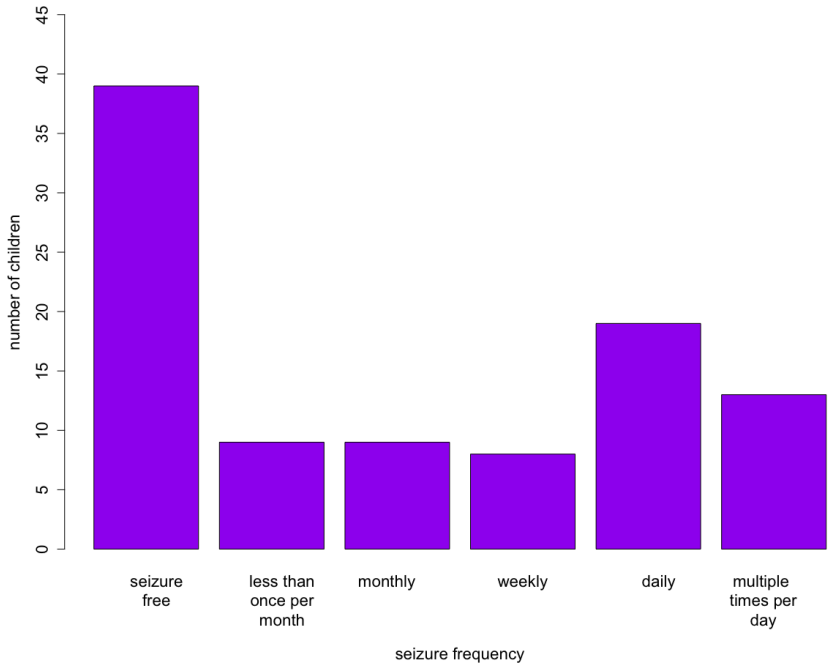

Figure 4.5: ***Seizure frequency.*** *Reported seizure frequency at the time the MRI scan was undertaken. (MRI: magnetic resonance imaging*

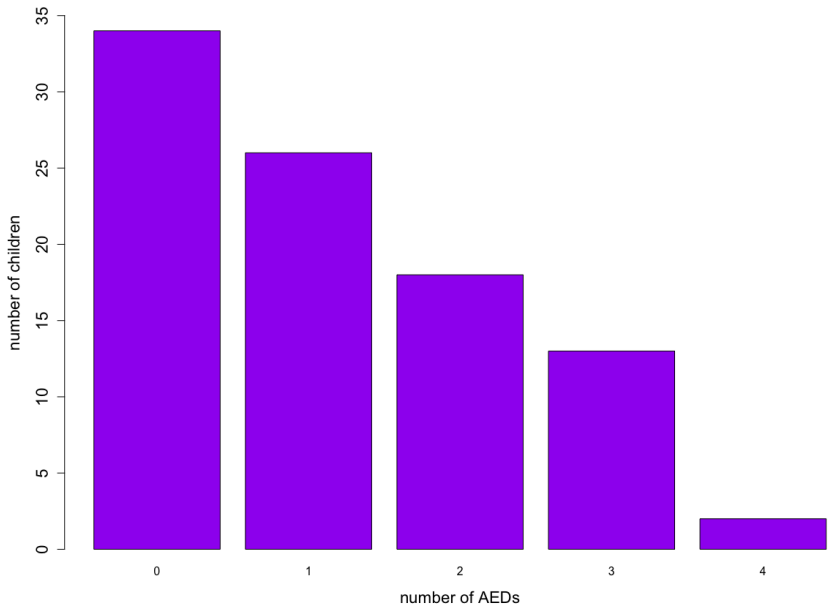

Figure 4.6: ***Number of AEDs.*** *The number of AEDs being taken at the time of MRI scanning (AED: anti-epileptic drug; MRI: magnetic resonance imaging)*

Twenty four (23%) patients had focal onset seizures, 69 (66%) patients had generalised onset seizures, and 12 (11%) patients were being investigated for episodes thought to be possible seizures, but the diagnosis was unclear at the time of scanning. Of the 24 patients with focal onset seizures, 11 had right sided onset and 13 had left sided onset. The side of onset was concordant on EEG, clinical semiology, and MRI in all cases. Aetiology of the focal onset seizures is shown in Table 4.1. In the MRI negative group, one patient had a small lesion in the ipsilateral globus pallidus not thought to be responsible for seizures, and one patient had an old infarct in the contralateral hemisphere to that likely to be responsible for seizures on EEG and clinical semiology. The remaining eight patients had normal MRI scans. Of the 69 patients with generalised onset seizures, 10 (15%) patients had experienced multiple febrile seizures (FS) or febrile status epilepticus. Aetiology of the remaining 59 generalised onset seizures is shown in Table 4.2. Genetic causes included one patient with an SCN1a mutation. Metabolic causes included two patients with mitochondrial disorders. Sixteen patients with generalised onset seizures had been diagnosed with electroclinical syndromes. These included benign epilepsy with centrotemporal spikes (BECTS)(1), epileptic encephalopathy with continuous spike-and-wave during sleep (CSWS)(1), CAE(2), epilepsy with myoclonic atonic seizures(1), FS plus(1), Lennox-Gastaut syndrome (LGS)(4), myoclonic epilepsy in infancy (MEI)(4), and mesial temporal sclerosis (MTS) on MRI with generalised onset seizures(2). Fifty-three (77%) of the 69 patients with generalised onset seizures had normal MRI scans, 7 (10%) patients had bilateral structural MRI abnormalities, and 9 (13%) patients had unilateral MRI abnormalities. These MRI abnormalities are described below in Section 4.5.1.5 and were not thought to be the direct cause of the seizures.

	Side	
Aetiology	Left	Right
Tumour	3	3
Focal Cortical Dysplasia	2	2
Hemimegalencephaly	1	0
Infarction	0	1
Mesial Temporal Sclerosis	1	0
MRI negative	6	5
Total	13	11

Table 4.1: ***Causes of focal onset seizures.*** *Frequency of each aetiology within the cohort.*

4.5.1.4 Neuropsychology

The results of neuropsychological assessment were available for 47 (45%) patients. Of these, nine had been unable to complete an IQ test due to severe cognitive impairment. The remaining 38 patients had achieved an IQ or DQ score following assessment. The distribution of IQ scores is shown in Figure 4.7, and the tests undertaken are listed in Table 4.3.

Forty-six (44%) patients had a documented diagnosis of an ID in their medical records or attended a school for children with special educational needs. These children formed the group with cognitive impairment. Fifty-two (50%) children were documented to have no concerns about their intellectual

Aetiology	
Genetic	3
Tuberous Sclerosis	4
Sturge-Weber	1
Infective	2
Infarction	1
Metabolic	5
Encephalopathy	2
Unknown	41
Total	59

Table 4.2: ***Causes of generalised onset seizures.*** *Frequency of each aetiology within the cohort.*

development or function at school or had achieved a score on an IQ test within two standard deviations of the population mean, and these formed the group without cognitive impairment. In 7 (7%) patients, there was no documentation in the child's medical records regarding their intellectual or cognitive function or progress at school and no documentation of a neuropsychological assessment. These children were excluded from the analyses of cognition.

The group without cognitive impairment had a mean IQ or DQ score of 91 points (SD:11) and the group with cognitive impairment had a mean IQ or DQ score of 60 points (SD:9). As expected, there was a statistically significant difference in IQ between these two groups ($p<0.001$). The group with cognitive impairment were younger at the time of imaging ($p=0.002$), younger at onset of epilepsy ($p=0.009$), had a longer duration between the time of the first seizure and the MRI ($p=0.03$), were more likely to be experiencing daily seizures ($p=0.001$), and more likely to be taking AEDs ($p=0.018$). There was no difference in the number of female patients or whether seizures were of focal or generalised onset between those with and without cognitive impairment.

Name of Assessment	Number of Children
Bayley Scales of Infant Development (BSID)	8
Wechsler Intelligence Scales for Children (WISC)	17
Snijders-Oomen Niet-verbale Intelligentietest (SON)	6
Wechsler Preschool and Primary Scales of Intelligence (WPPSI)	1
Kaufman Adolescent and Adult Intelligence Test (KAIT)	1
Unknown	5
Total	38

Table 4.3: ***Neuropsychological tests.*** *Frequency of use of each neuropsychological assessment in this cohort.*

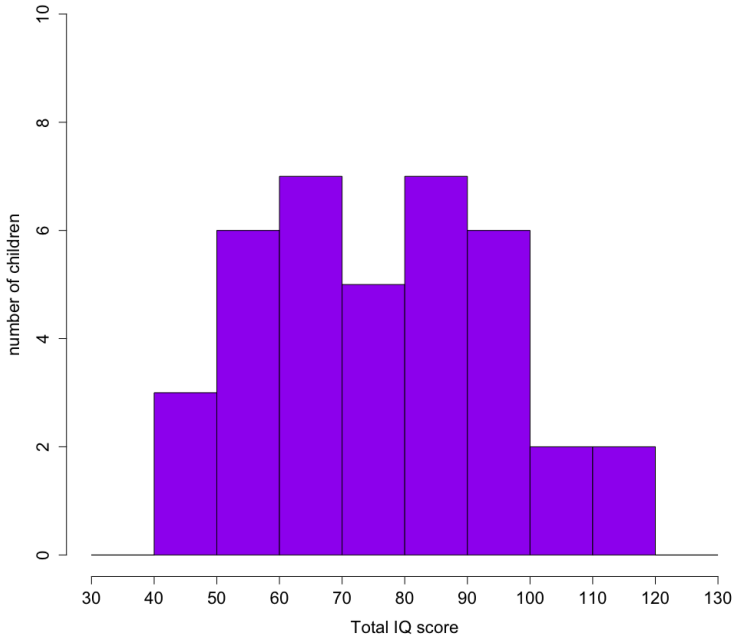

Figure 4.7: ***Total IQ score.*** *Distribution of combined total IQ and DQ scores of patients tested. (IQ: intelligence quotient; DQ: development quotient)*

4.5.1.5 MRI processing

Eighty-one (77%) MRI scans were acquired under general anaesthetic (GA). Seventy-two (69%) MRI scans were reported as being within normal limits, 16 (15%) had an abnormality limited to the right hemisphere, 10 (10%) had an abnormality limited to the left hemisphere, and 7 (7%) had bilateral or midline abnormalities involving both hemispheres. Of the 26 patients with unilateral abnormalities, 6 were limited to within a single lobe, 3 were multilobar, and 17 were hemispheric. Abnormalities that were likely causes of seizures are described in Section 4.5.1.3. In addition, 11 patients had corpus callosum abnormalities, and eight patients had small areas of white matter signal change. Arachnoid cysts were classified as normal variants.

Thirty (29%) MRI scans did not require manual intervention of the Freesurfer processing stream to achieve accurate segmentation and cortical parcellation. However, one scan required manual registration, 44 scans required manual editing of the brain mask after adjusting the skull strip settings, and 58 scans required editing of the white matter template using either control points or manual editing. Examples of manual editing of Freesurfer segmentations of MRI scans are shown in Figure 3.2 and Figure 3.3, and the descriptions of how scans were manually edited are in Section 3.7.2.

After manual editing, there were 100 MRI scans with accurate whole brain segmentations and parcellations. However, in 15 cases pathology interfered with accurate cortical thickness measurements in one hemisphere (6 left, 9 right). These 15 cases were excluded from whole brain cortical thickness analyses. The 11 patients with corpus callosum abnormalities were also excluded due to the large

influence of the corpus callosum on whole brain network characteristics. This left 85 patients for the whole brain cortical thickness analyses (see Figure 4.8).

Ninety-two patients had accurate parcellations and DTI of sufficient quality and accuracy to calculate DTI based connectomes. In 6 patients the DTI sequence was not acquired, and in 13 patients the DTI or freesurfer parcellations were not of sufficient quality to create connectomes. A further 12 patients were excluded due to pathology interfering with accurate connectome creation, or due to corpus callosum abnormalities. This left 80 patients for whole brain DTI connectome analyses (see Figure 4.8).

Some patients with inaccurate grey-white boundary approximations and inaccurate cortical thickness measurements had accurate regional parcellations and could be included in the DTI network analysis, and some patients who did not have the DTI sequence acquired had accurate cortical thickness measurements and could be included in the cortical thickness network analysis. Therefore, the group for cortical thickness analysis and the group for DTI analysis included different but overlapping groups of patients. The number of participants who were included in each type of network analysis and the reasons for exclusions are shown in Figure 4.8.

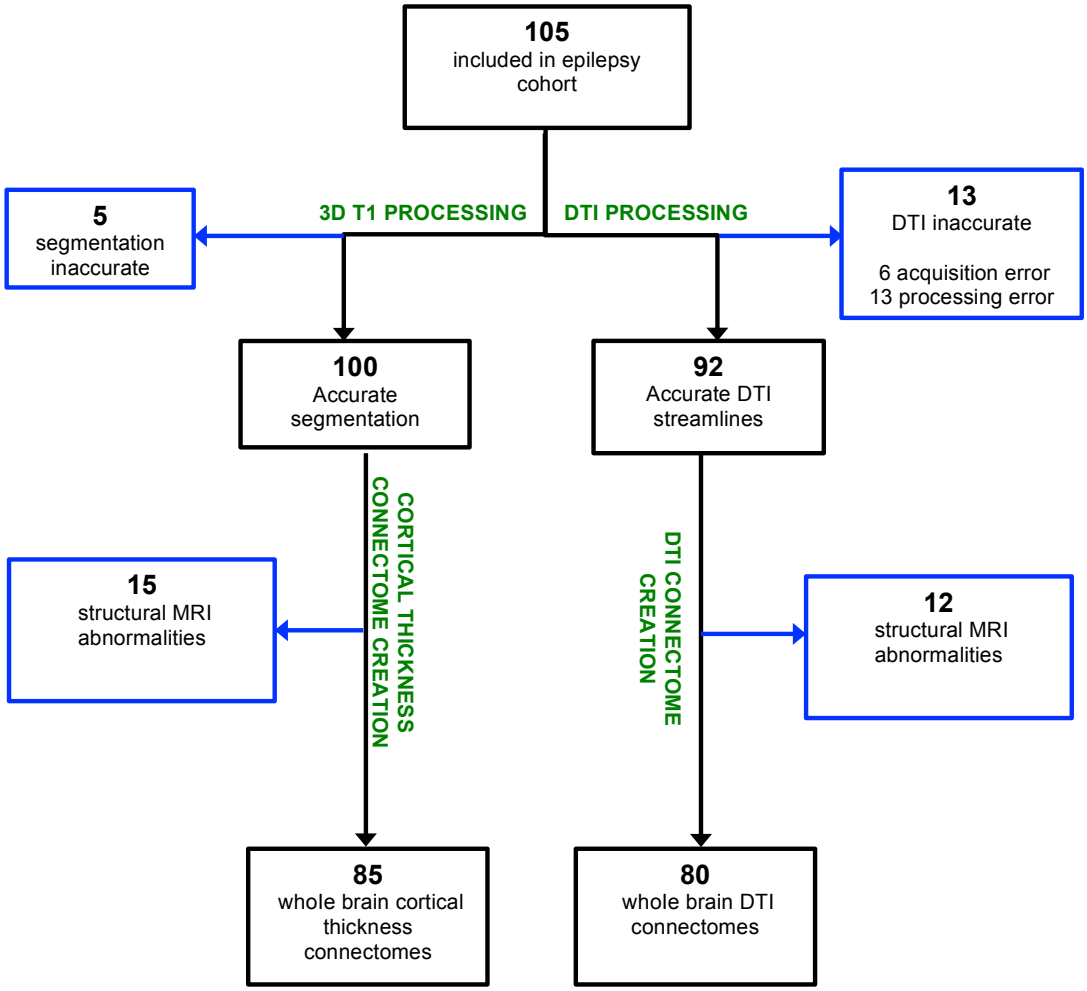

Figure 4.8: ***Image processing and exclusions.*** *Image processing pipeline and reasons for exclusions at each stage.*

4.5.2 Is cognitive impairment associated with structural network organisation in children with suspected epilepsy?

To assess whether structural network organisation differs between children with and without cognitive impairment, the suspected epilepsy cohort were divided into two groups. One group has a diagnosis of cognitive impairment and the other does not. Patients whose cognitive status was unknown were excluded from this analysis. First DTI derived connectomes were examined, and then cortical thickness derived connectomes.

4.5.2.1 Are DTI derived networks different in those with and without cognitive impairment?

Of the 80 patients with reliable DTI whole brain networks (see Figure 4.8), seven did not have information available regarding cognitive function, 30 (41%) patients had cognitive impairment as determined by a formal diagnosis of an ID or special educational needs, and 43 (59%) had normal cognitive function reported. The demographic and clinical features of these two groups are shown in Table 4.4. The group with cognitive impairment were younger at the time of their first seizure and were more likely to have daily or more frequent seizures. As expected, the group with cognitive impairment had lower IQ scores.

	Group		*p*
	cognitive impairment *n=30*	cognition intact *n=43*	
Female	18 (58%)	20 (48%)	*0.518*
Age at MRI (years)	5.3 (6.9)	5.5 (6.2)	*0.274*
Age at first seizure (years)	1.1 (3.0)	3.2 (5.9)	*0.004*
Interval from first seizure to MRI (months)	28.0 (37.8)	15.0 (42.3)	*0.374*
Daily or more frequent seizures	15 (48%)	5 (12%)	*0.001*
Number of AEDs	1.0 (1.0)	1.0 (2.0)	*0.087*
Focal onset seizures	8 (26%)	9 (21%)	*0.875*
Structural abnormality	13 (42%)	14 (33%)	*0.612*
IQ	59.0 (13.8)	92.5 (16.3)	*$<$0.001*

Table 4.4: ***DTI networks: demographic and clinical features by presence of cognitive impairment.*** *Comparison of demographic and clinical features between those with intact cognition and those with cognitive impairment. Data are count (percentage) for categorical data and median (interquartile range (IQR)) for numerical data except IQ which is mean (SD). Significance testing was carried out using X^2 tests for categorical data, Mann-Whitney U tests for numerical data except IQ, and t-tests for IQ. (AED: Anti-epileptic drug; IQ: total intelligence quotient; MRI: magnetic resonance imaging; IQR: interquartile range, SD: standard deviation)*

Global network characteristics were calculated for each individual patient network as described in Section 3.8.2. Network measures were calculated for networks derived from both the NOS and the FA averaged along the streamlines. NOS networks were initially examined using the raw NOS counts

without any adjustment of edge weights. Global metrics for the weighted networks for the groups with and without cognitive impairment are shown in Table 4.5. Patients with intact cognition had significantly higher network density, average node degree and average network strength in both the FA and the NOS networks. Average edge weight was statistically significantly higher in the group with intact cognition in the FA networks only. L was statistically significantly higher and network global efficiency was statistically significantly lower in the group with cognitive impairment in both types of network. When path length was normalised through comparison with random networks with the same number of nodes and edges to λ there was still a statistically significant difference between groups. The raw clustering coefficient was slightly higher in the group with intact cognition in the FA weighted networks only, but after normalisation of the C through comparison with random networks with the same numbers of nodes and edges to γ, clustering was statistically significantly higher in the group with cognitive impairment in both the FA and the NOS networks. All networks showed a small world organisation with γ greater than λ and $\sigma > 1$. The small world index was not significantly different between the two groups.

	FA			NOS		
	cognitive impairment	cognition intact	*p*	cognitive impairment	cognition intact	*p*
density	0.19 (0.01)	0.21 (0.02)	*0.001*	0.20 (0.01)	0.21 (0.02)	*0.002*
degree	16.2 (1.16)	17.4 (1.78)	*0.001*	16.4 (1.15)	17.6 (1.74)	*0.002*
S	5.86 (0.67)	6.65 (0.79)	*<0.001*	3222 (534)	3763 (878)	*0.003*
EW	0.36 (0.02)	0.38 (0.02)	*<0.001*	196 (29)	215 (55)	*0.077*
L	5.25 (0.44)	4.76 (0.34)	*<0.001*	0.01 (0.003)	0.01 (0.002)	*0.002*
λ	1.15 (0.03)	1.12 (0.03)	*<0.001*	1.48 (0.30)	1.33 (0.22)	*0.031*
C	0.27 (0.02)	0.28 (0.03)	*0.045*	0.02 (0.406)	0.02 (0.004)	*0.521*
γ	2.00 (0.24)	1.88 (0.20)	*0.031*	3.22 (0.34)	3.05 (0.24)	*0.031*
σ	1.75 (0.21)	1.68 (0.18)	*0.128*	2.23 (0.35)	2.32 (0.26)	*0.237*
E_{Glob}	0.22 (0.02)	0.24 (0.02)	*<0.001*	167 (30)	201 (44)	*0.002*

Table 4.5: ***Weighted DTI networks: global network characteristics by cognitive impairment.*** *Comparison of global network characteristics between those with cognitive impairment and those with intact cognition calculated from the weighted FA and NOS networks. Data are mean (SD). Statistical testing was carried out using t-tests and p values are adjusted using the FDR set at 5% for 32 comparisons (16 network measures - binary and weighted, and 2 network types). Adjusted p values are reported in the table. (FA: fractional anisotropy; NOS: number of streamlines; S: average network strength; EW: mean edge weight; L: average path length; λ: normalised average path length; C: clustering coefficient; γ: normalised clustering coefficient; σ: small worldness statistic; E_{Glob}: global efficiency; SD: standard deviation; FDR: false discovery rate)*

4.5.2.2 Which aspects of network structure account for the differences in DTI derived network organisation between those with and without cognitive impairment?

The group with cognitive impairment has lower mean density, degree, and strength. Average path lengths decrease and clustering coefficients increase with increasing network density, increasing network average strength and increasing average edge weights.[52] Correction to the normalised metrics

(λ and γ) partly corrects the path length and clustering coefficient by normalising to random networks of the same number of nodes and edges. However, this does not account for differences in network strength and edge weights in the weighted networks. To assess whether differences in path length and clustering between the groups are due to the differences in overall number and strength of edges, binary networks were created as described in Section 3.8.2. Analysing binary networks removes the influence of edge weights and therefore node strengths, but maintains edge arrangements and number. Correction of L and C to λ and γ in binary networks does account for the number of edges per node.

Binary network metrics are shown in Table 4.6. The group with cognitive impairment has statistically significantly higher L and λ and lower global efficiency in both the FA and NOS networks than the group with intact cognition. There are no differences in C between groups, but γ is statistically significantly higher in the group with cognitive impairment. The small world index (σ) is just statistically significantly higher in the group with cognitive impairment. As λ is higher in the group with cognitive impairment and σ is calculated from the ratio of γ to λ, this difference in σ must be attributable to a greater increase in γ than λ in the group with cognitive impairment. Normalisation of C to γ using values from random networks is less effective than normalisation of L to λ when networks show a small world organisation because in small world networks, whilst L is similar to random networks, C is more similar to lattice networks, and is therefore not well corrected by comparison to random networks.[52] Therefore, the differences between groups in γ may be spuriously created by the normalisation procedure, but the between group differences in L and λ are robust.

	FA			NOS		
	cognitive impairment	cognition intact	*p*	cognitive impairment	cognition intact	*p*
density	0.19 (0.01)	0.21 (0.02)	*0.002*	0.20 (0.01)	0.21 (0.02)	*0.002*
degree	16.2 (1.16)	17.4 (1.78)	*0.002*	16.4 (1.15)	17.6 (1.74)	*0.002*
L	2.10 (0.07)	2.04 (0.09)	*0.002*	2.10 (0.07)	2.04 (0.08)	*0.002*
λ	1.12 (0.02)	1.10 (0.02)	*0.002*	1.12 (0.02)	1.10 (0.02)	*0.002*
C	0.60 (0.02)	0.61 (0.01)	*0.534*	0.61 (0.01)	0.61 (0.01)	*0.356*
γ	2.13 (0.24)	2.00 (0.21)	*0.020*	2.14 (0.24)	2.01 (0.21)	*0.025*
σ	1.90 (0.19)	1.81 (0.16)	*0.040*	1.90 (0.19)	1.82 (0.16)	*0.046*
E_{Glob}	0.55 (0.02)	0.56(0.02)	*0.002*	0.55 (0.02)	0.56 (0.02)	*0.002*

Table 4.6: ***Binary DTI networks: global network characteristics by cognitive impairment.*** *Comparison of global network characteristics between those with cognitive impairment and those with intact cognition calculated from binarisation of the FA and NOS networks. Data are mean (SD). Statistical testing was carried out using t-tests and p values were adjusted using the FDR set at 5% for 32 comparisons (16 network measures - binary and weighted, and 2 network types). Adjusted p values are reported in the table. (FA: fractional anisotropy; NOS: number of streamlines; L: average path length; λ: normalised average path length; C: clustering coefficient; γ: normalised clustering coefficient; σ: small worldness statistic; E_{Glob}: global efficiency; SD: standard deviation; FDR: false discovery rate)*

An alternative method of investigating whether the node strengths and the edge weights play a part in determining the differences in network path lengths, global efficiency, and clustering between groups, is

to investigate whether changing the magnitude and distribution of network weights alters the findings. To do this, the NOS counts were normalised to be between zero and one and to follow a normal distribution as described in Section 3.8.2. Global network measures following normalisation of the NOS counts are shown in Table 4.7. After normalisation of streamline counts, there were no differences in mean network strength, edge weight, L, C, or global efficiency between the group with cognitive impairment and the group without. As the group differences in path length and clustering disappear when the group networks are adjusted to have similar edge weights and mean network strength, differences between groups may be attributable to differences in group network mean edge weights and overall node strengths. However, normalising the edge weights could also be a method of artificially removing the group differences in strength and edge weight through adjusting the network organisation.

	NOS		
	cognitive impairment	cognition intact	*p*
S	0.87 (0.16)	0.91 (0.17)	*0.359*
EW	0.05 (0.01)	0.05 (0.01)	*0.606*
L	38.2 (10.4)	33.4 (11.4)	*0.132*
C	0.02 (0.004)	0.02 (0.004)	*0.579*
E_{Glob}	0.05 (0.01)	0.05 (0.01)	*0.136*

Table 4.7: ***DTI networks: global weighted network characteristics of NOS networks after normalisation by cognitive impairment.*** *Comparison of global network characteristics between the those with cognitive impairment and those who are cognitively intact calculated from the weighted NOS networks after normalisation of network strengths. Data are displayed as mean (SD). Statistical testing was carried out using t-tests and p values were adjusted using FDR correction at 5% by substituting these values for those in Table 4.5. (FA: fractional anisotropy; NOS: number of streamlines; DTI: diffusion tensor imaging; S: average network strength; EW: mean edge weight; L: average path length; C: clustering coefficient; E_{Glob}: global efficiency; SD: standard deviation; FDR: false discovery rate)*

As there is no completely reliable method of correcting for differences in network degree, density, strength, and edge weight, an alternative method of assessing whether differences in path lengths and clustering coefficients in weighted networks are due to differences in numbers or strengths of edges or due to differences in underlying network topology was also investigated. Linear regressions with λ or γ as the dependent variable were performed using mean edge weight and presence of cognitive impairment as predictors for the weighted networks. Mean edge weight was added first as a predictor, and cognitive impairment second and the reduction in the residual sum of squares was assessed using the F statistic to compare the mean sum of squares to the residual mean sum of squares. Models for the weighted networks are shown in Table 4.8. Mean edge weight was chosen as the comparator as it reflects the overall number and strength of edges within the network. In both the FA and the NOS networks there is a statistically significant effect of adding the diagnosis of cognitive impairment as a predictor to λ, suggesting that there may be a difference in path length between the groups that is not accounted for by differences in total edge weight in the network. Models were also created using the mean edge weight from the NOS networks after normalisation of the edge weights. There was a significant effect of adding the cognitive impairment diagnosis to the models for both λ and γ in these

models. Therefore, mean edge weight of the network may not account for all of the differences in weighted λ and γ between the networks of the groups with and without cognitive impairment and weight placement and differing network organisation or topology may also be important.

	FA weighted			NOS weighted		
	sum squares	F	*p*	sum squares	F	*p*
λ						
EW	0.003	3.95	*0.051*	0.491	8.54	*0.005*
Cognitive Impairment	0.006	7.21	*0.009*	0.640	11.1	*0.001*
γ						
EW	0.565	13.4	*<0.001*	0.015	0.17	*0.678*
Cognitive Impairment	0.033	0.77	*0.381*	0.595	7.08	*0.009*

Table 4.8: ***DTI weighted networks: effect of cognitive impairment on association between mean edge weight and path length or clustering coefficient.*** *Linear regression modelling using λ, and γ as dependent variables and EW and the presence of cognitive impairment as predictors. Type I sums of squares were calculated for addition of cognitive impairment to EW as a predictor variable. (FA: fractional anisotropy; NOS: number of streamlines; EW: mean edge weight; DTI: Diffusion Tensor Imaging; γ: normalised clustering coefficient; λ: normalised path length)*

4.5.2.3 Conclusions regarding DTI network organisation in those with and without cognitive impairment

In conclusion, the group with cognitive impairment consistently showed a lower network density, degree, and global efficiency and higher L and λ in the binary networks, and a lower network strength, mean edge weight, L and λ in the weighted networks. Findings for the clustering coefficient were inconsistent across network construction and analysis methods. When the overall number of nodes and edges was taken into account by normalising L to λ, the group difference in path length remained. When network mean edge weight was regressed in a linear model the association between weighted λ and cognitive dysfunction remained. Therefore, although there may be a contribution to the group differences of the overall differences in number and weights of edges, there is evidence that the group differences in path lengths cannot be completely explained by these differences, and may be due to different topology of the networks between the groups.

4.5.2.4 Are cortical thickness derived networks different in those with and without cognitive impairment?

There were 85 patients with reliable cortical thickness measurements and cortical parcellations as described in Section 4.5.1.5 and in Figures 4.1 and 4.8. Seven of these patients did not have information available regarding whether or not they had cognitive impairment. Of the other 78 patients, 30 (39%) patients had documentation of cognitive impairment as described in Section 3.6 and the records of 48 (62%) patients documented normal cognitive function. The demographic and clinical features of the patients with cognitive impairment compared to those with intact cognition are shown in

Table 4.9. The group with cognitive impairment had no significant differences in their seizure characteristics compared to the group with intact cognition. This contrasts with the findings in Table 4.4 which compares the patients with and without cognitive impairment who have DTI networks for analysis. In the cohort investigated with DTI derived networks, the group with cognitive impairment had a higher likelihood of daily seizures and were younger at the age of their first seizure. In this group of patients with cortical thickness connectomes available, there are only non-significant trends for a lower age at first seizure and more frequent seizures in those with cognitive impairment.

	Group		*p*
	cognitive impairment *n=30*	cognition intact *n=48*	
Female	14 (46.7%)	22 (45.8%)	*1.00*
Age at MRI (years)	6.6 (7.2)	6.0 (6.2)	*0.914*
Age at first seizure (years)	1.3 (4.7)	3.0 (5.9)	*0.129*
Interval from first seizure to MRI	19.0 (32.0)	14.0 (32.3)	*0.450*
Daily or more frequent seizures	11 (36.7%)	8 (16.7%)	*0.083*
Number of AEDs	1.0 (2.0)	1.0 (2.0)	*0.089*
Focal onset seizures	3 (10.0%)	9 (18.8%)	*0.472*
Structural abnormality	9 (30.0%)	13 (27.1%)	*0.984*
IQ	59.0 (9.5)	91.0 (14.8)	*<0.001*

Table 4.9: ***Cortical thickness networks: demographic and clinical features by presence of cognitive impairment.*** *Comparison of demographic and clinical features between those with and without cognitive impairment. Data are count (percentage) for categorical data and median (IQR) for numerical data. Statistical testing was carried out using X^2 tests for categorical data and Mann-Whitney U tests for all numerical data except IQ, and t-tests for IQ. (AED: anti-epileptic drug; IQ: total intelligence quotient; MRI: magnetic resonance imaging; IQR: interquartile range)*

Group cortical thickness binary and weighted networks were constructed from both raw cortical thickness measurements and from the residual cortical thickness measurement after regressing the effects of age and sex in a linear model as described in Section 3.8.1.1. Networks were thresholded using a range of both proportional and absolute thresholds at 0.1 intervals from zero to one as described in Section 3.8.1.1. Networks were analysed after thresholding to find the lowest density at which the network remained fully connected to allow investigation of average path lengths and as described in previous analyses of cortical thickness connectomes.[83,173] The degree of each node in the network plotted against network density across the range of thresholds for networks constructed from raw cortical thickness measurements are shown in Figure 4.9 and Figure 4.10. The group network for the group with cognitive impairment is fully connected at lower densities than the group network for those with intact cognition following both methods of network construction using both raw cortical thickness values and age and sex corrected values. At a density of 0.7 or above, all networks were fully connected. To ensure that both groups had fully connected networks, global graph metrics were calculated at a proportional threshold that maintained the top 70% of edge weights and maintained a fixed network density of 0.7, and at an absolute threshold of 0.3 as removing all edges below 0.3 did not

cause the networks to disconnect.

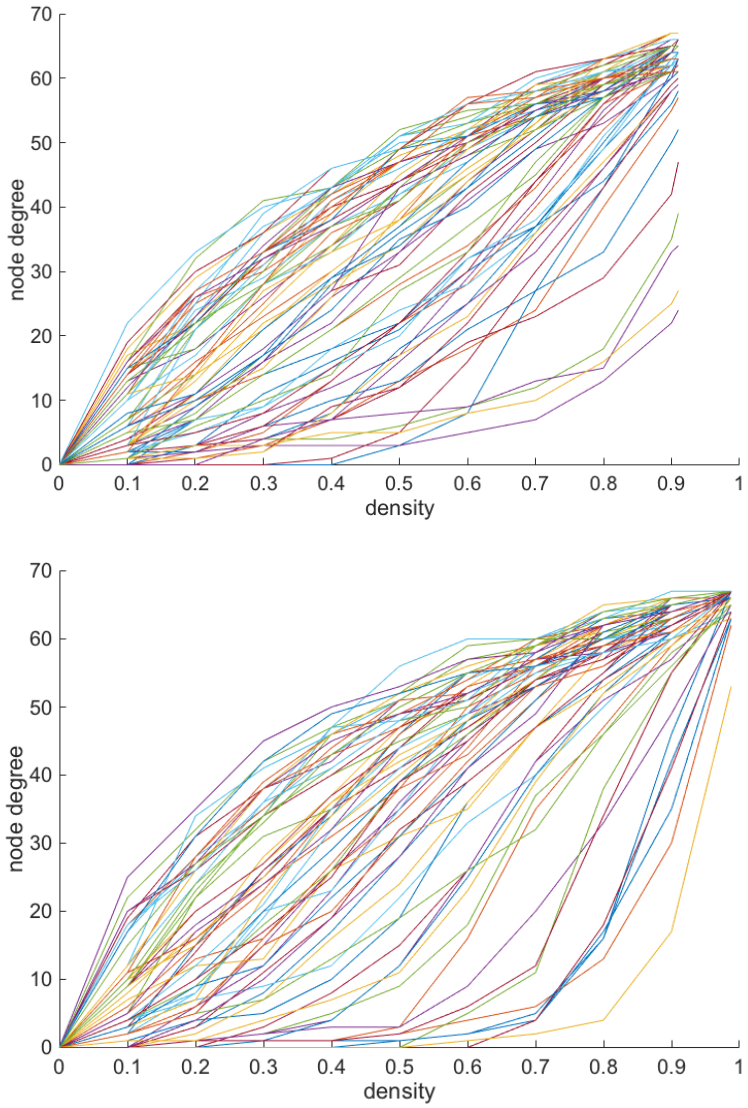

Figure 4.9: ***Node degree after proportional thresholding of raw cortical thickness networks.*** *The degree of each node is plotted against network density after applying proportional thresholds between zero and one to keep the top proportion of edge weights.* ***Top:*** *group network for those with cognitive impairment.* ***Bottom:*** *group network for those with intact cognition. Networks disconnect at lower densities in those with cognitive impairment.*

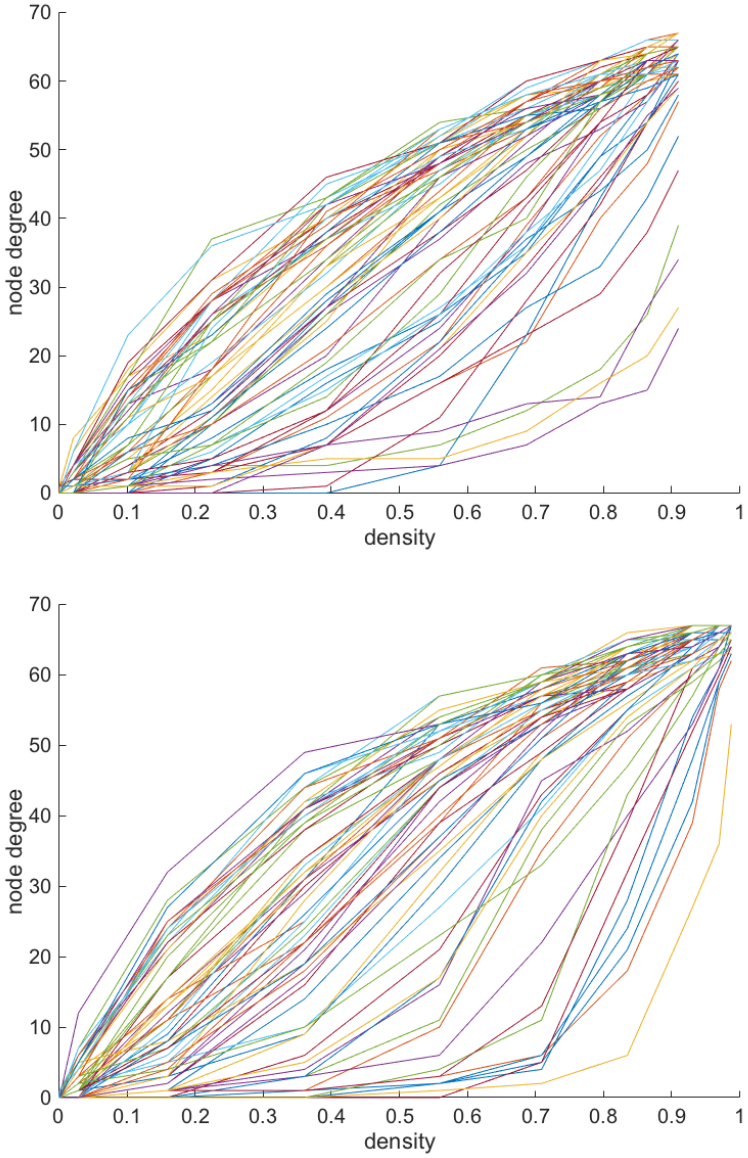

Figure 4.10: ***Node degree after absolute thresholding of raw cortical thickness networks.*** *The degree of each node is plotted against network density after applying an absolute threshold between zero and one to remove all edge weights lower than the threshold.* ***Top:*** *group network for those with cognitive impairment.* ***Bottom:*** *group network for those with intact cognition. Networks disconnect at lower densities in those with cognitive impairment.*

Global weighted and binary network metrics were calculated at the lowest proportional threshold that ensured both groups had fully connected networks and are shown in Table 4.10. Statistical testing was carried out using permutation tests. At a threshold that maintained the top 70% of edges, there were no significant differences between the group with cognitive impairment and the group with intact cognition in binary or weighted network strength, mean network edge weight, path length, global efficiency, clustering, or small worldness. In both the raw and age and sex corrected cortical thickness weighted networks λ was above one, but in the binary networks λ was equal to one in all groups. In all of the networks γ was around one, and σ was around one or less than one. Therefore, after proportional thresholding to maintain a density of 0.7, these networks do not show a small world organisation.

	Raw Cort.Thick.			Age & Sex Corrected Cort.Thick.		
	cognitive impairment	cognition intact	*p*	cognitive impairment	cognition intact	*p*
Binary Networks						
density	0.70	0.70	*1.00*	0.70	0.70	*1.00*
degree	46.9	46.9	*1.00*	46.9	46.9	*1.00*
L	1.31	1.31	*0.750*	1.30	1.30	*0.973*
λ	1.00	1.00	*1.00*	1.00	1.00	*0.973*
C	0.83	0.87	*0.696*	0.82	0.84	*0.973*
γ	1.02	0.96	*0.240*	1.04	1.01	*0.973*
σ	1.01	0.96	*0.640*	1.04	1.01	*0.973*
E_{Glob}	0.85	0.85	*0.750*	0.85	0.85	*0.973*
Weighted Networks						
S	24.9	28.4	*0.640*	23.0	21.9	*0.990*
EW	0.53	0.61	*0.640*	0.49	0.47	*0.990*
L	2.57	2.28	*0.640*	2.66	2.83	*0.990*
λ	1.15	1.10	*0.766*	1.11	1.11	*0.990*
C	0.48	0.55	*0.640*	0.44	0.43	*0.990*
γ	1.03	0.96	*0.640*	1.05	1.02	*0.990*
σ	0.90	0.88	*0.640*	0.95	0.92	*0.990*
E_{Glob}	0.45	0.51	*0.640*	0.43	0.40	*0.990*

Table 4.10: ***Cortical thickness networks, proportional thresholding: global network characteristics by cognitive impairment.*** *Comparison of global network characteristics between the those with cognitive impairment and those with intact cognition. Data are single values calculated from group networks with significance testing carried out using permutation of groups. The p values are adjusted for 32 multiple comparisons (16 network measures, 2 network types) using the FDR at 5%. Each network was thresholded to maintain the top 70% of edge weights. (Cort.Thick.: cortical thickness; S: average network strength; EW: mean edge weight; L: average path length; λ: normalised average path length; C: clustering coefficient; γ: normalised clustering coefficient; σ: small worldness statistic; E_{Glob}: global efficiency; FDR: false discovery rate)*

Binary and weighted global network measures after applying an absolute threshold to the networks to remove all edges with a weight of less than 0.3 are shown in Table 4.11. With the same absolute threshold applied, the density of the networks varied from 0.65 to 0.83. There were no statistically

significant differences between groups in network density or degree, but the values for density, degree, mean strength and mean edge weighted tended to be higher in the group with intact cognition, particularly in the raw cortical thickness networks. Similar to the proportionally thresholded networks, at these network densities, the thresholded networks showed a λ slightly higher than one in the weighted networks, but around one in the binary networks. These networks also had γ of around one, and σ of around one and did not show small world organisation.

	Raw Cort.Thick.			Age & Sex Corrected Cort.Thick.		
	cognitive impairment	cognition intact	*p*	cognitive impairment	cognition intact	*p*
Binary Networks						
density	0.69	0.83	*0.387*	0.65	0.66	*1.00*
degree	46.0	55.9	*0.387*	43.8	43.9	*1.00*
L	1.32	1.17	*0.387*	1.35	1.35	*1.00*
λ	1.01	1.00	*0.940*	1.00	1.00	*1.00*
C	0.83	0.92	*0.387*	0.80	0.82	*1.00*
γ	1.02	1.00	*0.940*	1.05	1.01	*1.00*
σ	1.01	1.00	*0.940*	1.05	1.01	*1.00*
E_{Glob}	0.84	0.92	*0.387*	0.83	0.83	*1.00*
Weighted Networks						
S	24.7	31.6	*0.810*	22.1	21.0	*0.990*
EW	0.54	0.57	*0.901*	0.50	0.48	*0.990*
L	2.57	2.20	*0.810*	2.66	2.84	*0.990*
λ	1.15	1.09	*0.960*	1.11	1.11	*0.990*
C	0.48	0.54	*0.810*	0.44	0.43	*0.990*
γ	1.04	1.00	*0.960*	1.07	1.02	*0.990*
σ	0.90	0.92	*0.960*	0.96	0.92	*0.990*
E_{Glob}	0.45	0.52	*0.810*	0.43	0.40	*0.990*

Table 4.11: ***Cortical thickness networks, absolute thresholding: global network characteristics by cognitive impairment.*** *Comparison of global network characteristics between the those with cognitive impairment and those with intact cognition. Data are single values calculated from group networks with significance testing carried out using permutation of groups. Adjusted p values are shown after FDR correction for 32 multiple comparisons (16 network measures, 2 network types) at 5%. All networks were thresholded to keep all edge weight values above 0.3. (Cort.Thick.: cortical thickness; S: average network strength; EW: mean edge weight; L: average path length; λ: normalised average path length; C: clustering coefficient; γ: normalised clustering coefficient; σ: small worldness statistic; E_{Glob}: global efficiency; FDR: false discovery rate)*

Because the cortical thickness group networks required high densities to maintain connected networks, and examining the networks at densities of 0.6-0.8 may not be representative of brain architecture,[43,70] and densely connected networks are known to be less likely to show a small world architecture,[70] networks were allowed to disconnect and were analysed across the range of densities from 0.1 to the full original density after removal of negative weights. Global efficiency was calculated at each threshold as this is not susceptible to the effects of network disconnections. The global efficiency of the group with

cognitive impairment compared to the group with intact cognition in the networks created from raw cortical thickness values are shown in Figure 4.11. After proportional thresholding from zero to one to maintain the top percentage of edge weights, the group with cognitive impairment have higher global efficiency across thresholds below 0.5. After applying absolute thresholds from zero to one which removed any edges with weights lower than the threshold, the group with intact cognition had a higher global efficiency. After creating 1000 random permutations of group assignments, none of the thresholds showed a significant difference using a *p* value cut off of 0.005 to account for 10 thresholds applied to the network. Global efficiency across the range of thresholded age and sex corrected networks is shown in Figure 4.12. The group with cognitive impairment appear to have slightly higher global efficiency between the thresholds of 0.1 and 0.6 in the proportionally thresholded graphs and between the thresholds of 0.2 and 0.7 in the graphs with absolute thresholds applied. However, after permutation testing, none of the thresholds showed a significant difference between groups using corrected *p* values.

Global network characteristics were also computed in sparsely thresholded networks for comparison with the network characteristics computed from the DTI networks. Network characteristics after proportional thresholding to keep only the top 20% of edge weights are shown in Table 4.12. The average path length was computed by removing infinity values from the distance matrix as described in Section 3.8.2. There were no statistically significant differences between the groups with and without cognitive impairment in strength or mean edge weight. Both L and λ were significantly higher in the raw cortical thickness networks at this threshold. In the age and sex corrected networks, only λ was significantly higher in the group with cognitive impairment. In the raw cortical thickness networks, there were no differences in C or γ between the two groups, but in the age and sex corrected networks, γ was significantly higher in the group with cognitive impairment in both the the binary and weighted networks. All of the proportionally thresholded networks at this density showed a small world organisation with γ higher than one, γ higher than λ, λ higher than one, and σ higher than one. In the group with cognitive impairment, σ was higher than in the group with intact cognition. As λ was also higher in the group with cognitive impairment, this must be due to the higher γ in the group with cognitive impairment.

To achieve network densities of around 0.2 to match the proportionally thresholded networks and the DTI networks, the raw cortical thickness networks were thresholded to keep all edge weights above 0.6, and the age and sex corrected cortical thickness networks were thresholded to keep all edge weights above 0.5. After absolute thresholding, density, degree, strength and edge weight were all higher in the group without cognitive impairment in the raw cortical thickness networks and in the group with cognitive impairment in the age and sex corrected networks. However none of these differences were statistically significant. The findings in the raw cortical thickness networks are similar to those in the DTI networks, whereas the networks constructed from age and sex corrected cortical thickness measurements seem to show opposite results. After absolute thresholding, both binary and weighted L and λ were higher in the raw cortical thickness networks in the group with cognitive impairment. There were no differences in γ between the groups with and without cognitive impairment. However, in both the binary and weighted networks, σ was statistically significantly higher in the group with cognitive impairment compared to the group with intact cognition. This must be driven by the non significant differences in γ as λ is higher in the group with cognitive impairment. In the age and sex corrected networks, there were no differences in path length between the groups, but γ and σ were statistically significantly higher in the weighted

networks.

	Raw Cort.Thick.			Age & Sex Corrected Cort.Thick.		
	cognitive impairment	cognition intact	*p*	cognitive impairment	cognition intact	*p*
Binary Networks						
density	0.20	0.20	*1.00*	0.20	0.20	*1.00*
degree	13.4	13.4	*1.00*	13.4	13.4	*1.00*
L	2.04	1.81	*0.00*	2.17	2.10	*0.184*
λ	1.05	0.96	*0.00*	1.11	1.07	*0.00*
C	0.60	0.54	*0.440*	0.57	0.53	*1.00*
γ	1.43	1.23	*0.440*	1.79	1.29	*0.027*
σ	1.36	1.28	*0.00*	1.61	1.21	*0.00*
E_{Glob}	0.46	0.39	*0.440*	0.53	0.46	*1.00*
Weighted Networks						
S	9.52	9.96	*0.626*	8.88	8.32	*1.00*
EW	0.71	0.74	*0.626*	0.66	0.62	*0.00*
L	2.87	2.41	*0.00*	3.27	3.36	*0.123*
λ	1.10	0.98	*0.00*	1.16	1.10	*0.00*
C	0.47	0.43	*0.493*	0.42	0.37	*0.00*
γ	1.45	1.24	*0.493*	1.81	1.31	*0.00*
σ	1.32	1.26	*0.00*	1.57	1.18	*0.00*
E_{Glob}	0.32	0.29	*0.536*	0.35	0.29	*1.00*

Table 4.12: ***Cortical thickness networks: global network characteristics by cognitive impairment after proportional thresholding to keep the top 20% of edge weights.*** *Comparison of global network characteristics between the those with cognitive impairment and those with intact cognition. Data are single values calculated from group networks with significance testing carried out using permutation of groups. The p values are adjusted for 32 multiple comparisons (16 measures, 2 network types) using the FDR at 5%. Each network was thresholded to maintain the top 20% of edge weights. (Cort.Thick.: cortical thickness; S: average network strength; EW: mean edge weight; L: average path length; λ: normalised average path length; C: clustering coefficient; γ: normalised clustering coefficient; σ: small worldness statistic; E_{Glob}: global efficiency; FDR: false discovery rate)*

	Raw Cort.Thick.			Age & Sex Corrected Cort.Thick.		
	cognitive impairment	cognition intact	*p*	cognitive impairment	cognition intact	*p*
Binary Networks						
density	0.22	0.36	*0.613*	0.31	0.26	*0.935*
degree	15.0	24.2	*0.613*	20.6	17.5	*0.935*
L	2.27	1.64	*0.027*	1.86	2.02	*0.931*
λ	1.20	0.99	*0.027*	1.06	1.11	*0.931*
C	0.59	0.65	*0.727*	0.62	0.63	*0.935*
γ	1.36	1.03	*0.680*	1.36	1.26	*0.935*
σ	1.13	1.04	*0.027*	1.28	1.13	*0.931*
E_{Glob}	0.51	0.56	*0.727*	0.63	0.56	*0.935*
Weighted Networks						
S	10.5	16.8	*0.752*	12.7	10.4	*0.867*
EW	0.70	0.70	*0.888*	0.62	0.60	*0.558*
L	3.27	2.35	*0.027*	2.98	2.39	*0.558*
λ	1.26	1.04	*0.027*	1.12	1.18	*0.558*
C	0.46	0.48	*0.888*	0.43	0.42	*0.925*
γ	1.37	1.03	*0.752*	1.38	1.27	*0.00*
σ	1.09	1.00	*0.027*	1.23	1.08	*0.00*
E_{Glob}	0.36	0.39	*0.888*	0.39	0.34	*0.764*

Table 4.13: ***Cortical thickness networks: global network characteristics by cognitive impairment after absolute thresholding.*** *Comparison of global network characteristics between the those with cognitive impairment and those with intact cognition. Data are single values calculated from group networks with significance testing carried out using permutation of groups. Adjusted p values are shown after FDR correction for 32 multiple comparisons (16 network measures, 2 network types) at 5%. Raw networks were thresholded to keep all edge weight values above 0.6 and age and sex corrected networks were thresholded to keep all edge weight values above 0.5. (S: average network strength; EW: mean edge weight; L: average path length; λ: normalised average path length; C: clustering coefficient; γ: normalised clustering coefficient; σ: small worldness statistic; E_{Glob}: global efficiency; FDR: false discovery rate*

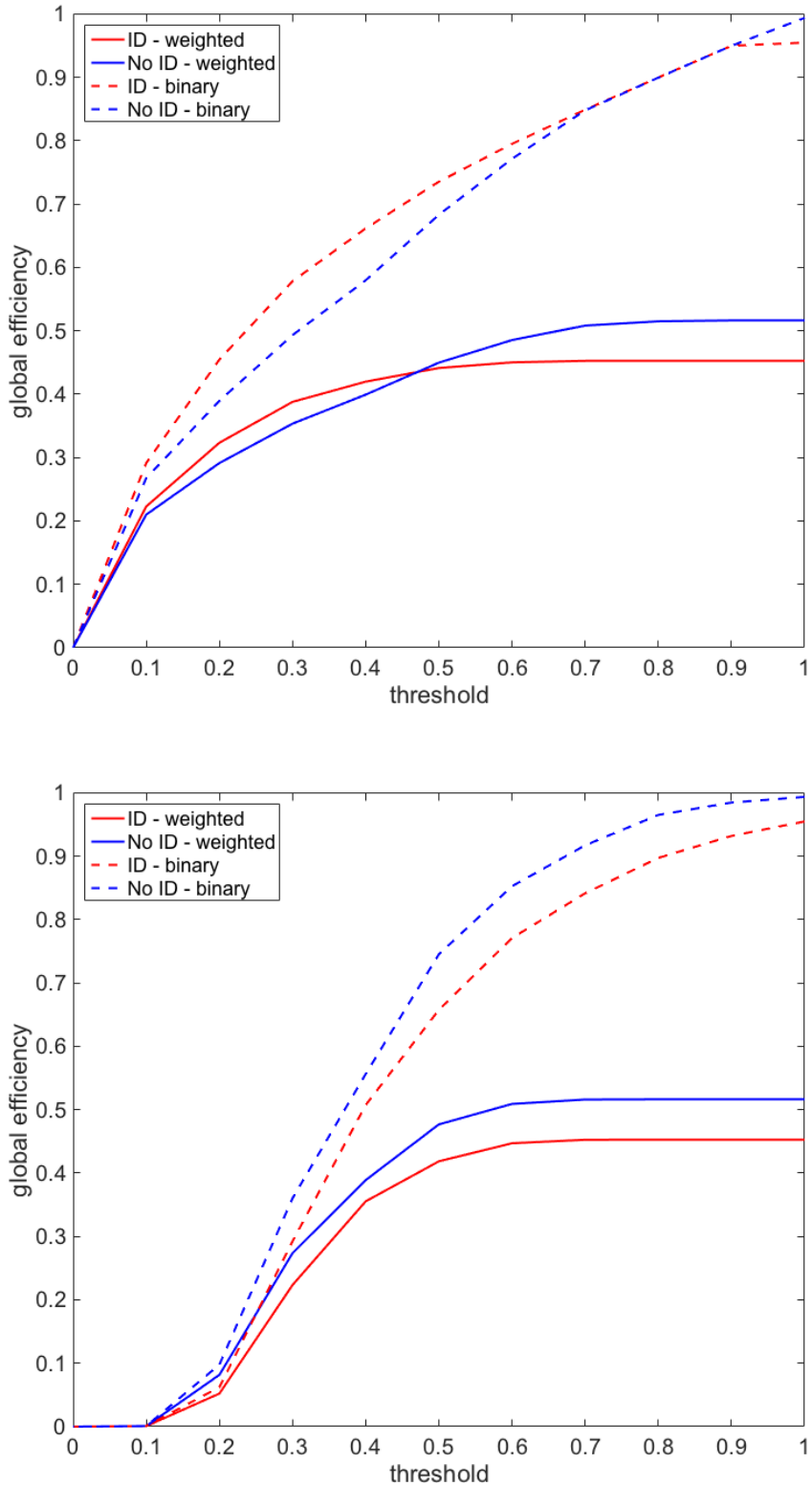

Figure 4.11: ***Global efficiency of raw cortical thickness networks by cognitive impairment*** *Network global efficiency of raw cortical thickness networks plotted across a range of network thresholds.* ***Top:*** *proportional thresholds were applied to keep the top percentage of the threshold value of edge weights.* ***Bottom:*** *absolute thresholds were applied to keep only edge weights above the threshold value. The group with cognitive impairment is shown in red and the group with intact cognition in blue. Solid lines are weighted network measures and dotted lines are binary network measures. (ID: cognitive impairment; Cort.Thick.: cortical thickness)*

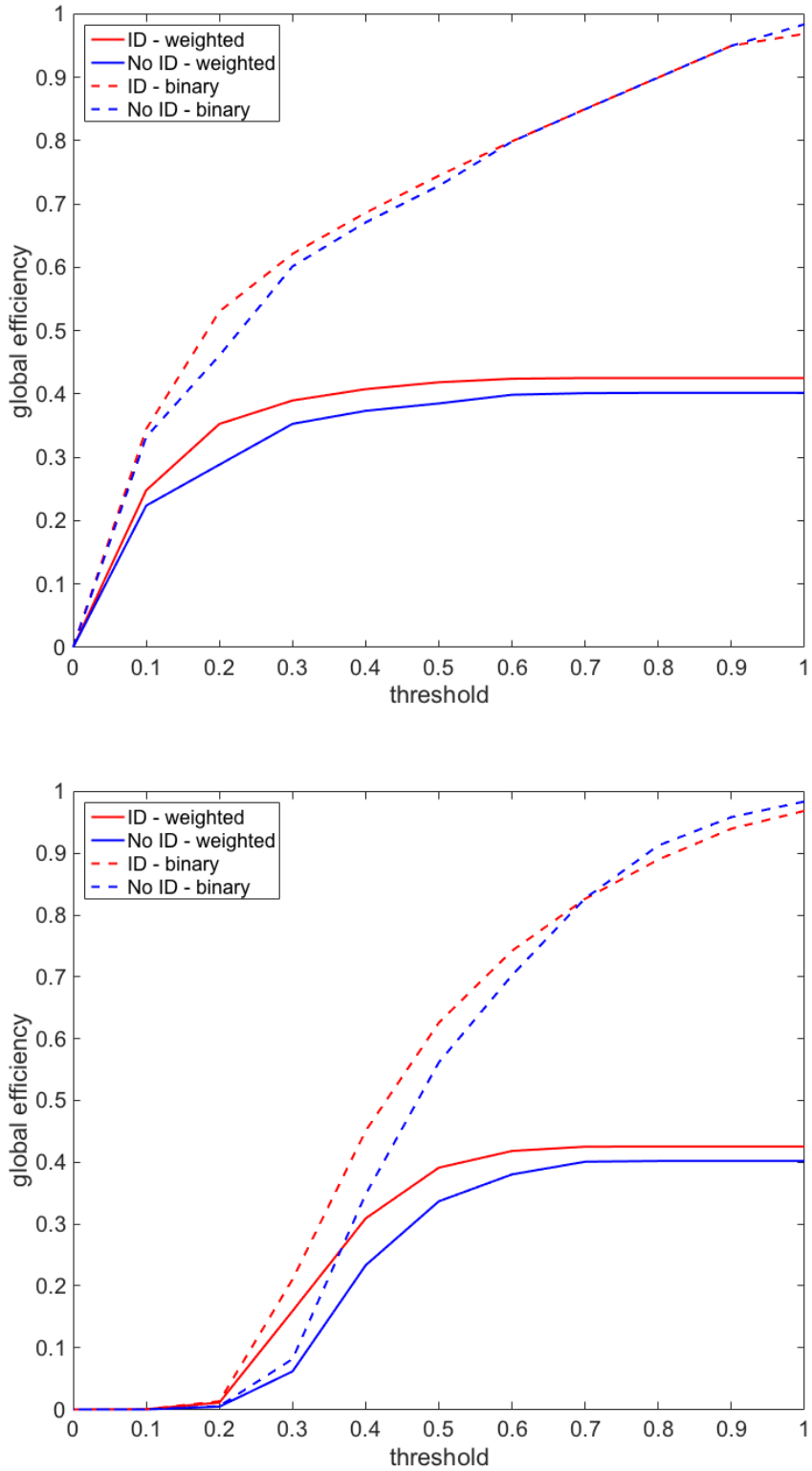

Figure 4.12: ***Global efficiency of corrected cortical thickness networks by cognitive impairment.*** *Network global efficiency of the age and sex corrected cortical thickness networks plotted across a range of network thresholds.* ***Top:*** *proportional thresholds were applied to keep the top percentage of the threshold value of edge weights.* ***Bottom:*** *absolute thresholds were applied to keep only edge weights above the threshold value. The group with cognitive impairment is shown in red and the group with intact cognition in blue. Solid lines are weighted network measures and dotted lines are binary network measures. (ID: cognitive impairment; Cort.Thick.: cortical thickness)*

4.5.2.5 Conclusions regarding cortical thickness network organisation in those with and without cognitive impairment

Cortical thickness networks were constructed from both raw and age and sex corrected cortical thickness measurements. Both binary and weighted networks were considered, and both proportional and absolute thresholds were applied to the networks. Prior to thresholding, networks were densely connected. After thresholding, networks had a tendency to disconnect and it was necessary to maintain high densities to examine fully connected networks. When fully connected networks at densities of 0.6-0.8 were examined, there were no differences between the groups with and without cognitive impairment. However, when networks were examined at lower densities (between 0.2-0.4) there were similar findings to the DTI networks with higher path length, higher clustering, and a higher small worldness statistic in the group with cognitive impairment. These differences were present in the raw cortical thickness networks after both proportional thresholding to maintain a density of 0.2 and after absolute thresholding where density was allowed to vary between groups, and therefore cannot be solely attributable to differences in density between groups. Networks constructed from the age and sex corrected cortical thickness measurements did not show a difference in L between groups after proportional thresholding, but did show a higher λ, γ and σ in the group with cognitive impairment. In the age and sex corrected networks, absolute thresholding of the cortical thickness measurements led to networks with no significant differences in network characteristics except that weighted γ and σ were higher in the group with cognitive impairment. At low densities, the findings in the cortical thickness networks were similar to those in the DTI networks with higher λ, γ, and σ in those with cognitive impairment. However, these findings did not hold in all types of network, and were not present when networks were examined at higher densities.

4.5.2.6 Comparison of DTI and cortical thickness derived network organisation in those with cognitive impairment

In the group with DTI connectomes there were some patients without cortical thickness connectomes and vice versa. This led to slight differences in the clinical characteristics between the groups with and without cognitive impairment as seen when comparing Table 4.4 and Table 4.9. To ensure that any differences in findings between the DTI networks and the cortical thickness networks were not due to different patient inclusions in the groups, DTI networks and cortical thickness networks were compared in the overlapping group with both types of connectome available. There were 65 patients with both cortical thickness and DTI connectomes available. Twenty-six (40%) patients had a documented diagnosis of cognitive impairment and 39 (60%) patients did not. The characteristics of the two groups are shown in Table 4.14. In this subset of patients, there is a significantly lower age at first seizure and a significantly higher likelihood of daily seizures in the group with cognitive impairment, similar to the findings in the group with DTI connectomes (Table 4.4).

DTI networks were compared to cortical thickness networks in the groups with and without cognitive impairment. Table 4.15 shows the network characteristics for the two groups in the FA weighted networks and the raw cortical thickness connectomes. The FA weighted networks were chosen for comparison as they are constructed so that edge weights fall between zero and one prior to any

	Group		*p*
	cognitive impairment *n=26*	cognition intact *n=39*	
Female	14 (54%)	19 (49%)	*0.879*
Age at MRI (years)	5.5 (6.2)	5.6 (6.2)	*0.520*
Age at first seizure (years)	1.3 (3.2)	3.9 (6.0)	*0.032*
Time from first seizure to MRI (months)	19.0 (32.5)	14.0 (35.0)	*0.465*
Daily or more frequent seizures	11 (42%)	5 (13%)	*0.016*
Number of AEDs	1.0 (1.0)	1.0 (2.0)	*0.111*
Focal onset seizures	3 (12%)	8 (21%)	*0.543*
Structural abnormality	8 (31%)	11 (28%)	*1.00*
IQ	59.0 (9.5)	95.0 (16.0)	<0.001

Table 4.14: ***Both network types: demographic and clinical features by cognitive impairment.*** *Comparison of demographic and clinical features between those with and without cognitive impairment in the subset with both cortical thickness and DTI data available. Data are count (percentage) for categorical data and median (IQR) for numerical data. Statistical testing was carried out using X^2 tests for categorical data and Mann-Whitney U tests for numerical data except IQ, for which t-tests were used. (AED: anti-epileptic drug; IQ: total intelligence quotient; MRI: magnetic resonance imaging; IQR: interquartile range)*

correction or normalisation, similar to structural covariance networks from cortical thickness measurements. As the FA weighted networks are not corrected for age, networks created from raw cortical thickness measurements were chosen for comparison. The raw cortical thickness connectomes were thresholded at an absolute threshold that maintained only edge weights above 0.8 to give densities that were not fixed across the groups and were similar in magnitude to the FA networks. As these cortical thickness networks were not fully connected, L was calculated across the network by removing entries of infinity from the distance matrix as described in Section 3.8.2. Both weighted and binary networks were compared.

The FA weighted and binary networks in this subgroup show similar results to those seen in the total group with DTI connectomes. The group with cognitive impairment has lower network densities, lower average degrees, lower average strength, lower average edge weights, lower global efficiency, and higher λ and γ than the group with intact cognition. In the cortical thickness networks the lower density, degree, strength, mean edge weight, and global efficiency in the group with cognitive impairment were not statistically significant. However, λ and γ were significantly higher in the group with cognitive impairment. In the FA weighted networks, γ was higher than λ and σ was greater than one, suggesting a small world organisation in both groups without any difference in σ between groups. In the cortical thickness networks, γ was greater than λ and σ was greater than one in the group with cognitive impairment but in the group with intact cognition, λ, γ, and σ were only just greater than one, which does not suggest a small world organisation.

The FA DTI networks and the raw cortical thickness networks were processed to try to keep the network

	FA DTI			Raw Cort.Thick.		
	cognitive impairment	cognition intact	*p*	cognitive impairment	cognition intact	*p*
Binary Networks						
density	0.19 (0.01)	0.21 (0.02)	*0.001*	0.12	0.20	*0.534*
degree	16.1 (1.12)	17.5 (1.66)	*0.001*	7.79	13.3	*0.534*
L	2.12 (0.07)	2.04 (0.08)	*0.001*	2.60	1.81	*0.00*
λ	1.12 (0.02)	1.10 (0.02)	*0.001*	1.16	1.00	*0.040*
C	0.60 (0.02)	0.61 (0.01)	*0.539*	0.43	0.51	*0.362*
γ	2.14 (0.24)	2.01 (0.20)	*0.034*	1.84	1.12	*0.00*
σ	1.91 (0.19)	1.82 (0.15)	*0.068*	1.59	1.11	*0.00*
E_{Glob}	0.55 (0.02)	0.56 (0.02)	*0.001*	0.34	0.39	*0.534*
Weighted Networks						
S	5.80 (0.65)	6.64 (0.73)	*<0.001*	6.03	10.2	*0.675*
EW	0.36 (0.02)	0.38 (0.02)	*0.001*	0.77	0.77	*0.879*
L	5.28 (0.44)	4.76 (0.33)	*<0.001*	3.39	2.35	*0.035*
λ	1.15 (0.03)	1.12 (0.03)	*0.001*	1.19	1.03	*0.400*
C	0.27 (0.02)	0.28 (0.03)	*0.023*	0.37	0.41	*0.675*
γ	2.01 (0.23)	1.90 (0.18)	*0.048*	1.87	1.12	*0.00*
σ	1.76 (0.20)	1.70 (0.16)	*0.200*	1.57	1.09	*0.035*
E_{Glob}	0.22 (0.02)	0.24 (0.02)	*<0.001*	0.26	0.30	*0.675*

Table 4.15: ***DTI and cortical thickness global network characteristics by cognitive impairment.*** *Comparison of global network characteristics between the those with cognitive impairment and those with intact cognition. Only patients with both DTI and cortical thickness networks are included. For the DTI FA networks data are mean (SD) and statistical comparison was carried out using t-tests. The raw cortical thickness networks are single values calculated from group networks after an absolute threshold of 0.7 was applied to remove all edge weights less than 0.7. For the cortical thickness networks group differences were tested statistically using permutation testing. All p values are adjusted following FDR correction at 5% for 32 comparisons (2 network types and 16 network measures). (DTI: diffusion tensor imaging; Cort.Thick.: cortical thickness; FA: fractional anisotropy; S: average network strength; EW: mean edge weight; L: average path length; λ: normalised average path length; C: clustering coefficient; γ: normalised clustering coefficient; σ: small worldness statistic; E_{Glob}: global efficiency; SD: standard deviation; FDR: false discovery rate)*

properties as similar to each other as possible. However, this meant the cortical thickness networks were not fully connected. This is reflected in the lower node degrees seen in the cortical thickness networks. The disconnections in the cortical thickness networks may have contributed to λ and γ being similar to regular networks and the lack of small world organisation. Thresholding the cortical thickness networks also led to high mean edge weights as the lower edge weights were removed, and also meant the mean edge weights were similar across the two groups. Despite the similar mean edge weights, weighted γ was still significantly higher in the group with cognitive impairment suggesting that this is due to different arrangements of weights in the cortical thickness networks rather than overall group differences in mean edge weight.

Connectivity matrices for the FA weighted networks are displayed in Figure 4.13. These can be compared with the connectivity matrices of the cortical thickness networks displayed in Figure 4.14. The DTI networks include subcortical areas, unlike the cortical thickness networks, leading to a higher number of nodes. The lower (blue coloured) weight connections can be appreciated in the DTI networks. These have been thresholded out in the cortical thickness networks, and only high edge weights remain. In both the DTI and cortical thickness networks, the greater network density in the group without cognitive impairment (bottom matrices) can be visually appreciated. There appears to be a greater number of interhemispheric connections in the cortical thickness networks than in the DTI networks. All of these differences in network structure arise from the methods involved in creating the connectivity matrices.

Overall, there are differences in path length and clustering in both the DTI networks and the cortical thickness networks in the groups with and without cognitive impairment. This suggests that network topology does differ between the group with cognitive impairment and the group with intact cognition. There are differences in findings between the DTI and the cortical thickness networks, and these differences may arise from the differences in network construction methodology. As similar findings do exist in networks created using very different techniques, this suggests the findings are robust and not an artefact of network creation techniques.

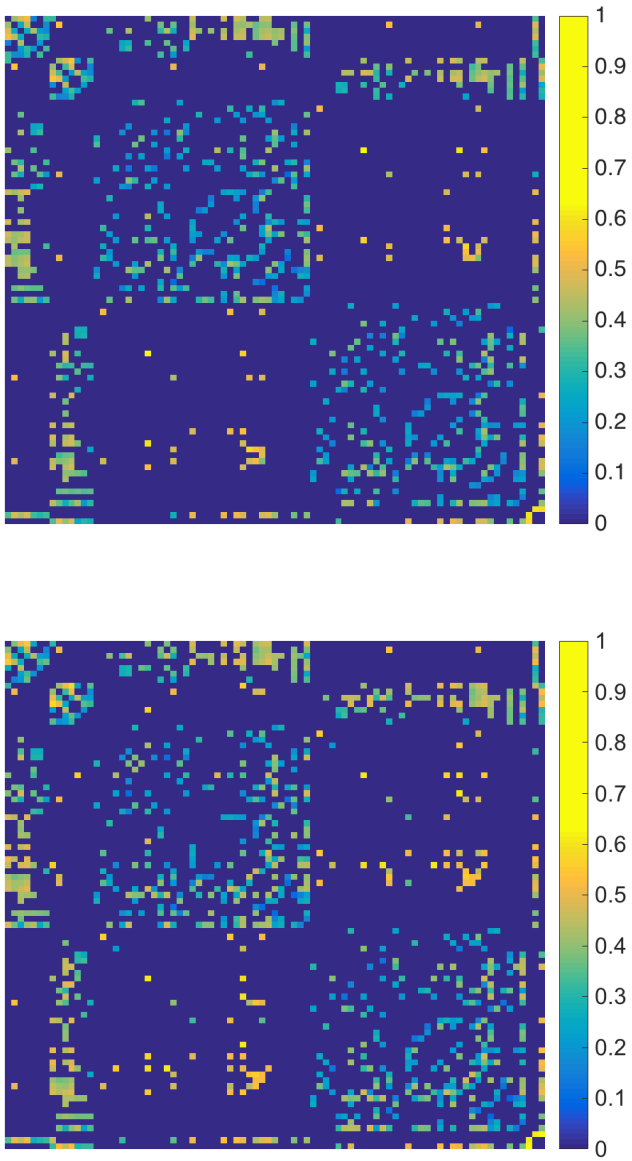

Figure 4.13: ***DTI FA weighted networks: group averaged connectivity matrices.*** *Group averaged weighted connectomes were constructed for both the group with cognitive impairment and the group with intact cognition. Connections were kept if they were present in more than 60% of the subjects within the group. Edges were weighted with the average group weight. The connectivity matrix is laid out with nodes running from top to bottom and left to right in the order given in Table 3.2.* ***Top:*** *group averaged weighted connectivity matrix for those with cognitive impairment.* ***Bottom:*** *group averaged weighted connectivity matrix for those with intact cognition. (FA: fractional anisotropy; DTI: diffusion tensor imaging)*

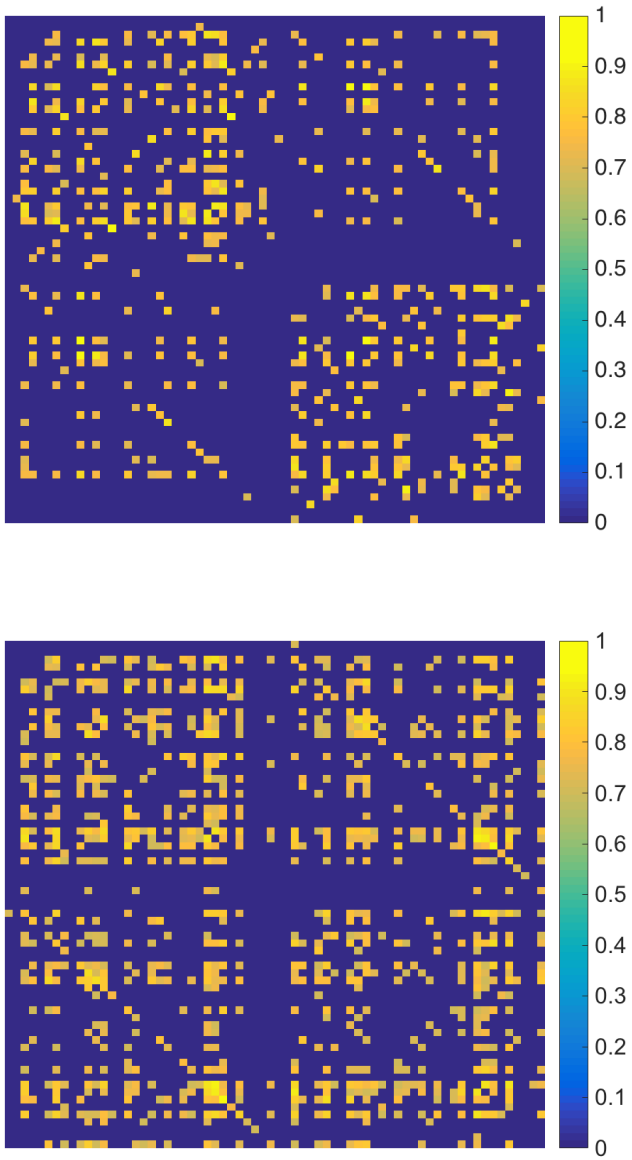

Figure 4.14: ***Raw cortical thickness weighted networks: connectivity matrices*** *Single group connectomes for those with cognitive impairment and those with intact cognition. The connectivity matrix is laid out with nodes running from top to bottom and left to right in the order given in Table 3.2.* ***Top:*** *group cortical thickness weighted connectivity matrix for those with cognitive impairment.* ***Bottom:*** *group cortical thickness weighted connectivity matrix for those with intact cognition (Cort.Thick.: cortical thickness)*

4.5.3 Is there an association between DTI network characteristics and IQ in children with suspected epilepsy?

To provide further evidence for an association between network characteristics and cognitive function, the subgroup of children with DTI networks and IQ scores available were investigated. IQ scores were correlated against network characteristics. DTI networks were chosen for this analysis rather than cortical thickness networks because they are constructed as individual networks rather than group networks. Of the 80 patients with DTI networks, 36 had undergone formal neuropsychological testing, and 32 had achieved a IQ score. Both binary and weighted FA and NOS networks were assessed. The normalised metrics were chosen for investigation as normalisation to random networks with the same number of edges, nodes, and node degrees should decrease the influence of overall network density and degree on the analyses. General linear models with the normalised network characteristic as the outcome measure, and IQ as a predictor were created and analysed. Models assessing binary normalised metrics included density as a covariate, and models assessing weighted normalised metrics included mean edge weight as a covariate to control for overall network number and strength of edges.

	FA				NOS			
	Estimate	Std Error	t	*p*	Estimate	Std Error	t	*p*
binary								
λ								
density	-0.776	0.143	-5.41	*<0.001*	-0.89	0.14	-6.39	*<0.001*
IQ	-0.0002	0.0001	-2.17	*0.039*	-0.0002	0.0001	-2.17	*0.078*
γ								
density	-10.2	1.82	-5.59	*<0.001*	-11.8	1.53	-7.72	*<0.001*
IQ	-0.001	0.001	-0.62	*0.538*	<0.001	0.001	-0.32	*0.752*
weighted								
λ								
EW	0.25	0.22	1.14	*<0.262*	0.67	4.06	0.17	*<0.870*
IQ	-0.0007	0.0002	-2.74	*0.010*	-0.002	0.002	-1.09	*0.283*
γ								
EW	-4.22	2.28	-1.85	*0.074*	8.25	4.45	1.85	*0.074*
IQ	-0.0009	0.002	-0.35	*0.729*	-0.004	0.002	-1.67	*0.105*

Table 4.16: ***DTI networks: prediction of normalised network characteristics using IQ.*** *Linear regression modelling using λ, and γ as dependent variables and density, mean edge weight, and IQ as predictors. (FA: fractional anisotropy; NOS: number of streamlines; DTI: diffusion tensor imaging; EW: mean edge weight; γ: normalised clustering coefficient; λ: normalised path length; IQ total intelligence quotient)*

The estimates, standard errors, t and *p* values for the linear models are shown in Table 4.16. The linear model predicting λ using density and IQ in the binary networks had an adjusted R^2 of 0.59 in the FA networks and 0.69 in the NOS networks. IQ was a significant predictor of λ in addition to density in the FA networks but not in the NOS networks. The models predicting γ in the binary networks had an adjusted R^2 of 0.54 in the FA networks and 0.69 in the NOS networks. Although density was a

significant predictor of γ in both network types, IQ was not. In the weighted networks, the adjusted R^2 for the model predicting λ from mean edge weight and IQ was only 0.17 in the FA networks and 0.03 in the NOS networks. Mean edge weight was not a significant predictor of λ in either type of network, and IQ was only a significant predictor of λ in the FA network. When γ was used as the outcome variable, the adjusted R^2 was 0.15 in the FA networks and 0.11 in the NOS networks. Neither IQ or mean edge weight were statistically significant predictors of γ. The combination of density and IQ accounts for a reasonable proportion of the variance in λ and γ in the binary networks (0.54-0.69). However, mean edge weight and IQ account for only a very small proportion of the variance (up to 0.17) in weighted γ and λ, suggesting that factors other than IQ and mean network edge strength must also be important in determining these weighted measures. In the FA networks, IQ is a significant predictor of both binary and weighted λ over and above density or mean edge weight. This is not seen in the NOS networks. IQ is not a significant predictor of γ in any of the networks.

Overall, there is a statistically significant association between IQ and λ in the FA weighted networks, and this persists even when controlling for the effects of density in the binary networks and mean edge weight in the weighted networks. However, this relationship is not seen in the NOS derived networks.

4.5.4 Is there an association between network characteristics, cognition, and seizure characteristics?

To investigate whether the group differences in frequency of seizures and age at onset of seizures can account for the differences in network characteristics between those with cognitive impairment and those without, the correlations between seizure characteristics, cognition, and network characteristics were examined. The correlation matrix for the binary metrics from the FA networks is shown in Figure 4.15, and the correlation matrix for the weighted metrics from the FA networks is shown in Figure 4.16. As can be appreciated from these figures, network characteristics are all highly correlated with each other. The measures of cognitive impairment and IQ are also highly correlated with each other. Measures of IQ and cognitive impairment are also correlated with network characteristics. The clinical seizure characteristics are also correlated with each other and then with cognitive and network characteristics to a lesser extent.

Initially models were built to assess the effect of seizure characteristics on IQ and cognitive impairment. The age at MRI, the interval from first seizure to MRI, and the age at onset of seizures were all highly correlated due to a large proportion of children undergoing MRI within a year of their first seizure (see Figure 4.4), and including all of these as predictor variables in linear or logistic regressions was not possible due to the problem of multicollinearity from correlated variables. The age at first seizure was chosen for inclusion as this correlated most strongly with the network and cognitive variables. Logistic regression with cognitive impairment as the dependent variable and the clinical features as predictors was performed. The included predictors, along with their estimates, standard errors, z values and *p* values are shown in Table 4.17. Only daily seizures were significantly predictive of cognitive impairment. Replacing the age at first seizure with the age at MRI or time from first seizure to MRI led to similar results. A linear model was built using the same predictors with IQ as the dependent variable and the estimates, standard errors and *p* values are shown in Table 4.18. The age at first seizure, number of

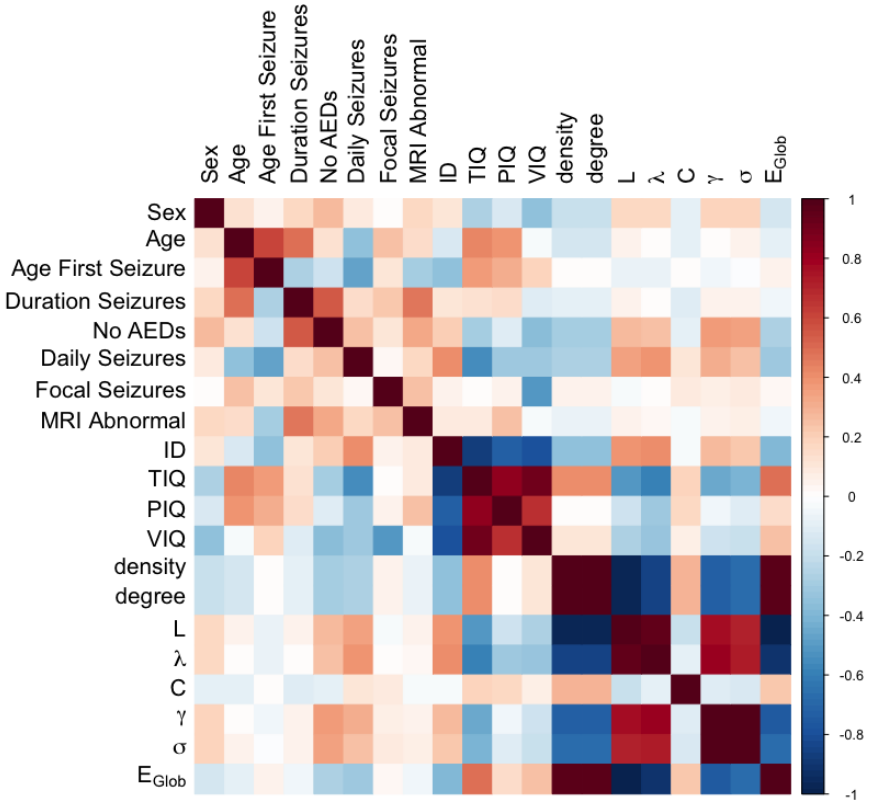

Figure 4.15: ***Network, cognitive, and clinical correlations for binary FA networks.*** *The spearman correlation coefficient was calculated for each of the network, clinical, and cognitive variables (FA: fractional anisotropy; ID: cognitive impairment; MRI: magnetic resonance imaging; AED: anti-epileptic drug; TIQ: total intelligence quotient; VIQ: performance intelligence quotient; PIQ: verbal intelligence quotient; L: average path length; λ: normalised average path length; C: clustering coefficient; γ: normalised clustering coefficient; σ: small worldness statistic; E_{Glob}: global efficiency)*

AEDs, and the presence of an MRI structural abnormality were all predictive of TIQ. The adjusted R^2 for this model was 0.48. Replacing the age of onset of seizures with the time from the first seizure to MRI or the age at MRI led to a similar model with either the interval from first seizure to MRI or the age at MRI being significant predictors of TIQ.

To check whether the difference in findings using IQ and cognitive impairment as the outcome was due to patient differences in the smaller cohort with IQ available, the model for cognitive impairment was repeated including only the 32 patients with IQ scores available. When only patients with IQ scores available were included, the age that seizures started was also significantly predictive of cognitive impairment in addition to the occurrence of daily seizures. Therefore, part of the difference in findings

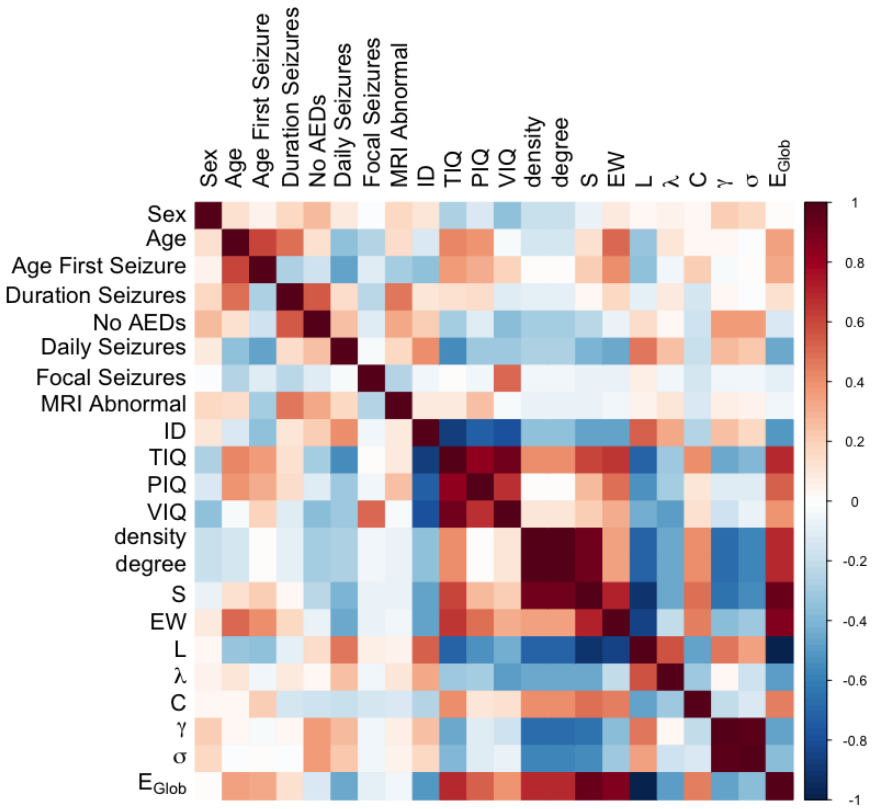

Figure 4.16: ***Network, cognitive, and clinical correlations for weighted FA networks.*** *The spearman correlation coefficient was calculated for each of the network, clinical, and cognitive variables (FA: fractional anisotropy; AED: anti-epileptic drug; MRI: magnetic resonance imaging; ID: cognitive impairment; TIQ: total intelligence quotient; VIQ: performance intelligence quotient; PIQ: verbal intelligence quotient; S: average network strength; EW: average network edge weight; L: average path length; λ: normalised average path length; C: clustering coefficient; γ: normalised clustering coefficient; σ: small worldness statistic; E_{Glob}: global efficiency)*

when using cognitive impairment and IQ as outcome variables relates to differences in the cohort of patients available for analysis.

The models predicting cognitive impairment and IQ were adjusted by adding binary or weighted λ or γ from the FA and NOS networks as predictors. Both binary and weighted λ had a significant prediction of cognitive impairment over and above the clinical features in the FA and NOS networks. In all of the networks except for the NOS weighted networks, the addition of λ to the model predicting cognitive impairment rendered the occurrence of daily seizures to become a non-significant predictor of cognitive impairment. In the linear model predicting IQ, adding binary or weighted λ from the FA or NOS networks

	Estimate	Standard Error	z	p
Female	-0.197	0.738	-0.973	*0.330*
Age at first seizure	0.005	0.008	0.66	*0.513*
Less than daily seizures	1.772	0.685	2.59	*0.010*
Number AEDs	-0.251	0.279	-0.90	*0.367*
Structural abnormality	0.568	0.694	0.82	*0.413*
Focal seizures	-0.605	0.691	-0.87	*0.382*

Table 4.17: ***Predicting cognitive impairment from clinical variables***. *Logistic regression model predicting cognitive impairment from clinical variables. (AED: anti-epileptic drug)*

	Estimate	Standard Error	t	p
Female	-11.9	8.18	-1.46	*0.156*
Age at first seizure	0.277	0.107	2.60	*0.015*
Less than daily seizures	17.7	7.89	2.24	*0.034*
Number AEDs	-10.3	3.40	-3.04	*0.005*
Structural abnormality	27.2	8.56	-3.17	*0.004*
Focal seizures	-7.24	7.81	-0.93	*0.362*

Table 4.18: ***Predicting IQ from clinical variables***. *Linear regression model predicting IQ from clinical variables. (AED: anti-epileptic drug)*

did not decrease the significance of the clinical predictors, and λ did not become a significant predictor. Adding binary or weighted λ increased the adjusted R^2 to 0.49-0.51. When the model predicting cognitive impairment was re-examined in just those patients in whom an IQ score was available, neither weighted or binary λ became a significant predictor of cognitive impairment and the clinical features remained significant. Therefore, λ is a significant predictor of cognitive impairment in the whole set of patients, but not in the subset with IQ scores available. When γ was added to the model predicting cognitive impairment instead of λ, daily seizures remained a significant predictor of cognitive impairment, and γ was not a significant predictor of cognitive impairment. Neither binary or weighted γ were significant predictors of IQ when added as predictors instead of λ, and the clinical seizure features remained significant predictors of IQ in these models. Adding γ as a predictor to the models increased the adjusted R^2 to 0.47.

General linear models were also built with λ and γ as the outcome variables, and the clinical seizure characteristics as predictors. The estimates, standard errors, t values and *p* values for each of the terms included in the models to predict λ are shown in Table 4.19. Daily seizures were predictive of binary λ in both the FA and NOS networks and were also predictive of weighted λ in the FA networks, but not in the NOS networks. However, the number of medications was predictive of weighted λ in the NOS networks. The adjusted R^2 for these models was only 0.16 for the binary NOS λ and 0.17 for the binary FA λ and 0.04 for weighted FA and 0.06 for weighted NOS. Adding cognitive impairment as a predictor variable to the binary models increased the R^2 to 0.21 in the FA model and 0.20 in the NOS models. In both these models, daily seizures remained predictive of λ. Cognitive impairment was significantly predictive of λ in the FA model with a *p* value of 0.04 but non significant in the NOS model with a *p* value of 0.05. Adding

IQ to the models instead of cognitive impairment rendered daily seizures non-significant, but was also itself not a significant predictor of λ, and increased the adjusted R^2 to 0.19 in the FA model and 0.16 in the NOS model. Therefore adding IQ explained less of the variance in λ than cognitive impairment, but may be more closely correlated with having daily seizures. Adding density to the models with cognitive impairment increased the R^2 to 0.70 in both the NOS model and in the FA model and rendered both daily seizures and cognitive impairment non significant in both models. Adding density to the models with IQ included as a predictor increased the R^2 to 0.60 in the FA model and 0.59 in the NOS model and again rendered all predictive variables non-significant. Density therefore accounts for much of the variance in binary λ. Cognitive impairment may account for more variance in binary λ than IQ, although the smaller sample size of patients with IQ scores available may be responsible for this difference.

	FA				NOS			
	Estimate	Std Error	t	*p*	Estimate	Std Error	t	*p*
Binary Networks								
λ								
Female	0.006	0.006	1.03	*0.308*	0.006	0.006	0.99	*0.326*
Age first seizure	-<0.001	<0.001	1.67	*0.100*	<0.001	<0.001	1.61	*0.112*
Not daily seizures	-0.020	0.006	-3.06	*0.003*	-0.019	0.006	-2.94	*0.005*
Number of AEDs	0.005	0.003	1.82	*0.074*	0.005	0.003	1.95	*0.056*
MRI abnormality	-0.009	0.006	-1.48	*0.143*	-0.009	0.006	-1.38	*0.172*
Focal seizures	0.003	0.006	0.44	*0.663*	0.003	0.007	0.40	*0.688*
Weighted Networks								
λ								
Female	0.004	0.008	0.47	*0.639*	0.022	0.061	0.37	*0.716*
Age first seizure	<0.001	<0.001	1.41	*0.164*	<0.001	0.001	0.06	*0.949*
Not daily seizures	-0.022	0.009	-2.46	*0.017*	-0.096	0.069	-1.39	*0.169*
Number of AEDs	0.002	0.003	0.62	*0.541*	0.057	0.027	2.08	*0.042*
MRI abnormality	-0.007	0.009	-0.76	*0.453*	-0.004	0.069	-0.06	*0.953*
Focal seizures	0.005	0.009	0.60	*0.553*	-0.008	0.069	-0.12	*0.903*

Table 4.19: ***DTI networks: prediction of λ using demographic and clinical features*** *Linear regression modelling using λ as the dependent variable and demographic and clinical features as predictors. (FA: fractional anisotropy; NOS: number of streamlines; DTI: diffusion tensor imaging; EW: edge weight; λ: normalised path length; MRI: magnetic resonance imaging; AED: anti-epileptic drug)*

Cognitive impairment was also added to the models predicting weighted λ. In the FA networks, cognitive impairment was a significant predictor of λ with a *p* value of 0.017, and daily seizures became non significant. In the NOS weighted networks, cognitive impairment was not a significant predictor of λ above the clinical characteristics but the number of AEDs remained significant. The adjusted R^2 became 0.12 in the NOS networks and 0.10 in the FA networks with the addition of cognitive impairment. When IQ was added to the model instead of cognitive impairment, the adjusted R^2 decreased to -0.01 in the FA model and 0.05 in the NOS model and none of the clinical factors or IQ were significant predictors of λ. Adding mean edge weight increased the adjusted R^2 to 0.02 in the

NOS and 0.04 in the FA models including IQ and to 0.19 in the NOS and to 0.11 in the FA models including cognitive impairment. The number of AEDs was still a significant predictor of λ after adding mean edge weight to the NOS weighted model. Adding density rather than mean edge weight did not increase the adjusted R^2 value any further. Thus cognitive impairment may also explain more of the variance in weighted λ than IQ, and the models show better fit without the IQ term, although again this may be due to the reduced sample size with IQ compared with cognitive impairment. Adding mean edge weight and cognitive impairment decreased the effect of daily seizures on λ in the FA networks but had no effect on the significant of the number of medications on λ in the NOS networks.

A similar experiment was performed using γ as the outcome variable rather than λ. The results are in Table 4.20. In the binary networks, daily seizures and the number of AEDs were significant predictors of γ. These models had an adjusted R^2 of 0.14 in the FA networks and 0.15 in the NOS networks. For weighted γ, daily seizures was a significant predictor in the FA networks, but the number of AEDs was not significant. In the NOS networks, the number of AEDs was significant but daily seizures were not significant with *p* values just above 0.05. The adjusted R^2 for the weighted γ models was 0.14 for the FA networks and 0.16 for the NOS networks. Adding cognitive impairment to these models rendered daily seizures a non-significant predictor of γ but the number of AEDs remained significant. The addition of cognitive impairment increased R^2 to 0.14 in both the NOS and FA networks. Cognitive impairment was not a significant predictor. When IQ was added to the models rather than cognitive impairment, this was also not a significant predictor, but it rendered all the clinical features non significant and increased the adjusted R^2 to 0.16 in the NOS networks and 0.15 in the FA networks. Adding density increased R^2 to 0.71 in the NOS and 0.69 in the FA networks, and was a significant predictor of γ in the models including IQ. Adding density also rendered all clinical variables non-significant predictors of γ. In the models including cognitive impairment, adjusted R^2 increased to 0.59 in the NOS networks and 0.57 in the FA networks, less than in the models including cognitive impairment. Again density was the only significant factor in the model.

In the weighted networks, the addition of cognitive impairment increased adjusted R^2 to 0.16 in the NOS networks and 0.13 in the FA networks, and the clinical factors remained significant. Adding IQ to the models instead of cognitive impairment gave an adjusted R^2 of 0.13 in the FA models and 0.17 in the NOS models and rendered all the clinical factors insignificant predictors. IQ was also an insignificant predictor of weighted γ. Adding mean edge weight to the models with IQ improved adjusted R^2 to 0.31 in the FA networks and 0.19 in the NOS networks. None of the clinical factors remained significant. Mean edge weight was itself a predictor of weighted γ in the FA networks but not in the NOS networks. Adding mean edge weight to the models with cognitive impairment increased R^2 to 0.22 in the the FA networks and 0.16 in the NOS networks. Adding density to the models instead of mean edge weight did not change the findings or increase R^2. Mean edge weight and the number of medications were significant predictors in the FA networks. In the NOS networks, only daily seizures were significant predictors of γ. Therefore, daily seizures and number of medications remained significant predictors of γ in the weighted networks after addition of cognitive impairment and mean edge weight to the models. For binary γ, the number of AEDs remained significant after the addition of cognitive impairment. Adding IQ to the models rendered all the clinical features non-significant, and IQ itself was also non-significant.

In conclusion, seizure, network, and cognitive variables are all correlated. The presence of cognitive

	FA				NOS			
	Estimate	Std Error	t	*p*	Estimate	Std Error	t	*p*
Binary Networks								
γ								
Female	0.067	0.057	1.16	*0.250*	0.066	0.057	1.16	*0.250*
Age first seizure	0.001	0.001	1.23	*0.226*	0.001	0.001	1.23	*0.223*
Not daily seizures	-0.138	0.065	-2.11	*0.039*	-0.136	0.065	-2.10	*0.040*
Number of AEDs	0.063	0.026	2.45	*0.017*	0.064	0.026	2.49	*0.016*
MRI abnormality	0.053	0.065	-0.82	*0.416*	-0.058	0.065	-0.89	*0.375*
Focal seizures	0.010	0.066	0.153	*0.879*	0.012	0.065	0.18	*0.855*
Weighted Networks								
γ								
Female	0.066	0.055	1.19	*0.240*	0.094	0.072	1.31	*0.197*
Age first seizure	0.001	0.001	1.07	*0.291*	0.001	0.001	1.65	*0.105*
Not daily seizures	-0.123	0.063	-1.96	*0.055*	-0.207	0.082	-2.53	*0.014*
Number of AEDs	0.061	0.025	2.46	*0.017*	0.065	0.032	2.00	*0.051*
MRI abnormality	-0.051	0.063	-0.81	*0.419*	-0.023	0.082	-0.29	*0.776*
Focal seizures	0.011	0.063	0.17	*0.868*	-0.012	0.082	-0.15	*0.879*

Table 4.20: ***DTI networks: prediction of γ using demographic and clinical features*** *Linear regression modelling using γ as the dependent variable and demographic and clinical features as predictors. (FA: fractional anisotropy; NOS: number of streamlines; DTI: diffusion tensor imaging; γ: normalised clustering coefficient; MRI: magnetic resonance imaging; AED: anti-epileptic drug)*

impairment is not only predicted by DTI network density, λ, and γ as shown in Section 4.5.2.1, but is also predicted by the presence of daily seizures after taking other clinical variables into account as seen in Table 4.17. In models predicting network characteristics in the FA networks, daily seizures were predictive of λ in the FA networks and the number of AEDs was predictive of λ in the NOS networks. γ was predicted by daily seizures and the number of AEDs in both the FA and NOS networks. Adding λ to models predicting cognitive impairment from clinical variables decreases the effect of the clinical variables. This suggests that λ may have a mediating effect on the association between seizure characteristics and cognition. Adding γ to the models predicting cognitive impairment from clinical variables did not have the same effect, and γ was not a significant predictor of cognitive impairment, suggesting γ does not have a similar mediating effect on cognition and is more closely associated with clinical variables than the presence of cognitive impairment. As models including the seizure characteristics also decrease the effect of λ on cognition, there could also be a mediating effect of seizure characteristics on the association between λ and cognitive impairment. However, including both seizure characteristics and network characteristics in models predicting cognitive impairment led to the highest adjusted R^2 values, suggesting that both seizure characteristics and network characteristics contribute to explaining whether or not a patient has cognitive dysfunction. The results for investigation of IQ scores are different to those for the cognitive impairment group, which is likely to be due to the smaller group size of patients with IQ scores available or the different statistical methods used for the

continuous IQ scores as opposed to the dichotomous cognitive impairment groups as all the patients in the cognitive impairment group had lower IQ scores than those in the group with intact cognition. In the binary networks, network density accounted for much of the variance in λ, but in the weighted networks, mean edge weight accounted for a much smaller proportion of the variance in λ. Adding density instead of mean edge weight to the models predicting weighted network characteristics did not change the findings.

4.5.5 Patients with a definite diagnosis of epilepsy

This suspected epilepsy cohort consists of patients investigated for suspected seizures. Some of these patients did not go on to receive a definite diagnosis of epilepsy. To assess whether the findings in this chapter are applicable to those with a definite diagnosis of epilepsy as well as to a cohort investigated for suspected epilepsy, the subgroup who were later diagnosed with epilepsy by their paediatric neurologist were investigated. As described in Section 4.5.1.3, twelve patients had an unclear diagnosis, and ten patients had experienced febrile seizures. These were excluded as they did not meet the criteria for a diagnosis of epilepsy.[99]

There were 41 children in the cohort with whole brain DTI connectomes and a definite diagnosis of epilepsy. Four patients did not have any documentation regarding cognitive impairment. Seventeen (46%) patients had cognitive impairment as described in Section 3.6, and twenty (54%) were cognitively intact. The demographic and clinical features of the two groups are shown in Table 4.21. There are no statistically significant differences detected between the two groups except in the IQ scores.

	Group		*p*
	cognitive impairment *n=17*	cognition intact *n=20*	
Female	10 (59%)	11 (55%)	*1.00*
Age at MRI (years)	6.4 (7.4)	6.8 (4.1)	*0.855*
Age at first seizure (years)	1.5 (4.3)	4.0 (4.5)	*0.141*
Time from first seizure to MRI (months)	14.5 (36.8)	14.0 (21.5)	*0.551*
Daily or more frequent seizures	8 (47%)	4 (20%)	*0.162*
Number of AEDs	1.5 (1.0)	1.0 (2.0)	*0.2402*
Focal onset seizures	2 (12%)	5 (25%)	*0.546*
IQ	59.6 (9.3)	92.1 (14.9)	$<$*0.001*

Table 4.21: ***DTI networks: demographic and clinical features by cognitive impairment in subgroup with definite epilepsy*** *Comparison of demographic and clinical features between those with and without cognitive impairment in the subgroup with definite epilepsy. Data are count (percentage) for categorical data and median (IQR) for numerical data except for IQ which is mean (SD). Significance testing was carried out using X^2 tests for categorical data and Mann-Whitney U tests for all numerical data except IQ, where a t-test was used. (AED: Anti-epileptic drug; IQ: intelligence quotient; MRI: magnetic resonance imaging; IQR: interquartile range; SD: standard deviation)*

Global network characteristics for the binary and weighted networks for the groups with and without cognitive impairment are shown in Table 4.22. There were no statistically significant differences in the global network measures calculated for binary networks between the group with cognitive impairment and the cognitively intact group. In the weighted networks, network strength was significantly higher in the group without cognitive impairment in both the networks constructed from FA and those constructed from the NOS. In the group with cognitive impairment average path length was higher and global efficiency lower in both the FA and NOS networks. However, there was no statistically significant difference in λ between the two groups.

	FA			NOS		
	cognitive impairment	cognition intact	*p*	cognitive impairment	cognition intact	*p*
Binary Networks						
density	0.19 (0.01)	0.20 (0.02)	*0.081*	0.19 (0.01)	0.20 (0.02)	*0.095*
degree	15.9 (1.08)	17.0 (1.68)	*0.081*	16.1 (1.07)	17.1 (1.68)	*0.095*
L	2.12 (0.07)	2.07 (0.09)	*0.081*	2.12 (0.07)	2.06 (0.09)	*0.095*
λ	1.12 (0.02)	1.11 (0.02)	*0.098*	1.12 (0.02)	1.11 (0.02)	*0.117*
C	0.60 (0.02)	0.60 (0.01)	*0.281*	0.60 (0.02)	0.61 (0.01)	*0.201*
γ	2.18 (0.25)	2.06 (0.22)	*0.171*	2.28 (0.24)	2.06 (0.21)	*0.165*
σ	1.93 (0.19)	1.85 (0.17)	*0.186*	1.94 (0.19)	1.85 (0.16)	*0.174*
E_{Glob}	0.54 (0.02)	0.56 (0.02)	*0.081*	0.55 (0.02)	0.56 (0.02)	*0.094*
Weighted Networks						
S	5.74 (0.61)	6.45 (0.71)	*0.007*	2993 (463)	3509 (734)	*0.041*
EW	0.36 (0.02)	0.38 (0.02)	*0.008*	186 (22)	205 (38)	*0.099*
L	5.25 (0.39)	4.82 (0.31)	*0.005*	0.01 (0.003)	0.01 (0.002)	*0.041*
λ	1.14 (0.02)	1.12 (0.03)	*0.061*	1.46 (0.33)	1.29 (0.12)	*0.099*
C	0.27 (0.02)	0.28 (0.03)	*0.040*	0.02 (0.005)	0.02 (0.004)	*0.230*
γ	2.04 (0.24)	1.94 (0.21)	*0.177*	3.28 (0.29)	3.11 (0.31)	*0.129*
σ	1.79 (0.22)	1.72 (0.18)	*0.301*	2.31 (0.36)	2.41 (0.16)	*0.309*
E_{Glob}	0.22 (0.02)	0.24 (0.01)	*0.005*	156 (27)	189 (42)	*0.041*

Table 4.22: ***DTI networks: global network characteristics by cognitive impairment in subgroup with definite epilepsy.*** *Comparison of global network characteristics between those with cognitive impairment and those without calculated from the FA and NOS networks. Data are mean (SD). Statistical testing was carried out using t-tests and p values are adjusted using the FDR set at 5% for 32 multiple comparisons (16 network measures, 2 network types). (FA: fractional anisotropy; NOS: number of streamlines; S: average network strength; EW: mean edge weight; L: average path length; λ: normalised average path length; C: clustering coefficient; γ: normalised clustering coefficient; σ: small worldness statistic; E_{Glob}: global efficiency; SD: standard deviation; FDR: false discovery rate)*

To assess whether the differences in L in the weighted networks between those with cognitive impairment and those without are due to the differences in mean network edge weight in the FA networks, a linear regression with L as the dependent variable and mean edge weight and cognitive impairment as predictors was created. Models for the weighted networks are shown in Table 4.23.

There is a statistically significant effect of adding the diagnosis of cognitive impairment as a predictor to L, confirming that there is a difference in L between groups that can not completely be accounted for by the differences in total edge weights between the networks.

	sum squares	F	*p*
L			
EW	5.12	88.2	*¡0.001*
Cognitive Impairment	0.312	7.21	*<0.026*

Table 4.23: ***DTI FA weighted networks: effect of mean edge weight on the association between cognitive impairment and average path length.*** *Linear regression modelling using L as the dependent variable and EW and the presence of cognitive impairment as predictors. Type I sums of squares were calculated for addition of cognitive impairment to EW as a predictor variable. (FA: fractional anisotropy; EW: mean edge weight; DTI: Diffusion Tensor Imaging; L: average path length)*

The association between network characteristics and IQ was also investigated in the group with definite epilepsy. In this subgroup, 17 (41.5%) had undergone formal neuropsychological testing, and 14 had achieved an IQ or DQ score. The other three were unable to complete testing and scores could not be assigned. The association of λ with IQ was investigated for both the binary and weighted FA and NOS networks. Scatter plots for the FA networks are shown in Figure 4.17. Pearson's correlation coefficient for the combined IQ or DQ scores with binary λ was -0.50 (*p=0.037*) for the FA derived networks and -0.55 (*p=0.041*) for the NOS derived networks. In the weighted networks, Pearson's correlation coefficient for the combined IQ or DQ scores with λ was -0.50 (*p=0.068*) for the FA derived networks and -0.353 (*p=0.215*) for the NOS derived networks.

In the subgroup with a definite diagnosis of epilepsy, the relationship between cognitive impairment and a longer path length that exists in the DTI networks in the whole cohort is present in the weighted networks but not the binary networks, and is only statistically significant for L and E_{Glob}, but not λ. The association between λ and IQ is also present in this subgroup.

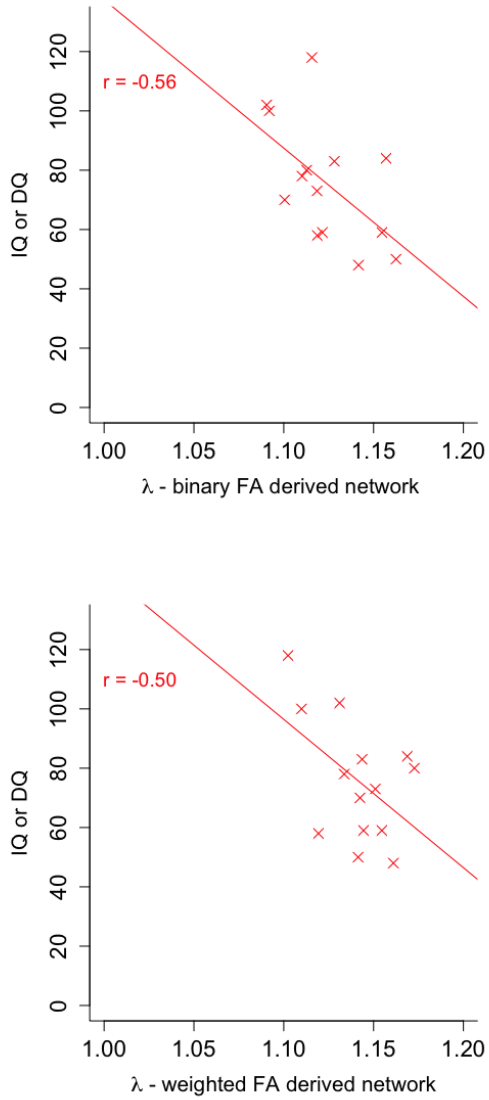

Figure 4.17: ***Association between IQ or DQ and λ in subgroup with definite epilepsy.*** *The normalised average path length (λ) from the FA derived networks is plotted against the combined DQ and IQ scores. Pearson's correlation coefficient is given on the graph along with the line representing the linear model fitted using linear regression with a gaussian model.* ***Top:*** *λ derived from FA weighted networks.* ***Bottom:*** *λ derived from FA binary networks (IQ: intelligence quotient; DQ: development quotient; λ: normalised weighted average path length; FA: fractional anisotropy; r: Pearson's product moment correlation coefficient)*

4.6 Discussion

4.6.1 Summary of findings

DTI networks were successfully created in 85 children with suspected epilepsy. Children with cognitive impairment had binary networks with lower density, average node degree, and global efficiency, and higher L and λ. Weighted networks had lower average node strength, average edge weight, and average global efficiency, and higher L and λ in those with cognitive impairment. This was consistent across networks constructed from NOS and streamline average FA. When cortical thickness networks were constructed to have a fixed density of 0.2 or proportional thresholding was used, aiming for network densities of around 0.2, similar findings of increased average path lengths in the the group with cognitive impairment were confirmed. The finding of an association between average path lengths with cognition was further strengthened by finding a dose response effect whereby IQ scores in the cohort were also associated with longer average path lengths.

To assess whether the association between average path length and cognition could be explained by an increase in the number and strength of network connections in children without cognitive impairment, L was normalised to λ by comparison with regular networks with the same number of nodes and edges, and the effects of network average edge weight were regressed. Neither of these steps were sufficient to remove the statistical association between average path length and cognitive function. This suggests that different network organisation rather than just number of connections plays a role in the determining the association between path length and cognitive function. However, regressing the effect of density did render the association between λ and cognitive dysfunction statistically insignificant in the binary networks. Further, normalising the NOS values to between zero and one, correcting raw cortical thickness values for age and sex, and creating cortical thickness networks with high densities also led to group differences no longer being present. This may be due to correction for confounding factors, or this may have been as a result of mathematical over-manipulation of networks causing real group differences to no longer be apparant.

The relationship between cognition, network average path length, and clinical features was explored to ensure that the findings of an association between average path length and cognition could not be explained by clinical features. The frequency of seizures and the number of AEDs were statistically significantly associated with network average path length and cognitive function. Including both the network average path length and the seizure frequency as predictors of cognition improved the amount of variance explained by the models, but adding average path length to the model decreased the effect of seizure frequency and vice versa. This suggests that there may be some mediation by structural network characteristics of associations between clinical epilepsy characteristics and the presence of cognitive impairment. Patients in whom a definite diagnosis of epilepsy was made after full investigation showed similar findings with increased path lengths associated with lower IQ values and cognitive impairment. However, these associations were not statistically significant in all network types, and this is likely due to a lack of power in this smaller subgroup analysis.

4.6.2 Limitations of findings

This suspected epilepsy cohort was created from a retrospective group of patients who all underwent MRI scanning with a particular protocol. However, out of 130 patients, both cortical thickness and DTI networks could be created for only 65 patients. Only 41 children in this cohort had a definite diagnosis of epilepsy following investigation and an accurate DTI whole brain connectome, and only 14 also had a documented IQ score. The small numbers within subgroups meant that subgroup analyses were underpowered. The models involving seizure characteristics, network characteristics and cognition were not repeated in the subgroup with a definite diagnosis of epilepsy due to the small number of patients in this group, and therefore the findings from these models may not apply to this subgroup. However, this cohort is a pragmatic representation of the clinical heterogeneity of patients assessed in a paediatric neurology department with suspected epilepsy, and therefore the findings in this cohort should be widely applicable to the majority of patients who are investigated for seizures. Although this was an undifferentiated cohort of children investigated for seizures, 56% underwent the MRI within one year of their first seizure, and 38% were not taking any AEDs, suggesting that for many children, this was their first imaging investigation for possible epilepsy. Several patients could not be included due to poor MRI quality or structural pathology interfering with MRI processing and interpretation, and this is representative of an undifferentiated cohort in clinical practice. Any research study is limited by the willingness of the participant to undergo the investigation, and children may particularly struggle with the noisy and claustrophobic MRI environment. Using scans acquired for clinical purposes ensures that there is a direct benefit to the participant of the investigation, but also means that data may be acquired that is sufficient for clinical diagnostic purposes where qualitative assessment is required, but may have too much artefact for research quantitative analysis. Automated quantitative MRI techniques are also usually tested on adult data from healthy volunteers, and therefore techniques may be more difficult to apply to clinical paediatric patients. Only 29% of MRI scans in this study did not require manual intervention in the Freesurfer processing pipeline to achieve accurate segmentation and parcellation, and this is likely due to the scans not being the homogenous research scans that automated analysis is trained on. It is not known whether the need for manual editing of processing has led to inconsistencies, or could influence the results of this study, but all scans were checked for errors, and patients with scans that could not be accurately processed were excluded.

Various different techniques of network construction were employed in this cohort. Two different methods of determining edge weights from DTI were investigated (NOS and FA), and findings were mostly consistent between these two methods. However, there were some differences, which shows that in the same patient group, network construction techniques will affect study findings. Raw streamline counts are problematic due to spurious results from seed points in white matter, a tendency to end at gyri, difficulty reconstructing long-range connections, and the possibility of an increased number beginning or ending at cortical nodes with larger volumes or surface areas.[175] Due to these problems with raw streamline counts, networks derived from tract averaged FA, normalised streamline counts, and binary networks were also examined. There were some differences in findings between networks constructed using different methods to determine edges. In particular, group differences were not evident after normalising the NOS edge weight distributions. Whilst this may represent an accurate correction of spurious results, it may also represent the overcorrection or over-normalisation of findings

to force data to fit models that actually removes the existing group differences. Correction of streamline counts for node volume or surface area to streamline density was not undertaken, and this is a limitation of this study. However, group differences remained present in binary networks, which do not use the weighting information, and correction to streamline density would not have altered the binary networks created from the number of streamlines information. The cortical thickness networks were thresholded for analysis with the aim of removing spurious connections without removing network topology through over correction. However, there is no established agreed technique for thresholding networks, and different thresholds in this cohort produced quite different findings. The three major approaches to thresholding in brain connectomics are to aim for a desired density, use a 5% significance level so only edges likely not to be due to chance are included, or to threshold so that all nodes are connected or a large as possible component exists.[52] When choosing the lowest threshold that ensured all nodes were connected, the cortical thickness networks were very dense (0.6-0.8), and such a high density means that small world architecture is not present, as although average path length decreases with density, clustering also increases.[70] The density at which the network is analysed can determine many features of the network,[52] and although brain networks are often analysed at low densities,[70] recent tract tracing studies in Macaque monkeys involving high resolution data have analysed brain networks with much higher densities, suggesting that with increasing technological advances, the density at which brain networks are analysed may well increase,[70,183] and what are currently thought of as spurious nuisance connections to discard may provide further enlightening information about brain structure. The reliance of network characteristics on network degree and density makes it unsurprising that group findings were different when the cortical thickness networks were analysed at 20% density rather than 60% density. It is also unsurprising that findings differed between DTI and cortical thickness networks. However, it is reassuring for the robustness of the conclusions of this analysis that networks constructed from cortical thickness covariance and networks constructed from DTI had similar between group findings when analysing the same group of patients with networks of approximately the same densities.

The practical definition of cognitive impairment employed in these analyses arose from a pragmatic approach to a cohort with a wide range of cognitive abilities. Even if neuropsychological assessment had been undertaken in every participant, some of the participants would not have achieved a valid IQ score due to their significant cognitive comorbidities. In some participants who were doing well at school, cognitive testing would not have changed their management, and therefore was not undertaken. However, the groups could be criticised for not having a formal dedicated assessment of the presence of intellectual disability or learning difficulties. The retrospective nature of this study meant that testing was not feasible, and data that was not recorded at the time of assessment was not possible to source. Employing a pragmatic definition of cognitive impairment ensures that the results of this study are applicable to general patient populations seen in clinical practice. The group differences were also corroborated by similar findings in the subgroup in whom IQ scores were available. The fact that the same findings were evident with IQ scores and the pragmatic definition provides some evidence for its use as a definition of cognitive impairment.

4.6.3 Comparison of findings to prior studies

This study has shown an association between cognitive impairment and low IQ scores with increased structural network average path length. This is in keeping with studies showing an association between a lower IQ with a longer average path length in functional and structural networks in schizophrenics,[82,86] an association between IQ and average path length in DTI derived networks in a healthy adult population[89], and a higher global efficiency with higher IQ in a healthy childhood population.[93] However, as shown within this study, this association is not consistently found in all network types and all populations. Nine patients with cognitive impairment and frontal lobe epilepsy did not show any statistically significant differences in network properties compared to those without cognitive impairment,[131] and there were no significant correlations between global network properties and IQ in a different group of patients undergoing epilepsy surgery.[135] In a larger study from the human connectome project there was no association between IQ and functional network characteristics.[88] Both the size and characteristics of the populations studied plus the network construction techniques may all play a role in the different findings between studies. Smaller studies may be underpowered to detect differences between populations. In addition, a small range of IQ scores or cognitive functioning may make differences more difficult to detect statistically. Many research studies are carried out in healthy volunteers or patients with near normal imaging and near normal cognition, and if the range of severely affected patients are not included in these studies, then the study results will not apply. For research findings that may be applied to a clinical population, it is important to study the clinical population who may benefit from the study results.

4.6.4 Biological mechanisms and future questions

This study found an association between an increased structural network average path length and cognitive impairment in children investigated for suspected epilepsy. Increased average path lengths occur in networks with poorer integration, fewer long range connections, and a more regular topology. Poorer network integration could be as a result of generalised whole brain disruption of brain structure. Epilepsy has been associated with widespread white matter changes,[136] as well as changes in cortical thickness.[137,138] Cognitive dysfunction in epilepsy has been previously shown to be associated with an early age of onset of epilepsy,[111,112] a longer duration of epilepsy,[113] an encephalopathic aetiology,[113,114] increased seizure frequency,[108,109] and the use of AEDs.[115] Many children in this study were not taking AEDs, and the MRI was the first investigation for potential seizures. As a higher path length in those with cognitive impairment was already present at the early stages of an epilepsy diagnosis, there is a suggestion that the cognitive dysfunction seen in epilepsy may be more as a result of the underlying problem responsible for the epilepsy, rather than as a result of the effects of seizure activity. However, including both seizure characteristics and network characteristics in models predicting cognitive impairment explained more model variance than either factor alone. This suggests that both seizure characteristics and network characteristics are important in determining cognitive dysfunction, and that network path lengths may not be solely dependent on epilepsy or seizure characteristics, but may also depend on the genetic and environmental background of the patient. Adding average path length to models predicting cognitive function from clinical epilepsy variables decreased the effect of the

clinical variables on cognition. This suggests that average path length may partially mediate this relationship. If increasing network average path length is a possible mechanism by which factors such as increased frequency of seizures, an early age of onset of epilepsy, and a longer duration of epilepsy are related to cognition, then it could function as a biomarker for cognitive dysfunction in epilepsy. However, it is still unclear as to why the path length in structural brain networks is increased in epilepsy, and whether this reflects an underlying structural cause for the epilepsy. If there were more patients available with IQ scores then factor analysis to combine epilepsy factors, followed by structural equation modelling would have been undertaken to try to tease out this relationship plus any mediation effects between network average path length, epilepsy characteristics, and cognitive function.

4.7 Conclusions

In a cohort of children with suspected epilepsy, the presence of cognitive impairment was associated with lower overall network densities, average node degrees, average node strengths, and average network edge weights. Children with cognitive impairment had higher average path lengths and lower global efficiencies in networks created from DTI NOS and streamline averaged FA. These findings persisted when corrections were made for differing network densities or average edge weights, suggesting network organisation as well as number and strength of edges contributes to the difference in network average path lengths between the groups. Cortical thickness networks thresholded to similar densities as the DTI networks also showed higher average path lengths in children with cognitive impairment. Longer network average path lengths were also associated with lower IQ scores. These findings were robust in the subgroup of children who later had a definite epilepsy diagnosis. The relationship between cognition and network average path length also remained significant when seizure frequency and number of AEDs were included in models. However, no group differences were evident in cortical thickness networks analysed at higher network densities, or in NOS derived networks after normalisation of the edge weights. This suggests that network construction and modelling methods have a strong influence on findings.

Chapter 5

Epilepsy Surgery Cohort

5.1 Chapter Abstract

An estimated one third of patients with epilepsy are resistant to AEDs and continue to experience seizures despite maximal medical therapy. Surgery to resect the epileptogenic focus or disrupt seizure pathways may be considered in patients with medication resistant epilepsy. The main aim of epilepsy surgery is to stop or reduce seizures. However, changes in cognitive function following surgery may greatly influence the perceived benefits of surgery for the patient and their family. This chapter investigates the pre-operative structural network characteristics in the healthy non-operated hemisphere in a cohort of children undergoing contralateral resective epilepsy surgery. First the cohort was divided into those with a pre-operative IQ greater than or equal to 70 and those with a pre-operative IQ less than 70. There were no statistically significant differences in cortical thickness measurements or cortical thickness networks within the healthy hemisphere between the two groups. Next, the cohort was divided into a group who had a post-operative increase in IQ of at least 10 points at two years and a group whose IQ changed less than 10 points post-operatively. The group with an increase in IQ post-operatively showed higher cortical thickness network global efficiency across a range of network thresholds. The group with an increase in IQ post-operatively also had a shorter duration of epilepsy pre-operatively. The structural connectome of the healthy hemisphere may therefore be a marker of the capacity for cognitive improvement following epilepsy surgery.

5.2 Introduction

Medication resistant epilepsy requires significant health and social care resources and can affect quality of life due to the effects of poor seizure control and developmental and cognitive deterioration or delay.[114] The frequency of cognitive impairment in epilepsy varies with aetiology, with low grade neoplasms being associated with a very low likelihood of intellectual disability and epileptic encephalopathies being highly associated with cognitive dysfunction.[113,114] However, an early age of onset of epilepsy,[111,112] longer duration of epilepsy,[112,113] and increased seizure frequency[108] are associated with worse cognition regardless of the epilepsy aetiology. Thus it is not clear what

contribution the underlying aetiology and the effect of seizure activity have on cognition. Cognitive deficits may be the result of epileptic activity in structurally normal brains, but equally both cognitive deficits and uncontrollable seizures may be determined by the same underlying structural pathological process.

Children undergoing focal surgical resection for epilepsy provide an excellent model to study cognitive dysfunction in epilepsy as surgical procedures aim to remove the epileptogenic focus and prevent seizures spreading, but do not alter the underlying pathological process that has led to epilepsy. Epilepsy surgery candidates are fully assessed pre and post-operatively with a full clinical and neuropsychological assessment. Children with medication resistant epilepsy referred for epilepsy surgery have a high frequency of cognitive dysfunction with around 60% having a pre-operative IQ lower than 80.[111,113] Meta-analyses of post-operative changes in IQ following epilepsy surgery have reported pooled estimates of a 16-19% chance of a gain in IQ post-operatively.[124,125] Determining which factors are associated with better cognitive outcomes following epilepsy surgery could aid pre-operative outcome prediction, provide better information for patients and families, and could lead to a better understanding of how epilepsy affects cognition, which could lead to improved interventional strategies that aim to preserve or improve the factors associated with improved cognition.

Widespread structural changes have been reported in focal onset epilepsies, with reduced FA and cortical thinning in both the ipsilateral and contralateral hemispheres.[117–119,137] The structure of the brain can be modelled as a network, known as a connectome, with anatomical regions as nodes and either white matter streamlines determined from DTI or covariance of ROI thickness or volume as edges.[47] Networks can be mathematically analysed using graph theory.[46] The global changes in brain structure seen in epilepsy can be reflected in alterations in measures used to analyse and describe structural connectomes. Chapter 2 reviews the findings of studies investigating differences in structural networks derived from MRI between patients with epilepsy and healthy controls and concludes that studies have a tendency to show an increased network average path length in patients with epilepsy.[133,135,142,150,151] Better network efficiency with shorter average path lengths or higher global efficiency has been associated with improved cognitive function in healthy research participants and some patient groups.[82,89–91,93] In Chapter 4, an association between whole brain network higher average path lengths and cognitive impairment or lower IQ was shown in a group of patients investigated for suspected epilepsy. A small number of other studies have also investigated the association between structural network characteristics and cognition in epilepsy and found a less efficient network organisation in those with lower scores on cognitive assessments.[133,134]

This chapter builds on the findings of Chapter 4 by investigating whether similar changes in network structure in the healthy hemisphere are associated with pre-operative IQ in a group of children undergoing resective epilepsy surgery for an abnormal epileptogenic focus in their contralateral hemisphere. This will determine whether similar methods of investigating network structure can be applied to paediatric patients with an abnormality within one hemisphere. The association of brain network structure with post-operative change in IQ will then also be investigated. As all children undergoing resective epilepsy surgery have focal onset seizures, and many have a structural abnormality visible on MRI, the non-operated, contralateral hemisphere will be investigated so that any changes in network structure directly attributable to an obvious focal structural abnormality are not

included in the analysis. Assessing whether differences in pre-operative network organisation within the non-operated hemisphere are associated with post-operative change in IQ scores could lead to a better understanding of whether cognitive function is constrained by pre-existing brain structural organisation, and could help in determining structural correlates of cognition and how structural brain organisation leads to changes in cognitive function in epilepsy.

5.3 Aims

This chapter aims to address the following questions in a cohort of children undergoing unilateral resective epilepsy surgery.

- Is pre-operative network average path length or global efficiency related to pre-operative IQ?
- Is pre-operative network average path length or global efficiency related to post-operative change in IQ?

As the networks are derived from cortical thickness measurements, the association of cortical thickness with IQ is also assessed to ensure that any differences in network structure are not due to differences in absolute cortical thickness measurements.

5.4 Methods

5.4.1 Epilepsy surgery cohort

An epilepsy surgery cohort was identified as described in Chapter 3, Section 3.3.2. The details of 259 consecutive patients who had undergone epilepsy surgery between 1994 and 2014 and who had been assessed both pre and post-operatively in the paediatric neuropsychological department at the UMCU were extracted from the hospital electronic records. PACS was searched for each patient and MRI brain scans carried out before the date of surgery were reviewed. Those with a pre-operative 3D volume T1-weighted non contrast enhanced sequence available on the UMCU PACS system were included. Patients under the age of one year at the time of the MRI scan or 18 years or older at the time of undergoing surgery were excluded. Patients with significant artefact on MRI which precluded accurate analysis were excluded, and examples of patients excluded due to MRI artefacts are shown in Figure 3.1 in Chapter 3, Section 3.7.2. Patients with bilateral pathological findings on MRI or bilaterally arising seizures on EEG and those who had undergone bilateral or midline procedures were excluded to create a cohort with an apparently healthy hemisphere contralateral to the side of the operation. This contralateral hemisphere was termed the 'healthy hemisphere.' The number of patients excluded at each stage with reasoning is shown in the flow diagram in Figure 5.1. In total, there were 99 patients from the original 259 who met the inclusion criteria for this epilepsy surgery cohort.

For all included patients, clinical and demographic details were collected from the electronic record system of the UMCU, the Dutch paediatric epilepsy surgery database, and other surgical epilepsy

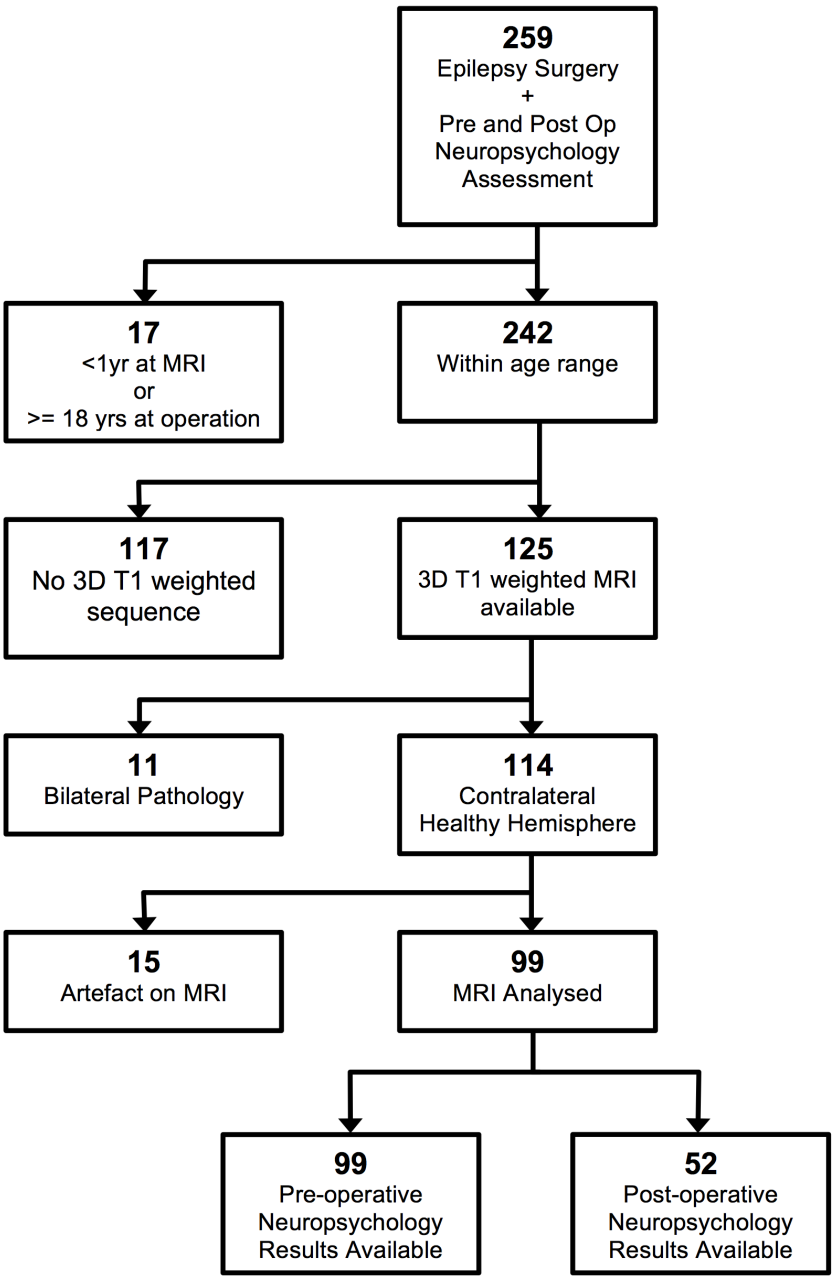

Figure 5.1: ***Epilepsy Surgery Cohort.*** *Numbers of patients initially identified in the consecutive cohort and reasons for exclusion from analyses.*

databases held by researchers and clinicians at the paediatric neurology department. Data collected included relevant demographics, epilepsy characteristics, medication, and surgical outcomes.

5.4.2 MRI processing

All patients had pre-operatively undergone one of the 3D T1-weighted MRI sequences described in Section 3.7.1. MRI data were extracted from PACS, converted to NifTI format, and processed with

Freesurfer sorftware as described in detail in Section 3.7.2. In 5 (5%) cases MRI scans required manual registration to the Talairach atlas, in 10 (10%) cases scans required manual editing of the brain mask to achieve an accurate skull strip even after adjusting the skull stripping watershed threshold, and in 24 (24%) cases scans required editing of the white matter template using either control points or manual editing. As some scans required manual intervention at multiple stages of the Freesurfer pipeline, 28 (28%) scans in total underwent manual editing and 71 (72%) did not require any manual editing. Editing was completed to achieve accurate segmentation and parcellation of the healthy, non-operated hemisphere, but the operated hemisphere was not corrected as this was not analysed. Hemispheres were run separately within the steps of the Freesurfer processing stream where this was feasible to allow the healthy hemisphere to be processed when abnormal anatomy prevented accurate processing of the pathological hemisphere.

Cortical thickness measurements for each region of the Desikan-Killiany atlas[48] were extracted. Mean hemisphere cortical thickness measurements as calculated across vertices in Freesurfer and across ROIs were compared with clinical and neuropsychological variables. Cortical thickness networks were created in MATLAB as described in detail in Section 3.8.1.1. For each group investigated, 34 single hemisphere cortical regions of the Desikan-Killiany atlas[48] as listed in Table 3.2 in Section 3.8.1.1 were used as network nodes to create a healthy hemisphere group network. The pearson product moment correlation coefficient between the cortical thickness of each network region was calculated and this was taken as the edge weight between each pair of nodes to create a single within hemisphere network for each patient group from their healthy, non-operated hemisphere similar to the description of the creation of cortical thickness networks in previous studies.[83,134,143] Self-self connections were set to zero and negative correlations were removed from the group connectivity matrices to allow analysis of networks using graph theory methods.[47,74] Matrices were thresholded using absolute thresholds to remove all edges with weights below the threshold value in steps of 0.05. Network metrics were calculated at two different thresholds. The first was the highest threshold value that maintained a completely connected network without any disconnected nodes as per previous studies of cortical thickness networks.[83,173] The second threshold was chosen to create networks with a density as close as possible to 0.2, as this is a common density at which previous studies have examined brain structural and functional connectomes.[52,70,86] To create binary networks, all existing edge weights were set to one with non-existent edges set to zero.

Connectivity matrices were analysed using the Brain Connectivity Toolbox[74] in MATLAB Release 2015b (The Mathworks Inc, Massachusetts, United States). Network density, degree, node strengths, edge weights, path lengths, global efficiency, clustering coefficients, and small world indices were calculated as described in Section 3.8.2. Group healthy hemisphere cortical thickness network measures were compared with each other using permutation testing. The subjects were permuted into 1000 random group allocations and network measures were computed for these random permuted group networks. The *p* values were calculated using the number of times the absolute difference between the randomly permuted groups was greater than the absolute difference between the experimental groups divided by the number of permutations, as described in Section 3.9.

5.4.3 Neuropsychology analysis

Neuropsychological testing was carried out both pre and post-operatively in the paediatric neuropsychology department of the UMCU by trained clinical paediatric neuropsychologists as part of the Dutch national paediatric epilepsy surgery programme. Age and developmental stage appropriate testing methods were used to evaluate the IQ of the child. When IQ testing was not able to be carried out, but the assessing neuropsychologist deemed it to be clinically appropriate, they assigned a DQ score to the child as described in Section 3.6. Not all children had a numerical IQ or DQ score assigned as some children were too impaired to be able to complete assessments. The age appropriate instruments used to assess IQ and the frequency of their use in this cohort are shown in Table 5.1. All children were tested post-operatively with the same test as pre-operatively except for three children. Two children were assessed pre-operatively with the BSID at ages 25 and 42 months and post-operatively with the SON at ages 4 years and 5 years and one child was assessed pre-operatively with the WISC at age 16 years and post-operatively with the Wechsler Adult Intelligence Scales (WAIS) at 19 years old.

Results of neuropsychological assessments were available pre-operatively for all patients, but only 52 (53%) patients had results of the post-operative tests undertaken available from the neuropsychology department. The number of patients with available neuropsychology assessments is included in Figure 5.1. The post-operative score was always the two year follow up score where this was available. When a score was available at one year but not at two years, this was used as the post-operative score. The final post-operative neuropsychological testing used in the analyses was undertaken between 13 and 38 months post-operatively, with a mean of 24 months.

Only TIQ or DQ scores were used for the analyses presented in this chapter rather than subscores as all neuropsychological assessments in use assigned either a TIQ or DQ score with a population normal mean of 100 points and a standard deviation of 15 points. The difference between pre-operative and post-operative scores was calculated as the post-operative score minus the pre-operative score. When assessing IQ change only children tested using the same instrument and who scored within the assessable range of the instrument at both time points were included. The assessable range for IQ assessments across tests was a score of greater than 55 points. Children who were not assigned a score on initial testing did not achieve a score of more than 65 on repeat post-operative testing in any cases and were not included in assessments of IQ change.

To assess the difference in network characteristics between those with cognitive impairment and those without, children were divided into two groups based on IQ scores. Children with scores between 70-130, which are within two standard deviations of the population mean were considered to have scored within the normal range of the test. Those who scored below 70 points, or who were unable to be assigned an IQ or DQ score due to severe impairment were considered to have cognitive impairment. No children in this cohort scored above 130 points.

To assess the association of network characteristics with change in IQ, children were divided into a group who showed an increase in at least 10 IQ points post-operatively, and those who did not. Ten points was taken as the clinically meaningful change in IQ score as per previous studies of IQ changes following epilepsy surgery.[125]

Neuropsychological Test	Number Tested	Age Range
Wechsler Intelligence Scales for Children (WISC)	64	5-17 years
Wechsler Adult Intelligence Scales (WAIS)	5	16-17 years
Snijders-Oomen Niet-verbale Intelligentietest (SON)	10	3-7 years
Kaufman Adolescent and Adult Intelligence Test (KAIT)	3	15-17 years
Bayley Scales of Infant Development (BSID)	17	16-165 months
Total	99	

Table 5.1: ***Frequency of use of pre-operative IQ tests.*** *The number of patients and age range assessed with each type of neuropsychological assessment.*

5.4.4 Statistical analysis

Statistical testing was carried out using R version 3.4.0 "You Stupid Darkness" (The R Foundation for Statistical Computing, 2017). Statistical analysis was carried out using t tests for normally distributed data, Mann Whitney U tests for numerical data that did not follow a normal distribution, and X^2 tests for categorical data as described in Section 3.9. FDR corrected *p* values [181] are reported where multiple comparisons were performed for network measures. For each network analysis, the *p* values were adjusted for 32 comparisons (2 network types and 16 network measures, for example the values in Table 5.5). For multivariable analyses, logistic regressions were performed for categorical outcome data and linear (gaussian) regressions were performed for numerical data. For all models, the model fit, residuals and standard errors were analysed.

5.5 Results

5.5.1 Demographics and clinical features

5.5.1.1 Demographics

There were 99 patients included in the final epilepsy surgery cohort as described in Figure 5.1. All patients underwent surgery between 2001 and 2014 at the UMCU. Age at the time of the operation ranged between one year and 17 years and the age distribution is shown in Figure 5.2. The median age at the time of the procedure was 10 years. There were 50 (51%) male patients in the cohort.

5.5.1.2 Epilepsy characteristics

Epilepsy aetiology according to post-operative histological and imaging findings is shown in Table 5.2. All included patients had a focal onset epilepsy. In six (6%) cases a formal diagnosis was unable to be reached from the resected tissue or imaging.

Fifty (51%) patients had undergone a resective surgical procedure on the left hemisphere and the other 49 (50%) on the right hemisphere. There were 78 (79%) procedures that were limited to within a single

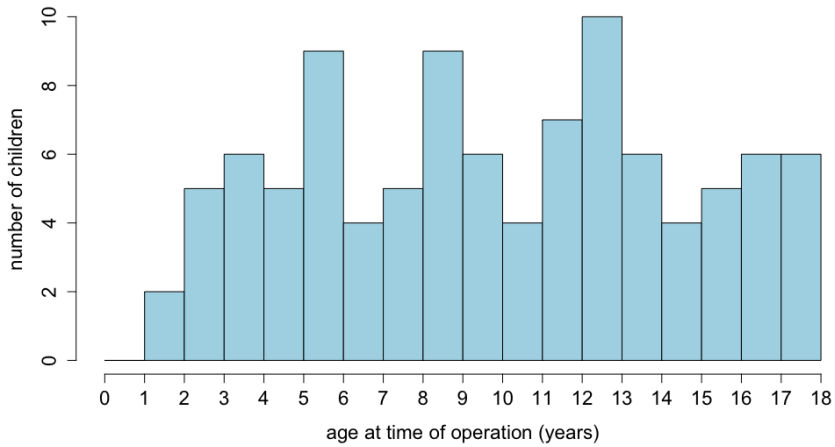

Figure 5.2: ***Age at time of operation.*** *Age distribution at the time of the surgical procedure*

Aetiology	Total
Malformation of Cortical Development	**36**
Focal Cortical Dysplasia	29
Hemimegalencephaly	2
Other	5
Tumour	**28**
Ganglioglioma	19
DNET	5
Oligodendroglioma	2
Glioneuronal	1
Harmartoma	1
Hippocampal sclerosis	**11**
Vascular	**11**
Ischaemic	6
Haemorrhagic	3
Cavernoma	2
Neurocutaneous	**7**
Tuberous Sclerosis	5
Other	2
No tissue diagnosis	**6**
Total	99

Table 5.2: ***Epilepsy aetiology.*** *Diagnostic categories determined by histology and imaging findings. (DNET: dysembryoplastic neuroepithelial tumour)*

lobe. Seventeen (17%) procedures were hemispheric and four (4%) involved a wider area than a single lobe but not the whole hemisphere. The breakdown by site and side of procedure is shown in Table 5.3.

The age at onset of epilepsy ranged from the first year of life to 14 years. The distribution of the age at

onset is plotted in Figure 5.3. Twenty-one (21%) patients had their first seizure within the first year of life, and 53 (54%) had an onset before the age of 3 years. The duration of epilepsy at the time of surgery ranged from six months to 16 years. Epilepsy duration at the time of surgery is shown in Figure 5.4. Forty-three (43%) patients underwent surgery within five years of onset of epilepsy, but only 8 (8%) patients underwent epilepsy surgery within two years of onset.

	Side	
Site	Left	Right
Single Lobe	**42**	**36**
Frontal	15	15
Temporal	25	18
Parietal	2	1
Occipital	0	2
Multilobar	**2**	**2**
Hemispheric	**6**	**11**
Total	50	49

Table 5.3: ***Side and site of operation.*** *Multilobar includes any operation extending to more than one lobe but less than the whole hemisphere.*

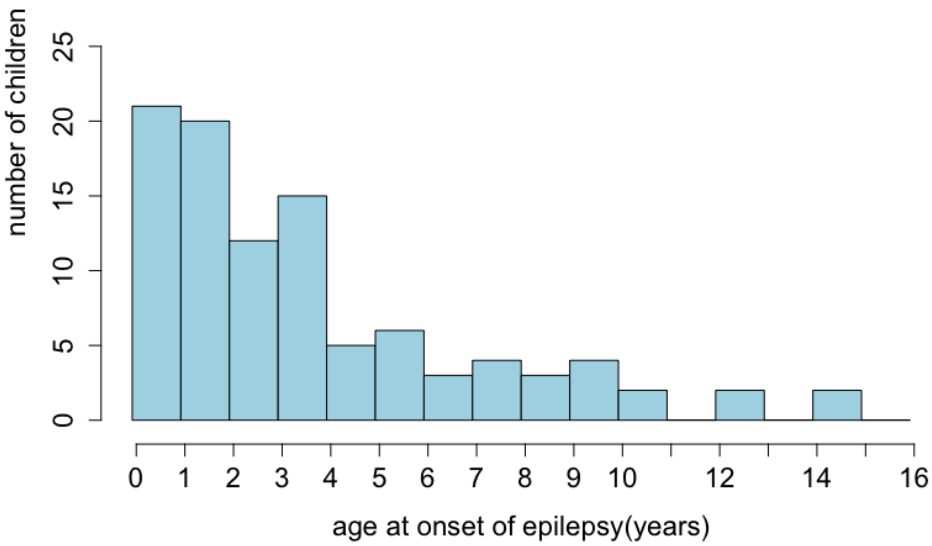

Figure 5.3: ***Age at onset of epilepsy.***

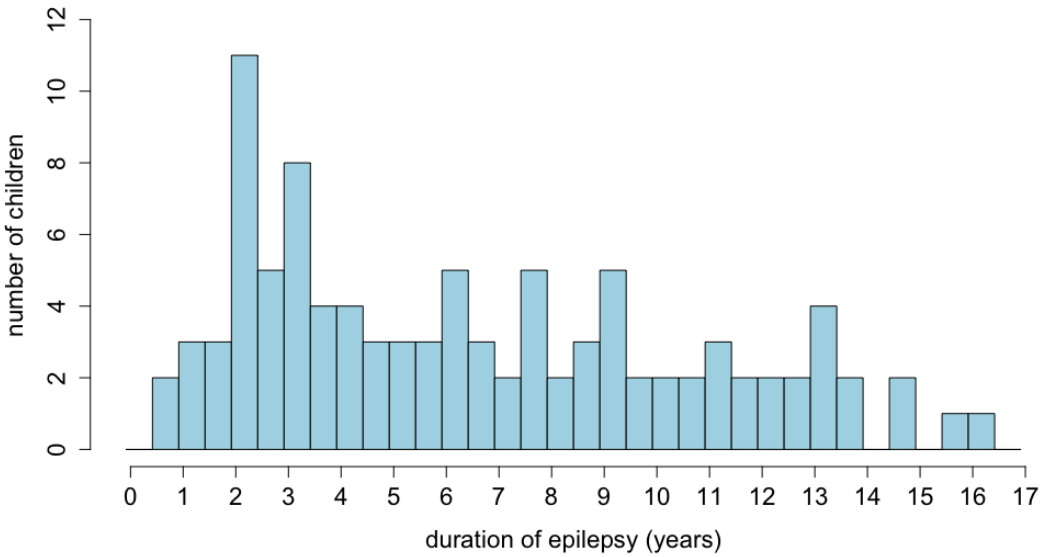

Figure 5.4: ***Duration of epilepsy.*** *Duration of epilepsy at the time of operation*

5.5.1.3 Seizure outcomes

Engel scores were available for 94 patients at one year post-operatively and of these 74 (79%) patients were seizure free with an Engel score of 1A. At two years post-operatively, Engel scores were available for 88 patients, of whom 61 (69%) were seizure free with an Engel score of 1A. The last available Engel score after 2 years of follow up is shown in Figure 5.5. In the six patients in whom Engel scores were not available at two years, but were available at one year, the one year post-operative score was carried over as the last available Engel score. AED use at two years or the last post-operative assessment was determined for 92 patients. Of these 34 (37%) had stopped taking all AEDs.

An Engel score of 1A at the last available follow up was associated with a shorter duration of epilepsy (*p=0.022*) and a diagnosis of hippocampal sclerosis (*p=0.047*). The Engel score was not associated with the age at operation, or the age of onset of epilepsy. An Engel score of 1A was associated with being AED free post-operatively (*p=0.002*).

5.5.2 Neuropsychological assessments

All patients had undergone pre and post-operative neuropsychological assessment. The results for all 99 pre-operative assessments were available. Seven patients had not been able to complete age and development appropriate assessments of IQ or DQ and scores could not be assigned. Sixty nine (70%) children completed an IQ assessment and achieved a score of greater than 55 points, and within the assessable range of the assessment. Twenty-three (23%) children were either assigned a DQ using the BSID or were assigned a score that was lower than 55 on the other instruments. The range of pre-operative IQ and DQ scores are shown in Figure 5.6.

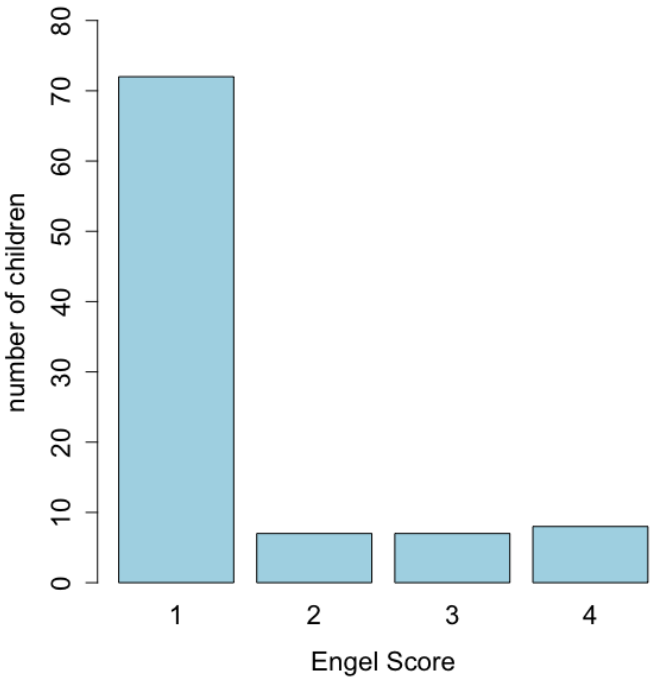

Figure 5.5: ***Engel score at two years.*** *Distribution of Engel scores by numerical category at 2 years post-op or last follow up available prior to this.*

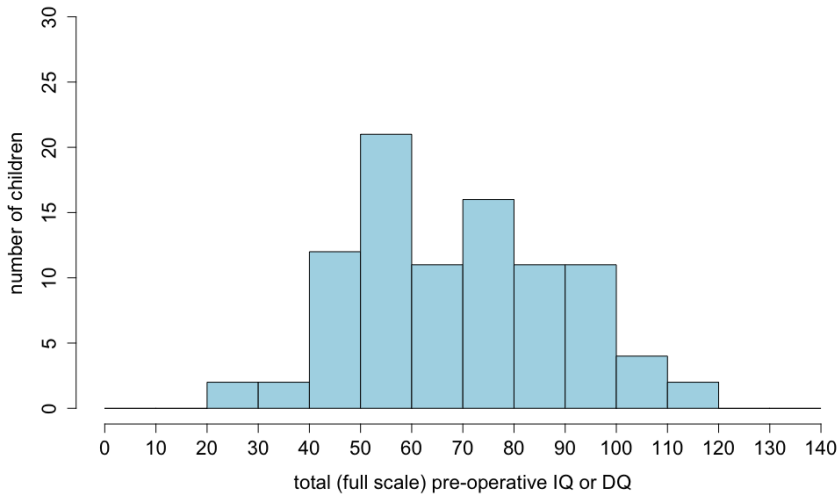

Figure 5.6: ***Pre-operative IQ score.*** *Distribution of combined pre-operative IQ and DQ scores. (IQ: intelligence quotient; DQ: developmental quotient)*

Neuropsychological assessment was completed in all patients post-operatively. However, the results of the assessment could only be sourced for 50 patients at one year and 41 patients at two years of follow up. There was an available result of the post-operative assessment for 52 (53%) patients in total. There was no difference in demographics, epilepsy characteristics, or outcome between the group with

post-operative scores available and the group without post-operative IQ scores available. Of the 52 patients with post-operative IQ or DQ scores available, 35 had scored greater than 55 points on their pre-operative assessment and were included in the analysis of change in IQ. A change in IQ of 10 points was taken as a clinically meaningful change.[125,126,165] In total there were 11 of 35 (31%) patients who scored more than 55 points on their pre-operative assessment and whose score increased by at least 10 points post-operatively. There were 24 of 35 (69%) patients whose IQ score did not increase more than 10 points. Within this group of 24 patients, none had an IQ score decrease of over 10 points from the pre-operative assessment to the post-operative assessment. None of the patients who had a IQ of less than 55 points pre-operatively increased to a IQ score of greater than 65 post-operatively. There was no statistically significant difference in the cohort between the mean IQ scores pre-operatively and post-operatively.

The age at which the neuropsychology assessment was undertaken was associated with the IQ and DQ combined scores ($p<0.001$). Age at testing is plotted against the pre-operative and post-operative IQ or DQ scores in Figure 5.7.

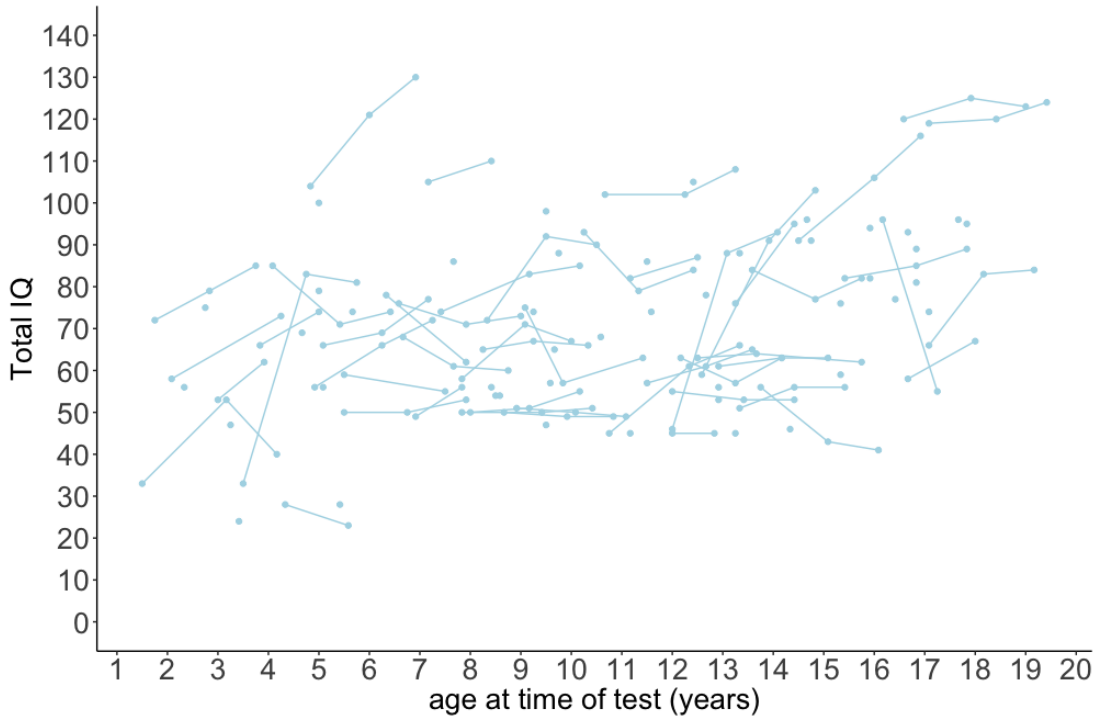

Figure 5.7: ***Change in IQ or DQ score and age at testing.*** *Dots represent scores. All assigned pre-operative DQ or IQ scores are included in the graph. Lines join each individuals pre-operative score to their one or two year follow up score where this is available. Single dots without lines represent patients in whom no post-operative score was available. (IQ: intelligence quotient; DQ: developmental quotient)*

Children at younger ages were assessed using instruments designed to measure DQs as can be seen in Table 5.1 and therefore lower scores were possible. When only those with a IQ of greater than 55 were considered, age was still associated with pre-operative IQ ($p=0.008$). The age of onset of epilepsy was associated with both the pre-operative combined IQ and DQ scores ($p<0.001$) and the IQ scores in those who scored greater than 55 points ($p<0.001$), with an earlier age of onset of epilepsy associated

with a lower IQ score. Pre-operative IQ was not statistically significantly associated with the duration of epilepsy. Multilobar procedures were associated with lower pre-operative combined DQ and IQ scores (mean:57.6, SD:12.1 vs mean:72.9, SD:20.6 $p<0.001$) and when only IQ scores greater than 55 were considered (mean:65.4, SD:16.3 vs mean:79.9, SD:8.7 , $p<0.001$). The side of operation and aetiology categories were not associated with pre-operative IQ.

In the 52 patients with post-operative IQ or DQ scores available, the post-operative IQ was strongly correlated with the pre-operative IQ score (r=0.73, $p<0.001$). The post-operative IQ score was also associated with the age at onset of epilepsy ($p=0.013$). However, the post-operative IQ score was not associated with the age at assessment, the duration of epilepsy pre-operatively, the side of operation, multilobar procedures, or the aetiology of epilepsy. The post-operative IQ score was higher in those who had an Engel score of 1A post-operatively (mean:86.6, SD:20.9 vs mean:68.4, SD:10.2, $p<0.001$). The post-operative IQ was not associated with post-operative cessation of AEDs.

5.5.3 Is cortical thickness associated with pre-operative IQ?

Mean cortical thickness measurements of the healthy, non-operated hemisphere were obtained from the pre-operative 3D T1-weighted MRI scans. Mean healthy hemisphere cortical thickness is plotted against age at MRI scan in Figure 5.8. Cortical thickness decreased with age (r=-0.55, $p<0.001$). Cortical thickness is plotted against the combined pre-operative IQ and DQ scores in Figure 5.9. Mean cortical thickness had a linear correlation with the combined IQ and DQ scores (r=-0.26, $p=0.011$), but not with the IQ scores alone (r=-0.15, $p=0.22$), suggesting that the relationship was influenced heavily by the few lower DQ scores.

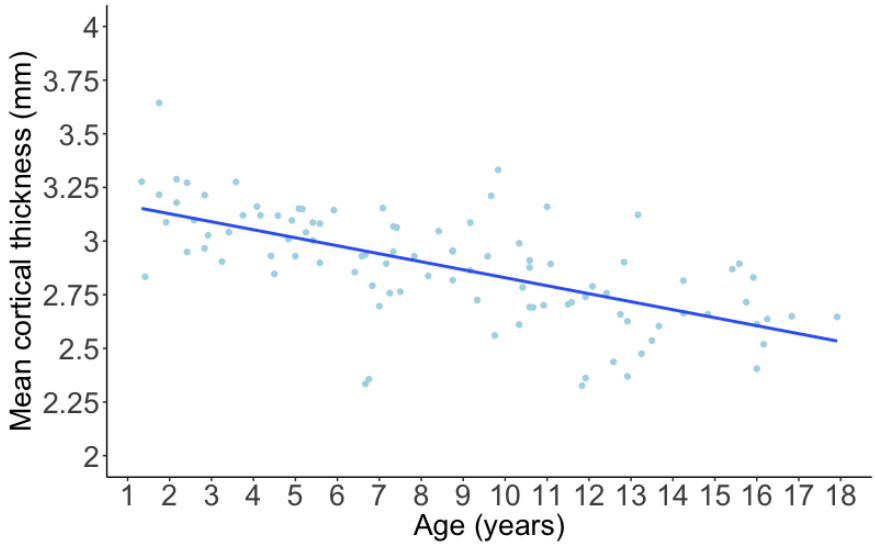

Figure 5.8: ***Cortical thickness by age.*** *Mean cortical thickness of the healthy hemisphere pre-operatively, plotted against age at time of MRI. (mm: millimetres; MRI: magnetic resonance imaging)*

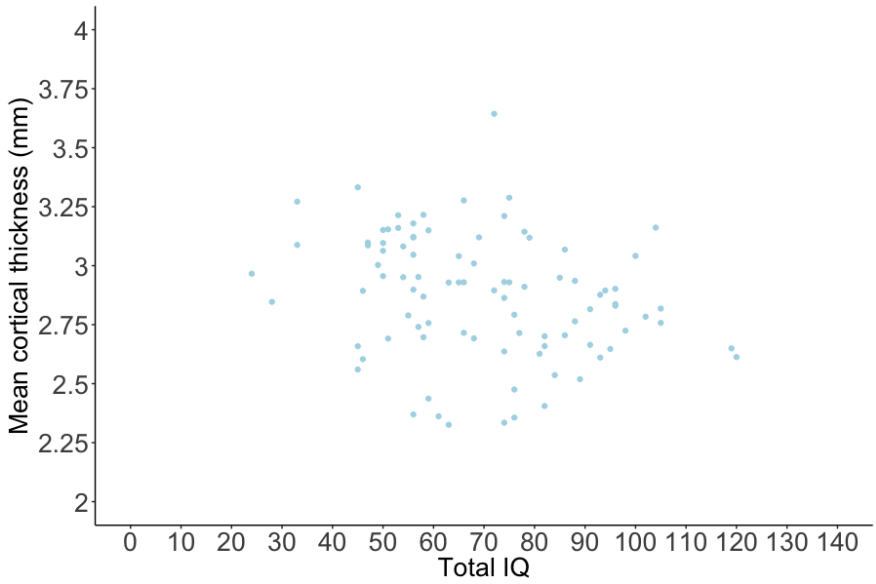

Figure 5.9: ***Cortical thickness with IQ*** *Mean cortical thickness of the healthy hemisphere pre-operatively, plotted against combined IQ and DQ scores. (IQ: intelligence quotient; DQ: developmental quotient; mm: millimetres)*

5.5.4 Are cortical thickness network characteristics in the healthy hemisphere related to pre-operative IQ in children undergoing epilepsy surgery?

To assess whether cortical thickness network characteristics are related to pre-operative IQ, the cohort was divided into two groups. One group consisted of those with pre-operative IQ scores within two standard deviations of the population mean, who were considered to have scored within the normal range of the test. This group had IQ scores between 70-130. The second group consisted of those who scored below 70 on testing, and included those who were unable to be assigned a IQ or DQ score due to severe impairment. The characteristics of the two groups are shown in Table 5.4. The groups are similar in sex and duration of epilepsy, but the group with higher pre-operative IQ is older at the time of surgery, older at the time of onset of epilepsy, more likely to be undergoing a procedure within a single lobe, more likely to have hippocampal sclerosis or tumour aetiology, and has lower mean cortical thickness measurements.

Group cortical thickness networks were created for the group of patients with pre-operative IQ scores greater than 70, and for the group of patients who scored lower than 70 on IQ or DQ pre-operatively. The group cortical thickness networks are displayed in Figure 5.10. Visual inspection of the networks suggests that the group with IQ greater than 70 have a larger proportion of higher edge weights (yellow coloured).The networks were thresholded to remove all edge weights below the absolute threshold value in steps of 0.05. Networks were analysed at the highest threshold value that allowed a completely connected network. This was 0.25. Both networks were thresholded to remove all edges with weights below 0.25 and the thresholded networks are displayed in Figure 5.11 as anatomical networks. Again, it appears from these figures that there are more edges with higher edge weights in the group with higher pre-operative IQ scores. Networks were also examined using a threshold value of 0.7, as this was the value that created sparse networks with a density as close to 0.2 as possible. Binary networks were

	Group		
	IQ≥70	IQ<70	*p*
	n=44	*n=55*	
Female	25 (56.8%)	24 (43.6%)	*0.271*
Age at Operation (years)	12.2 (8.0-15.9)	8.5 (5.1-12.1)	*<0.001*
Age at First Seizure (years)	4.0 (2.0-7.0)	1.3 (0.5-2.8)	*<0.001*
Duration of Epilepsy (years)	6.3 (2.8-10.4)	5.6 (3.2-9.2)	*0.908*
Left Hemisphere Operated	27 (61.4%)	23 (41.8%)	*0.084*
Operation within Single Lobe	40 (90.9%)	38 (69.1%)	*0.017*
Aetiology			
cortical dysplasia	14 (31.8%)	22 (40.0%)	
hippocampal sclerosis	8 (18.2%)	3 (5.5%)	
neurocutaneous	2 (4.5%)	5 (9.1%)	
tumour	16 (36.4%)	12 (21.8%)	
vascular	4 (9.1%)	7 (12.7%)	
unknown	0 (0%)	6 (10.9%)	*0.040*
Mean Cortical Thickness (mm)	2.8 (0.25)	2.9 (0.24)	*0.015*
IQ	87.2 (12.2)	53.8 (10.0)	*0.030*

Table 5.4: ***Comparison of demographic and clinical features by pre-operative IQ.*** *Comparison of demographic and clinical features between those with a pre-operative IQ score over 70 and those with a score lower than 70. Data are count (percentage) for categorical data, median (IQR) for age and years, and mean (SD) for cortical thickness and IQ scores. Significance testing was carried out using tests for categorical data, Mann-Whitney U tests for age and years, and t-tests for IQ scores and cortical thickness measures. (IQ: intelligence quotient; IQR: interquartile range; SD: standard deviation)*

created by setting the weights of all present edges to one. Global network metrics were calculated across the range of threshold values. Average path length and global efficiency across the range of threshold values for the binary and weighted networks is shown in Figure 5.12. Network metrics for both the dense networks without any disconnected nodes (threshold value 0.25), and the sparse networks, aiming for a density as close as possible to 0.2 in each group (threshold value 0.7) are shown in Table 5.5.

Those with a pre-operative IQ score less than 70 had lower network global efficiency across threshold values from 0-0.8 and higher network average path lengths across threshold values from 0-0.5 (see Figure 5.12). However, these differences did not reach statistical significance (see Table 5.5). There were no statistically significant differences between the two groups in any of the network characteristics investigated.

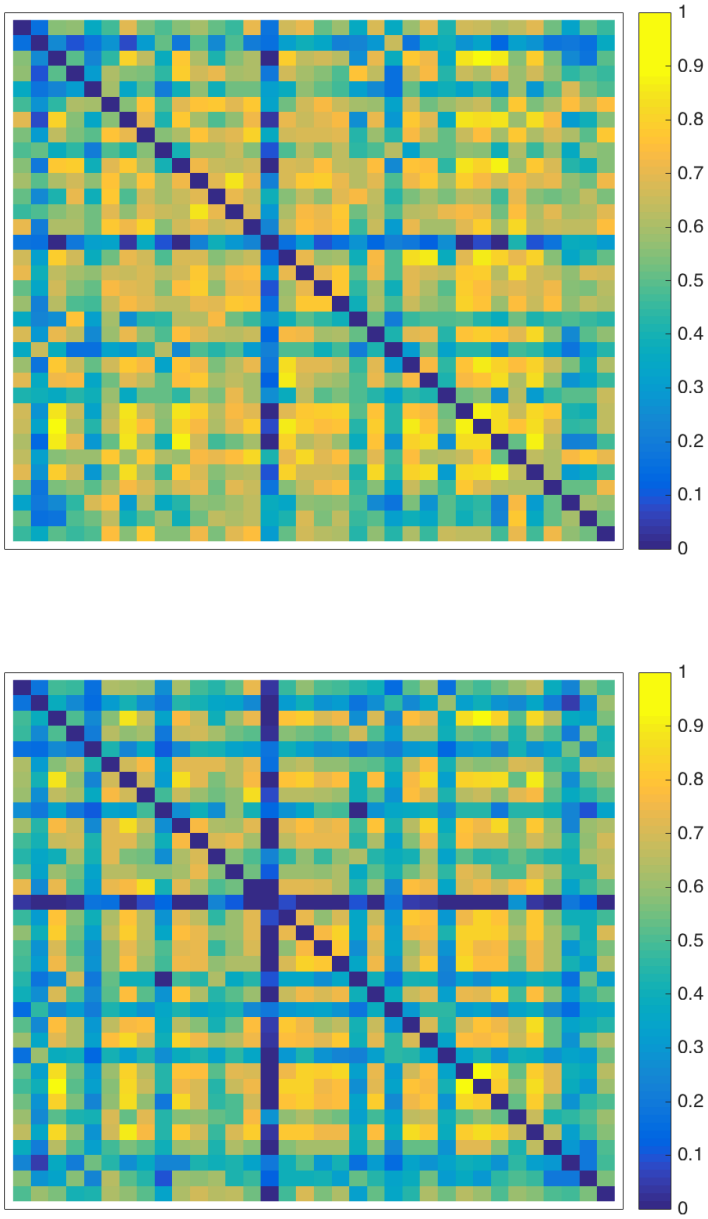

Figure 5.10: ***Cortical thickness networks and pre-operative IQ.*** *Networks are displayed with regions of the Desikan-Killiany atlas along the left and top axes and edge weights within the matrix. Regions are ordered as in Table 3.2. Edge weights correspond to the key given. Negative and self-self connections have been removed.* ***Top:*** *Group network for those with a pre-operative IQ greater than 70.* ***Bottom:*** *Group network for those with a pre-operative IQ or DQ score less than 70. (IQ: intelligence quotient; DQ: developmental quotient)*

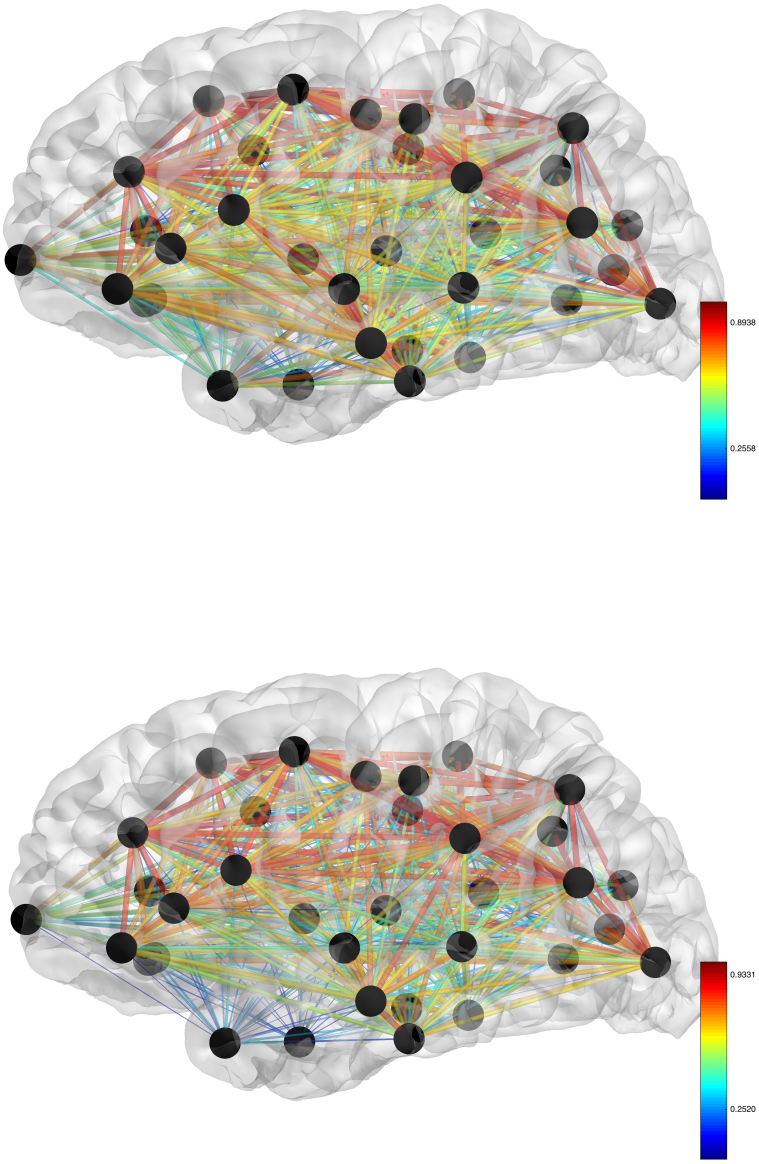

Figure 5.11: ***Cortical thickness networks by pre-operative IQ.*** *Networks are displayed with nodes represented by black dots in anatomical space overlaid on a representative left hemisphere cortex. Networks have been thresholded to remove all edge weights below 0.25 and self-self connections have been removed. Edge weights correspond to the colour key given and thicker edges represent larger edge weights.* ***Top:*** *Group network for those with a pre-operative IQ greater than 70.* ***Bottom:*** *Group network for those with a pre-operative IQ or DQ score less than 70. (IQ: intelligence quotient; DQ: developmental quotient)*

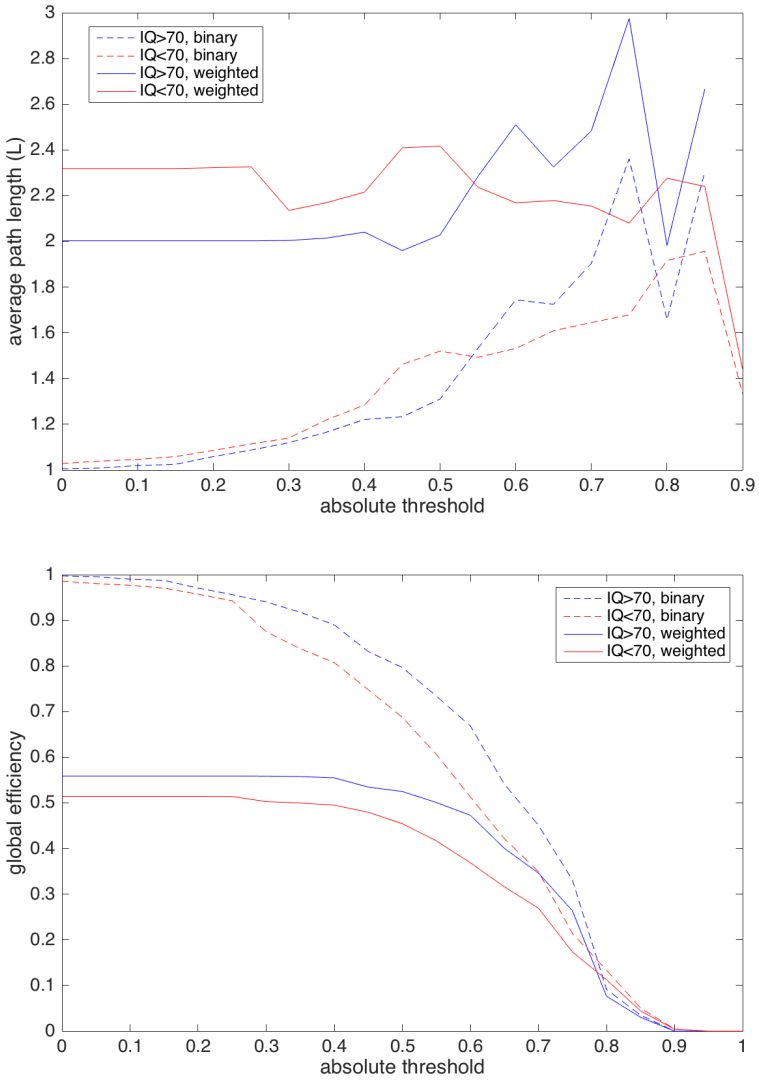

Figure 5.12: ***Network measures by threshold and IQ.*** *Network measures from the cortical thickness networks are displayed across a range of thresholds. Absolute thresholds were applied so that all edges with weights lower than the threshold value were removed prior to calculation of the network measure. Binary network measures are shown with dashed lines and weighted network measures are solid lines. Red lines show data for those with an IQ score less than 70. Blue lines show data for those with an IQ score greater or equal to 70.* ***Top:*** *Average path length.* ***Bottom:*** *Global efficiency. (IQ: intelligence quotient; L: average path length)*

	Dense			Sparse		
	IQ≥70	IQ<70	*p*	IQ≥70	IQ<70	*p*
Binary Networks						
density	0.91	0.89	*0.699*	0.23	0.22	*0.949*
degree	30.1	29.2	*0.696*	7.65	7.35	*0.941*
L	1.09	1.11	*0.713*	1.90	1.64	*0.413*
λ	1.00	1.00	*1.00*	1.05	1.01	*0.610*
C	0.95	0.92	*0.503*	0.52	0.52	*0.972*
γ	1.00	1.00	*0.980*	1.40	1.07	*0.080*
σ	1.00	1.00	*0.940*	1.34	1.06	*0.130*
E_{Glob}	0.96	0.94	*0.722*	0.45	0.35	*0.446*
Weighted Networks						
S	17.6	16.1	*0.559*	5.86	5.71	*0.967*
EW	0.58	0.55	*0.479*	0.77	0.77	*0.429*
L	2.00	2.33	*0.268*	2.48	2.15	*0.466*
λ	1.05	1.01	*0.890*	1.07	1.05	*0.730*
C	0.61	0.54	*0.225*	0.45	0.43	*0.880*
γ	1.00	1.00	*0.960*	1.40	1.07	*0.080*
σ	0.96	0.99	*0.990*	1.31	1.02	*0.110*
E_{Glob}	0.56	0.51	*0.480*	0.35	0.27	*0.475*

Table 5.5: ***Global network characteristics by pre-operative IQ.*** *Comparison of global network characteristics between those with a pre-operative IQ equal to or above 70 and those with a pre-operative IQ below 70. Values are calculated from both binary and weighted networks. Networks were thresholded to create completely connected dense networks by removing all values less than the threshold value of 0.25. Networks were also thresholded to create sparse networks using a threshold value of 0.7 to remove all edge weights lower than this, aiming for networks with a density as close as possible to 0.2. Permutation testing using 1000 group permutations was used to calculate p values, which were then corrected for the 32 multiple comparisons in the table using the FDR. The p values shown are corrected values. (S: mean network strength; EW: mean network edge weight; L: average path length;* λ*: normalised average path length; C: clustering coefficient;* γ*: normalised clustering coefficient;* σ*: small worldness statistic;* E_{Glob}*: global efficiency)*

5.5.5 Are cortical thickness network characteristics in the healthy hemisphere related to post-operative change in IQ following epilepsy surgery?

To assess whether cortical thickness network characteristics are related to change in IQ after epilepsy surgery, only patients who scored within the assessable range of the IQ instrument (IQ>55) were considered so that reliable changes in IQ could be investigated. These patients were divided into two groups based on whether or not they had a clinically meaningful increase in IQ score post-operatively of at least 10 points. The characteristics of the two groups are shown in Table 5.6. Patients with an increase of at least 10 points in IQ post-operatively had a shorter duration of epilepsy pre-operatively. There were no patients with hippocampal sclerosis in the group that improved more than 10 points post-operatively, although aetiology was not statistically significantly different between the groups. Those who improved more than 10 points had slightly lower IQ scores pre-operatively and slightly thicker mean cortical thickness measurements, but these differences were not statistically significant.

	Group		
	Change IQ≥10	Change IQ<10	*p*
	n=11	*n=24*	
Female	6 (54.5%)	11 (45.8%)	*0.909*
Age at Operation (years)	8.2 (5.0-13.1)	11.4 (7.1-13.9)	*0.234*
Age at first seizure (years)	3.0 (2.0-6.8)	2.8 (1.0-5.0)	*0.454*
Duration of epilepsy (years)	3.1 (2.0-5.4)	5.8 (3.2-12.0)	*0.033*
Left Hemisphere Operated	5 (45.5%)	11 (45.8%)	*1.00*
Operation within Single Lobe	10 (90.9%)	22 (91.7%)	*1.00*
Aetiology			
cortical dysplasia	6 (54.5%)	8 (33.3%)	
hippocampal sclerosis	0 (0%)	4 (16.7%)	
neurocutaneous	1 (9.1%)	1 (4.2%)	
tumour	3 (27.3%)	7 (29.2%)	
vascular	1 (9.1%)	2 (8.3%)	
unknown	0 (0%)	2 (8.3%)	*0.559*
Last Engel Score 1A	9 (81.8%)	14 (58.3%)	*0.329*
AED Free	4 (36.4%)	5 (20.8%)	*0.576*
Pre Op IQ	72.2 (14.5)	78.0 (19.4)	*0.336*
Change in IQ	19.6 (9.5)	2.3 (11.3)	*<0.001*
Mean Cortical Thickness (mm)	2.9 (0.39)	2.8 (0.26)	*0.478*

Table 5.6: ***Comparison of demographic and clinical features by change in IQ.*** *Patients with a post-operative IQ score more than 10 points above their pre-operative IQ score are compared to those without a change in IQ. Data are count (percentage) for categorical data, median (IQR) for age and years, and mean (SD) for cortical thickness and IQ scores. Significance testing was carried out using X^2 tests for categorical data, Mann-Whitney U tests for age and years, and t-tests for IQ and cortical thickness measures. (IQ: intelligence quotient; IQR: interquartile range; SD: standard deviation; AED: anti-epileptic drug)*

Group cortical thickness networks were created for these two groups as described in Section 5.4.2 and are shown in Figure 5.13. The group with a post-operative increase in IQ of at least 10 points appear to have more edges with higher edge weights as there are a higher number of bright yellow squares in preference to green or blue coloured squares in the matrix.

The networks were thresholded to remove all edge weights below the threshold value in steps of 0.05. Networks were analysed at two threshold values. The first was the highest threshold value that maintained a completely connected network in both groups with no disconnected nodes - this was a threshold value of 0.3. Both networks were thresholded to remove all edges with weights below 0.3 and the thresholded networks are displayed in Figure 5.14 in anatomical space. There still appears to be a higher number of higher edge weights in the group with an increase of at least 10 point in IQ post-operatively. Networks were also analysed at a higher threshold, aiming for sparse networks with a density as close as possible to 0.2. The threshold value that achieved this was 0.8. Binary networks were created from both the sparse and the dense networks by setting all existing edge weights to one. Global network metrics for both the dense and the sparse networks were calculated using both weighted and binary networks, and are displayed in Table 5.7. Average path length and global efficiency across the range of thresholds are shown in Figure 5.15.

Figure 5.15 shows that the group who increased at least 10 points in IQ score post operatively have shorter average path lengths and higher network global efficiency across threshold values of 0-0.8. In the weighted networks, the difference in global efficiency was statistically significant in both the dense and the sparse networks. The difference in average path length was statistically significant in the dense networks but not the sparse networks. There was no statistically significant difference in λ between the groups. Although the aim was to create sparse networks with a density as close as possible to 0.2, the group network for those with a change in IQ of at least 10 points had a density of 0.39 and the group network for those with a change in IQ of less than 10 points had a density of 0.12, which is substantially, although not statistically significantly lower. A difference in L and global efficiency without a difference in λ could mean that the the difference in L is actually due to the increased number and weight of connections in the group network for those with a change in IQ of at least 10 points. However, the differences in network density, degree, strength and mean edge weight did not reach statistical significance themselves.

	Dense			Sparse		
	Change IQ≥10	Change IQ<10	*p*	Change IQ≥10	Change IQ<10	*p*
Binary Networks						
density	0.98	0.86	*0.113*	0.39	0.12	*0.139*
degree	32.3	28.4	*0.114*	13.06	4.00	*0.140*
L	1.02	1.15	*0.068*	1.74	1.75	*0.982*
λ	1.00	1.01	*0.940*	1.04	0.85	*0.090*
C	0.98	0.91	*0.182*	0.67	0.43	*0.286*
γ	1.00	0.99	*0.960*	1.27	1.58	*0.690*
σ	1.00	0.99	*0.960*	1.22	1.85	*0.230*
E_{Glob}	0.99	0.93	*0.228*	0.68	0.21	*0.042*
Weighted Networks						
S	23.99	18.0	*0.145*	11.3	3.38	*0.142*
EW	0.75	0.64	*0.138*	0.87	0.84	*0.370*
L	1.43	2.06	*0.044*	2.00	2.07	*0.142*
λ	1.01	1.11	*0.690*	1.06	0.86	*0.090*
C	0.75	0.62	*0.211*	0.60	0.40	*0.302*
γ	1.00	1.01	*0.960*	1.28	1.59	*0.690*
σ	0.99	0.91	*0.790*	1.21	1.85	*0.210*
E_{Glob}	0.74	0.58	*0.014*	0.59	0.18	*0.044*

Table 5.7: ***Global network characteristics by change in IQ.*** *Comparison of global network characteristics between those whose post-operative IQ increased at least 10 points and those whose post-operative IQ score did not increase. Network measures are calculated from both the binary and weighted networks thresholded at 0.3 to create dense completely connected networks with no disconnected nodes and at 0.8 to create sparse networks, aiming for a density of 0.2. Permutation testing using 1000 group permutations was used to calculate p values, which were then corrected for the 32 multiple comparisons in the table using the FDR. The p values shown are corrected values. (IQ: intelligence quotient, S: mean network strength; EW: mean network edge weight; L: average path length; λ: normalised average path length; C: clustering coefficient; γ: normalised clustering coefficient; σ: small worldness statistic; E_{Glob}: global efficiency)*

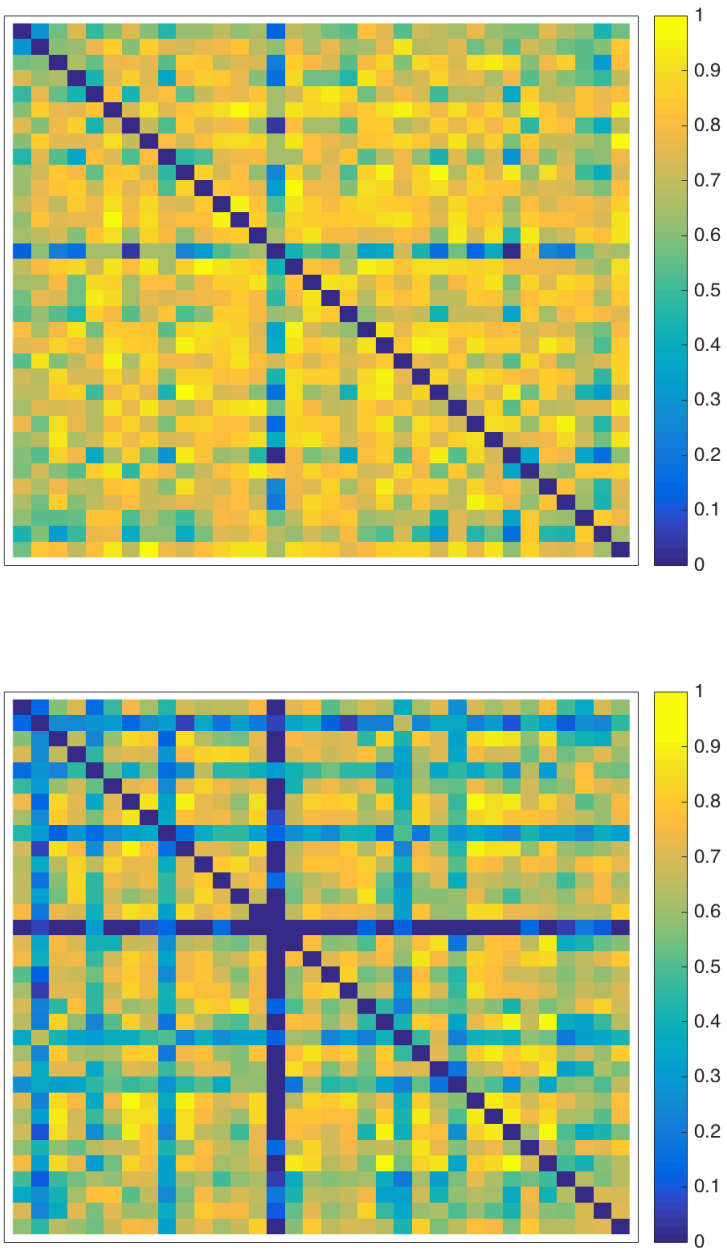

Figure 5.13: ***Cortical thickness networks and change in IQ.*** *Networks are displayed with regions of the Desikan-Killiany atlas along the left and top axes and edge weights within the matrix. Regions are ordered as in Table 3.2. Edge weights correspond to the key given. Negative and self-self connections have been removed.* ***Top:*** *Group network for those with a post-operative increase in IQ of 10 or more points.* ***Bottom:*** *Group network for those with a post-operative change in IQ of less than 10 points. (IQ: intelligence quotient)*

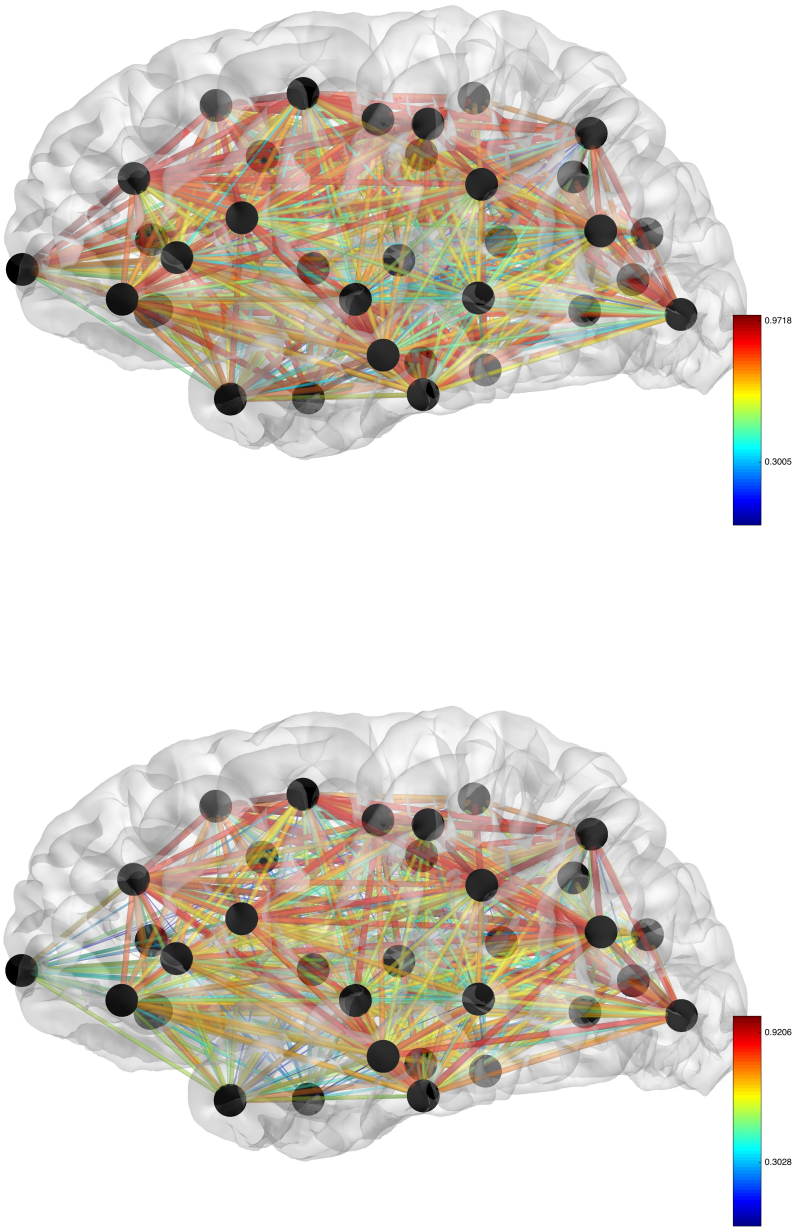

Figure 5.14: ***Anatomical representation of cortical thickness networks by change in IQ.*** *Networks are displayed with nodes represented by black dots in anatomical space overlaid on a representative left hemisphere cortex. Networks have been thresholded to remove all edge weights below 0.3 and self-self connections have been removed. Edge weights correspond to the colour key given and thicker edges represent larger edge weights.* ***Top:*** *Group network for those with a post-operative increase in IQ of 10 or more points.* ***Bottom:*** *Group network for those with a post-operative change in IQ of less than 10 points.(IQ: intelligence quotient)*

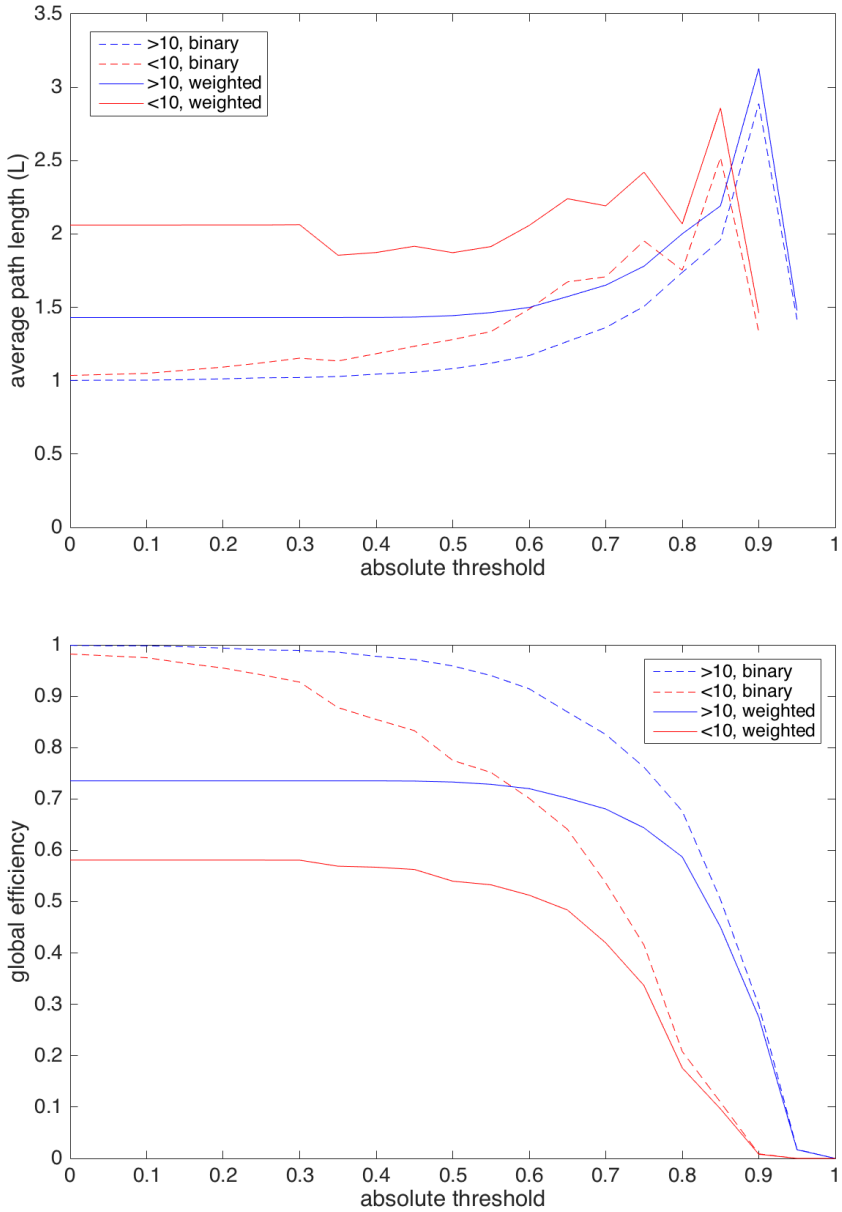

Figure 5.15: ***Network measures by threshold and IQ change.*** *Network measures from the cortical thickness networks are displayed across a range of thresholds. Absolute thresholds were applied so that all edges with weights lower than the threshold value were removed prior to calculation of the network measure. Binary network measures are shown with dashed lines and weighted network measures are solid lines. Red lines show data for those with a post-operative change in IQ score less than 10. Blue lines show data for those with a post-operative change in IQ score greater or equal to 10.* ***Top:*** *Average path length.* ***Bottom:*** *Global efficiency. (IQ: intelligence quotient; L: average path length)*

5.6 Discussion

5.6.1 Summary of findings

This chapter has investigated the association between structural network measures in the healthy hemisphere with pre-operative IQ and post-operative change in IQ in children undergoing contralateral resective epilepsy surgery. Global network characteristics of the healthy hemisphere cortical thickness networks were not statistically significantly different between those with a pre-operative IQ score less than 70 and those with a pre-operative IQ score greater than 70. However, the group of patients who had a greater than 10 point increase in IQ post-operatively had lower average path lengths and higher network global efficiency than those whose IQ did not increase more than 10 points post-operatively. The group with an increase in post-operative IQ of at least 10 points had a shorter duration of epilepsy pre-operatively. In addition, post-operative IQ scores were positively correlated with pre-operative IQ scores and the age at onset of epilepsy. Higher pre-operative IQ scores were associated with an older age at testing, an older age at onset of epilepsy, and undergoing a single lobe procedure rather than a multilobar procedure. Mean cortical thickness was associated with age, but did not show a statistically significant correlation with IQ score.

5.6.2 Comparison to previous studies

For inclusion in this study, participants had to have an apparently healthy hemisphere contralateral to the side of operation, an available 3D T1-weighted MRI scan without significant artefact, and available documentation of an IQ or DQ assessment. Of 259 patients initially investigated only 99 (38%) were included in the pre-operative analyses and only 52 (20%) in the post-operative analyses. These smaller cohorts were compared to the previously published overall population data for those undergoing paediatric epilepsy surgery at the UMCU.[184] The cohorts are very similar in age, sex, duration of epilepsy, age at seizure onset, and aetiology.[184] The groups were also similar in terms of outcomes, although this cohort has 72% in Engel class I at two years and the larger cohort has 81% in Engel class I, and this cohort has 35% AED free at 2 years and the wider cohort has 29% AED free at 2 years.[184] Overall, this smaller cohort with complete MRI and neuropsychology data is representative of the wider population undergoing paediatric epilepsy surgery who may have been excluded due to incomplete data, and therefore these results should be applicable to the larger cohort.

In the cohort studied in this chapter, there were no statistically significant differences in healthy hemisphere cortical thickness network measures between the group with an IQ greater than or equal to 70 and the group with an IQ less than 70. In Chapter 4, the group with cognitive impairment (mean IQ:59, SD:10) and the group with intact cognition (mean IQ:91, SD:15) (see Table 4.9) also did not show any statistically significance differences in cortical thickness whole brain network measures when networks were analysed at densities of 0.6-0.8 using either proportional thresholding to remove a stated proportion of edge weights or absolute thresholding to remove all edge weights below the threshold value. However, when sparse networks were analysed at densities of 0.2-0.3 the group with cognitive impairment analysed in Chapter 4 had higher whole brain network average path lengths and higher

network average clustering coefficients in the networks derived from raw cortical thickness measurements. This difference is unlikely to be explained by cohort size as the group in Chapter 4 consisted of 78 patients whereas the surgical cohort in this chapter (Chapter 5) contained 99 patients. However, it is possible that the results are influenced by the spread of IQ scores, which was smaller in the paediatric epilepsy surgery cohort whose results are presented in this chapter as there were fewer participants with high IQ scores (IQ≥ 70: mean IQ:87, SD:12 vs IQ< 70: mean IQ:54, SD:10; see Table 5.4 compared to Table 4.9). A previous study of 45 children undergoing epilepsy surgery with near normal IQ scores (mean IQ:97, SD:12) also failed to show any statistical association between IQ and global network properties from DTI derived networks,[135] and this study also seems to have a small spread of IQ scores. It is possible not to find any differences between the groups if the groups are too similar. A study investigating the differences in cortical thickness network topology between a group of high performing (mean PIQ:120, SD:9) vs normal performing (mean PIQ:100, SD:7) healthy children found higher global efficiency in the high performing group when PIQ was investigated, but not when VIQ was investigated.[93] It is also therefore possible that the different findings between the cohorts in Chapters 4 and 5 arise from the different methods of classifying the participants into two groups. In Chapter 4, the presence of cognitive impairment was established either by a documented diagnosis of an ID or by IQ testing or attendance at a special educational school, whereas in this chapter (Chapter 5), the groups were created from performance on tests of IQ and DQ only. The method of classification may have affected the group differences seen. In addition, in Chapter 4 whole brain connectomes were analysed, whereas in Chapter 5 only the healthy hemisphere unilateral connectome was analysed. Differences in findings may be due to differences in within hemisphere networks compared to whole brain networks.

The change in IQ score post-operatively in this cohort is consistent with previous descriptions of paediatric epilepsy surgery cohorts.[113,124,125] In a meta-analysis, an improvement of 5-15 points in IQ was seen in 29% of children undergoing hemispherectomy and 11% of epilepsy surgery in general, which is similar to the 31% with an increase in IQ seen in this study.[125] The results in this chapter are probably more similar to the hemispherectomy results as those undergoing palliative procedures, and those with a contralateral hemisphere that was structurally abnormal on imaging or had epileptic EEG discharges were excluded in this study. Change in IQ following epilepsy surgery has been previously associated with age at surgery, duration of epilepsy, aetiology, pre-operative IQ, post-operative seizure freedom, post-operative AED use, and socioeconomic factors.[122,125–127,185] The only statistically significant group difference between those with an increase of at least 10 points in IQ post-operatively and those without was a shorter duration of epilepsy (see Table 5.6). This difference in study findings is likely due to different sample sizes and different statistical techniques. For example, previous studies have considered mean changes as low as 5.3 IQ points where they are statistically significant within the cohort.[185] Dichotomising the groups to include only those with an increase greater than 10 IQ points as in this chapter, increases the number of subjects required and the score change required to identify a statistically significant result. No-one has previously investigated the association of structural networks with change in IQ scores post-operatively in epilepsy surgery, but the results are consistent with a previous study that showed that contralateral MRI abnormalities are associated with poorer cognitive outcomes following hemispherectomy.[126]

5.6.3 Limitations of findings

In this chapter cortical thickness networks were created on a group level - one group network for each group investigated. Permutation testing was used to assess statistical significance by randomly permuting the groups. Although this takes into account group size, and randomly switches group labels, it is not possible to specifically control for potential confounding factors as in general linear models. The group with higher pre-operative IQ scores were older at the time of operation, older at the time of their first seizure, and were more likely to be undergoing a procedure within a single lobe rather than a multilobar procedure (see Table 5.4). The group whose post-operative IQ score increased at least 10 points had a shorter duration of epilepsy pre-operatively (see Table 5.6). There were also trends for a younger age at operation, a shorter duration of epilepsy, and a higher proportion who were seizure free and AED free, although these trends did not reach statistical significance. It is a limitation of this study that it is not known whether one or several of these differences in seizure and epilepsy characteristics are more related to the the difference in group network characteristics than the difference in IQ or change in IQ. Cognitive function, and change in IQ scores have been previously demonstrated to be dependent on several seizure and epilepsy characteristics,[109,112,113] so it is likely that all of these epilepsy, seizure, structural, and cognitive factors interact in the complex association between epilepsy and cognition.

Creating networks from DTI data rather than covariance of cortical thickness data would have allowed individual rather than group networks to be created. However, this study was carried out retrospectively, and very few of the children undergoing epilepsy surgery had DTI data available historically for analysis, hence this study was restricted to cortical thickness network analysis. Creating DTI networks for each individual would have allowed general linear models to be built using each individual's data, which could have helped investigate the relationships between epilepsy characteristics and cognition or changes in IQ. However, DTI networks also have the disadvantage that they are dependent on white matter tract integrity and the processing pathways used to determine streamlines. Cortical thickness networks and DTI networks have been shown to produce similar models of brain structure,[43,59] but cortical thickness networks have the advantage of more accurately reflecting long range connections or instances of crossing fibres.[58,61]

Although all of the networks investigated in this chapter were created from the same underlying dataset, post processing of the data allows networks with very different characteristics to be created. Two different thresholds were chosen for network analysis and both binary and weighted networks were examined. Global efficiency and average path length across the range of thresholds are shown in Figures 5.12 and 5.15. These figures show that although these two network characteristics tend to show the same pattern of difference across different thresholds and with binary and weighted networks, absolute numbers can be very different. Further, at the extreme threshold values, differences between networks can become reversed or very unstable. This is particularly true of the average path length, and is likely due to the disconnections in the networks. When shortest path lengths were calculated in disconnected networks, the values of infinity were removed from the distance matrix and set to zero and the mean shortest path length was calculated on only non zero entries in the matrix. Calculation of network global efficiency uses the mean of the inverse shortest path length and so does not have this issue.[177] The absolute values of the calculated network measures in Tables 5.5 and 5.7 between the

sparse and the dense networks show the numerical differences that can be produced through the use of different thresholds. The consistency of the finding of increased global efficiency in the healthy hemisphere of those with a greater than 10 point increase in IQ post op across all network construction methods except for the dense binary networks, suggests that this is not a spurious finding. The fact that the opposite finding occurs in L in the dense weighted networks is extra evidence for a difference in organisation in the structural network of the healthy hemisphere between the two groups.

5.6.4 Potential mechanisms and future questions

The higher network global efficiency described in the healthy hemisphere of the group who increased at least 10 points in IQ post-operatively could be accounted for by differences in the overall number and weight of connections in the group networks. However, this is unlikely as there were no statistically significant differences in network density, mean node degree, mean node strength, or mean edge weight. This suggests that it is the overall pattern of cortical thickness correlations within the group that is different. Mean cortical thickness measurements were not statistically significantly different between the two groups (2.9mm vs 2.8mm, see Table 5.6). Thus the group differences are unlikely to be accounted for by overall differences in cortical thickness measurements. Mean cortical thickness decreased with age in this cohort, as has previously been described.[186,187] Cortical thickness and histology is known to be associated with the function of the cortical region,[6,59] and changes in correlations in cortical thickness between regions have been attributed to environmental influences such as learning, or genetic and developmental influences, such as disease states.[43,63–65] The less organised cortical thickness correlations in the healthy hemisphere of the group who did not show an increase in IQ post-operatively may therefore represent a lack of development of cortical thickness correlations that prevents efficient brain network usage and increase in IQ scores post-operatively once seizures and AEDs have been removed. This lack of cortical organisation in the healthy hemisphere could be as a result of uncontrolled seizure activity preventing normal development, or due to an underlying aetiology of disordered cortical thickness correlations that causes epilepsy. If the underlying cause for disordered cortical thickness correlations with higher path lengths is related to the cause of the epilepsy, then you would expect seizures to continue post-operatively, and there was a non-significant trend for a lower proportion of children to be seizure free at two years post-operatively.

In a study of healthy adolescent volunteers, the global efficiency of DTI FA structural networks increased with age, and the association of global efficiency with IQ became stronger with increasing age.[98] This suggests that networks can become more efficient with development and older childhood ages. The group without a post-operative change in IQ had longer average path lengths and lower global efficiency, but were slightly older at the time of operation. If network efficiency increases with age during childhood, which fits with previous studies of increased correlations between regions with learning,[65] then it is unlikely that the differences in average path length between the groups with and without an increase in post-operative IQ can be explained by the different ages of the groups, as it would be expected that the older group had increased global efficiency and shorter average path lengths.

Longer term cognitive outcomes more than five years following epilepsy surgery are known to be better than shorter term outcomes, and improvements in cognition have been associated with cessation of

AEDs and differences in grey matter volume.[122] Thus, longer term follow up with re-assessment of post-operative cortical thickness connectomes would be necessary to assess whether the organisation of the healthy hemisphere can change post-operatively to facilitate cognitive improvement and development or whether the pre-operative existing structure determines outcomes.

A prospective study of epilepsy surgery candidates with individual and group networks computed using DTI and cortical thickness covariance methods both pre-operatively and post-operatively would allow regression of individual level epilepsy characteristics from network measures and facilitate assessment of changes in structure post-operatively. This could lead to further insight into the plasticity of networks in the healthy hemisphere, and help lead to improved surgical planning and timing to facilitate better post-operative network structure. A prospective study design would hopefully lead to fewer items of missing data than occurred in this study, leading to a larger number of subjects that could be studied. To increase the number of subjects studied, a multi-centre study could be considered. However, the MRI data acquired on different centres' scanners would need to be robustly assessed for scanner and sequence related differences prior to analysis of networks. Even a perfectly designed study would not be able to account for the subjects who move in the scanner leading to movement artefact or those who fail to attend for follow up appointments.

5.7 Conclusions

This chapter has investigated a cohort of children undergoing epilepsy surgery. Group cortical thickness networks were successfully created from this clinical cohort. There were no statistically significant differences in cortical thickness network measures in the healthy hemisphere between children with a pre-operative IQ score greater than or equal to 70 and children with a pre-operative IQ score less than 70. In the 35 children with both pre-operative and post-operative IQ scores greater than 55, those who showed an increase in IQ of at least 10 points post-operatively had higher network global efficiencies across a range of network thresholds in weighted networks and in sparse binary networks.
Post-operative IQ scores were associated with pre-operative IQ scores and the group who improved post-operatively had a shorter duration of epilepsy pre-operatively. The structural organisation of the healthy hemisphere is therefore associated with cognitive improvement following epilepsy surgery.

Chapter 6

Discussion

6.1 Summary of Findings

Brain structure can be modelled as a network of anatomical grey matter regions and the connections between them. The structure of model brain networks created from MRI has been investigated in patients with epilepsy, children with suspected epilepsy, and children undergoing epilepsy surgery. Epilepsy can be described as a whole brain network disorder in which seizures spread through epileptic networks, and widespread MRI structural changes occur. Cognitive impairment is a common comorbidity in epilepsy, and this may be associated with uncontrolled seizure activity, the underlying aetiology of the epilepsy, or brain structural changes. This thesis aimed to investigate whether structural brain networks are altered in epilepsy, whether structural network characteristics are associated with cognitive impairment in those investigated for suspected epilepsy, and whether structural network characteristics are associated with an improvement in IQ following epilepsy surgery.

In Chapter 2 a systematic literature review was undertaken to assess structural network differences between those with epilepsy and healthy controls. This identified 27 studies using DTI or ROI covariance methods to construct networks from MRI. Some studies, using different network construction methods, identified increased network average path lengths and decreased network global efficiency in patients with epilepsy compared to healthy controls. However, this finding was not consistent across studies. Covariance networks also identified increased average clustering coefficients in patients with epilepsy, but this was not found in studies investigating networks constructed from DTI. There were no overall differences identified in the normalised graph metrics γ or λ or in the small worldness statistic (σ) between those with epilepsy and healthy controls. Meta-analysis was not undertaken due to the heterogeneity of network construction and analysis methods and the heterogeneity of numerical estimates of network measures.

In Chapter 4 structural cortical thickness and DTI networks were created in a cohort of children undergoing MRI to investigate suspected epilepsy. In this cohort, cognitive impairment was associated with lower overall network densities, average node degrees, average node strengths, and average network edge weights. Children with cognitive impairment had higher average path lengths and lower global efficiencies in networks created from DTI NOS and streamline averaged FA, and these findings

persisted when corrections were made for differing network densities or average edge weights. Network average path lengths were also negatively associated with IQ scores. After correction for seizure frequency and number of AEDs the relationship between cognitive dysfunction and higher average path lengths persisted. When sparse cortical thickness networks were investigated at densities similar to the DTI networks, higher network average path lengths were also found in those with cognitive impairment. However, these findings were not reproducible at high network densities in the cortical thickness networks.

Chapter 5 describes a cohort of paediatric patients undergoing epilepsy surgery. The global efficiency of the pre-operative cortical thickness network derived from the healthy contralateral non-operated hemisphere was found to be higher in the group with a post-operative improvement in IQ score of at least 10 points. However, there were no statistically significant differences in cortical thickness network measures in the healthy hemisphere between children with a pre-operative IQ score greater than or equal to 70 and those with a pre-operative IQ score less than 70. The group who improved post-operatively had a shorter duration of epilepsy pre-operatively but no overall differences in pre-operative IQ scores or mean cortical thickness measurements.

This thesis has provided evidence to support the theory that global network characteristics are altered in epilepsy and that within groups of children investigated for suspected epilepsy or undergoing epilepsy surgery, a more efficient organisation of modelled brain networks with lower average path lengths and higher global efficiency is associated with better cognitive function and capacity for improvement in cognitive function. However, different network construction and analysis methods can lead to different numerical estimates of network measures.

6.2 Study Limitations

6.2.1 Experimental study design

This study used retrospective analysis of existing data sets from clinical cohorts. This has the advantage of not requiring any further clinical assessments such as MRI or neuropsychological assessments that children, particularly those with cognitive impairment, may find difficult to tolerate. However, retrospective studies rely on existing data that may be incomplete, inaccurate, or impossible to find. The initial plan for the epilepsy surgery cohorts was to conduct a multi-centre study using DTI derived structural networks. This required ethical approval across three different countries, and international data sharing agreements. It became apparent that very few paediatric epilepsy surgery candidates across the centres had undergone pre-operative DTI, and that widely varying protocols and scanner manufacturers were used. This meant that data from two sites were not used in this thesis and that data from the third were restricted to cortical thickness network analyses only. This problem could have been avoided by ensuring that all potential collaborators checked existing data thoroughly and provided estimates of numbers of patients with complete datasets prior to embarking on ethical approvals and data sharing agreements.

Although all epilepsy surgery programmes aim to thoroughly investigate candidates pre and

post-operatively with neuropsychological assessments and imaging, not all of the imaging or neuropsychological assessments and clinical details could be sourced. This led to missing data or the exclusion of candidates. It is very difficult to address this in a retrospective study design. Although the amount of missing data through inability to find records may be reduced using a prospective study design, a prospective study design will not address missing data that occurs when subjects fail to attend for assessments.

The clinical cohorts consisted of children who were either being investigated for suspected epilepsy or who were undergoing epilepsy surgery. These patients may have found it difficult to tolerate assessments. Four patients in the suspected epilepsy cohort and 15 patients in the epilepsy surgery cohort could not be included due to significant artefact on MRI, the majority of which was movement artefact (see Figures 4.1 and 5.1). In addition, patients with bilateral pathology or pathological structural changes too extensive for automated MRI analyses were excluded from these cohorts. When investigating patients with clinical disease using methods developed for research using healthy structurally normal brains, it is inevitable that some patients will need to be excluded because the methods simply will not work for them or are not applicable to them. An example is measuring cortical thickness in patients with tuberous sclerosis and multiple cortical tubers. This is not possible using automated methods because of the influence of the cortical tubers on MRI signal intensity, which prevents software from accurately identifying the grey-white junction. Chapter 5 examined the healthy hemisphere - that is the hemisphere contralateral to the side of the surgical procedure that was reported as normal on clinical imaging and EEG analyses. This was to allow patients with unilateral pathology to be investigated. The use of automated segmentation and parcellation techniques developed in healthy adults with MRI pathology and paediatric brains meant that manual intervention was required in 71% of patients in the suspected epilepsy cohort and 38% of patients in the epilepsy surgery cohort. Manual intervention of the image processing pipeline in skull stripping, registration, white matter template editing, and segmentation editing improved the qualitative appearance of the segmentations, but may have affected the quantitative results. However, the only way to ensure that automated MRI methods are able to deal with all scans without manual intervention would have been to restrict the study to healthy volunteers with structurally normal scans, and this would have meant that the results of the study might not have been applicable to those presenting in clinical practice.

6.2.2 Network construction

Network characteristics are heavily influenced by the number of nodes and edges in a network.[52] The systematic review in Chapter 2 identified many different parcellation schemes and methods of establishing network edges from DTI and structural covariance (see Table 2.6). Different parcellation schemes lead to different numbers of nodes and different sizes of adjacency matrices, and therefore calculated metrics can be numerically quite different.[52] If a fixed volume, such as a brain, is being investigated, and the number of edges is fixed, then decreasing the number of nodes by increasing the size of the regions used as nodes will increase the number of edges per node and lead to higher density graphs. In Chapters 4 and 5 only one parcellation scheme was used - the Freesurfer Desikan-Killiany atlas.[48] However, cortical thickness networks and DTI derived networks still had different numbers of

nodes as only cortical regions were used in the cortical thickness networks, but DTI derived networks included subcortical grey matter regions as additional nodes (see Table 3.2 for region descriptions). The difference in the number of nodes could have accounted for some of the differences between the findings of the cortical thickness networks and the DTI derived networks.

Methods of determining edge weights and thresholding edges also influence network characteristics.[52,74] This was clearly seen in this thesis when two methods of determining DTI edge weights were compared and when different thresholds were used to determine the density at which cortical thickness networks were examined. Tables 4.5 and 4.6 show the different metrics produced when edge weights are determined by the NOS between regions compared to when edges are determined by the average FA along the streamlines. There is no consensus as to which is the most accurate method of determining edges in DTI networks, and several other variations have been investigated and are in wide use, including those described in Table 2.6. Each method has philosophical or mathematical advantages and disadvantages and counteracts the disadvantages of using DTI streamlines to differing extents.[55,58] FA weighting falls naturally between zero and one which aids in mathematical modelling of network measures, but the total number of streamlines takes into account the cross-sectional area or potential bandwidth of the ROI.[188] Converting NOS weights by normalising to a normal distribution and ensuring values fell between zero and one completely erased all group differences between those with cognitive impairment and those with intact cognition in the suspected epilepsy cohort, as displayed in Tables 4.5 and 4.7 and this shows the extent of manipulation of edge weights on network measures and group differences.

Networks derived from the covariance of ROI thickness or volume measures will not have the difficulties with underrepresentation of local connectivity due to poor resolution or the under-representation of long range connections due to small errors seen with DTI derived networks.[188] Cortical thickness measurements on MRI have been shown to reflect histological post mortem cortical thickness,[59] and networks constructed from cortical thickness correlations show similar patterns of connectivity to those constructed from DTI or tract tracing data.[43,60,61] However, different methods of thresholding cortical thickness covariance adjacency matrices may lead to networks with very different characteristics and calculated network measures. The three most commonly used methods for thresholding network data are to use a 5% significance level and discard all values that do not meet this threshold, choose a value that obtains a fixed density or degree distribution for the network, or choose the largest threshold that guarantees that all nodes are connected.[52] In Chapters 4 and 5 two of these methods were used. The largest threshold that guaranteed all nodes had at least one edge led to the creation of dense networks with densities greater than 0.6. Therefore, a threshold that created a sparse network with a density closest to 0.2, similar to the DTI networks was also chosen, and the two network types were compared. Global efficiency was also examined over a range of thresholds in both cohorts. The aim of thresholding networks is to remove spurious connections, but removing too many connections may remove real connections and substantially affect graph properties.[52] More densely connected graphs do not tend to show a small world organisation when using σ as the measure of small worldness.[70] This is because although networks with an increased number and weight of edges will show lower average path lengths and higher clustering,[47,74] to calculate σ, both L and C are normalised by dividing their values by those from random networks with the same number of edges and nodes.[75] As small world networks have path

lengths similar to random networks, but clustering similar to lattices, the path length will normalise independently of network density, leading to values of λ that are consistent across network densities, but values of γ will remain dependent on network density with lower values at higher densities.[52] This leads to lower values of σ ($\frac{\gamma}{\lambda}$) at higher densities,[52,70] and explains why the completely connected cortical thickness networks with high densities have lower values of σ than the sparsely connected networks.

Both proportional and absolute thresholds were used in Chapter 4 in the suspected epilepsy cohort. Proportional thresholds remove a particular proportion of values in each adjacency matrix and therefore create networks across groups with a fixed density. This can be very useful as many network measures are affected by network density.[52,70] However, this may also remove group differences by fixing networks with very different numbers of edges to the same density. Tables 4.12 and 4.13 show the different network measures obtained in the two groups of the suspected epilepsy cohort when proportional vs absolute thresholding is applied to the same adjacency matrices to create different networks, and it can be seen in these tables that the network measures become more similar across the groups when proportional thresholding was used.

Binary and weighted networks were both calculated for the networks in Chapters 4 and 5. Binary networks are more straightforward for mathematical interpretation and analysis, but creating binary networks from MRI data that is naturally weighted may remove important information from the dataset. Binary networks can be useful in determining whether it is the arrangement of network edges between nodes or the edge weights that determine differences in network metrics. Comparing Tables 4.5 and 4.6 for the weighted and binary versions of the same networks suggests that because the differences in L, λ, γ, σ, and global efficiency are present in the binary networks as well as the weighted networks, these cannot be solely attributed to the distributions of weights on the edges. However, as the networks in Table 4.6 differ in density and degree between the two groups, group differences in L may still be due to the overall number of nodes and edges. The group difference in λ suggests this is unlikely to be the case. In addition, it can be seen in Table 4.6 that using binary versions of the NOS networks removes the mathematical difficulties encountered in calculated network measures when the edge weights do not fall between zero and one. Thus binary networks have several mathematical advantages as well as advantages in understanding mechanisms behind network differences, even if they remove edge weight information from the analysis.

Another important consideration in analysing networks is whether they have been constructed as group networks where a single network represents a group, or whether there is a network for each individual. There are no generally accepted methods for creating individual cortical thickness covariance networks, although attempts have been described.[189] In addition, several authors of seminal connectome studies have preferred to create group networks from DTI data using methods that only include edges found in a specific proportion of subjects as this ensures spurious connections are not included.[81] In this thesis, DTI networks were analysed at an individual level because this allowed network metrics to be modelled along with epilepsy characteristics using traditional statistical techniques. Cortical thickness networks were analysed as group networks using permutation testing which randomly reallocated groups to each subject. It is not possible to use permutation testing to account for group differences in demographics or clinical characteristics. However, some authors have adjusted the cortical thickness measurements prior to calculating the correlation across networks to remove the effects of age, sex, or epilepsy

characteristics (see Table 2.6 for examples).[83,84,143,149,159] Age and sex were regressed from the raw cortical thickness measurements in the suspected epilepsy cohort and the resultant networks were compared to those created from the raw cortical thickness measurements (see Tables 4.12, 4.13, and 4.13, and Figures 4.11 and 4.12). Regressing the effects of age and sex on cortical thickness prior to construction of the networks may be controlling for the effects of age and sex and rendering group differences smaller due to the group differences being truly reliant on age and sex. Alternatively, regressing the effects of age and sex may be removing data from construction of the networks and spuriously eliminating real group differences. The lack of overall difference in age at MRI between the two groups (mean 6.6 years vs mean 6.0 years, see Table 4.9) supports analysis without age correction.

Due to the different network construction techniques described in the literature, and summarised in this section, and their relative advantages and disadvantages, networks were constructed using a variety of different techniques in this thesis. That the overall findings in the two experimental chapters were mostly consistent across different network construction techniques, suggests that these are valid and robust findings in these cohorts. The heterogeneity of network measure estimates reported in Chapter 2 is likely as a result of the different network construction techniques used in the studies analysed, and is the reason that meta-analysis was not undertaken. However, where there is consistency of findings across different network construction techniques, this suggests that the findings are valid representations of underlying brain structure.

6.3 Context and Implications

6.3.1 Network characteristics in epilepsy

The systematic review in Chapter 2 investigating differences in network structure between those with epilepsy and healthy control subjects identified 27 studies of both adults and children with epilepsy. Of these, 17 investigated patients with TLE and only six included paediatric populations, which suggests that these results are mostly applicable to adults with TLE. In general, studies included few numbers of patients, with epilepsy groups ranging from 7 to 156 participants per study. Increasing the number of participants in each group would increase the power of the studies to detect any real differences between those with epilepsy and healthy controls. However, the low numbers are likely a reflection of the intensity of image processing and network matrix processing and analysis required to create and analyse MRI derived structural networks.

Due to the heterogenous study designs, study populations, and network construction techniques, numerical estimates of network measures varied substantially and so meta-analysis was not undertaken. Despite this variety, a majority of studies investigating average path length or global efficiency as measures of integration found that patients with epilepsy had an increased path length or a lower global efficiency compared to healthy controls. However, studies investigating λ found no difference between patients with epilepsy and controls. If there is a difference in L but not λ this suggests that the difference is due to overall network characteristics such as a lower number of edges or edge weights in the networks of the patients with epilepsy. Results were similar for studies of network

average clustering coefficients with more studies finding differences in average clustering coefficients than in normalised clustering coefficients, which supports this theory. However, investigation of L and λ did not always occur in the same studies (see Tables 2.8 and 2.9), and therefore patient populations and network construction techniques may also have played a role in producing different results. This theory is supported by the observation that studies which found an increased average clustering coefficient (C) in epilepsy all used covariance methods to construct networks, whilst studies which found a decreased clustering coefficient in epilepsy all used DTI methods to construct networks.

If an increase in L but not in λ and C but not γ is due to an overall increase in number or strength of edges, this could be accounted for pathologically by structural changes in epilepsy that lead to lower overall edge numbers or node strengths. A global loss of white matter has been described in patients with epilepsy.[117,136,137] In addition, local and generalised cortical thinning have been described in epilepsy, and this could lead to decreased co-ordination and correlation of changes across the whole brain, leading to a decreased number of edges in networks.[138,163] The cause for these underlying structural changes in epilepsy is unknown. Structural changes may be accounted for by the underlying pathological process that has led to the development of epilepsy.[117,138] However, seizures themselves may also produce widespread brain structural changes via methods such as excitotoxicity.[117,139]

6.3.2 Association of network characteristics with cognitive function

The association of network characteristics with cognitive function was investigated in a paediatric cohort with suspected epilepsy in Chapter 4. This cohort consisted of a group of children who were investigated for possible seizures with a specific MRI protocol. Not all of the children in this group had a final diagnosis of epilepsy following investigation and follow up. This cohort is a pragmatic representation of a clinical group likely to be investigated with MRI for suspected epilepsy. Fifty-six percent underwent the MRI within one year of their first seizure, and 38% were not taking any AEDs, suggesting that for many children, this was likely the first investigation for seizures. Thus the results from this cohort should be widely applicable to those investigated for possible epilepsy. In Section 4.5.5 a subgroup analysis of only those who had a final diagnosis of epilepsy was carried out, which confirmed the results were also applicable to those with a diagnosis of epilepsy.[99] The association of network characteristics with IQ was also investigated in Chapter 5 in the paediatric epilepsy surgery cohort. This cohort consisted only of children with medication resistant partial epilepsy and a structurally normal contralateral hemisphere who were candidates for epilepsy surgery, and therefore the results from this cohort are only applicable to this particular population. This thesis did not investigate adults with epilepsy in any of the experimental cohorts and therefore the findings may have limited applicability to adults.

The definition of cognitive impairment used in the suspected epilepsy cohort in Chapter 4 is a pragmatic description to include all children in the cohort with a wide range of cognitive abilities who were investigated as clinically appropriate rather than according to a strict research schedule. This should make the results widely applicable. Neuropsychological assessment and formal IQ testing was not undertaken when it was clinically unnecessary as there were no concerns regarding the child's cognitive development or school attainment. At the other end of the spectrum, some children were attending special education due to a diagnosis of an ID and this was appropriate for their level of function, but

recent IQ testing had not been undertaken. Although the definition of cognitive impairment as a documented diagnosis of ID or attendance at a special educational school was pragmatic and facilitated inclusion of most of the patients within the cohort in the analyses, using IQ scores would be a more accurate method of assessing cognitive impairment. The analyses were repeated in the subgroup with IQ scores, and similar results were found, suggesting that the pragmatic definition was appropriate.

In the epilepsy surgery cohort, there were no statistically significant differences in cortical thickness network measures between the group with an IQ greater than or equal to 70 and the group with an IQ less than 70. This contradicts the findings in the suspected epilepsy cohort where both cognitive impairment and IQ were associated with network average path lengths in both the DTI and the sparse cortical thickness networks. The difference in findings may be due to to the different range and cut off of IQ values. There were fewer participants with high IQ scores in the epilepsy surgery cohort (IQ≥ 70: mean IQ: 87, SD:12 vs IQ< 70: mean IQ: 54, SD:10; see Table 5.4) compared to the suspected epilepsy cohort (cognitive impairment: mean IQ: 59, SD:10 vs intact cognition: mean IQ: 91, SD: 15; see Table 4.9). Alternatively it may reflect differences between whole brain and single hemisphere network characteristics. The epilepsy surgery cohort had a greater number of participants in this analysis (n=99) compared to the suspected epilepsy cohort (n=78), so the difference in findings is unlikely to be due to the number of participants. The association between cognitive impairment and increased average path length is in keeping with previous studies showing an association between a lower IQ with a longer average path length in functional and structural networks in schizophrenics,[82,86] an association between IQ and average path length in DTI derived networks in a healthy adult population,[89] and a higher global efficiency with higher PIQ in a healthy childhood population.[93]

A few studies have specifically investigated the association of network characteristics with cognition in epilepsy. A study of 45 children undergoing epilepsy surgery did not show an association between DTI derived network properties and IQ,[135] similar to the epilepsy surgery cohort described in Chapter 5. However, in 39 children with new onset epilepsy, the ratio of clustering coefficient to characteristic path length derived from cortical thickness networks was found to be reduced in those with lower IQ scores,[134] similar to the findings from the paediatric suspected epilepsy cohort in Chapter 4. In a group of 39 adults wth focal epilepsy, cognitive impairment was associated with lower clustering coefficients and higher path lengths.[133] Thus the findings of studies investigating an association between cognition and network characteristics within patients with epilepsy may be dependent of the characteristics of the groups studied and the network creation methods as well as the range of cognitive disabilities studied. This thesis adds to the previous work by confirming an association of increased average path length in a heterogenous group of patients with cognitive impairment being investigated for seizures. However, this thesis also confirms that in a homogenous group of patients selected for epilepsy surgery with a low range of IQ scores, no association between IQ and average path length was found.

6.3.3 Association of network characteristics with change in IQ following epilepsy surgery

Chapter 5 investigated the association between structural network measures derived from cortical thickness networks of the healthy hemisphere with post-operative change in IQ in children undergoing

contralateral resective epilepsy surgery. In the group of patients who had a greater than 10 point increase in IQ post-operatively, higher network global efficiency was found in both the binary and weighted networks when networks were thresholded to remove all edge weights below 0.8, and in the weighted networks when networks were thresholded to remove all weights below 0.3. The consistency of the finding across different network construction methods suggests that this is a robust finding. As there are no differences between groups in network density, average node degree, mean edge weight or mean node strength (see Table 5.7), it is unlikely that the difference in global efficiency is due to overall differences in network construction rather than network topology. Mean cortical thickness measurements were not statistically significantly different between the two groups (see Table 5.6), and therefore the differences are also unlikely to be due to overall differences in cortical thickness measurements. The group whose post-operative IQ score increased at least 10 points had a shorter duration of epilepsy pre-operatively (see Table 5.6). Because it was not possible to take group differences into account using permutation testing, it is not known whether differences in epilepsy characteristics contribute to differences in group network characteristics.

No studies have previously investigated the association of structural networks with change in IQ scores post-operatively in epilepsy surgery, but the results are consistent with a study that showed that contralateral MRI abnormalities are associated with poorer cognitive outcomes following hemispherectomy.[126] Changes in mean cortical thickness in different ROIs or changes in correlations in cortical thickness between ROIs have been described following environmental, genetic, and developmental influences.[43,63–65] The more efficient organisation of the group cortical thickness network in the healthy hemisphere in those with an increase in IQ post operatively may represent more advanced development pre-operatively or prior to the onset of epilepsy, and more efficient organisation may facilitate cognitive development post-operatively.

6.4 Interaction of Networks, Cognition, and Epilepsy

Epilepsy is frequently associated with cognitive impairment,[113] and this thesis has shown that epilepsy is associated with disorganised structural networks with higher path lengths. Epilepsy is known to cause widespread structural changes in cortical thickness and white matter pathways.[136–138] This thesis has also provided evidence that higher network average path lengths are associated with cognitive impairment and lower IQ. Understanding the association of network characteristics with cognition and clinical epilepsy characteristics could provide some insight into whether the organisation of structural networks mediates the association between epilepsy and cognitive dysfunction.

Cognitive dysfunction in epilepsy has been associated with an early age of onset,[111,112] a longer duration of epilepsy,[113] increased seizure frequency,[108,109] and the use of AEDs.[115] These markers suggest that more severe epilepsy is more likely to be associated with cognitive impairment. These findings were confirmed in this thesis, as the presence of cognitive impairment in the suspected epilepsy cohort was associated with a younger age at first seizure and an increased seizure frequency, and in the epilepsy surgery cohort, a lower pre-operative IQ was associated with a younger age at operation, a younger age at onset of epilepsy, and single lobe pathology. In the suspected epilepsy

cohort, the frequency of seizures and the number of AEDs were statistically significantly associated with the network average path length and cognitive dysfunction. Including both the network average path length and the seizure frequency as predictors of cognition improved the amount of variance explained by the model, suggesting there is some mediation by structural network characteristics of associations between clinical epilepsy characteristics and cognition.

6.5 Future Questions

This thesis has suggested that epilepsy, cognition, and network characteristics are all inter-related, but has insufficient data to assess to what extent network characteristics mediate the association between epilepsy and cognition. As epilepsy characteristics are strongly correlated with each other (see Figures 4.15 and 4.16) and network characteristics are also strongly correlated with each other, it is difficult to accurately control for all of the potentially confounding factors in general linear models. Instead, in a large group of patients with epilepsy, detailed cognitive testing, network characteristics, and clinical characteristics could be included in a structural equation model to establish the relative influences and mediation of structural network characteristics on the relationship between epilepsy and cognition. Whether there is a stronger pathway directly from epilepsy to cognition or whether there is a stronger pathway from epilepsy via structural network characteristics to cognition would help determine whether structural network characteristics are mediating the association between epilepsy and cognition.[190] With multiple correlating epilepsy, cognitive, and network characteristics, factor analysis could help tease out which of the correlating characteristics are providing more influence in the model such as whether the VIQ or PIQ subtests are more strongly associated with different network characteristics. This planned model is shown graphically in Figure 6.1.

The study design that would facilitate building this model is a prospective observational study of a large group of patients with epilepsy with a wide range of epilepsy characteristics and cognitive functioning. Individual structural networks would be required for this analysis, and these would be built using a range of different DTI methods to determine edge weights to ensure network findings were robust across a range of construction methods. Complete neuropsychological testing of multiple cognitive domains would be undertaken in each patient. Ideally all MRI scans would be acquired on the same scanner with the same sequence parameters.

The second question that this thesis has raised is to what extent plasticity in structural networks occurs. Plasticity occurs via changes in synapses[191] and plasticity in cognitive function can occur over months to years, for example with the change in the location of eloquent cortex surrounding low grade gliomas.[192] Studying post-operative structural networks could address whether network plasticity also occurs. Improvements in cognition following epilepsy surgery can be associated with changes in grey matter volume.[122] Longer term follow up after epilepsy surgery with assessment of five year post-operative cortical thickness or DTI connectomes and comparison to pre-operative connectomes and change in IQ scores would assess to what extent the organisation of the healthy hemisphere can change post-operatively to facilitate cognitive improvement and development.

In the future, pre-operative modelling of the resection of epileptogenic tissue during epilepsy and the

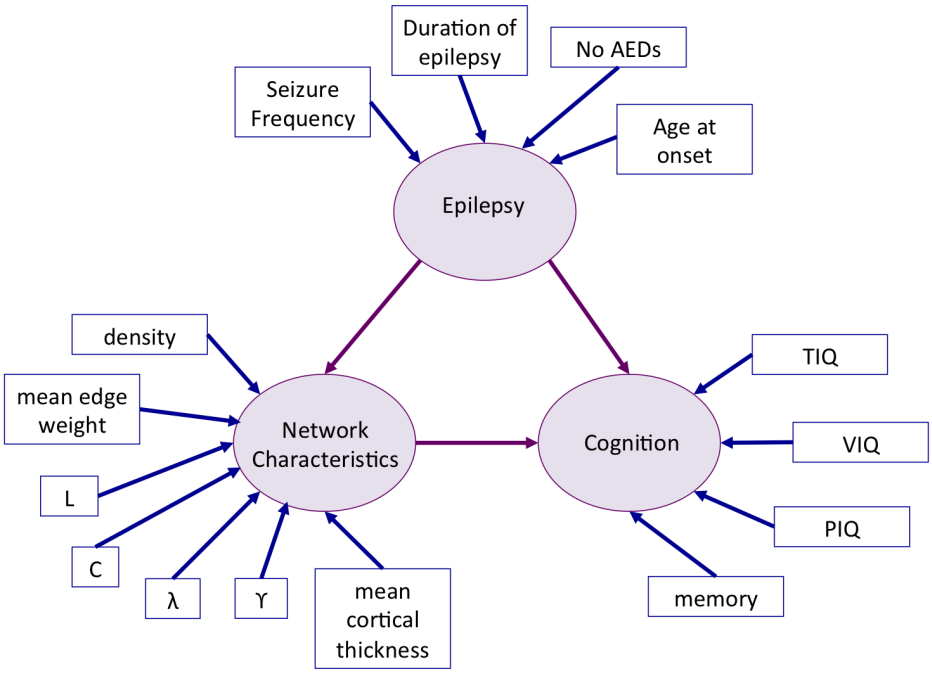

Figure 6.1: ***Planned structural equation model***. *Circles are the three latent variables. Squares are the measured variables contributing to each of those latent variables. Mediation is assessed by whether the association between epilepsy and network characteristics and the association between network characteristics and cognition are stronger than that between epilepsy and cognition when the model is fit. (AED: anti-epileptic drug; TIQ: total intelligence quotient; PIQ: verbal intelligence quotient; VIQ: performance intelligence quotient; L: average path length; λ: normalised average path length; C: clustering coefficient; γ: normalised clustering coefficient)*

effects of extent or location of resections on network structures and associated cognitive outcomes could help improve cognitive outcomes by maintaining or improving network structures that facilitate cognition. However, this would require modelling of network structure within and around the epileptogenic focus, which would be difficult using current automated methods of segmentation and parcellation, and very time consuming if this was performed manually for each patient. Therefore, this approach is not currently feasible for patients with a structural MRI abnormality, but would be feasible in the increasing number of patients undergoing epilepsy surgery who do not have a macroscopic abnormality visible on MRI.

6.6 Conclusions

This thesis has achieved the aims laid out in Section 1.4 and demonstrated that in epilepsy, structural networks show an increased average path length compared to healthy controls. However, there is no difference in the normalised average path length between patients with epilepsy and healthy controls. In the paediatric suspected epilepsy cohort, increased average path length, increased normalised average path length, and decreased global efficiency were found in structural networks of children with cognitive

impairment. These findings were not accounted for by differences in network number and strength of connections, and likely represent a less efficient network topology in those with cognitive impairment. In a paediatric epilepsy surgery cohort, a post-operative improvement in IQ of at least 10 points was associated with increased pre-operative global efficiency in the contralateral hemisphere.

Bibliography

[1] O'Rahilly R, Müller F. Significant features in the early prenatal development of the human brain. Ann Anat. 2008;190(2):105–18. doi:10.1016/j.aanat.2008.01.001.

[2] Bystron I, Blakemore C, Rakic P. Development of the human cerebral cortex: Boulder Committee revisited. Nat Rev Neurosci. 2008;9(2):110–22. doi:10.1038/nrn2252.

[3] ten Donkelaar HJ, Yamada S, Shiota K, van der Vliet T. Overview of the Development of the Human Brain and Spinal Cord. In: Clinical Neuroembryology. Springer; 2014.

[4] Müller F, O'Rahilly R. The human brain at stages 21-23, with particular reference to the cerebral cortical plate and to the development of the cerebellum. Anat Embryol (Berl). 1990;182(4):375–400.

[5] Azevedo FAC, Carvalho LRB, Grinberg LT, Farfel JM, Ferretti REL, Leite REP, et al. Equal Numbers of Neuronal and Nonneuronal Cells Make the Human Brain an Isometrically Scaled-Up Primate Brain. J Comp Neurol. 2009;513(5):532–541. doi:10.1002/cne.21974.

[6] Brodmann K. Vergleichende Lokalisationslehre der Großhirnrinde : in ihren Prinzipien dargestellt auf Grund des Zellenbaues. Leipzig: Barth; 1909.

[7] Judas M, Cepanec M, Sedmak G. Brodmann's Map of the Human Cerebral Cortex - or Brodmann's Maps? Transl Neurosci. 2012;3(1):67–74. doi:10.2478/s13380-012-0009-x.

[8] Penfield W, Jasper H. Epilepsy and the Functional Anatomy of the Human Brain. J and A Churchill Ltd; 1954.

[9] Ojemann G, Mateer C. Human language cortex: localization of memory, syntax, and sequential motor-phoneme identification systems. Science. 1979;205(4413):1401–3.

[10] De Benedictis A, Duffau H. Brain hodotopy: from esoteric concept to practical surgical applications. Neurosurgery. 2011;68(6):1709–23; discussion 1723. doi:10.1227/NEU.0b013e3182124690.

[11] Fuster JM. The cognit: a network model of cortical representation. Int J Psychophysiol. 2006;60(2):125–32. doi:10.1016/j.ijpsycho.2005.12.015.

[12] Yousem M D, Grossman I R. Neuroradiology: The Requisites. Third edition ed. Elsevier; 2010.

[13] Le Bihan D, Breton E, Lallemand D, Grenier P, Cabanis E, Laval-Jeantet M. MR imaging of intravoxel incoherent motions: application to diffusion and perfusion in neurologic disorders. Radiology. 1986;161(2):401–407. doi:10.1148/radiology.161.2.3763909.

[14] Basser PJ, Pierpaoli C. Microstructural and physiological features of tissues elucidated by quantitative-diffusion-tensor MRI. Journal of Magnetic Resonance - Series B. 1996;111(3):209–219.

[15] Beaulieu C. The basis of anisotropic water diffusion in the nervous system - a technical review. NMR Biomed. 2002;15(7-8):435–55. doi:10.1002/nbm.782.

[16] Beaulieu C, Allen PS. Water diffusion in the giant axon of the squid: implications for diffusion-weighted MRI of the nervous system. Magn Reson Med. 1994;32(5):579–83.

[17] Moseley ME, Cohen Y, Kucharczyk J, Mintorovitch J, Asgari HS, Wendland MF, et al. Diffusion-weighted MR imaging of anisotropic water diffusion in cat central nervous system. Radiology. 1990;176(2):439–45. doi:10.1148/radiology.176.2.2367658.

[18] Gulani V, Webb AG, Duncan ID, Lauterbur PC. Apparent diffusion tensor measurements in myelin-deficient rat spinal cords. Magn Reson Med. 2001;45(2):191–5.

[19] Wimberger DM, Roberts TP, Barkovich AJ, Prayer LM, Moseley ME, Kucharczyk J. Identification of ”premyelination” by diffusion-weighted MRI. J Comput Assist Tomogr. 1995;19(1):28–33.

[20] Takahashi M, Ono J, Harada K, Maeda M, Hackney DB. Diffusional anisotropy in cranial nerves with maturation: quantitative evaluation with diffusion MR imaging in rats. Radiology. 2000;216(3):881–5. doi:10.1148/radiology.216.3.r00se41881.

[21] Mori S, Crain BJ, Chacko VP, van Zijl PC. Three-dimensional tracking of axonal projections in the brain by magnetic resonance imaging. Ann Neurol. 1999;45(2):265–9.

[22] Basser PJ, Pajevic S, Pierpaoli C, Duda J, Aldroubi A. In vivo fiber tractography using DT-MRI data. Magn Reson Med. 2000;44(4):625–32.

[23] Behrens TEJ, Berg HJ, Jbabdi S, Rushworth MFS, Woolrich MW. Probabilistic diffusion tractography with multiple fibre orientations: What can we gain? Neuroimage. 2007;34(1):144–55. doi:10.1016/j.neuroimage.2006.09.018.

[24] Behrens TEJ, Woolrich MW, Jenkinson M, Johansen-Berg H, Nunes RG, Clare S, et al. Characterization and propagation of uncertainty in diffusion-weighted MR imaging. Magn Reson Med. 2003;50(5):1077–88. doi:10.1002/mrm.10609.

[25] Hagmann P, Kurant M, Gigandet X, Thiran P, Wedeen VJ, Meuli R, et al. Mapping human whole-brain structural networks with diffusion MRI. PLoS One. 2007;2(7):e597. doi:10.1371/journal.pone.0000597.

[26] Parker GJM, Haroon HA, Wheeler-Kingshott CAM. A framework for a streamline-based probabilistic index of connectivity (PICo) using a structural interpretation of MRI diffusion measurements. J Magn Reson Imaging. 2003;18(2):242–54. doi:10.1002/jmri.10350.

[27] Tuch DS, Reese TG, Wiegell MR, Makris N, Belliveau JW, Wedeen VJ. High angular resolution diffusion imaging reveals intravoxel white matter fiber heterogeneity. Magn Reson Med. 2002;48(4):577–82. doi:10.1002/mrm.10268.

[28] Wedeen VJ, Hagmann P, Tseng WYI, Reese TG, Weisskoff RM. Mapping complex tissue architecture with diffusion spectrum magnetic resonance imaging. Magn Reson Med. 2005;54(6):1377–86. doi:10.1002/mrm.20642.

[29] Iturria-Medina Y, Sotero RC, Canales-Rodríguez EJ, Alemán-Gómez Y, Melie-García L. Studying the human brain anatomical network via diffusion-weighted MRI and Graph Theory. Neuroimage. 2008;40(3):1064–76. doi:10.1016/j.neuroimage.2007.10.060.

[30] Parker GJM, Stephan KE, Barker GJ, Rowe JB, MacManus DG, Wheeler-Kingshott CAM, et al. Initial demonstration of in vivo tracing of axonal projections in the macaque brain and comparison with the human brain using diffusion tensor imaging and fast marching tractography. Neuroimage. 2002;15(4):797–809. doi:10.1006/nimg.2001.0994.

[31] Clayden JD, Storkey AJ, Bastin ME. A probabilistic model-based approach to consistent white matter tract segmentation. IEEE Trans Med Imaging. 2007;26(11):1555–61. doi:10.1109/TMI.2007.905826.

[32] Dauguet J, Peled S, Berezovskii V, Delzescaux T, Warfield SK, Born R, et al. Comparison of fiber tracts derived from in-vivo DTI tractography with 3D histological neural tract tracer reconstruction on a macaque brain. Neuroimage. 2007;37(2):530–8. doi:10.1016/j.neuroimage.2007.04.067.

[33] Catani M, Thiebaut de Schotten M, Slater D, Dell’Acqua F. Connectomic approaches before the connectome. Neuroimage. 2013;80:2–13. doi:10.1016/j.neuroimage.2013.05.109.

[34] Azadbakht H, Parkes LM, Haroon HA, Augath M, Logothetis NK, de Crespigny A, et al. Validation of High-Resolution Tractography Against In Vivo Tracing in the Macaque Visual Cortex. Cereb Cortex. 2015;25(11):4299–309. doi:10.1093/cercor/bhu326.

[35] Zumsteg D, Wieser HG. Presurgical evaluation: current role of invasive EEG. Epilepsia. 2000;41 Suppl 3:S55–60.

[36] Glover GH. Overview of functional magnetic resonance imaging. Neurosurg Clin N Am. 2011;22(2):133–9, vii. doi:10.1016/j.nec.2010.11.001.

[37] Farrell B, Godwin J, Richards S, Warlow C. The United Kingdom transient ischaemic attack (UK-TIA) aspirin trial: final results. J Neurol Neurosurg Psychiatry. 1991;54(12):1044–54.

[38] Teasdale G, Jennett B. Assessment of coma and impaired consciousness. A practical scale. Lancet. 1974;2(7872):81–4.

[39] Kaufman A, Lichtenberger E. Assessing Adolescent and Adult Intelligence. 3rd ed. Wiley; 2006.

[40] Booth T, Bastin ME, Penke L, Maniega SM, Murray C, Royle NA, et al. Brain white matter tract integrity and cognitive abilities in community-dwelling older people: the Lothian Birth Cohort, 1936. Neuropsychology. 2013;27(5):595–607. doi:10.1037/a0033354.

[41] White JG, Southgate E, Thomson JN, Brenner S. The structure of the nervous system of the nematode Caenorhabditis elegans. Philos Trans R Soc Lond B Biol Sci. 1986;314(1165):1–340.

[42] Eichler K, Li F, Litwin-Kumar A, Park Y, Andrade I, Schneider-Mizell CM, et al. The complete connectome of a learning and memory centre in an insect brain. Nature. 2017;548(7666):175–182. doi:10.1038/nature23455.

[43] He Y, Chen ZJ, Evans AC. Small-world anatomical networks in the human brain revealed by cortical thickness from MRI. Cereb Cortex. 2007;17(10):2407–19. doi:10.1093/cercor/bhl149.

[44] Stephan KE, Kamper L, Bozkurt A, Burns GA, Young MP, Kötter R. Advanced database methodology for the Collation of Connectivity data on the Macaque brain (CoCoMac). Philos Trans R Soc Lond B Biol Sci. 2001;356(1412):1159–86. doi:10.1098/rstb.2001.0908.

[45] Scannell JW, Blakemore C, Young MP. Analysis of connectivity in the cat cerebral cortex. J Neurosci. 1995;15(2):1463–83.

[46] Bullmore E, Sporns O. Complex brain networks: graph theoretical analysis of structural and functional systems. Nat Rev Neurosci. 2009;10(3):186–98. doi:10.1038/nrn2575.

[47] Sporns O, Tononi G, Kötter R. The human connectome: A structural description of the human brain. PLoS Comput Biol. 2005;1(4):e42. doi:10.1371/journal.pcbi.0010042.

[48] Desikan RS, Ségonne F, Fischl B, Quinn BT, Dickerson BC, Blacker D, et al. An automated labeling system for subdividing the human cerebral cortex on MRI scans into gyral based regions of interest. Neuroimage. 2006;31(3):968–80. doi:10.1016/j.neuroimage.2006.01.021.

[49] Fischl B, Salat DH, Busa E, Albert M, Dieterich M, Haselgrove C, et al. Whole brain segmentation: automated labeling of neuroanatomical structures in the human brain. Neuron. 2002;33(3):341–55.

[50] Tzourio-Mazoyer N, Landeau B, Papathanassiou D, Crivello F, Etard O, Delcroix N, et al. Automated anatomical labeling of activations in SPM using a macroscopic anatomical parcellation of the MNI MRI single-subject brain. Neuroimage. 2002;15(1):273–89. doi:10.1006/nimg.2001.0978.

[51] Friston KJ. Commentary and opinion: II. Statistical parametric mapping: ontology and current issues. J Cereb Blood Flow Metab. 1995;15(3):361–70. doi:10.1038/jcbfm.1995.45.

[52] van Wijk BCM, Stam CJ, Daffertshofer A. Comparing brain networks of different size and connectivity density using graph theory. PLoS One. 2010;5(10):e13701. doi:10.1371/journal.pone.0013701.

[53] Zalesky A, Fornito A, Harding IH, Cocchi L, Yücel M, Pantelis C, et al. Whole-brain anatomical networks: does the choice of nodes matter? Neuroimage. 2010;50(3):970–83. doi:10.1016/j.neuroimage.2009.12.027.

[54] Mårtensson G, Pereira JB, Mecocci P, Vellas B, Tsolaki M, Kłoszewska I, et al. Stability of graph theoretical measures in structural brain networks in Alzheimer's disease. Sci Rep. 2018;8(1):11592. doi:10.1038/s41598-018-29927-0.

[55] Qi S, Meesters S, Nicolay K, Romeny BMTH, Ossenblok P. The influence of construction methodology on structural brain network measures: A review. J Neurosci Methods. 2015;253:170–82. doi:10.1016/j.jneumeth.2015.06.016.

[56] Stanley ML, Moussa MN, Paolini BM, Lyday RG, Burdette JH, Laurienti PJ. Defining nodes in complex brain networks. Front Comput Neurosci. 2013;7:169. doi:10.3389/fncom.2013.00169.

[57] Vaessen MJ, Hofman PAM, Tijssen HN, Aldenkamp AP, Jansen JFA, Backes WH. The effect and reproducibility of different clinical DTI gradient sets on small world brain connectivity measures. Neuroimage. 2010;51(3):1106–16. doi:10.1016/j.neuroimage.2010.03.011.

[58] Buchanan CR, Pernet CR, Gorgolewski KJ, Storkey AJ, Bastin ME. Test-retest reliability of structural brain networks from diffusion MRI. Neuroimage. 2014;86:231–43. doi:10.1016/j.neuroimage.2013.09.054.

[59] Popescu V, Klaver R, Versteeg A, Voorn P, Twisk JWR, Barkhof F, et al. Postmortem validation of MRI cortical volume measurements in MS. Hum Brain Mapp. 2016;37(6):2223–33. doi:10.1002/hbm.23168.

[60] Lerch JP, Evans AC. Cortical thickness analysis examined through power analysis and a population simulation. Neuroimage. 2005;24(1):163–73. doi:10.1016/j.neuroimage.2004.07.045.

[61] Bernhardt BC, Worsley KJ, Besson P, Concha L, Lerch JP, Evans AC, et al. Mapping limbic network organization in temporal lobe epilepsy using morphometric correlations: insights on the relation between mesiotemporal connectivity and cortical atrophy. Neuroimage. 2008;42(2):515–24. doi:10.1016/j.neuroimage.2008.04.261.

[62] Bassett DS, Bullmore E, Verchinski BA, Mattay VS, Weinberger DR, Meyer-Lindenberg A. Hierarchical organization of human cortical networks in health and schizophrenia. J Neurosci. 2008;28(37):9239–48. doi:10.1523/JNEUROSCI.1929-08.2008.

[63] Maguire EA, Gadian DG, Johnsrude IS, Good CD, Ashburner J, Frackowiak RS, et al. Navigation-related structural change in the hippocampi of taxi drivers. Proc Natl Acad Sci U S A. 2000;97(8):4398–403. doi:10.1073/pnas.070039597.

[64] Bullmore ET, Woodruff PW, Wright IC, Rabe-Hesketh S, Howard RJ, Shuriquie N, et al. Does dysplasia cause anatomical dysconnectivity in schizophrenia? Schizophr Res. 1998;30(2):127–35.

[65] Bailey JA, Zatorre RJ, Penhune VB. Early musical training is linked to gray matter structure in the ventral premotor cortex and auditory-motor rhythm synchronization performance. J Cogn Neurosci. 2014;26(4):755–67.

[66] Andrews TJ, Halpern SD, Purves D. Correlated size variations in human visual cortex, lateral geniculate nucleus, and optic tract. J Neurosci. 1997;17(8):2859–68.

[67] Alexander-Bloch A, Raznahan A, Bullmore E, Giedd J. The convergence of maturational change and structural covariance in human cortical networks. J Neurosci. 2013;33(7):2889–99. doi:10.1523/JNEUROSCI.3554-12.2013.

[68] Rakic P. Specification of cerebral cortical areas. Science. 1988;241(4862):170–6. doi:10.1126/science.3291116.

[69] Yeh CH, Smith RE, Liang X, Calamante F, Connelly A. Correction for diffusion MRI fibre tracking biases: The consequences for structural connectomic metrics. Neuroimage. 2016;142:150–162. doi:10.1016/j.neuroimage.2016.05.047.

[70] Bassett DS, Bullmore ET. Small-World Brain Networks Revisited. Neuroscientist. 2017;23(5):499–516. doi:10.1177/1073858416667720.

[71] Börner K, Sanyal S, Vespignani A. Network science. Annual Review of Information Science and Technology. 2007;41(1):537–607. doi:10.1002/aris.2007.1440410119.

[72] Watts DJ, Strogatz SH. Collective dynamics of 'small-world' networks. Nature. 1998;393(6684):440–2. doi:10.1038/30918.

[73] Milgram S. The small world problem. Psychology Today. 1967;1:61–67.

[74] Rubinov M, Sporns O. Complex network measures of brain connectivity: uses and interpretations. Neuroimage. 2010;52(3):1059–69. doi:10.1016/j.neuroimage.2009.10.003.

[75] Humphries MD, Gurney K. Network 'small-world-ness': a quantitative method for determining canonical network equivalence. PLoS One. 2008;3(4):e0002051. doi:10.1371/journal.pone.0002051.

[76] Eguíluz VM, Chialvo DR, Cecchi GA, Baliki M, Apkarian AV. Scale-free brain functional networks. Phys Rev Lett. 2005;94(1):018102. doi:10.1103/PhysRevLett.94.018102.

[77] van den Heuvel MP, Stam CJ, Boersma M, Hulshoff Pol HE. Small-world and scale-free organization of voxel-based resting-state functional connectivity in the human brain. Neuroimage. 2008;43(3):528–39. doi:10.1016/j.neuroimage.2008.08.010.

[78] Stam CJ, Jones BF, Nolte G, Breakspear M, Scheltens P. Small-world networks and functional connectivity in Alzheimer's disease. Cereb Cortex. 2007;17(1):92–9. doi:10.1093/cercor/bhj127.

[79] Sporns O, Honey CJ, Kötter R. Identification and classification of hubs in brain networks. PLoS One. 2007;2(10):e1049. doi:10.1371/journal.pone.0001049.

[80] Liang X, Yeh CH, Connelly A, Calamante F. Robust Identification of Rich-Club Organization in Weighted and Dense Structural Connectomes. Brain Topogr. 2019;32(1):1–16. doi:10.1007/s10548-018-0661-8.

[81] van den Heuvel MP, Sporns O. Rich-club organization of the human connectome. J Neurosci. 2011;31(44):15775–86. doi:10.1523/JNEUROSCI.3539-11.2011.

[82] Yeo RA, Ryman SG, van den Heuvel MP, de Reus MA, Jung RE, Pommy J, et al. Graph Metrics of Structural Brain Networks in Individuals with Schizophrenia and Healthy Controls: Group Differences, Relationships with Intelligence, and Genetics. J Int Neuropsychol Soc. 2016;22(2):240–9. doi:10.1017/S1355617715000867.

[83] Bernhardt B C, Chen Z, He Y, Evans A C, Bernasconi N. Graph-theoretical analysis reveals disrupted small-world organization of cortical thickness correlation networks in temporal lobe epilepsy. Cerebral Cortex. 2011;21(9):2147–2157.

[84] Besson P, Dinkelacker V, Valabregue R, Thivard L, Leclerc X, Baulac M, et al. Structural connectivity differences in left and right temporal lobe epilepsy. Neuroimage. 2014;100:135–144.

[85] Bonilha L, Helpern J A, Sainju R, Nesland T, Edwards J C, Glazier S S, et al. Presurgical connectome and postsurgical seizure control in temporal lobe epilepsy. Neurology. 2013;81(19):1704–1710.

[86] van den Heuvel MP, Stam CJ, Kahn RS, Hulshoff Pol HE. Efficiency of functional brain networks and intellectual performance. J Neurosci. 2009;29(23):7619–24. doi:10.1523/JNEUROSCI.1443-09.2009.

[87] Pamplona GSP, Santos Neto GS, Rosset SRE, Rogers BP, Salmon CEG. Analyzing the association between functional connectivity of the brain and intellectual performance. Front Hum Neurosci. 2015;9:61. doi:10.3389/fnhum.2015.00061.

[88] Kruschwitz JD, Waller L, Daedelow LS, Walter H, Veer IM. General, crystallized and fluid intelligence are not associated with functional global network efficiency: A replication study with

the human connectome project 1200 data set. NeuroImage. 2018;171:323 – 331. doi:https://doi.org/10.1016/j.neuroimage.2018.01.018.

[89] Li Y, Liu Y, Li J, Qin W, Li K, Yu C, et al. Brain anatomical network and intelligence. PLoS Comput Biol. 2009;5(5):e1000395. doi:10.1371/journal.pcbi.1000395.

[90] Kocevar G, Suprano I, Stamile C, Hannoun S, Fourneret P, Revol O, et al. Brain structural connectivity correlates with fluid intelligence in children: A DTI graph analysis. Intelligence. 2019;72:67 – 75. doi:https://doi.org/10.1016/j.intell.2018.12.003.

[91] Fischer FU, Wolf D, Scheurich A, Fellgiebel A. Association of structural global brain network properties with intelligence in normal aging. PLoS One. 2014;9(1):e86258. doi:10.1371/journal.pone.0086258.

[92] Zalesky A, Fornito A, Seal ML, Cocchi L, Westin CF, Bullmore ET, et al. Disrupted axonal fiber connectivity in schizophrenia. Biol Psychiatry. 2011;69(1):80–9. doi:10.1016/j.biopsych.2010.08.022.

[93] Khundrakpam BS, Lewis JD, Reid A, Karama S, Zhao L, Chouinard-Decorte F, et al. Imaging structural covariance in the development of intelligence. Neuroimage. 2017;144(Pt A):227–240. doi:10.1016/j.neuroimage.2016.08.041.

[94] Deary IJ, Penke L, Johnson W. The neuroscience of human intelligence differences. Nat Rev Neurosci. 2010;11(3):201–11. doi:10.1038/nrn2793.

[95] Jung RE, Haier RJ. The Parieto-Frontal Integration Theory (P-FIT) of intelligence: converging neuroimaging evidence. Behav Brain Sci. 2007;30(2):135–54; discussion 154–87. doi:10.1017/S0140525X07001185.

[96] Basten U, Hilger K, Fiebach CJ. Where smart brains are different: A quantitative meta-analysis of functional and structural brain imaging studies on intelligence. Intelligence. 2015;51:10–27. doi:10.1016/j.intell.2015.04.009.

[97] Brouwer RM, van Soelen ILC, Swagerman SC, Schnack HG, Ehli EA, Kahn RS, et al. Genetic associations between intelligence and cortical thickness emerge at the start of puberty. Hum Brain Mapp. 2014;35(8):3760–73. doi:10.1002/hbm.22435.

[98] Koenis MMG, Brouwer RM, Swagerman SC, van Soelen ILC, Boomsma DI, Hulshoff Pol HE. Association between structural brain network efficiency and intelligence increases during adolescence. Hum Brain Mapp. 2018;39(2):822–836. doi:10.1002/hbm.23885.

[99] Fisher RS, Acevedo C, Arzimanoglou A, Bogacz A, Cross JH, Elger CE, et al. ILAE official report: a practical clinical definition of epilepsy. Epilepsia. 2014;55(4):475–82. doi:10.1111/epi.12550.

[100] Bernhardt BC, Bonilha L, Gross DW. Network analysis for a network disorder: The emerging role of graph theory in the study of epilepsy. Epilepsy Behav. 2015;50:162–70. doi:10.1016/j.yebeh.2015.06.005.

[101] van Diessen E, Zweiphenning WJEM, Jansen FE, Stam CJ, Braun KPJ, Otte WM. Brain Network Organization in Focal Epilepsy: A Systematic Review and Meta-Analysis. PLoS One. 2014;9(12):e114606. doi:10.1371/journal.pone.0114606.

[102] van Diessen E, Diederen SJH, Braun KPJ, Jansen FE, Stam CJ. Functional and structural brain networks in epilepsy: what have we learned? Epilepsia. 2013;54(11):1855–65. doi:10.1111/epi.12350.

[103] Lin JJ, Mula M, Hermann BP. Uncovering the neurobehavioural comorbidities of epilepsy over the lifespan. Lancet. 2012;380(9848):1180–92. doi:10.1016/S0140-6736(12)61455-X.

[104] Hunter MB, Yoong M, Sumpter RE, Verity K, Shetty J, McLellan A, et al. Neurobehavioral problems in children with early-onset epilepsy: A population-based study. Epilepsy Behav. 2019;93:87–93. doi:10.1016/j.yebeh.2019.01.019.

[105] Reilly C, Atkinson P, Das KB, Chin RFMC, Aylett SE, Burch V, et al. Neurobehavioral comorbidities in children with active epilepsy: a population-based study. Pediatrics. 2014;133(6):e1586–93. doi:10.1542/peds.2013-3787.

[106] Shankar R, Rowe C, Van Hoorn A, Henley W, Laugharne R, Cox D, et al. Under representation of people with epilepsy and intellectual disability in research. PLoS One. 2018;13(6):e0198261. doi:10.1371/journal.pone.0198261.

[107] Ferro MA, Camfield CS, Levin SD, Smith ML, Wiebe S, Zou G, et al. Trajectories of health-related quality of life in children with epilepsy: a cohort study. Epilepsia. 2013;54(11):1889–97. doi:10.1111/epi.12388.

[108] Baker GA, Nashef L, van Hout BA. Current issues in the management of epilepsy: the impact of frequent seizures on cost of illness, quality of life, and mortality. Epilepsia. 1997;38 Suppl 1:S1–8.

[109] Czochańska J, Langner-Tyszka B, Losiowski Z, Schmidt-Sidor B. Children who develop epilepsy in the first year of life: a prospective study. Dev Med Child Neurol. 1994;36(4):345–50.

[110] Aldenkamp AP, Bodde N. Behaviour, cognition and epilepsy. Acta Neurol Scand Suppl. 2005;182:19–25. doi:10.1111/j.1600-0404.2005.00523.x.

[111] Cormack F, Cross JH, Isaacs E, Harkness W, Wright I, Vargha-Khadem F, et al. The development of intellectual abilities in pediatric temporal lobe epilepsy. Epilepsia. 2007;48(1):201–4. doi:10.1111/j.1528-1167.2006.00904.x.

[112] Vasconcellos E, Wyllie E, Sullivan S, Stanford L, Bulacio J, Kotagal P, et al. Mental retardation in pediatric candidates for epilepsy surgery: the role of early seizure onset. Epilepsia. 2001;42(2):268–74.

[113] D'Argenzio L, Colonnelli MC, Harrison S, Jacques TS, Harkness W, Vargha-Khadem F, et al. Cognitive outcome after extratemporal epilepsy surgery in childhood. Epilepsia. 2011;52(11):1966–72. doi:10.1111/j.1528-1167.2011.03272.x.

[114] van Rijckevorsel K. Cognitive problems related to epilepsy syndromes, especially malignant epilepsies. Seizure. 2006;15(4):227–34. doi:10.1016/j.seizure.2006.02.019.

[115] Lagae L. Cognitive side effects of anti-epileptic drugs. The relevance in childhood epilepsy. Seizure. 2006;15(4):235–41. doi:10.1016/j.seizure.2006.02.013.

[116] Yoong M, Hunter M, Stephen J, Quigley A, Jones J, Shetty J, et al. Cognitive impairment in early onset epilepsy is associated with reduced left thalamic volume. Epilepsy Behav. 2018;80:266–271. doi:10.1016/j.yebeh.2018.01.018.

[117] Yogarajah M, Duncan JS. Diffusion-based magnetic resonance imaging and tractography in epilepsy. Epilepsia. 2008;49(2):189–200. doi:10.1111/j.1528-1167.2007.01378.x.

[118] Otte WM, van Eijsden P, Sander JW, Duncan JS, Dijkhuizen RM, Braun KPJ. A meta-analysis of white matter changes in temporal lobe epilepsy as studied with diffusion tensor imaging. Epilepsia. 2012;53(4):659–67. doi:10.1111/j.1528-1167.2012.03426.x.

[119] Braakman HMH, Vaessen MJ, Jansen JFA, Debeij-van Hall MHJA, de Louw A, Hofman PAM, et al. Pediatric frontal lobe epilepsy: white matter abnormalities and cognitive impairment. Acta Neurol Scand. 2014;129(4):252–62. doi:10.1111/ane.12183.

[120] Baulac M, de Boer H, Elger C, Glynn M, Kälviäinen R, Little A, et al. Epilepsy priorities in Europe: A report of the ILAE-IBE Epilepsy Advocacy Europe Task Force. Epilepsia. 2015;56(11):1687–95. doi:10.1111/epi.13201.

[121] Tellez-Zenteno JF, Dhar R, Wiebe S. Long-term seizure outcomes following epilepsy surgery: a systematic review and meta-analysis. Brain. 2005;128(Pt 5):1188–98. doi:10.1093/brain/awh449.

[122] Skirrow C, Cross JH, Cormack F, Harkness W, Vargha-Khadem F, Baldeweg T. Long-term intellectual outcome after temporal lobe surgery in childhood. Neurology. 2011;76(15):1330–7. doi:10.1212/WNL.0b013e31821527f0.

[123] Téllez-Zenteno JF, Dhar R, Hernandez-Ronquillo L, Wiebe S. Long-term outcomes in epilepsy surgery: antiepileptic drugs, mortality, cognitive and psychosocial aspects. Brain. 2007;130(Pt 2):334–45. doi:10.1093/brain/awl316.

[124] Sherman EMS, Wiebe S, Fay-McClymont TB, Tellez-Zenteno J, Metcalfe A, Hernandez-Ronquillo L, et al. Neuropsychological outcomes after epilepsy surgery: systematic review and pooled estimates. Epilepsia. 2011;52(5):857–69. doi:10.1111/j.1528-1167.2011.03022.x.

[125] Schooneveld MMJV, Braun KPJ. Cognitive outcome after epilepsy surgery in children. Brain and Development. 2013;35(8):721 – 729. doi:https://doi.org/10.1016/j.braindev.2013.01.011.

[126] Boshuisen K, van Schooneveld MMJ, Leijten FSS, de Kort GAP, van Rijen PC, Gosselaar PH, et al. Contralateral MRI abnormalities affect seizure and cognitive outcome after hemispherectomy. Neurology. 2010;75(18):1623–30. doi:10.1212/WNL.0b013e3181fb4400.

[127] Boshuisen K, Lamberink HJ, van Schooneveld MM, Cross JH, Arzimanoglou A, van der Tweel I, et al. Cognitive consequences of early versus late antiepileptic drug withdrawal after pediatric epilepsy surgery, the TimeToStop (TTS) trial: study protocol for a randomized controlled trial. Trials. 2015;16:482. doi:10.1186/s13063-015-0989-2.

[128] Ponten SC, Bartolomei F, Stam CJ. Small-world networks and epilepsy: graph theoretical analysis of intracerebrally recorded mesial temporal lobe seizures. Clin Neurophysiol. 2007;118(4):918–27. doi:10.1016/j.clinph.2006.12.002.

[129] Bartolomei F, Bettus G, Stam CJ, Guye M. Interictal network properties in mesial temporal lobe epilepsy: a graph theoretical study from intracerebral recordings. Clin Neurophysiol. 2013;124(12):2345–53. doi:10.1016/j.clinph.2013.06.003.

[130] Wang J, Qiu S, Xu Y, Liu Z, Wen X, Hu X, et al. Graph theoretical analysis reveals disrupted topological properties of whole brain functional networks in temporal lobe epilepsy. Clin Neurophysiol. 2014;125(9):1744–56. doi:10.1016/j.clinph.2013.12.120.

[131] Vaessen M J, Jansen J F, Braakman H M, Hofman P A, De Louw A, Aldenkamp A P, et al. Functional and structural network impairment in childhood frontal lobe epilepsy. PLoS ONE [Electronic Resource]. 2014;9(3):e90068–e90068.

[132] Bonilha L, Nesland T, Martz G U, Joseph J E, Spampinato M V, Edwards J C, et al. Medial temporal lobe epilepsy is associated with neuronal fibre loss and paradoxical increase in structural connectivity of limbic structures. Journal of Neurology, Neurosurgery & Psychiatry. 2012;83(9):903–909.

[133] Vaessen M J, Jansen J F, Vlooswijk M C, Hofman P A, Majoie H J, Aldenkamp A P, et al. White matter network abnormalities are associated with cognitive decline in chronic epilepsy. Cerebral Cortex. 2012;22(9):2139–2147.

[134] Bonilha L, Tabesh A, Dabbs K, Hsu D A, Stafstrom C E, Hermann B P, et al. Neurodevelopmental alterations of large-scale structural networks in children with new-onset epilepsy. Human Brain Mapping. 2014;35(8):3661–3672.

[135] Widjaja E, Zamyadi M, Raybaud C, Snead O C, Doesburg S M, Smith M L. Disrupted Global and Regional Structural Networks and Subnetworks in Children with Localization-Related Epilepsy. Ajnr: American Journal of Neuroradiology. 2015;36(7):1362–1368.

[136] Yogarajah M, Focke NK, Bonelli SB, Thompson P, Vollmar C, McEvoy AW, et al. The structural plasticity of white matter networks following anterior temporal lobe resection. Brain. 2010;133(Pt 8):2348–64. doi:10.1093/brain/awq175.

[137] Laufs H. Functional imaging of seizures and epilepsy: evolution from zones to networks. Curr Opin Neurol. 2012;25(2):194–200. doi:10.1097/WCO.0b013e3283515db9.

[138] Ogren JA, Tripathi R, Macey PM, Kumar R, Stern JM, Eliashiv DS, et al. Regional cortical thickness changes accompanying generalized tonic-clonic seizures. Neuroimage Clin. 2018;20:205–215. doi:10.1016/j.nicl.2018.07.015.

[139] Kim JA, Chung JI, Yoon PH, Kim DI, Chung TS, Kim EJ, et al. Transient MR signal changes in patients with generalized tonicoclonic seizure or status epilepticus: periictal diffusion-weighted imaging. AJNR Am J Neuroradiol. 2001;22(6):1149–60.

[140] Whiting PF, Rutjes AWS, Westwood ME, Mallett S, Deeks JJ, Reitsma JB, et al. QUADAS-2: a revised tool for the quality assessment of diagnostic accuracy studies. Ann Intern Med. 2011;155(8):529–36. doi:10.7326/0003-4819-155-8-201110180-00009.

[141] Moher D, Liberati A, Tetzlaff J, Altman DG. Preferred reporting items for systematic reviews and meta-analyses: the PRISMA statement. J Clin Epidemiol. 2009;62(10):1006–1012. doi:10.1016/j.jclinepi.2009.06.005.

[142] Xue K, Luo C, Zhang D, Yang T, Li J, Gong D, et al. Diffusion tensor tractography reveals disrupted structural connectivity in childhood absence epilepsy. Epilepsy Research. 2014;108(1):125–138.

[143] Curwood E K, Pedersen M, Carney P W, Berg A T, Abbott D F, Jackson G D. Abnormal cortical thickness connectivity persists in childhood absence epilepsy. Annals of Clinical & Translational Neurology. 2015;2(5):456–464.

[144] Caeyenberghs K, Powell H W, Thomas R H, Brindley L, Church C, Evans J, et al. Hyperconnectivity in juvenile myoclonic epilepsy: a network analysis. NeuroImage Clinical. 2015;7:98–104.

[145] Zhang Z, Liao W, Chen H, Mantini D, Ding J R, Xu Q, et al. Altered functional-structural coupling of large-scale brain networks in idiopathic generalized epilepsy. Brain. 2011;134(Pt 10):2912–2928.

[146] Li X, Morgan PS, Ashburner J, Smith J, Rorden C. The first step for neuroimaging data analysis: DICOM to NIfTI conversion. J Neurosci Methods. 2016;264:47–56. doi:10.1016/j.jneumeth.2016.03.001.

[147] Garcia-Ramos C, Lin JJ, Bonilha L, Jones JE, Jackson DC, Prabhakaran V, et al. Disruptions in cortico-subcortical covariance networks associated with anxiety in new-onset childhood epilepsy. Neuroimage Clin. 2016;12:815–824. doi:10.1016/j.nicl.2016.10.017.

[148] Besseling R M, Jansen J F, Overvliet G M, van der Kruijs S J, Ebus S C, de Louw A J, et al. Delayed convergence between brain network structure and function in rolandic epilepsy. Frontiers in Human Neuroscience. 2014;8(704).

[149] Liao W, Zhang Z, Mantini D, Xu Q, Wang Z, Chen G, et al. Relationship between large-scale functional and structural covariance networks in idiopathic generalized epilepsy. Brain Connectivity. 2013;3(3):240–254.

[150] Liu M, Chen Z, Beaulieu C, Gross D W. Disrupted anatomic white matter network in left mesial temporal lobe epilepsy. Epilepsia. 2014;55(5):674–682.

[151] Xu Y, Qiu S, Wang J, Liu Z, Zhang R, Li S, et al. Disrupted topological properties of brain white matter networks in left temporal lobe epilepsy: a diffusion tensor imaging study. Neuroscience. 2014;279:155–167.

[152] Sone D, Matsuda H, Ota M, Maikusa N, Kimura Y, Sumida K, et al. Graph Theoretical Analysis of Structural Neuroimaging in Temporal Lobe Epilepsy with and without Psychosis. PLoS One. 2016;11(7):e0158728. doi:10.1371/journal.pone.0158728.

[153] Wirsich J, Perry A, Ridley B, Proix T, Golos M, Bénar C, et al. Whole-brain analytic measures of network communication reveal increased structure-function correlation in right temporal lobe epilepsy. Neuroimage Clin. 2016;11:707–718. doi:10.1016/j.nicl.2016.05.010.

[154] DeSalvo M N, Douw L, Tanaka N, Reinsberger C, Stufflebeam S M. Altered structural connectome in temporal lobe epilepsy. Radiology. 2014;270(3):842–848.

[155] Lemkaddem A, Daducci A, Kunz N, Lazeyras F, Seeck M, Thiran J P, et al. Connectivity and tissue microstructural alterations in right and left temporal lobe epilepsy revealed by diffusion spectrum imaging. NeuroImage Clinical. 2014;5:349–358.

[156] Yasuda C L, Chen Z, Beltramini G C, Coan A C, Morita M E, Kubota B, et al. Aberrant topological patterns of brain structural network in temporal lobe epilepsy. Epilepsia. 2015;56(12):1992–2002.

[157] Li, R, Liao, W, Y, et al. Disrupted structural and functional rich club organization of the brain connectome in patients with generalized tonic-clonic seizure; Ovid.

[158] Kamiya K, Amemiya S, Suzuki Y, Kunii N, Kawai K, Mori H, et al. Machine Learning of DTI Structural Brain Connectomes for Lateralization of Temporal Lobe Epilepsy. Magnetic Resonance in Medical Sciences. 2016;15(1):121–129.

[159] Raj A, Mueller S G, Young K, Laxer K D, Weiner M. Network-level analysis of cortical thickness of the epileptic brain. Neuroimage. 2010;52(4):1302–1313.

[160] Fang P, An J, Zeng L L, Shen H, Chen F, Wang W, et al. Multivariate pattern analysis reveals anatomical connectivity differences between the left and right mesial temporal lobe epilepsy. NeuroImage Clinical. 2015;7:555–561.

[161] Munsell B C, Wee C Y, Keller S S, Weber B, Elger C, da Silva L A, et al. Evaluation of machine learning algorithms for treatment outcome prediction in patients with epilepsy based on structural connectome data. Neuroimage. 2015;118:219–230.

[162] Douw L, DeSalvo M N, Tanaka N, Cole A J, Liu H, Reinsberger C, et al. Dissociated multimodal hubs and seizures in temporal lobe epilepsy. Annals of Clinical & Translational Neurology. 2015;2(4):338–352.

[163] Bernhardt BC, Rozen DA, Worsley KJ, Evans AC, Bernasconi N, Bernasconi A. Thalamo-cortical network pathology in idiopathic generalized epilepsy: insights from MRI-based morphometric correlation analysis. Neuroimage. 2009;46(2):373–81.

[164] Scheffer IE, Berkovic S, Capovilla G, Connolly MB, French J, Guilhoto L, et al. ILAE classification of the epilepsies: Position paper of the ILAE Commission for Classification and Terminology. Epilepsia. 2017;58(4):512–521. doi:10.1111/epi.13709.

[165] Moffitt TE, Caspi A, Harkness AR, Silva PA. The natural history of change in intellectual performance: who changes? How much? Is it meaningful? J Child Psychol Psychiatry. 1993;34(4):455–506.

[166] Ségonne F, Dale AM, Busa E, Glessner M, Salat D, Hahn HK, et al. A hybrid approach to the skull stripping problem in MRI. Neuroimage. 2004;22(3):1060–75. doi:10.1016/j.neuroimage.2004.03.032.

[167] Dale AM, Fischl B, Sereno MI. Cortical surface-based analysis. I. Segmentation and surface reconstruction. Neuroimage. 1999;9(2):179–94. doi:10.1006/nimg.1998.0395.

[168] Fischl B, Sereno MI, Dale AM. Cortical surface-based analysis. II: Inflation, flattening, and a surface-based coordinate system. Neuroimage. 1999;9(2):195–207. doi:10.1006/nimg.1998.0396.

[169] Fischl B, Dale AM. Measuring the thickness of the human cerebral cortex from magnetic resonance images. Proc Natl Acad Sci U S A. 2000;97(20):11050–5. doi:10.1073/pnas.200033797.

[170] Andersson JLR, Skare S. A model-based method for retrospective correction of geometric distortions in diffusion-weighted EPI. Neuroimage. 2002;16(1):177–99. doi:10.1006/nimg.2001.1039.

[171] Chang LC, Jones DK, Pierpaoli C. RESTORE: robust estimation of tensors by outlier rejection. Magn Reson Med. 2005;53(5):1088–95. doi:10.1002/mrm.20426.

[172] Mori S, van Zijl PCM. Fiber tracking: principles and strategies - a technical review. NMR Biomed. 2002;15(7-8):468–80. doi:10.1002/nbm.781.

[173] He Y, Chen Z, Evans A. Structural insights into aberrant topological patterns of large-scale cortical networks in Alzheimer's disease. J Neurosci. 2008;28(18):4756–66. doi:10.1523/JNEUROSCI.0141-08.2008.

[174] van den Heuvel MP, Sporns O, Collin G, Scheewe T, Mandl RCW, Cahn W, et al. Abnormal rich club organization and functional brain dynamics in schizophrenia. JAMA Psychiatry. 2013;70(8):783–92. doi:10.1001/jamapsychiatry.2013.1328.

[175] Sotiropoulos SN, Zalesky A. Building connectomes using diffusion MRI: why, how and but. NMR Biomed. 2019;32(4):e3752. doi:10.1002/nbm.3752.

[176] Dijkstra EW. A note on two problems in connexion with graphs. Numerische Mathematik. 1959;1(1):269–271. doi:10.1007/BF01386390.

[177] Latora V, Marchiori M. Efficient behavior of small-world networks. Phys Rev Lett. 2001;87(19):198701. doi:10.1103/PhysRevLett.87.198701.

[178] Onnela JP, Saramäki J, Kertész J, Kaski K. Intensity and coherence of motifs in weighted complex networks. Phys Rev E Stat Nonlin Soft Matter Phys. 2005;71(6 Pt 2):065103. doi:10.1103/PhysRevE.71.065103.

[179] Freeman LC. Centrality in social networks conceptual clarification. Social Networks. 1978;1(3):215–239. doi:10.1016/0378-8733(78)90021-7.

[180] Xia M, Wang J, He Y. BrainNet Viewer: a network visualization tool for human brain connectomics. PLoS One. 2013;8(7):e68910. doi:10.1371/journal.pone.0068910.

[181] Benjamini Y, Hochberg Y. Controlling the false discovery rate: A practical and powerful approach to multiple testing. J R Stat Soc. 1995;57(1):289–300.

[182] Kim DJ, Davis EP, Sandman CA, Sporns O, O'Donnell BF, Buss C, et al. Children's intellectual ability is associated with structural network integrity. Neuroimage. 2016;124(Pt A):550–556. doi:10.1016/j.neuroimage.2015.09.012.

[183] Markov NT, Ercsey-Ravasz M, Van Essen DC, Knoblauch K, Toroczkai Z, Kennedy H. Cortical high-density counterstream architectures. Science. 2013;342(6158):1238406. doi:10.1126/science.1238406.

[184] Lamberink HJ, Boshuisen K, van Rijen PC, Gosselaar PH, Braun KPJ, Dutch Collaborative Epilepsy Surgery Program (DCESP). Changing profiles of pediatric epilepsy surgery candidates over time: A nationwide single-center experience from 1990 to 2011. Epilepsia. 2015;56(5):717–25. doi:10.1111/epi.12974.

[185] Meekes J, van Schooneveld MMJ, Braams OB, Jennekens-Schinkel A, van Rijen PC, Hendriks MPH, et al. Parental education predicts change in intelligence quotient after childhood epilepsy surgery. Epilepsia. 2015;56(4):599–607. doi:10.1111/epi.12938.

[186] Sowell ER, Peterson BS, Thompson PM, Welcome SE, Henkenius AL, Toga AW. Mapping cortical change across the human life span. Nat Neurosci. 2003;6(3):309–15. doi:10.1038/nn1008.

[187] Raznahan A, Shaw P, Lalonde F, Stockman M, Wallace GL, Greenstein D, et al. How does your cortex grow? J Neurosci. 2011;31(19):7174–7. doi:10.1523/JNEUROSCI.0054-11.2011.

[188] Clayden JD. Imaging connectivity: MRI and the structural networks of the brain. Funct Neurol. 2013;28(3):197–203. doi:10.11138/FNeur/2013.28.3.197.

[189] Tijms BM, Seriès P, Willshaw DJ, Lawrie SM. Similarity-based extraction of individual networks from gray matter MRI scans. Cereb Cortex. 2012;22(7):1530–41. doi:10.1093/cercor/bhr221.

[190] Iacobucci D, Saldanha N, Deng X. A Meditation on Mediation: Evidence That Structural Equations Models Perform Better Than Regressions. Journal of Consumer Psychology. 2007;17(2):139–153.

[191] Kandel R E. Principles of Neural Science. Kandel R E, editor. Appleton and Lange, Norwalk; 1991.

[192] Duffau H. New concepts in surgery of WHO grade II gliomas: functional brain mapping, connectionism and plasticity – a review. Journal of Neuro-Oncology. 2006;79(1):77. doi:10.1007/s11060-005-9109-6.